A Model-Based Methodology for Managing Technological Risk

Rodrigo Francisco Blanco Gutiérrez

A thesis submitted for the degree of Doctor of Philosophy of the University of London and Diploma Membership of Imperial College

Centre for Process Systems Engineering
Department of Chemical Engineering
Imperial College London
London SW7 2AZ, United Kingdom

August 2007

BIBL
LONDON
UNIV.

I declare that the work is my own and that the work of others is acknowledged appropriately. Rodrigo Francisco Blanco Gutiérrez

Contents

List of Figures viii

List of Tables x

Abstract xi

Acknowledgements xiii

1 Introduction and Motivation 1

1.1 Technological Risk in Process Design 1

1.1.1 Illustrative Example 2

1.2 Objectives 3

1.3 Thesis outline 3

2 Process Design under Uncertainty - An Overview **4**

2.1 Process Synthesis and Design 4

2.1.1 Knowledge-based process design 5

2.1.2 Optimisation-based process design 6

2.2 Process Design and Operability under Uncertainty 8

2.2.1 Process modelling and uncertainty 8

2.2.2 Classification of uncertainty 9

2.2.3 Problem formulation 10

2.3 Stochastic Programming for Process Design under Uncertainty 11

2.3.1 Recourse models 11

2.3.2 Robust stochastic programming 17

2.3.3 Value of information and R&D costs 19

2.3.4 Investment in the presence of technological change 21
2.4 Summary 22

3 Overview of the Proposed Methodology **25**
3.1 Introduction 25
3.2 Problem definition 26
3.2.1 Objectives 26
3.2.2 Modelling assumptions 28
3.2.3 Mathematical representation 29
3.3 Solution Strategy 30
3.3.1 Step 1: Model construction and validation 31
3.3.2 Step 2: Deterministic optimisation - Nominal design 33
3.3.3 Step 3: Stochastic design 33
3.3.4 Step 4: R&D investment decisions 36
3.4 Summary 36

4 Global Sensitivity/Feasibility Analysis **38**
4.1 Introduction 38
4.2 Overview of Sensitivity Approaches 40
4.2.1 Local methods 41
4.2.2 Overview of global methods 44
4.2.3 Sampling methods 45
4.2.4 Point evaluation 47
4.2.5 Analysis of results – Sensitivity indices 50
4.3 Global Sensitivity/Feasibility Analysis and Risk Quantification 64
4.3.1 Choice of sampling technique 64
4.3.2 Feasibility analysis 65
4.3.3 Risk quantification 66
4.3.4 Identification of critical parameters 69
4.4 GSFA Implementation 70
4.4.1 Code structure 70
4.4.2 Input files 73
4.4.3 Output files 74
4.4.4 Code performance 75

4.5 Summary 79

5 Scenario-Based Optimisation **81**

5.1 Introduction 81

5.2 Pseudo-Dynamic Approach 83

5.3 Scenario Generation 88

5.3.1 Reduction of scenarios using first-order sensitivity indices 88

5.3.2 Reduction of scenarios using higher-order sensitivity indices 90

5.4 Summary 92

6 Case Study **93**

6.1 Overview 93

6.2 Catalytic Tubular Reactor 93

6.2.1 Description and data 94

6.2.2 Description of the uncertainty 96

6.3 Iteration I 98

6.3.1 Deterministic optimisation 98

6.3.2 First stochastic design - GSFA 99

6.3.3 First stochastic design - Scenario-based optimisation 118

6.3.4 Second stochastic design - GSFA 122

6.3.5 Second stochastic design - Scenario-based optimisation 128

6.3.6 Third stochastic design - GSFA 132

6.4 Iteration II 140

6.4.1 First stochastic design - GSFA 141

6.5 Summary 149

7 Conclusions and future work **150**

7.1 Conclusions 150

7.2 Future Work 152

7.2.1 Extension to dynamic systems 152

7.2.2 Improvements to sensitivity index calculations 153

7.2.3 Model reduction 153

Bibliography **155**

A Dynamic Optimisation **164**

A.1 PDAE Solution 164

A.2 Optimisation of Dynamic Problem 166

B GSA Files **167**

B.1 Input file for GSA implementation (input.txt) 167

B.2 gPROMS file example to call the simpleEventFOI foreign object 168

C Phosgene Reactor Model **171**

C.1 Nomenclature 171

C.2 Model equations 173

List of Figures

2.1 Hierarchical approach by J. M. Douglas, 1988 6
2.2 Discretisation of uncertain parameter θ 13
2.3 Confidence intervals for two uncertain parameters by Rooney and Biegler, 1999 14
2.4 Two-level dynamic decision making by Cheng *et al.*, 2003 23

3.1 Overview of the proposed methodology. Text in italics and dashed lines indicate information passed between two tasks. 31
3.2 Overview of Step 3 of the proposed methodology. Text in italics and dashed lines indicate information passed between two tasks. 34

4.1 Two-dimensional sampling of 256 points using different methods (a) Uniform sampling, (b) Random sampling based on uniform distribution, (c) Random sampling based on normal distribution, (d) Sobol' sequence . . . 45
4.2 Points needed for a 2-dimensional sample or trial 59
4.3 Probability for key performance indicator 68
4.4 Code structure for GSFA implementation 71
4.5 Parallel implementation structure 72
4.6 Convergence of S_1/S_1^{Tot} to the value of 1 as a function of the number of sample points for Sobol' and uniform random sampling for function (4.99), n=2 76
4.7 Convergence of $\sum S_i$ to the value of 1 as a function of the number of sample points for Sobol' and uniform random sampling for function (4.99) for n=2 76
4.8 Convergence of S_1/S_1^{Tot} and $\sum S_i$ to analytical values for function (4.100) for n=2 77

4.9 Convergence of S_1/S_1^{Tot} and $\sum S_i$ to analytical values for function (4.100) for n=10 78
4.10 Convergence of S_1/S_1^{Tot} and $\sum S_i$ to analytical values for function (4.101) for n=2 78
4.11 Convergence of S_1/S_1^{Tot} and $\sum S_i$ to analytical values for function (4.101) for n=10 79

5.1 Graphical representation of the traditional scenario-based optimisation . . 84
5.2 Pseudo-dynamic optimisation approach 85
5.3 Homotopy approach 86
5.4 Representation of scenario reduction in a 2-dimensional space: a) a uniform grid is used to capture interactions between parameters; b) the number of sample points is reduced when a second-order sensitivity index calculation indicates there is no interaction between parameters. 91

6.1 Schematic of catalytic tubular reactor 94
6.2 Annualised profit probability distribution for the nominal design in iteration I (uniform case) 105
6.3 Coolant flowrate histogram for the nominal design in iteration I (uniform case) 105
6.4 Carbon monoxide feed partial pressure histogram for the nominal design in iteration I (uniform case) 106
6.5 Chlorine feed partial pressure histogram for the nominal design in iteration I (uniform case) 106
6.6 Feed stream velocity histogram for the nominal design in iteration I (uniform case) 107
6.7 Infeasible points for the nominal design in iteration I using Sobol' sampling 108
6.8 Annualised profit probability distribution for the nominal design in iteration I using Sobol'-normal sampling 111
6.9 Coolant flowrate histogram for the nominal design in iteration I using Sobol'-normal sampling 111
6.10 Carbon monoxide feed partial pressure histogram for the nominal design in iteration I using Sobol'-normal sampling 112

6.11 Chlorine feed partial pressure histogram for the nominal design in iteration I using Sobol'-normal sampling 112
6.12 Feed stream velocity histogram for the nominal design in iteration I using Sobol'-normal sampling 113
6.13 Comparison of infeasible points found by Sobol' and Sobol'-normal sampling for the nominal design in iteration I 114
6.14 Annualised profit probability distribution for the nominal design in iteration I using Sobol' sampling with weight factors 115
6.15 Coolant flowrate histogram for the nominal design in iteration I using Sobol' sampling with weight factors 116
6.16 Carbon monoxide feed partial pressure histogram for the nominal design in iteration I using Sobol' sampling with weight factors 116
6.17 Chlorine feed partial pressure histogram for the nominal design in iteration I using Sobol' sampling with weight factors 117
6.18 Feed stream velocity histogram for the nominal design in iteration I using Sobol' sampling with weight factors 117
6.19 36 scenarios generated from the 2-dimensional space of critical parameters 119
6.20 Scenarios used in the first stochastic design step of iteration I, when assuming that the infeasibility probability is unacceptable 121
6.21 Annualised profit probability distribution for design 2 in iteration I (uniform case) 125
6.22 Coolant flowrate histogram for design 2 in iteration I (uniform case) 125
6.23 Carbon monoxide feed partial pressure histogram for design 2 in iteration I (uniform case) 126
6.24 Chlorine feed partial pressure histogram for design 2 in iteration I (uniform case) 126
6.25 Feed stream velocity histogram for design 2 in iteration I (uniform case) . . 127
6.26 Infeasible points identified in the second GSFA for new design in iteration I 127
6.27 Annualised profit probability distribution for design 2 (normal case) in iteration I 129
6.28 Normal coolant flowrate histogram for design 2 (normal case) in iteration I 129
6.29 Carbon monoxide feed partial pressure histogram for design 2 (normal case) in iteration I 130

6.30 Chlorine feed partial pressure histogram for design 2 (normal case) in iteration I 130
6.31 Feed stream velocity histogram for design 2 (normal case) in iteration I . . 131
6.32 Sample points used for the scenario-based optimisation in the second stochastic design loop of iteration I 131
6.33 Annualised profit probability distribution for design 3 in iteration I (uniform case) 134
6.34 Coolant flowrate histogram for design 3 in iteration I (uniform case) 134
6.35 Carbon monoxide feed partial pressure histogram for design 3 in iteration I (uniform case) 135
6.36 Chlorine feed partial pressure histogram for design 3 in iteration I (uniform case) 135
6.37 Feed stream velocity histogram for design 3 in iteration I (uniform case) . . 136
6.38 Annualised profit probability distribution for design 3 (normal case) in iteration I 137
6.39 Normal coolant flowrate histogram for design 3 (normal case) in iteration I 138
6.40 Carbon monoxide feed partial pressure histogram for design 3 (normal case) in iteration I 138
6.41 Chlorine feed partial pressure histogram for design 3 (normal case) in iteration I 139
6.42 Feed stream velocity histogram for design 3 (normal case) in iteration I . . 139
6.43 Profit probability using Sobol'-normal sampling for nominal design in iteration II 146
6.44 Coolant flowrate histogram using Sobol'-normal sampling for nominal design in iteration II 147
6.45 Carbon monoxide histogram using Sobol'-normal sampling for nominal design in iteration II 147
6.46 Chlorine histogram using Sobol'-normal sampling for nominal design in iteration II 148
6.47 Feed stream velocity histogram using Sobol'-normal sampling in iteration II 148

A.1 Schematic representation of Method of Lines 165
A.2 Schematic representation for solution of dynamic optimisation problem . . 166

List of Tables

4.1 Analytical values for Sobol' sensitivity indices of test functions. 75

6.1 Gas-phase physical properties 95
6.2 Reaction kinetics 95
6.3 Data for the gas stream 96
6.4 Cost data 97
6.5 8 Uncertain parameters 97
6.6 Optimal design and control variables in nominal design for Iteration I . . . 99
6.7 One-at-a-time sensitivity analysis results for simulation-based approach . . 100
6.8 GSFA results for first-order Sobol' indices for the nominal design in iteration I (uniform case) 102
6.9 GSFA results for higher-order Sobol' indices for the nominal design in iteration I 103
6.10 Mean value and standard deviation for profit and control variables for the nominal design in iteration I (uniform case) 107
6.11 GSFA results for first-order Sobol' indices for the nominal design in iteration I (normal case) using Sobol'-normal sampling 110
6.12 Mean value and standard deviation for profit and control variables for the nominal design in iteration I using Sobol'-normal sampling 113
6.13 Mean value and standard deviation for profit and control variables for the nominal design in iteration I using Sobol'-normal sampling and Sobol' sampling with weight factor 115
6.14 Infeasibility index for the nominal design in iteration I using Sobol'-normal sampling and Sobol' sampling with weight factor approach 118

6.15 Pseudo-dynamic optimisation results for the 40-scenario optimisation problem in iteration I (design 2) 122
6.16 GSFA results for first-order Sobol' indices for design 2 in iteration I 123
6.17 GSFA results for second-order Sobol' indices for design 2 in iteration I . . . 123
6.18 Mean value and standard deviation for profit and control variables in iteration I for design 2 (uniform case) 124
6.19 Mean value and standard deviation for profit and control variables in iteration I for design 2 using Sobol' sampling with weight factors 128
6.20 Pseudo-dynamic optimisation results for the 44-scenario optimisation problem in iteration I (design 3) 132
6.21 GSFA results for first-order Sobol' indices for design 3 in iteration I 132
6.22 GSFA results for second-order Sobol' indices for design 3 in iteration I . . . 133
6.23 Mean value and standard deviation for profit and control variables in iteration I for design 3 (uniform case) 133
6.24 Mean value and standard deviation for profit and control variables in iteration I for design 3 (normal case) 137
6.25 Uncertain parameters for iteration II 141
6.26 Comparison of GSFA results for first-order Sobol' indices for nominal design between iterations I and II 142
6.27 GSFA results for higher-order Sobol' indices for nominal design in iteration II 142
6.28 Mean value and standard deviation for profit and control variables for nominal design in iteration II using Sobol' sampling 143
6.29 Comparison of GSFA results for first-order Sobol' indices using a Sobol'-normal sampling between iterations I and II (normal case, nominal design) 144
6.30 GSFA results for higher-order Sobol' indices using Sobol'-normal sampling in iteration II 145
6.31 Comparison of standard deviations for nominal designs using Sobol'-normal sampling in iterations I and II 145

Abstract

Technological risk is often the consequence of incomplete knowledge when developing new products and processes. As with any other innovation process, uncertainty is likely to be present. Technological development almost inevitably implies increased risk with respect to safety, operability and sustainability. Although the risk can often be reduced by spending additional time and resources in R&D activities, the increased time and cost can significantly reduce the competitive advantage obtained from the new technology. Therefore, the potential risk implications have to be weighed against the potential benefits of the technology deployment.

This work considers the problem of process design under technological risk arising from limitations in the understanding of the new technology. It presents a systematic methodology to manage the technological risk in process design using mathematical models sufficiently detailed to quantify risk. While simple models can be acceptable for simple units, it is the details, such as reaction microkinetics, the spatial variation of properties, such as temperature and pressure variations along a reactor's length, and finite rates of mass/energy transfer, that often distinguish new technologies from existing ones.

The aim of the methodology is to identify the resulting uncertainty in key performance indicators (KPIs) of a process, for a certain level of model accuracy; to generate a list of critical model aspects on which further R&D is needed if the risk is unacceptable; and to find the best design that can deal with the residual model uncertainty.

The approach consists of a series of steps from model building to robust design. In the first step, a detailed process model is built and validated. The model is expressed in the form of a mixed system of partial differential and algebraic equations (PDAEs). A key output of the validation process is the set of confidence intervals for the uncertain model parameters.

In the second step, a deterministic optimisation identifies an optimal design and control strategy for the nominal or most probable value of the uncertain parameters. The result of the deterministic optimisation is used as initial guess for the following steps.

In the following step, a global sensitivity/feasibility analysis (GSFA) is used to identify critical parameters affecting key performance indicators. The approach exploits the flexibility of the process by using the control variables to optimise the operation for every

sampled point. Sobol' sensitivity indices are approximated by a parallelised code using gPROMS. The solution of several optimisation problem in the GSFA is used to generate histograms of key performance indicators. These histograms are used to quantify the risk arising from the existing parameter uncertainty for a given design. The results of the GSFA are also used to calculate the probability of the design leading to infeasible operation.

If the results of the previous step are deemed as acceptable, the nominal design can be used if the variability in the KPIs is sufficiently small. Otherwise, a scenario-based optimisation is performed. A reduced set of scenarios is generated by sampling the reduced uncertain space formed by the critical uncertain parameters. A pseudo-dynamic optimisation approach is proposed to solve the scenario-based problem. The proposed method is able to deal with a large number of scenarios and can handle large nonlinear models while avoiding numerical convergence difficulties.

When the results of the GSFA are unacceptable, the method can proceed to find a new design employing the pseudo-dynamic approach to reduce the variability of the KPIs. Otherwise, additional R&D resources can be focused on the critical parameters aiming at reducing the parametric uncertainty.

The benefits and capabilities of the proposed methodology are illustrated on the design of a catalytic tubular reactor.

Acknowledgements

First of all, I want to thank my parents and my brother for the great support they have given me to get to this point.

A very special acknowledgement to Liliana who is the one who has had to cope with me all these years. You worked hard to show me that the distance was not a problem to make me feel your love and support. You are behind this and without you this wouldn't have been possible.

I am very grateful to my supervisors Claire and Costas for giving me the opportunity to work with them on this project. It has been a very rewarding and amazing experience to work with both of you. You have each brought something to complement this work and my learning experience. Thanks so much for all your great help and support.

Thanks as well to CONACyT and CPSE for the very much needed financial support for living in a place like London.

I want to mention several people who allowed me to do this work at CPSE and PSE. Graham and Terrence at CPSE, thanks for the help provided to get my code running in the cluster. I am also very grateful to Adam, Luke and Duane at PSE for all the support on the gPROMS side and for showing me some of the wonders of gPROMS, such as the Costas Help Desk =).

Thanks to Sergei Kucherenko for the initial sensitivity analysis code and for helping me with the different modifications, ideas and discussions that improved this work.

Thanks as well to people at Dow Chemical who helped me with this project. To Alfonso German who was one of the main guy supporting my idea of doing a PhD. And thanks to Philippe Hayot and Jan W. Verwijs who provided some direction to this project.

A special mention to some great friends at CPSE. Vini, thanks for the warm welcome to the center and for being such a social character. Tim, thanks for you help with Latex and for the coffee bar legacy. To Mark Pinto for all those great moments and sangria sharing, and to Milica who was a nice support and a great friend.

A big acknowledgement to all the people who made my time in London one of my best experiences. All my friends at Clayponds: Veronica, Olli, Juan, Michaela, Elle, Costas. Andreina, Idalina, Saurabh, and Mark and Sue Tyrer.

And finally, there is no way to show how grateful I am to my great flatmates who became part of my family: Takis, Mike and Amy. You were just there all the time. Thanks a lot!

Chapter 1

Introduction and Motivation

1.1 Technological Risk in Process Design

Innovative process design is subject to technological risk, especially when new process chemistry and/or new process technology is involved. The risk usually arises because of uncertainty in the operation, reliability and performance of the new technology. In today's rapidly changing business environment, existing technologies are exposed to uncertainty in future operation, profitability and sustainability under new developments in the field. This risk is currently being addressed in a rather ad hoc fashion, primarily relying on an expert review process. The potential implications of the risk have to be weighed against the potential benefits that may be realised by the deployment of new technology. The shortage of methods to evaluate risk leaves decision-makers in process design without a proper guide to coordinate efforts and optimise resources, thus favouring conservative approaches rather than new technologies. If a method is developed to deal with this type of risk as an integral part of the process design, the result will be a competitive advantage, which will save time and costs by optimising the available resources. The development of a method to manage technological risk as an integral part of process design will allow users to gain a competitive advantage by deploying and focusing their R&D efforts in a way which brings risk down to an acceptable level.

1.1.1 Illustrative Example

Consider the following example. A company produces a chemical under a conventional process technology when a new process chemistry is developed. Adopting the new technology implies designing and investing in a new reactor, bringing about lower expected operational costs, and improving the economic performance of the process. The business managers need to decide on the best R&D strategy and timing to start-up the new operation based on the balance of two factors: expected financial gain and level of risk. An earlier start-up allows the company to reap the benefits of the new technology sooner but reduces the amount of time available for uncertainty reduction through R&D. For a fast implementation of the new technology, some parameters could have a large associated uncertainty, reflected in large ranges of values or wide probability distribution functions. Therefore, the design will have a higher level of uncertainty in its performance, but the benefits of lower costs could be felt faster. On the other hand, if the start-up is delayed, R&D can be focused on the reduction of the uncertainty to acceptable levels, increasing the cost and time to introduce the product to the market. The decision should be based on an acceptable level of risk as determined by measures such as downside and other indicators of the effect of uncertainty.

In conventional design techniques, deterministic parameter values are used to generate solutions. When these methodologies are used under uncertainty, the uncertain parameters should be assigned nominal values which are usually the mean or average within a specified range. If the realisation of the uncertain parameters is not the one used in the deterministic design, the proposed design could have an unexpected behaviour. The extent of the deviation from expected operation will depend on the overall effect that the uncertain parameter has on the performance variable.

Without a proper methodology to address this problem, the use of existing process design techniques could result in the implementation of a process with low performance or, in the worst case, one that fails to meet the required specifications. Performance targets, quality constraints or even safe operation limits could be violated. Ultimately, the overall process life cycle could be affected because of decreased profits.

1.2 Objectives

The aim of this thesis is to tackle the problem of design under technological risk. In this thesis, a methodology to address the following questions is presented:

- What is the risk inherent in a given process design in which a new technology is used?
- What is the best design, when using a new technology, that minimises the risk inherent in its use?
- How can additional R&D expenses be best targeted to reduce the risk when the current level is too high?

In this work, internal and external uncertainties are considered, but it is assumed that a model which captures all relevant phenomena is available. This typically requires the use of detailed (distributed) models. Emphasis is placed on deriving a reliable and quantitative assessment of the risk associated with a given process and a given level of uncertainty.

1.3 Thesis outline

This thesis is organised as follows. In chapter 2, a literature review of research in the area of process design with emphasis on process design under uncertainty is presented. Different solution approaches are shown to tackle this problem.

In chapter 3, a general overview of the proposed methodology is given. In chapter 4, the literature on sensitivity analysis methods is reviewed and an approach for global sensitivity/feasibility analysis and risk quantification is described. The last step of the methodology, scenario-based optimisation, is detailed in chapter 5. The methodology is then applied to the design of a phosgene reactor in chapter 6. Finally, the conclusions are discussed in chapter 7 along with some suggestions for future work.

Chapter 2

Process Design under Uncertainty - An Overview

2.1 Process Synthesis and Design

Process synthesis and process design can be regarded as closely related activities. On one hand, process synthesis is the generation of the general topology of a flowsheet, the sequence of unit operations and estimated operating conditions for each piece of equipment. On the other hand, process design is concerned with equipment design within a flowsheet. In the context of this thesis, *process design* will be used as a single term to cover both activities.

Process design techniques have been developed during the past several decades with the main objective of providing the industry with profitable designs (Ishii, 1997). This development is the result of the industry's needs and business conditions that demand cleaner, more efficient, more reliable and cost competitive plants. For many years, the focus of process design was on large plants which meant better economic profit for long life-cycle products. Having a plant with high production capacity for a single product implied lower manufacturing costs and higher profits. However, the development of new products with shorter life cycles, an increased focus on specific markets, tightening environmental regulations and the need for greater business competitiveness have changed the constraints placed on process design. This has made the design of smaller plants, more integrated operations and faster product and process development high priorities in the race to reduce costs and optimise resources.

Process design has also seen developments in the scale of its application. The level of application can be divided in three scales: macro-scale, meso-scale and micro-scale (Li and Kraslawski, 2004). Chronologically, the meso-scale is the first category that was explored (1960's to 1980's), focusing on the concept of unit operations. The macro-scale followed as a result of increased regulation and competition. These constraints led to the incorporation of factors such as market and environmental requirements in design. The micro-scale is the most recent scale to be considered (mid 1990's) and deals with the details of molecular structure, fluid dynamics and chemical reactions to come up with designs for new unit operations.

Process design is an activity which considers multiple choices and requires multidisciplinary action (Siirola, 1996). The different approaches to process design can be divided in two categories: knowledge-based and optimisation-based (Li and Kraslawski, 2004). Knowledge-based methods make use of experience as the basis to produce acceptable designs. These two types of approaches are reviewed in the remainder of this section. Methods to handle uncertainty are the focus of the rest of this chapter.

2.1.1 Knowledge-based process design

Different methods in knowledge-based process design are differentiated by the way the problem is decomposed and solved. The most representative are heuristic methods, means-ends analysis and evolutionary approaches. Heuristics can be defined as rules-of-thumb derived from practical or computational experience and, as such, they rely on intuition, engineering knowledge and physical principles to deliver process design. The work by Douglas (1988) is a representative approach for heuristic methods in process design. The decisions are taken in a specific order, which can be seen in figure 2.1.

Means-ends analysis operates on the opportunistic difference between two well-defined states. In process design, these two defined states are generally the raw material and the desired product. The means-ends analysis systematically identifies property differences, such as chemical identity, amount, concentration, phase, temperature, pressure, form, which can be exploited to reach a new state (Siirola, 1996).

Finally, the evolutionary approach works using existing designs as a basis. The method is probably one of the most used by process designers (Stephanopoulos and Westerberg, 1976). In this approach, existing systems are analysed and changed in different ways to

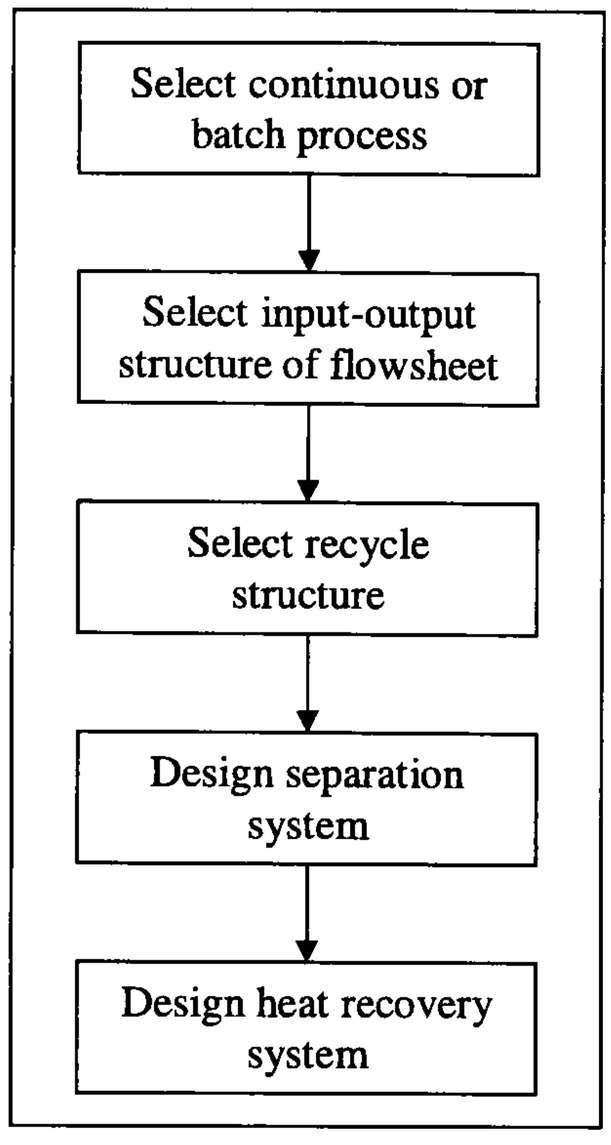


Figure 2.1: Hierarchical approach by J. M. Douglas, 1988

improve them. For new processes where a similar process is available, the modifications are done based on the feedback obtained from plant operation and known problems. In other cases, an existing flowsheet is selected which matches most of the characteristics for the new product and is modified appropriately. Such an approach maintains the strengths of the existing design in the process of finding an improved process. A drawback of this method is that it needs a considerable amount of expertise. Applications of the evolutionary approach can be found in King et al. (1972) and Stephanopoulos and Westerberg (1976).

2.1.2 Optimisation-based process design

On the other hand, optimisation-based methods are based on a mathematical formulation of the design problem which is solved via optimisation techniques. The process model consists of equations in the form of equalities and inequalities. The equalities describe the process behaviour, taking into account mass, energy and possibly momentum balances and any relevant physical or chemical behaviour. The inequalities represent operation limits and design constraints. These are set to follow specific design and operational

guidelines for safety, environmental or economic reasons. The variables and parameters can be continuous, such as temperature or flowrate, or discrete, such as equipment sizes or number of units.

Optimisation-based methods have been applied to several areas within process design such as heat and mass exchanger networks, reactor networks and distillation sequences. A significant contribution in the synthesis of heat exchanger networks was given by Hohman (1971), Linnhoff and Flower (1978a) and Umeda et al. (1979). They proposed a formulation of the problem based on thermodynamic principles. It matches hot streams with cold streams and where no match can be found, external utilities are included to minimise the capital and operational costs. This heat integration approach is known as pinch technology. Further development of the pinch technology has found application in fields such as the heat integration of distillation columns (Linnhoff et al., 1983; Floudas and Paules-IV, 1988; Yeomans and Grossmann, 1999), heat integration of reactors (Glavič et al., 1988) and total site integration (Dhole and Linnhoff, 1992).

A similar thermodynamic approach for heat integration has been used in the synthesis of mass exchange networks (El-Halwagi and Manousiouthakis, 1990). The objective is to design a network of mass exchangers to transfer compounds from rich streams to lean streams at a minimum cost. Hallale and Fraser (1998) apply this methodology in the synthesis of networks for waste water minimisation. Papalexandri and Pistikopoulos (1994) propose a methodology for the synthesis of combined heat and mass exchange networks. A mixed integer nonlinear programme (MINLP) is formulated and transformed into a multiperiod problem when inlet conditions are allowed to vary and described by discrete values. The objective function is the minimisation of capital and operating costs for both heat and mass exchange networks.

Optimisation-based methods have also been applied in the field of reactor network synthesis. Hildebrandt and Glasser (1990) propose a formulation based on geometric representations for systems of reaction and mixing. A different approach is given by Kokossis and Floudas (1990) who show a systematic methodology for schemes working under isothermal operation. A reactor network superstructure is presented containing a series of continuous stirred tank reactors (CSTRs) and plug flow reactors (PFRs). An extension of the formulation has been used in the synthesis of multiphase reaction systems (Mehta and Kokossis, 1998).

The work by Biegler et al. (1997) presents an approach for the design of distillation

sequences. A mixed integer linear programming (MILP) is formulated from some assumptions such as 100% recovery for key components, which help to model the problem in terms of total feed flowrates. The simplest model assumes that all heating and cooling duties are supplied by utilities. Heat integration and pressure effects are later included to obtain complex column arrangements reducing capital and operating costs. Finally, they present a rigorous MINLP model to determine the optimal feed location and number of trays in a column, which uses tray-by-tray calculations.

The complexity of the models used in optimisation approaches depends on the process studied and on the level of assumptions and simplifications used. The model can be a set of linear equations, in the simplest case, or it can be a system of partial differential and algebraic equations (PDAEs), in the most complex case. The development of the optimisation methods and level of complexity in the formulation has been closely linked with advances in computer technology (Westerberg, 2004). Recent developments in computing and numerical methods have allowed the solution of thousands of equations in a relatively small amount of time. This makes it feasible to use complex high-fidelity models for process design.

The main advantage of using optimisation-based techniques for process design is the provision of a systematic way to evaluate the performance and cost of different configurations along with their interactions. However, the disadvantage is that the search for optimal solutions is done within the space defined by the proposed superstructure. This may result in missed opportunities, especially for systems where the automatic generation of such configurations is not possible. Another disadvantage is that there is no guarantee of global solution for large complex NLP and MINLP with current solution methods.

Much recent work has been focused on optimisation-based methods. However, in an industrial context, design is usually undertaken via a combination of knowledge-based and optimisation-based methods.

2.2 Process Design and Operability under Uncertainty

2.2.1 Process modelling and uncertainty

Process modelling is used in knowledge-based and optimisation-based process design to reproduce the behaviour of a system. Depending on the process or unit to be studied, mod-

els incorporate details at one or more scales: distillation columns are typically modelled at the macro-scale, while a reactor model may incorporate micro-scale kinetics modelling. or meso-scale computational fluid dynamics modelling in addition to macro-scale effects. Depending on the needs and tools used to solve the models, the size and complexity of the model can vary significantly from a few equations to thousands of equations, requiring the integration of different solvers.

A model is a mathematical approximation of the real behaviour and as such it is subject to uncertainty. This uncertainty can be the result of one or more factors. Firstly, the model itself can give rise to uncertainty when assumptions and/or simplifications are used to represent the behaviour of the system. Sometimes, these assumptions and simplifications are made to reduce the size of the problem and to make its solution tractable with available tools. Secondly, the parameters used within the model can also be a source of uncertainty. This is due to a lack of information, primarily in the form of experimental data. This is the type of uncertainty this thesis focuses on.

2.2.2 Classification of uncertainty

Assuming a "good" model representation which captures all relevant physical phenomena, the remaining uncertainty can be classified in the following categories (Pistikopoulos, 1995):

- Model-inherent uncertainty, which is related to parameters within the model whose values are obtained from experiments or pilot plant tests, like kinetic constants or physical properties. They can be described by probability distribution functions.

- Process-inherent uncertainties are variations encountered in the process variables such as temperature, flowrate or stream quality properties and some can be defined as disturbances.

- External uncertainty depends on factors not related to the model itself like product demands, prices and availability.

- Discrete uncertainty is related to equipment availability which can be described by discrete probability functions.

In this thesis, we tackle the problem of process design taking into account model-inherent uncertainties arising from the lack of knowledge about a new technology, and process-inherent uncertainty.

Research activity on uncertainty and risk applied to process design has increased in the last decade. The literature can be divided in two general areas: (1) process design and operational planning under uncertainty, and (2) investment under uncertainty. The first area deals with issues related directly with design and operational variables within the process design context. Investment under uncertainty on the other hand addresses the problem from a management and decision-making point of view. The following sections give a brief review of representative research done in these areas.

Research on process design and operational planning under uncertainty has focused on process and product design, production planning, scheduling and capacity expansion.

2.2.3 Problem formulation

The formulation and solution strategies are affected by the representation of the uncertainty. As discussed by Bernardo et al. (2001), this can be scenario-based, stochastic (using a continuous probability distribution function (pdf) for the uncertain parameters) and parametric. The scenario-based approach is particularly suitable for parameters with discrete realisations, but it can also be used to approximate continuous distributions.

Sahinidis (2004) presents a review of the theory and methodologies developed for optimisation problems under uncertainty. The main approaches are divided in three areas:

1. Stochastic programming

2. Stochastic dynamic programming

3. Fuzzy mathematical programming

Within stochastic programming, several types of problems can be distinguished (Sahinidis, 2004): stochastic linear programming, stochastic integer programming, stochastic NLP, robust stochastic programming and probabilistic programming. The first three categories refer to formulations with different types of models and uncertainty representations, but where the objective function is based on an expected value. The fourth category brings a measure of risk into the objective function through the introduction of a penalty term

based on variability measure. The last approach, probabilistic programming, differs from the others because of the use of soft constraints in which a given condition is satisfied with a prescribed probability.

The second class of approach, dynamic programming, is based on the idea of sequential decision-making. The problem is decomposed in several stages. It takes into account the conditions in the current stage as well as expected results for future scenarios. This is done by breaking every decision sequence in two parts: the first one takes the value of the immediate decision by evaluating current conditions and states. The second part accounts for all the remaining decisions. This is used to work back starting from the final stage and going all the way to the initial condition or stage (Bellman, 1957). This approach has been used by Cheng et al. (2003), Yin et al. (2003), and by Dixit and Pindyck (1994) for investment under uncertainty (see section 2.3.4).

Fuzzy programming, the third class of approach, differs from the previous approaches in the way it handles uncertainty. Stochastic and dynamic programming use discrete or continuous probability functions to represent uncertain parameters. Fuzzy programming uses fuzzy numbers and fuzzy sets. Violation of constraints is allowed to a certain degree using membership functions (Bellman and Zadeh, 1970). These functions represent the degree of satisfaction and the expectation of the decision maker about the objective function level. Liu and Sahinidis (1997) apply this solution method to a production planning and capacity expansion problem and Kraslawski and Nyström (1994) apply fuzzy sets to the calculation of flexibility indices.

In this work, we focus on stochastic programming. Rather than attempting an exhaustive review of this area, we introduce key concepts and refer the reader to the reviews of Sahinidis (2004) and Biegler and Grossmann (2004) for further reading.

2.3 Stochastic Programming for Process Design under Uncertainty

2.3.1 Recourse models

In the recourse models, design decisions are taken in a first stage before the realisation of the uncertain parameters. In the second stage, values for the control variables are selected to be applied once the uncertain values are known. The general form for this type of

problem is shown in (2.1) using the notation of Pistikopoulos and Ierapetritou (1995).

Design stage:

$$\begin{aligned} &\max_{d} E_{R_{n(d)}}\{f'(d,\theta)\} \\ &\qquad R_{n(d)} = \{\theta \in \Theta | \exists (z,y,x) : h(d,z,x,\theta) = 0 \wedge g(d,z,x,\theta) \leq 0\} \\ &\qquad d \in D, \theta \in \Theta \end{aligned} \tag{2.1}$$

Operating stage:

$$\begin{aligned} f'(d,\theta) \quad &= \quad \max_{z,x} f(d,z,x,\theta) \\ \text{subject to} \quad &\qquad h(d,z,x,\theta) = 0 \\ &\qquad g(d,z,x,\theta) \leq 0 \\ &\qquad z \in Z, x \in X \end{aligned}$$

where x represents the state variables, z the control variables, θ the vector of uncertain parameters, n is the number of uncertain parameters in the formulation, f is a scalar function which is the main performance indicator, and function f' is obtained by maximising the value of f for fixed design variable vector d and uncertain parameter values θ, subject to equalities h and constraints g. $E_{R_{n(d)}}$ is the expectation operator over the region R_n, defined by (2.2),

$$E_{R_{n(d)}}\{f(d,\theta)\} = \int_{R_{n(d)}} f(d,\theta) j(\theta) d\theta \tag{2.2}$$

where $j(\theta)$ is the probability of parameter realisation θ.

The different types of algorithms that have been proposed to solve the two-stage stochastic programming model are discussed next: single-level algorithms and two-level algorithms.

Single-level algorithms

In single-level algorithms, the problem is reformulated as a multiperiod optimisation problem, or scenario-based problem, in which the optimisation is performed over a number of scenarios, using a traditional deterministic optimisation technique. In the case of problems with discrete uncertainty, the generation of scenarios is straightforward. However, sampling-based approaches are needed when the uncertain parameters are defined by continuous probability distribution functions, as illustrated in figure 2.2. Each scenario has

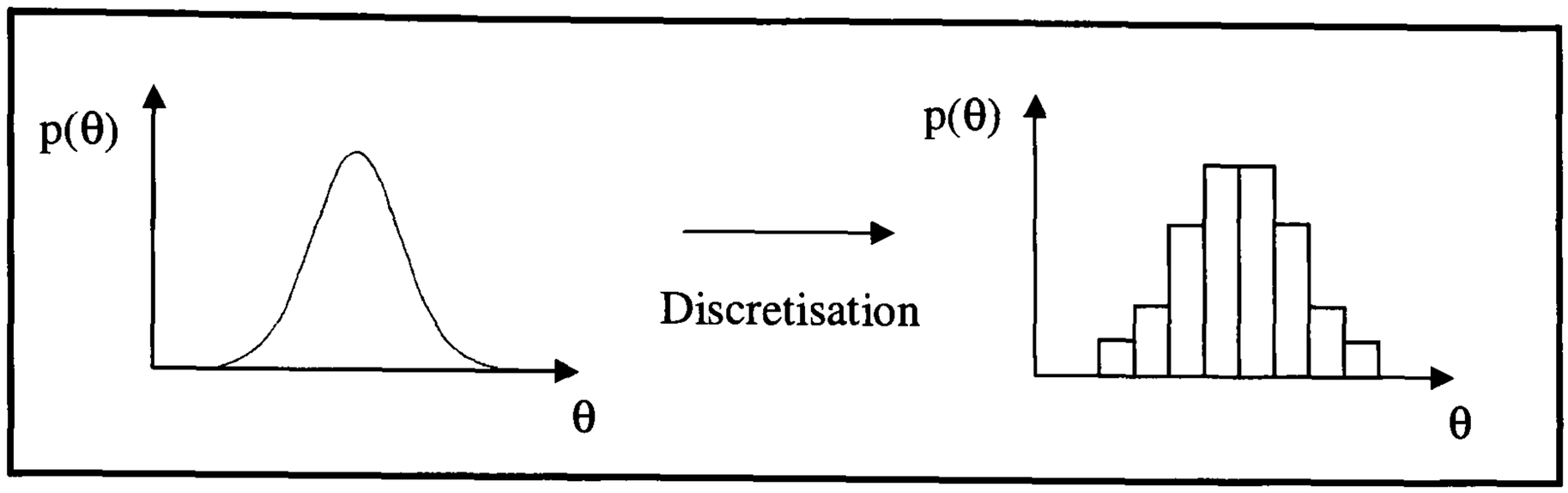


Figure 2.2: Discretisation of uncertain parameter θ

an associated weight factor which measures the relative contribution of the scenario to the expected result.

The general formulation of the multiperiod problem is

$$\max_{d,z,x} f_o(d) + \sum_{p=1}^{P} w_p f(d, z_p, x_p, \theta_p) \tag{2.3}$$

$$\begin{aligned} s.t. \quad & h(d, z_p, x_p, \theta_p) = 0 \;\; p = 1, \ldots, P \\ & g(d, z_p, x_p, \theta_p) \leq 0 \;\; p = 1, \ldots, P \\ & d \in D, z \in Z, x \in X \end{aligned}$$

where d represents design variables, x state variables, z control variables, θ represents the uncertain parameters and w_p the weight factor for period, or scenario, p. P denotes the total number of scenarios. This approach is used by Varvarezos et al. (1994), Paules and Floudas (1992) and Ahmed and Sahinidis (1998), among others.

In the common case where the uncertainty parameters are continuous, the number of scenarios and the value of the parameters chosen have an impact on the quality of the approximation, by a discrete sum, of the expected value. Several authors have proposed methods to choose scenarios in order to obtain a good approximation and/or keep the problem size as small as possible.

Ierapetritou and Pistikopoulos (1995) and Ierapetritou et al. (1996b) use a quadrature formula for scenario generation, given box constraints on the values of the uncertain parameters. Bernardo et al. (1999) use special integration techniques to reduce the

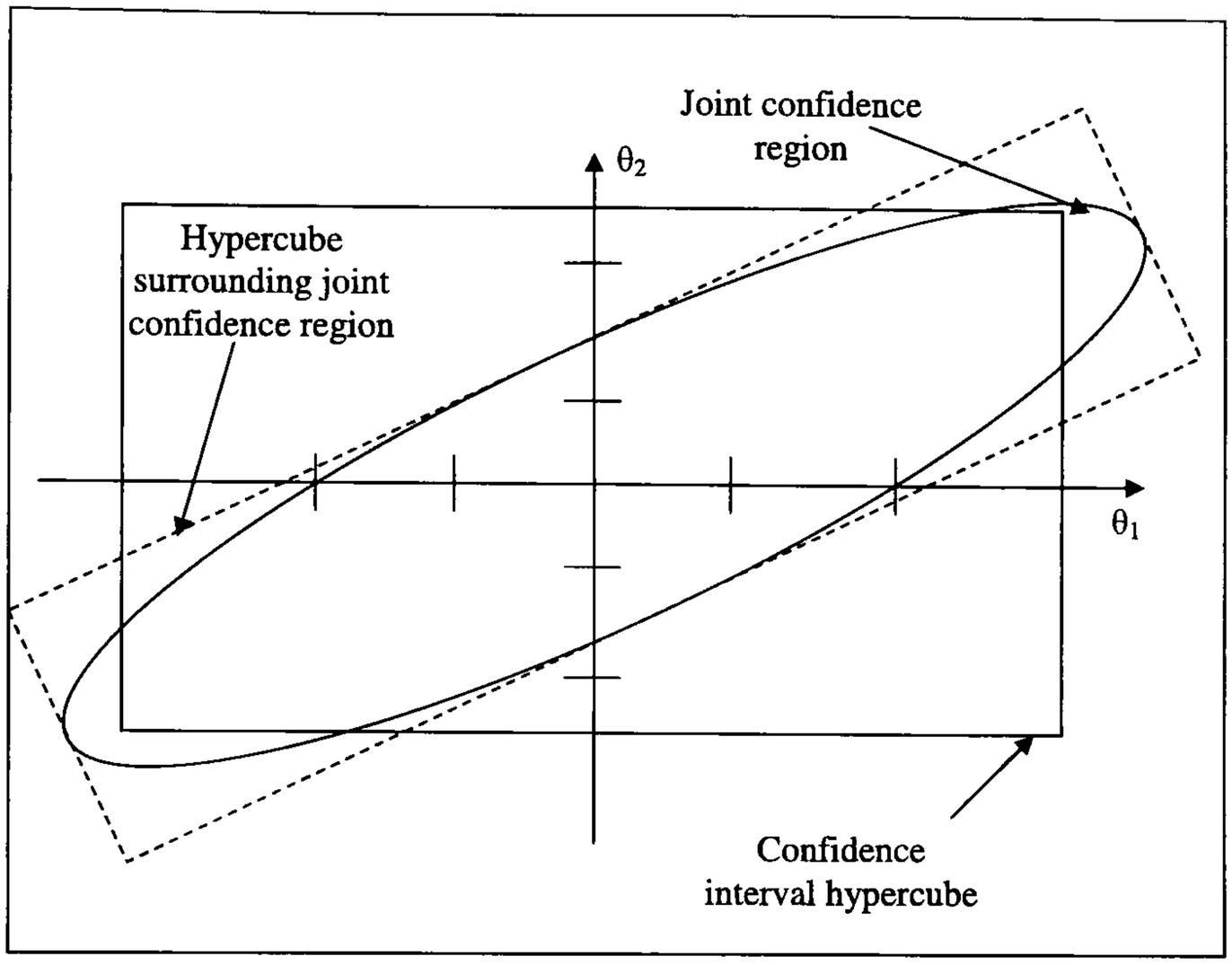


Figure 2.3: Confidence intervals for two uncertain parameters by Rooney and Biegler, 1999

computational cost required by assuming that the uncertain parameters follow normal distributions and by exploiting the mathematical properties of Gaussians.

Rooney and Biegler (1999) use joint confidence regions to represent uncertainty. In some cases, the individual confidence region for variables cannot give the greatest expected uncertainty which is only obtained when combined confidence regions are used. The method uses the covariance matrix to obtain points which reflect the greatest expected uncertainty in the model, as shown in figure 2.3. These points are used to generate scenarios to be optimised. One of the advantages of this method is that it provides a systematic way to choose points based on statistical analysis, thus avoiding the exponential growth of the problem, as fewer scenarios are required. However, the approach has two main disadvantages. First, it requires the use of the covariance matrix, which could be challenging and expensive to find. The second is that the method relies on the feasibility test, which must be checked over an infinite combination of uncertain parameters.

Rooney and Biegler (2001) extend their previous work on joint confidence regions (Rooney and Biegler, 1999). In this new approach, the nonlinearity of the model is accounted for by using confidence regions derived from the likelihood ratio test. The multi-

period problem is optimised with respect to design variables only yielding a conservative solution. The solution algorithm generates a number of scenarios from the confidence region.

Diwekar (2003) proposes the formulation of a large scale problem by using a quasi-Monte Carlo sampling technique, the Hammersley sequence sampling. They show that this approach provides an improved convergence with the number of sample points when compared to Monte Carlo sampling. While such a method results in good accuracy, it leads to a large scale problem which is solved using an algorithm based on simulated annealing.

Finally, Wei and Realff (2004) present an algorithm for stochastic convex MINLPs based on the concept of sample average approximation (SAA). Rather than solving a large multiperiod optimisation problem, an upper bound on the solution is obtained by solving several small multiperiod problems to generate an average solution. This average solution is then assessed through the evaluation of performance over a large set of scenarios yielding a lower bound. An iterative procedure is proposed to allow convergence of the bounds.

Regardless of the approach chosen for scenario generation, a realistic evaluation of performance over the uncertain parameter space requires the solution of a large optimisation problem. This problem has a special structure since only the design variables appear in all constraints, which has been exploited by several authors to reduce computational requirements.

Varvarezos et al. (1994) present a new decomposition algorithm for multiperiod problems. The main disadvantage when using general purpose optimisation methods for multiperiod problems is the increasing size of the problem with the number of periods or scenarios. This increase may be quadratic or even cubic as the number of periods increases. The proposed approach decomposes the multiperiod problem by making use of the diagonal block structure which is characteristic of this type of problems. The methodology reduces the computational effort by making it linearly dependent on the number of scenarios. The approach was applied to 4 case studies, 2 of which are process synthesis related.

Bhatia and Biegler (1999) further develop the algorithm of Varvarezos et al. (1994) with the incorporation of interior point methods within the successive quadratic programming (SQP) framework. A bottleneck of the Varvarezos et al. (1994) algorithm is the use of an active set strategy to solve the quadratic programming subproblem as this is combinatorial

in the number of active constraints. The proposed methodology replaces this by an interior point method to make the quadratic programming (QP) problem solution independent of the active set.

The use of a finite number of scenarios in the evaluation of the expected value necessarily leads to an approximation and may even result in an infeasible design at some non-sampled points in the uncertain space. Ierapetritou and Pistikopoulos (1995) and Ierapetritou et al. (1996a) present a multiperiod formulation for the problem of batch plant design under uncertainty. They relax the condition of feasibility by introducing a penalty term for unfilled orders and partial feasibility. They propose ways in which the structure of the problem can be exploited to arrive at reliable (global) solutions efficiently.

Two-level algorithms

In two-level algorithms, the issue of ensuring feasibility over the entire space of uncertain parameters is tackled explicitly. The algorithms proposed build on the work in the area of process flexibility (see Grossmann and Straub (1991) and Pistikopoulos (1995) for a review) and in the area of semi-infinite programming (Gustafson, 1981).

In two-level algorithms, an iterative procedure which alternates between the solution of two problems is adopted. A multiperiod problem is formulated based on scenarios chosen to approximate the expected performance measure. This problem is solved to obtain an initial design. A second problem, the feasibility problem, is then posed: it consists of the verification of the feasibility of the design over the entire parameter space through some form of maximisation of constraint violation. If a scenario θ^c is found to violate the constraints (a critical scenario), it is added to the set of constraints in the multiperiod optimisation problem.

Recent work in this area has been devoted to new problem formulations to deal with different types of uncertainty or to allow a better treatment of flexibility by taking its cost into account.

Pistikopoulos and Ierapetritou (1995) lift the requirement of feasibility over a specified uncertainty range, and focus on the simultaneous computation of the expected economic performance and the boundaries of the feasible region. These boundaries are obtained by solving a series of small feasibility subproblems. The quadrature points for the evaluation of the expected profit for the current design are then chosen based on the boundaries of the feasible region, allowing a more accurate computation than when using fixed quadrature

points. The problem is tackled using a decomposition approach based on the Generalised Benders Decomposition. Further improvements to the algorithm have been reported by Ierapetritou et al. (1996a) and Ahmed et al. (2000).

In Rooney and Biegler (2003), the uncertainty is divided into unknown model parameters, such as kinetic constants, which can never be known precisely, and process variability such as inlet temperature or flowrate, which can be measured during operation. It is assumed that uncertain parameters cannot be compensated for by adjusting control variables, while process variability can be handled through control. There must therefore exist one control action which results in feasible operation for all values of the uncertain parameters. A two-level algorithm is used to solve this problem. At the first-stage (design) level, scenarios in the multiperiod problem are initially chosen based on a quadrature formula. Critical scenarios identified in the second-stage (feasibility) problem are added as constraints in the multiperiod problem. They do not appear in the objective function (quadrature approximation). To deal with the two types of uncertain parameters, a new formulation of the feasibility problem is given, based on a multilevel max-min-max-max problem. A solution strategy based on the aggregation of inequality constraints using KS functions (Kreisselmeier and Steinhauser, 1983) is proposed. The methodology was applied to a linear retrofit problem, a reactor-cooler design and to the Williams-Otto process.

A similar strategy is followed by Ostrovsky et al. (2004), who independently proposed a formulation similar to that of Rooney and Biegler (2003). Their solution strategy is based on the derivation of lower and upper bounds for the solution of the feasibility problem, as first presented by Ostrovsky et al. (1998).

2.3.2 Robust stochastic programming

In the robust stochastic approach, the recourse problem is modified to take into account a variability measure, *e.g.* variance. Two different formulations can be seen. In the first one, the robustness measure can be included as an extra constraint in the operating stage (2.4).

Design stage:

$$\begin{aligned} &\max_{d} E_{R_{n(d)}}\{f'(d,\theta)\} \\ &\qquad d \in D, \theta \in \Theta \\ &\qquad R_{n(d)} = \{\theta \in \Theta | \exists (z,y,x) : h(d,z,x,\theta) = 0 \wedge g(d,z,x,\theta) \leq 0\} \end{aligned} \tag{2.4}$$

Operating stage:

$$\begin{aligned} f'(d,\theta) &= \max_{z,x,y} f(d,z,x,\theta) \\ \text{subject to} \quad & h(d,z,x,\theta) = 0 \\ & g(d,z,x,\theta) \leq 0 \\ & g_q(y,y^\star) \leq 0 \\ & d \in D, z \in Z, x \in X, y \in Y, \theta \in \Theta \end{aligned}$$

In this case, function g_q measures the variance of a quality variable y around a desired $y^\star$ value and is included as a constraint in the operating stage.

Problem (2.4) shows quality constraints as hard constraints as they must be met within the specified intervals. Following Georgiadis and Pistikopoulos (1999), these hard constraints are relaxed by making use of Taguchi loss functions which penalise the objective function for deviations from desired quality targets, giving place to the second approach:

Design stage:

$$\max_{d} E_{R_{n(d)}}\{f'(d,\theta)\} - C_q(y,y^\star) \qquad (2.5)$$
$$d \in D, z \in Z, x \in X, \theta \in \Theta$$

Operating stage:

$$\begin{aligned} & f'(d,\theta) = \max_{z,x} f(d,z,x,\theta) \\ \text{subject to} \quad & h(d,z,x,\theta) = 0 \\ & g(d,z,x,\theta) \leq 0 \\ & z \in Z, x \in X \end{aligned}$$

where C_q is a term penalising the deviation from a desired quality value $y^\star$. The process robustness criterion can be incorporated in the formulation as a statistical constraint on the quality variable y:

$$\begin{aligned} Mean \quad & \mu_y \geq \mu_{min} \\ Variance \quad & \sigma_y^2 \leq \sigma_{max}^2 \end{aligned}$$

The relaxation of the hard constraints allows the expectation operator in (2.5) to be evaluated over the entire Θ domain. Therefore, the evaluation of the expected value can

be performed by integration techniques over this domain, reducing the problem to a single stage problem:

$$\max_{d,z_i,x_i,y_i} \sum_{i=1}^{N_p} w_i f(d, z_i, x_i, \theta_i) - C_q(y_i, y^\star) \tag{2.6}$$

$$\text{subject to} \quad \left.\begin{array}{l} h(d, z_i.x_i, \theta_i) = 0 \\ g(d, z_i.x_i, \theta_i) \leq 0 \\ z_i \in Z, x_i \in X, y_i \in Y, \theta_i \in \Theta \end{array}\right\} i = 1, \ldots, N_p$$
$$d \in D \tag{2.7}$$

2.3.3 Value of information and R&D costs

As seen in the above approaches, the presence of uncertainty in process design changes the optimisation problem from deterministic to stochastic. In the stochastic problem, the optimal solution is based on the calculation of an expected value of the objective function. A different and usually better optimal solution would be found if the uncertain parameter realisations were known a priori and a deterministic problem could be solved. The difference between these two solutions gives an estimate of how important the effect of the parameter uncertainty is on the final design. This difference, known as the value of information, can be used as an indication of where and to what extent resources should be focused to minimise the effect of uncertainty. The few efforts that have been made on the use of the value of information in the context of process design are reviewed next.

Ierapetritou et al. (1996b) extend previous work on planning under uncertainty (Ierapetritou and Pistikopoulos, 1994) to define better the maximum regret and formulate it as the Expected Value of Perfect Information (EVPI). The definition of the EVPI is the expected difference between *wait-and-see* and *here-and-now* decisions:

$$EVPI(\bar{x}_1) = E_\Theta\{F_1(\theta) - F_2(\bar{x}_1, \theta)\} \tag{2.8}$$

where F_1 is the wait-and-see objective function (where one delays decision making until the uncertainty has been resolved) and F_2 is the here-and-now objective function (where first-stage decisions are made now, and second decisions are left until the uncertainty is resolved).

This information is useful in addressing the following questions:

- "what would be the benefit if it were possible to eliminate uncertainty before executing a plan?"
- "what is the loss of opportunity associated with a plan involving uncertainty?"
- "how much the DM (decision maker) is willing to pay to obtain perfect information – if the information regarding uncertainty realization were available at a cost?"
- "what is the price of having to deal with uncertainty?"

The authors propose an integrated metric to measure future plan feasibility and potential economic risk – or Value of Perfect Information, VPI – in the face of uncertainty. The solution algorithm of Ierapetritou and Pistikopoulos (1994) is used. The results shown for the case studies provide a solution with a minimum value – or minimum expected value – of perfect information, giving the decision maker an insight into the level of risk related to the uncertain parameter realisation.

A framework to address directly issues related to uncertainty and R&D effort is proposed by Bernardo et al. (2000). The uncertainty is divided in two categories:

1. uncertain parameters whose variability can be reduced by getting more information (R&D), and
2. random parameters whose variability cannot be controlled, such as prices or demands.

The proposed approach focuses on uncertain parameters defined in the first category to quantify the spending needed on R&D to reduce the uncertainty by altering the objective function (cost minimisation) in the stochastic two-stage problem. A multiperiod version of the proposed change is formulated as:

$$\min_{d,b,\epsilon,z,x,y} \sum_{i=1}^{N_p} w_i f_q(d, z_i, x_i, y_i, y^\star, \theta_i) - C_I(b,\epsilon) \tag{2.9}$$

$$C_I(b,\epsilon) = \sum_{j \in J} \left[b_j C_{If,j} + \alpha_j \left(\frac{1}{\epsilon_j} - \frac{1}{\epsilon_j^N} \right) \right]$$

where f_q can be defined as:

$$f_q(d, z, x, y. y^\star, \theta) = f(d, z, x, \theta) - C_q(y, y^\star) \tag{2.10}$$

and C_I is the R&D spending to reduce the uncertainty in the parameters, which is composed of two terms. The first one represents fixed costs $C_{If,j}$ associated with reducing the uncertainty for each parameter θ_j, while the second one represents variable costs. The value of ϵ_j defines the relative error associated with uncertain parameter θ_j, where the nominal relative error is ϵ_j^N. If no reduction is selected, the binary variable b_j takes the value of 0.

The formulation takes into account profitability, robustness in terms of quality as per Bernardo et al. (1999) and a new R&D expense term, as shown in (2.9). The problem is reduced from a two-stage to a single-stage optimisation using special integration techniques (Bernardo et al., 1999). The framework considers the design problem by balancing profitability, robustness and R&D spending.

Two case studies show the results of the method. One takes the mean value of the uncertain parameter as known and the objective is to define the optimal expense on R&D to reduce the variability around this mean value. The second, and more realistic case study, is where the mean uncertain parameter value is not known, so the objective is to find the optimal spending to reduce the uncertainty level around an unknown mean parameter value.

In this second case, all the uncertain parameters are screened individually to identify those which have a greater economic impact on the objective function. For this subset, the optimal spending to reduce the variability is defined. The main drawback of this approach is that by screening the parameters individually, it does not take into account the interaction between two or more parameters on the main performance measure.

2.3.4 Investment in the presence of technological change

The impact of technological change on investment has been studied mainly in the economics and management fields. The most representative contributions are reviewed here.

Investment in new equipment is not an easy task because of its initial high costs and its impact on future operating performance. The work by Nair (1995) addresses the issue of modelling strategic investment decisions under the presence of technological change. The general assumptions made are:

- technological changes are sequential;
- newer technologies generate at least as much revenue as the previous technology;

- revenues and costs related to each technology are known from the beginning.

Uncertainty arises from the probability that a new technology appears in the following period. If a particular technology did not appear in a specific period, the chances of it becoming available in the next one are higher. The solution approach to this problem uses forecast horizon-based methods showing whether to keep or replace the existing technology. The model only deals with costs related to new technologies and revenues in each period.

Rajagopalan et al. (1998) present a capacity expansion and replacement model that takes in consideration technological breakthroughs. The framework models the costs of acquiring new equipment and the costs of replacement and salvage of old technologies. Two scenarios are shown, one in which the technology evolution is predictable and a second where technological evolution is uncertain. Some key properties are used to reduce the computational effort required and it is solved using a regeneration point-based dynamic programming algorithm.

Within the process design framework, the recent work by Cheng et al. (2003) includes the issue of technology evolution. The way in which the approach takes into account the development of new technologies and other uncertainties is through the use of Markov models.

The problem is formulated over a time period which is divided in time intervals. Decisions are taken at each time interval depending on the current state and expected outcome for the following period. At each period, decisions at two levels, design and production, are being made, as can be seen in figure 2.4 (Cheng et al., 2003).

The formulation integrates multiple decision criteria such as profitability, minimisation of risks and process lifetime under uncertainty incorporating technology evolution. The problem is solved using dynamic programming.

2.4 Summary

It can be seen from the overview of the literature that the problem of process design under technological risk has been tackled in two main separate areas. On one hand, the field of process design under uncertainty addresses issues closely related to the process itself, such as design variables, operating conditions and production plans. On the other hand, the management and economics areas have produced a number of papers on investment under

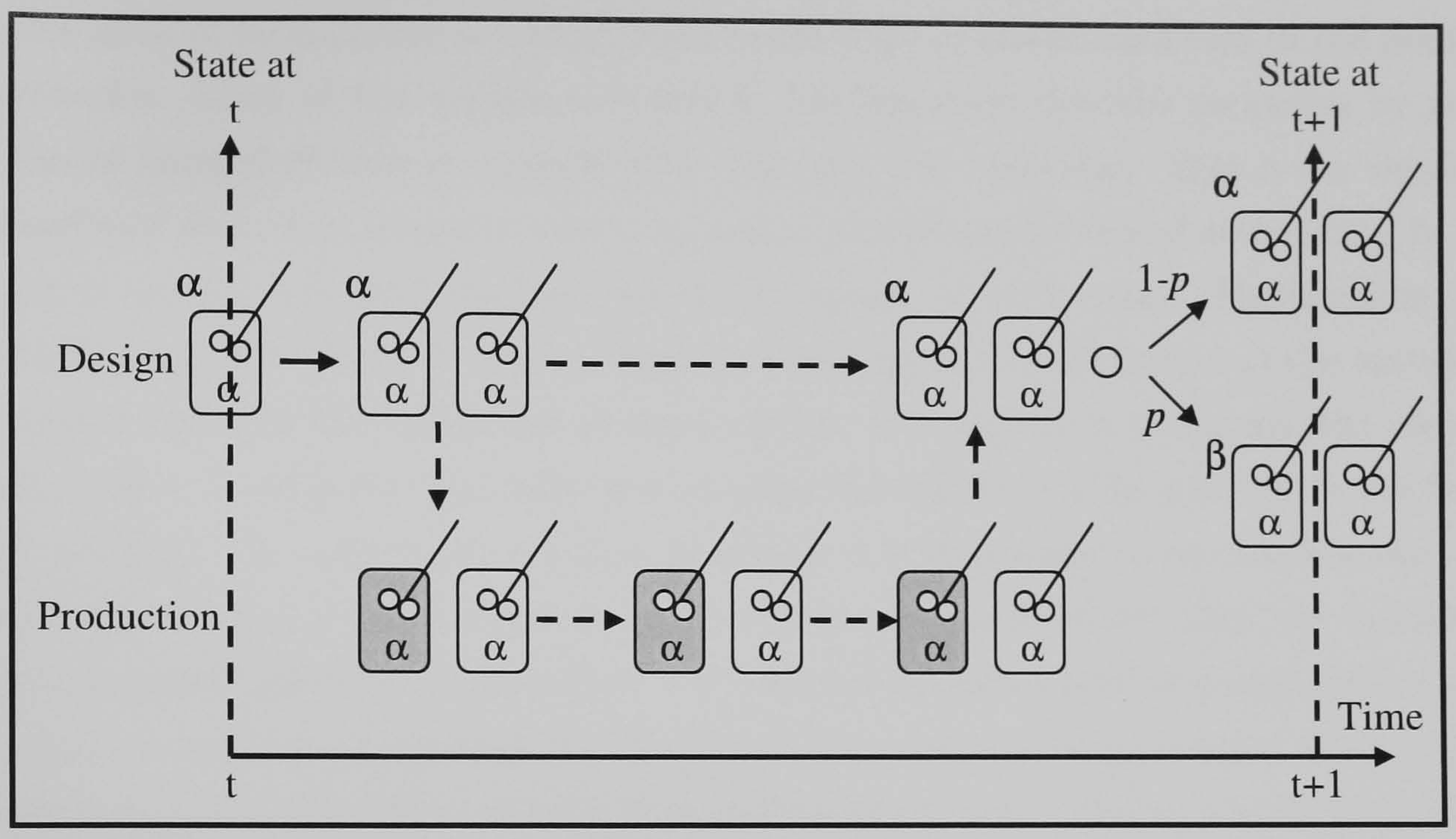


Figure 2.4: Two-level dynamic decision making by Cheng *et al.*, 2003

uncertainty, working on higher-level decisions. This research is more focused on long-term decisions which could affect the overall performance of a process, and takes into account the uncertainty associated with technological evolutions.

Some of the key challenges discussed in the literature include

- the handling of different types of uncertainty,
- the formulation of the design problem to capture the uncertain parameter space with sufficient accuracy,
- the solution of the resulting large scale optimisation problems,
- the quantification and optimisation of performance measures such as feasibility and risk, as well as profitability.

Although significant progress has been made on these fronts, there remains much work to be done to tackle problems of industrial scale and complexity. In this context, one can identify three important issues: the formulation of sufficiently accurate scenario-based design problems, their solution, and the generation of suitable information to support high-level decision-making, such as R&D investment.

The issue of formulation is related both to the type of model used and to the number of scenarios. Most of the models reviewed in the literature describe processes by making use of lumped-parameter models with relatively few equations. This is the result of assumptions and simplifications which introduce an additional level of uncertainty to the results presented and limit the analysis of the impact of uncertainty. Furthermore, the representation of uncertainty is often limited by the use of a small sample of the uncertain parameter values in the calculation of expectations. For nonconvex problems, the use of a small number of scenarios also calls into question the validity of the solution to the feasibility problem. To tackle more realistic problems, it is important to use models that can capture the sources of risk adequately, and to choose scenarios which allow the variability of process performance to be quantified. The choice of scenarios has been addressed in part by using the solution of the feasibility problem to identify critical scenarios. This implies choosing scenarios that have an impact on performance, and choosing a sufficiently large number of scenarios.

The issue of problem solution has been tackled through the development of algorithms which exploit problem structure (Varvarezos et al., 1994; Ierapetritou and Pistikopoulos, 1995) and through the use of the sample average approximation (Wei and Realff, 2004), but problem size remains a bottleneck in the solution of realistic problems.

Finally, to support high-level decision-making, one must provide information beyond expected profit, in order to quantify the cost of uncertainty. This can take the form of downside risk, or probability distribution functions for process performance. It should allow the decision-maker to decide whether any efforts should be made to mitigate risk by reducing uncertainty through investment in R&D, and to identify the sources of uncertainty towards which this expenditure should be directed.

The development of a framework which takes into account both managerial and process decisions based on the risk analysis of a detailed process representation can bring a competitive advantage in industry. Some of the benefits include minimisation of life cycle costs, reduction of risks, R&D management and overall process and product sustainability.

Chapter 3

Overview of the Proposed Methodology

3.1 Introduction

Current market conditions and business competitiveness push companies to develop and deliver new products faster. By innovating and bringing a product or process into production before competitors, one can gain a leading market share and increase company profitability. However, the price to pay for this competitive advantage is usually that of working under conditions where information about the process or product is not complete or fully understood.

In process design, this lack of information leads to technological risk, especially when new process chemistry and/or new process technology is involved. The risk usually arises from uncertainty in the operation, reliability, safety and performance of the new technology. Thus, decision-makers must weigh the potential implications of the risk against the potential benefits that may be realised by the deployment of new technology.

In practice, technological risk is currently addressed in a rather *ad hoc* fashion, primarily by relying on an expert review process which can be costly and time-consuming, and can often result in overdesign. The lack of adequate quantitative methods to evaluate risk leaves decision-makers without proper guidance to prioritise and optimise the deployment of resources on different process design activities. This encourages conservative approaches rather than the adoption of new technologies.

In contrast, the use of model-based methodologies in process design and operation,

as reviewed in Chapter 2, provides a faster and relatively cheap way to address the issue of technological risk. Such approaches can accelerate R&D activities by complementing experimental investigations at the laboratory, pilot plant and industrial plant scales. In principle, instead of searching the, often large, space of possible designs and operations, experimental R&D can first be focused on deriving an accurate model (*e.g.* by identifying the fundamental chemistry associated with a new catalyst). In a second step, the model can then be used for the relatively rapid and inexpensive consideration and screening of many alternatives. Each alternative design can be assessed for its economic performance, but also for the degree of risk it entails. Finally, in a third step, once one or more promising alternatives are identified, their predicted performance may be verified again experimentally (*e.g.* using pilot plants).

Clearly, the effectiveness of this three-step approach depends crucially on the accuracy of the model derived at the first step. Recent years have witnessed significant advances in this context. It is now practically feasible to use detailed models of experimental apparatus to interpret experimental measurements correctly, estimating multiple model parameters from measurements taken from multiple steady-state and/or dynamic experiments. *A posteriori* statistical significance analysis can provide estimates of the errors in the parameter estimates. We also have at our disposal model-based techniques for experiment design which can determine the optimal conditions for executing further experiments aiming at achieving maximum model accuracy (Benabbas et al., 2005; Chen and Asprey, 2003).

Building on these developments, a systematic model-based methodology that can explicitly deal with technological risk and can help achieve a competitive advantage at reduced cost is developed in this thesis. This chapter provides a more precise definition of the problem being tackled and an overview of the steps of the proposed methodology.

3.2 Problem definition

3.2.1 Objectives

In the present work, a methodology and tools to evaluate and mitigate the risk associated with the introduction of new technology are developed. This problem can be approached by answering the following questions:

1. For a given parameter uncertainty, can the uncertainty in key performance indicators

(KPIs) of a process or product be quantified using a model?

2. For the given parameter uncertainty, can a design be found which has optimal expected performance, and for which the risk is below an acceptable threshold?

3. If no design can be found with an acceptable risk level, or if a better expected performance is sought, what are the critical sources of uncertainty on which R&D should focus resources?

To address the first question, a description of the probability distributions of the KPIs over the parameter uncertainty space is needed. For example, when a new catalyst is introduced in an existing reactor, the kinetic parameters associated with this catalyst are unlikely to be known precisely, but a range of values, or a probability distribution, may be known from small-scale laboratory experiments and parameter estimation studies. One would like to quantify how KPIs such as production rate, selectivity, and maximum reactor temperature are likely to be affected by this new technology. The starting point to obtaining this information is a model representing the system or process in sufficient detail to capture the KPI variability arising from the uncertainty. For instance, the presence of hot spots can only be detected if a spatially distributed model of heat transfer is used. The main difficulty here is to provide a realistic evaluation of uncertainty based on a sound process model and an accurate evaluation of the KPI distributions.

The second question concerns the determination of a new design which takes into account the model uncertainty to optimise expected performance and to ensure that the risk is acceptable (low variation in performance, low probability of experiencing poor performance). The handling of this risk in process design includes decisions that may be parametric, like operating conditions in different units, or structural, in the form of process flowsheet modifications. For example, it may be possible to reduce the risk by introducing new equipment in the flowsheet so that any variability in performance can be remedied by downstream units. The reduction of risk must be balanced against any potential reductions in expected performance to accommodate the uncertainty. The main difficulty in tackling this issue is to formulate and solve an optimisation problem which captures all the design decisions and gives an appropriate description of the uncertainty.

In some cases, it may not be possible to find a design which is acceptable in terms of risk. In this case, further R&D is needed to reduce the KPI uncertainty by targeting the model's input uncertainty and to increase confidence in the process or product.

Similarly, uncertainty may be reduced via R&D in order to allow a design with better expected performance to be found. Since the model can have a large number of uncertain parameters, a significant amount of R&D resources may need to be consumed to reduce the uncertainty level for all parameters. Quantitative information on the sources of risk is therefore required to decide on appropriate R&D targets.

The aim of this work is to provide decision-support tools that answer the three questions posed above. In order to define more precisely the problem to be addressed the assumptions made and mathematical representations of the problem are described next.

3.2.2 Modelling assumptions

Structural uncertainty

A central assumption in this work is the availability of a mathematical model free of structural uncertainty. Structural uncertainty arises when the form of the equations used does not allow the prediction of the key performance indicators even when all the model parameters are known precisely. This erroneous representation of the actual process may be due to a lack of knowledge of the underlying phenomena or due to excessive simplifications made in the modelling activity. Thus, the model used should be high-fidelity, providing a sufficiently detailed representation of the process under study to capture the behaviour of the key performance indicators. Fortunately, high-fidelity models now exist for a large number of technologies and are becoming easier to develop.

Types of uncertainty addressed

Based on the uncertainty classification given by Pistikopoulos (1995) and reviewed in section 2.2.2, the proposed methodology aims to deal with model-inherent and process-inherent uncertainties. Rooney and Biegler (2003) classify uncertainty into unknown parameters, that can never be known precisely, and variable parameters, that can be measured or specified at a later date. Their treatment of unknown parameters assumes that it is not possible to adapt to different realisations of these parameters because they cannot be known. This is the case, for instance, of an uncertain feed composition for a batch process, where it may be impossible to take on-line measurements of the inlet or batch compositions, and therefore corrective control action is not feasible. Here, it is assumed that, even when a parameter cannot be measured, it is possible to take control action. In

other words, key performance indicators such as temperature or composition can be measured on-line and manipulated variables are available to take compensatory action when these vary.

Additionally, the uncertainty can be represented by discrete or continuous probability distribution functions (pdf). The uncertainty associated with some parameters can be reduced by different means, such as laboratory or pilot plant testing (*e.g.* kinetic parameters, equilibrium constants). For those parameters which are measured directly, the pdf is known from the measurement equipment. For those parameters which are inferred from other measurements, the pdf can be obtained as part of the solution of the parameter estimation problem in the form of confidence intervals. Finally, parameters such as output fluctuations from process controllers can fall in either of these two classes. While, in some cases, it may be possible to reduce the variability by installing or improving a control system, in other cases, it may not be possible to achieve any reduction. Therefore, if further R&D is to be undertaken to improve the risk profile of a given design, this can result in a reduction in parameter uncertainty only for those parameters within our control.

3.2.3 Mathematical representation

In order to achieve the objectives of this work, process performance will need to be evaluated. For a fixed design $d \in D$ and a given realisation of the uncertain parameters $\theta \in \Theta$, this task can be represented mathematically by the maximisation of a performance objective with respect to the control variables

$$\begin{aligned} \Phi^*(d,\theta) = \quad & \max_{u} && \Phi(d,u,x,\theta) \\ & \text{subject to} && f(d,u,x,\theta) = 0 \\ & && g(d,u,x,\theta) \leq 0 \\ & && y = \mathcal{Y}(d,u,x,\theta) \\ & && y \leq \overline{y} \\ & && u \in U, x \in X, y \in Y \end{aligned} \tag{3.1}$$

where u and x are vectors of control and state variables respectively and y represents the different KPIs. The process model equations, *e.g.* mass and energy balances or equilibrium relationships, are represented by the vector of functions f. The function vector g describes inequalities which define hard constraints on operation, quality, safety and/or

environmental requirements. The vector function $\mathcal{Y}$ defines the key performance indicators. The scalar function Φ measures the process performance to be optimised, which is normally defined as economic profit. Finally, vector $\overline{y}$ defines targets for the key performance indicators. These targets may be considered to be soft constraints. At the solution (x^*, u^*) of problem (3.1), the KPI values are denoted $Y(d, \theta)$.

3.3 Solution Strategy

The approach to risk management proposed here is based around two main tools: global sensitivity/feasibility analysis (GSFA) and scenario-based optimisation. The global sensitivity/feasibility analysis allows the expected values, variances and probability distribution functions to be estimated with good accuracy and thus provides an answer to the first question in Section 3.2.1. Once it is possible to evaluate the uncertainty in the KPIs for given parameter uncertainty and fixed design, the issue of design can be addressed (question 2). As discussed in Chapter 2, this has often been addressed as a scenario-based optimisation problem. However, the limited number of scenarios means that design decisions are made based on a low-accuracy estimate of the expected value and, in the case of robust design strategies, of the variance. Here, we propose an approach based on GSFA and scenario-based optimisation, in which the results of the GSFA help to choose scenarios that describe the impact of the parameter uncertainty well. Once a satisfactory design has been obtained, the variability of the KPIs can be assessed to answer question 3. If the design is found to present too high a risk, further R&D should be undertaken if it is likely to result in a reduction of the risk. This can be determined based on the results of the GSFA, which also indicate which sources of uncertainty should be targeted in R&D.

The risk management strategy, summarised in figure 3.1, consists of four steps:

1. Model construction and validation;

2. Initial design: deterministic optimisation;

3. Stochastic design through iterative solution of:

   (a) global sensitivity/feasibility analysis (GSFA)

   (b) scenario-based optimisation

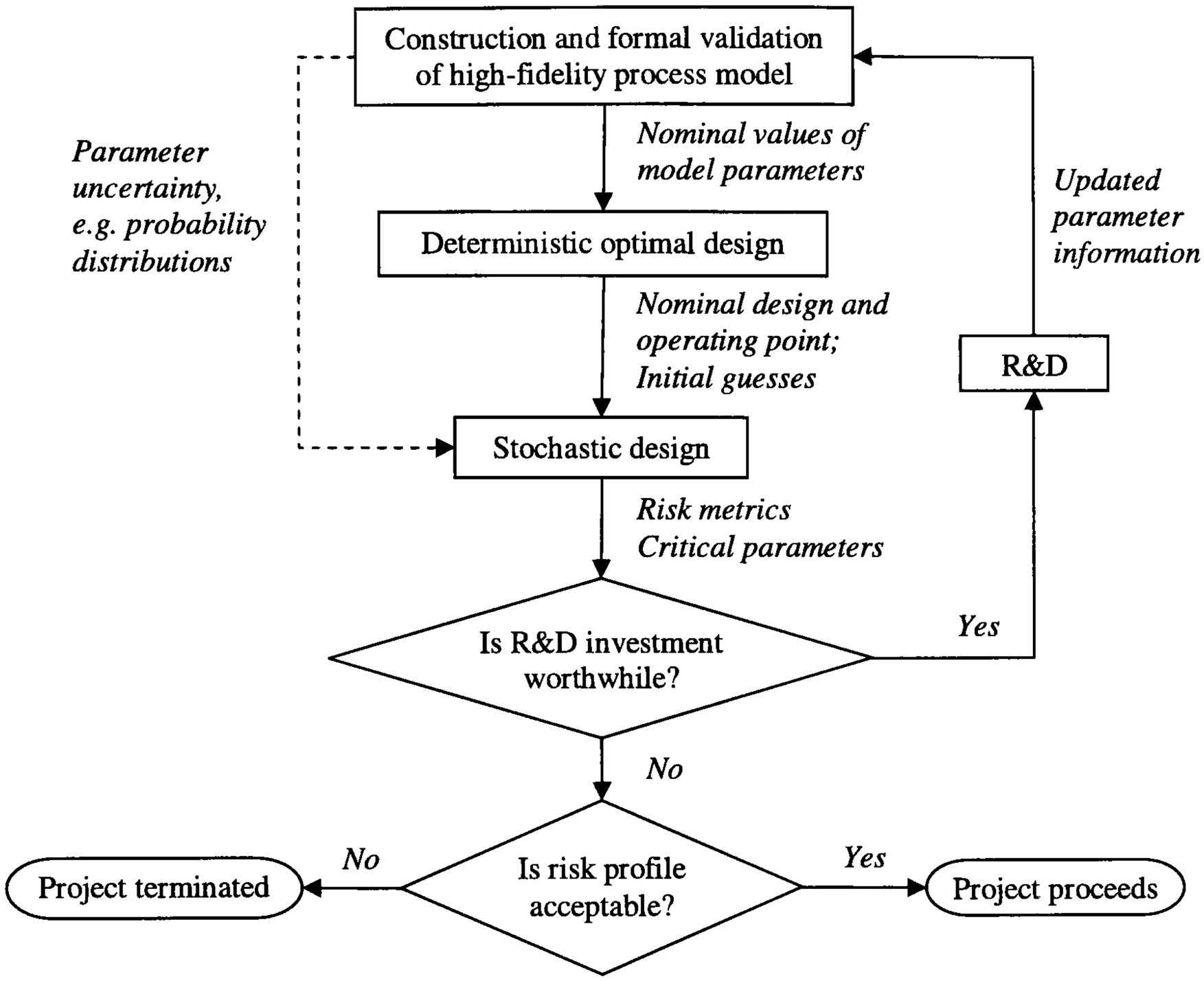


Figure 3.1: Overview of the proposed methodology. Text in italics and dashed lines indicate information passed between two tasks.

4. Is further R&D investment is worthwhile?

   (a) if so, carry out R&D and return to Step 1;

   (b) if not, decide whether project should proceed to next phase based on current risk level.

An overview of each step of the methodology is given in the remainder of this chapter.

3.3.1 Step 1: Model construction and validation

The construction and validation of a mathematical model representing the system under study (Step 1) yields a set of model equations, as well as nominal (most probable) values of

the uncertain parameters, and statistical information on the uncertainty space. The validated model and the description of the parameter uncertainty are then used in subsequent steps.

Special care must be taken when using model-based methodologies as the quality of the results depends directly on the quality of the model used. Most of the methodologies reviewed in Chapter 2 have been applied to simple models, involving a small number of uncertain parameters which can be explored using a small number of scenarios. The processes are commonly represented using a few algebraic equations. This reflects the many simplifications and assumptions made during the model development. While for some simple systems these model approximations can be justified and are acceptable, it is details such as reaction microkinetics, the spatial variation of properties, and the finite rates of mass transfer, rather than generic operational characteristics (*e.g.* reaction in a tube, vapour/liquid phase equilibrium) that often distinguish new technologies from existing ones. Therefore, a model is useful for the quantification of technological risk only if it captures the low-level phenomena that are the sources of risk, *e.g.* the formation of undesirable side-products or the occurrence of hot spots through imperfect mixing. In most cases, such models will typically be distributed models involving a large system of partial differential and algebraic equations (PDAEs). Any methodology based on these models must be able to cope with the increased complexity. The notation of eq.(3.1) can be modified as follows to account for the distributed nature of the model:

$$
\begin{aligned}
& \max_{u} \Phi(d, u, x(z), x_z(z), x_{zz}(z), \theta) && && (3.2)\\
\text{s.t.} \quad & f(d, u, x(z), x_z(z), x_{zz}(z), \theta) = 0 && \forall\, z \in \Omega \\
& h(d, u, x(z), x_z(z), x_{zz}(z), \theta) = 0 && \forall\, z \in \Gamma(\Omega) \\
& g(d, u, x(z), x_z(z), x_{zz}(z), \theta) \leq 0 && \forall\, z \in \Omega \\
& y = \mathcal{Y}(d, u, x(z), x_z(z), x_{zz}(z), \theta) && \forall\, z \in \Omega \\
& y \leq \overline{y} \\
& u \in U, x \in X, y \in Y
\end{aligned}
$$

where $x_z \equiv \nabla_z x$ and $x_{zz} \equiv \nabla_z^2 x$. Note that the equality constraints h are the boundary conditions valid at $\Gamma(\Omega)$, where Ω defines the spatial domain. All other symbols are defined as in formulation (3.1).

The model validation process typically involves estimating parameters using available

experimental data, so that the uncertainty associated with the different parameters can be quantified. Some parameters may also be estimated from first principles, such as computational chemistry calculations. Any further development of the model can be treated as part of an interactive process involving R&D activities. If model accuracy needs to be improved, the model can be used to design experiments to reduce the uncertainty in some of the model parameters. Thus, model-based methodologies such as experiment design and parameter estimation can be used to complement the experimental investigations and accelerate R&D activities.

3.3.2 Step 2: Deterministic optimisation - Nominal design

Once the model has been constructed and validated, a deterministic optimisation is performed to identify the nominal design. The values of the uncertain parameters are fixed to their nominal or most probable value, θ^{μ}. The formulation for this problem is as follows:

$$\max_{d,u} \Phi(d, u, x(z), x_z(z), x_{zz}(z), \theta^{\mu}) \tag{3.3}$$

$$\begin{aligned}
\text{s.t.} \quad & f(d, u, x(z), x_z(z), x_{zz}(z), \theta^{\mu}) = 0 && \forall\, z \in \Omega \\
& h(d, u, x(z), x_z(z), x_{zz}(z), \theta^{\mu}) = 0 && \forall\, z \in \Gamma(\Omega) \\
& g(d, u, x(z), x_z(z), x_{zz}(z), \theta^{\mu}) \leq 0 && \forall\, z \in \Omega \\
& y = \mathcal{Y}(d, u, x(z), x_z(z), x_{zz}(z), \theta^{\mu}) && \forall\, z \in \Omega \\
& y \leq \overline{y} \\
& d \in D, u \in U, x \in X, y \in Y
\end{aligned}$$

The above problem is solved using standard deterministic optimisation techniques. The result gives a nominal design and nominal operating conditions which will be used as initial guesses in the subsequent steps.

3.3.3 Step 3: Stochastic design

In Step 3, the aim is to identify an optimal design with an acceptable risk profile. Several strategies, such as those discussed in Chapter 2, could be used to produce this design. Instead of attempting to solve a very large scale scenario-based optimisation problem that captures the uncertainty accurately, an iterative approach is proposed here, as illustrated in figure 3.2. The key idea is to alternate between a reliable evaluation of the impact of

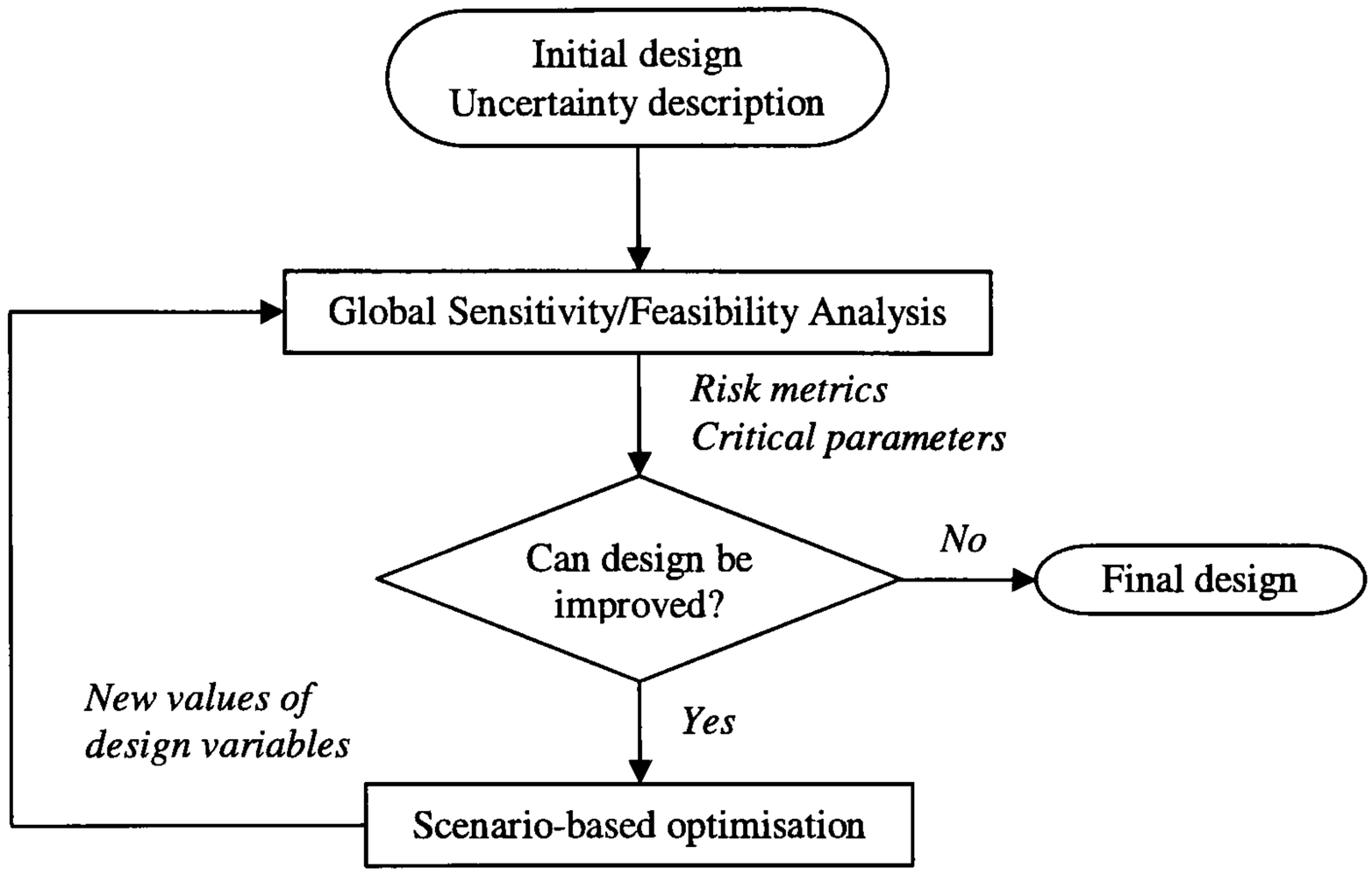


Figure 3.2: Overview of Step 3 of the proposed methodology. Text in italics and dashed lines indicate information passed between two tasks.

uncertainty (GSFA – Step 3a) and the solution of a design problem in which the salient features of the uncertainty space are represented (scenario-based optimisation – Step 3b). In addition to providing risk metrics, the results of the GSFA are also used to identify the key sources of uncertainty in the form of "critical parameters", i.e. parameters that have the greatest effect on the KPIs. This information is used to formulate the scenario-based optimisation problem. The risk metrics for the new design are obtained through another GSFA. The iterations are terminated if one of the following heuristic criteria is met:

- the risk metrics obtained for the current design are acceptable,
- there was no significant change in the risk metrics during the last design iteration,
- there was no significant change in the critical parameters during the last design iteration.

Step 3a: Global sensitivity/feasibility analysis (GSFA)

A global sensitivity/feasibility analysis is carried out to quantify the risk and feasibility associated with the current design (*e.g.* the nominal design) and to identify those parame-

ters that affect the key performance indicators (KPIs) the most. The uncertain parameter space is sampled by generating a series of points. The performance of the process at each point is then evaluated by solving the optimisation problem given in eq. (3.2). Reliable risk metrics, including a feasibility index, and a ranking of critical parameters are obtained by analysing the results of many evaluations (usually several thousands).

The risk is assessed by plotting histograms representing the probability distribution functions for the objective function and KPIs. The means and variances which provide a quantitative measure of the average, upside and downside performance of the process are also calculated. This information can be used to decide whether further R&D is needed and whether to proceed with the project.

The uncertain parameters are ranked in terms of their impact on KPIs through the use of Sobol' sensitivity indices (Sobol', 2001a). This analysis is based on the ANOVA (analysis of variances) decomposition of a nonlinear function. This information is used in the formulation of a scenario-based design problem (Step 3b). It is also used to decide where further R&D should focus by identifying critical parameters.

In some cases the initial design may not be feasible for some of the parameter values sampled. In this case, the analysis of the GSFA results can be useful in identifying the infeasible region(s) and to estimate an infeasibility index. Some of the infeasible points identified can be used in the scenario-based optimisation of Step 3b to help find a more feasible design.

The methodology and implementation for this step are described in detail in chapter 4.

Step 3b: Scenario-based optimisation

The main difficulties in solving scenario-based optimisation problems arise from the maximum number of scenarios that can be used and the lack of numerical robustness which makes it difficult to solve large nonlinear models. The scenario-based optimisation proposed here overcomes some of these limitations.

First, scenarios which provide good coverage of the uncertain parameter space while maintaining problem size at a minimum are chosen by using results from the GSFA step. The scenarios can be generated from the reduced space of the critical uncertain parameters.

Despite this reduction in the size of the uncertain parameter space, a large problem is obtained. It is solved by using a formulation in which the scenarios are considered

over a pseudo-time domain. The approach is similar to formulating an optimal control problem, where the different scenarios are treated as disturbances over pseudo-time. The disturbances remain constant for a period of time before changing to a new set of values and hence a new scenario. This problem is solved through the use of dynamic optimisation. The main advantages are that a larger number of scenarios can be handled than by considering all scenarios simultaneously and that the numerical problems that usually arise during the initialisation of the different scenarios are eliminated. Only one initial guess for the first scenario is needed, instead of the individual guesses required for each scenario in the simultaneous approach. This is particularly important in the context of distributed models.

A more detailed description of this step is given in chapter5.

3.3.4 Step 4: R&D investment decisions

The possibility of reducing the current level of risk, as computed by GSFA, is examined by trading off the cost of uncertainty against the cost of R&D to reduce the uncertainty in the critical parameters. The cost of uncertainty may be quantified in several ways. For example, the difference between the performance of the deterministic design and the expected performance of the stochastic design may be used. Alternatively, the difference between the expected performance of the stochastic design and its worst-case performance may be considered. If it appears worthwhile to undertake R&D, experiments are performed to estimate the critical parameters more precisely. The new information gathered can be used to re-validate the model in Step 1 and repeat the entire procedure.

If no R&D is undertaken, the current design is considered optimal and the level of risk associated with the new technology can be assessed to make business-level decisions. If the risk is acceptable, the design is put forward to the next phase of the project. Otherwise, the new technology is judged too risky and is abandoned.

3.4 Summary

The systematic methodology proposed in this chapter is aimed at managing technological risk using a model-based approach. Technological risk arises from incomplete knowledge during process development. The approach is based around the use of mathematical

models that are sufficiently detailed to address the sources of risk and to quantify its effect on key performance indicators (KPIs).

A global sensitivity/feasibility analysis is proposed to quantify the risk associated with the uncertain parameters. This is done by sampling the uncertain parameter space and solving for each point an optimisation problem to evaluate the optimal process performance. The results also help to identify those parameters affecting the process KPIs the most.

This analysis is used to formulate a scenario-based optimisation which captures the main sources of uncertainty. This allows a stochastic design to be obtained. The risk associated with this design can then be assessed reliably by applying the GSFA. The scenario-based optimisation and GSFA are repeated until no improvement appears possible.

The risk metrics for the final stochastic design are used to determine whether further R&D should be undertaken, and to decide whether the project should proceed to the next phase.

Chapter 4

Global Sensitivity/Feasibility Analysis

4.1 Introduction

The three main outcomes of the proposed global sensitivity/feasibility analysis (GSFA) are a risk evaluation, in the form of histograms for the key performance indicators, an infeasibility evaluation, in the form of a probability of failing to meet process constraints, and the identification of "critical" uncertain parameters. These results are then used to make decisions based on the existing risk and to simplify the subsequent steps in the methodology. Sensitivity analysis thus lies at the heart of the proposed GSFA.

Sensitivity analysis is a discipline which is closely related to mathematical modelling. In simple terms, sensitivity analysis can be defined as the study of changes in model outputs with respect to input (or parameter) variations. The application of this mathematical tool is as wide as the environments in which mathematical modelling is used, *e.g.* engineering, science, economics and finance. It can be used for two general purposes. The first one is to support model development and validation by comparing how well the model represents the system under study. On the other hand, the second objective is to study the effect of input variations on the model's outputs.

The use of sensitivity analysis during model development, as reported by Cacuci (2003) and Saltelli et al. (2000), is aimed at answering questions such as:

1. How well does the model represent the actual system or process under study?

2. How far can we extrapolate the results obtained with the model without reducing the confidence in the results?

3. How can we improve the model based on experimental results?

4. How do we design experiments to extract the most information possible while minimising the number of trials?

5. Is it possible to simplify the model without affecting the quality of the results?

These questions focus on the model itself compared to the actual system it represents. They aim to identify how close predicted behaviour is to actual behaviour, how widely applicable the model is and how to improve it.

On the other hand, sensitivity analysis can be focused on the study of the system that the model represents. This assumes that the model being used has been validated and approximates the behaviour observed in the real system. The focus is then on how disturbances affect the outputs of the model. Some of the uses of sensitivity analysis in this context are:

1. Identification of the parameters that most affect the output.

2. Identification of groups of parameters that have an important combined effect on the system.

3. Ranking of uncertain parameters based on their effect on output variables.

4. Identification of input regions for which the model variation is important.

In the context of the methodology proposed in this thesis, sensitivity analysis is used for the analysis of the system.

Several methods have been proposed to perform a sensitivity analysis. They range from simple one-input one-output techniques to complex multiparameter analysis and can be classified as local or global methods. Some techniques provide qualitative results, while others provide quantitative results. The different methods available are briefly described in section 4.2. An optimisation-based method for global sensitivity/feasibility analysis is then presented in section 4.3. Finally, the implementation of the GSFA is presented.

4.2 Overview of Sensitivity Approaches

Most sensitivity analysis methods use a series of common steps:

1. Define parameters to be studied.

2. For each parameter or combination of parameters,
   (a) Evaluate a point (or series of sampled points for global analysis)
   (b) Analyse the output obtained, relating it to the input from which it came.
   (c) Calculate a measure of sensitivity.

The methods differ in the way in which the inputs are determined and in which the information obtained is processed. The simplest methods are based on the analysis of few sampled points for a one-input one-output relation giving qualitative, rather than quantitative, measures of sensitivity. This can be useful when dealing with simple models, when analysing sensitivity around a given point and when the interactions between the different parameters can be neglected. On the other hand, some methods are based on multiparameter analysis for complex systems where parameter ranges are large and interactions are important.

Different types of sensitivity measures can be obtained depending on the method used to process the information and the type of model on which they are based. The simplest measures are for steady-state systems, where the sensitivity is calculated with respect to input parameters. For dynamic systems on the other hand, sensitivities can be calculated with respect to input factors but also to initial conditions. These sensitivity values can be calculated at the initial time or at any other time and the results depend on the time at which the inputs were perturbed. Finally, sensitivities in distributed dynamic systems have similar characteristics to those in dynamic systems. When adding a spatial domain, the associated boundary conditions are similar to the initial conditions in the time dependent problem. Therefore, sensitivities in distributed models have an increased complexity in that they can vary spatially depending on where the input parameters were perturbed.

The appropriate choice of method depends on the scope of the problem, its complexity, the required information and the resources available to solve the problem. The following sections describe some of the sensitivity analysis methods classified in two general groups: local and global methods.

4.2.1 Local methods

Local sensitivity methods measure the impact of input factors on the model's outputs around a nominal input point. These methods are useful when the parameter ranges are relatively small or when the interest is only around a nominal input value. Local techniques generally use partial derivatives of the model's outputs with respect to input factors to estimate the model's sensitivity and they can be extended to multiparameter analysis. However, the main disadvantage is that the results cannot be extended beyond the nominal value, especially with nonlinear input-output relations or high parameter uncertainty.

The work by Rabitz et al. (1983) provides a good description of local methods which are described briefly in the following sections.

One-at-a-time method

The one-at-a-time analysis is a local method and one of the simplest to perform. It can also be classified as a screening method. Screening methods are a computationally economical alternative to analyse models with a large number of input parameters. They can be used as a first option to identify the group of parameters that have the greatest impact on the model outputs before performing a deeper analysis. They work on the assumption that, in a model with several input parameters, only a few will have a large influence on the output.

In the one-at-a-time method, the model is initially evaluated with the input parameters at their nominal or standard value, generating base values of the outputs. Then, the input values are changed one at a time, while keeping the rest at their nominal value. Normally, for the selected input, two extreme values are chosen around the nominal point. The difference between the evaluation at the nominal value and that at the modified parameter value gives a measure of the parameter's importance. The procedure is repeated for every input and the results are compared to select the group of critical parameters.

Daniel (1973) focuses on one-at-a-time methods for experimental work or design, and describes the above method as "standard" one-at-a-time (o.a.t.). He identifies a further four variants of o.a.t.:

1. In strict o.a.t., one factor is changed from the preceding point.

2. In paired o.a.t., two measurements are taken at the same time leading to one comparison.

3. In free o.a.t., one input factor is changed to any value which may seem useful after analysing previously evaluated points.

4. In nested or curved o.a.t., the input factor which is easiest to vary is changed while keeping the others constant.

One disadvantage of the one-at-a-time method is its inability to account for parameter interactions. However, the different methods described by Daniel (1973) can provide more information than simple one-at-a-time techniques. By following one-at-a-time sampling or trial paths, these methods allow individual parameter effects to be identified by eliminating the two-factor interactions.

Another disadvantage of one-at-a-time methods is that the results generally cannot be extrapolated easily, especially when dealing with non-linear models. Book and Chernik (1991) are able to extrapolate sensitivity results around the nominal value by estimating the outputs' three-sigma deviations using one-at-a-time evaluations.

Cotter's method

Cotter's method (Cotter, 1979) is another type of sensitivity analysis which can also be classified as a screening method. This approach requires $2n+2$ tests for n factors or input parameters. Two levels are used for each factor: high and low. The first test involves all factors at their low level. n trials or evaluations of the output are then performed with all inputs at their low level except one which is at its high value. In the following n tests, all input values are at their high level except for one which is at its low value. Finally, in the last test, all input values are at their high level. This sequence of scenarios is called systematic fractional replicate design.

The combined effects of different input parameters can be estimated based on the results of the systematic fractional replicate design. The combined effect is calculated in two blocks or groups: one estimates the combined effect of odd interaction orders (3rd, 5th and so on) while the other calculates the combined effect of even (2nd, 4th and so on) interaction orders. However, this method does not provide a direct calculation of a parameter's main, or individual, effect. It can only be calculated under special circumstances

where third and higher-order interactions are zero. The main disadvantage of this method is its lack of precision, although it benefits from not requiring any prior assumption on the parameter interactions.

Sensitivity in time-dependent problems

Consider the time-dependent problem:

$$\frac{dy}{dt} = f(y,\theta) \qquad y(0) = y^0 \tag{4.1}$$

where y is the vector of process performance variables, θ the vector of n input (uncertain) parameters, y^0 the value of y at the initial time and t the time domain. The first-order local sensitivity indices for the output variables with respect to input parameter θ_i can be calculated by finite differences.

$$\frac{\partial y(t)}{\partial \theta_i} = \frac{y(t,\theta_i + \Delta\theta_i) - y(t,\theta_i)}{\Delta\theta_i} \tag{4.2}$$

This is similar to a one-at-a-time strategy where input parameter θ_i is changed while keeping the remaining parameters constant. $\Delta\theta_i$ is the perturbation applied to θ_i, which Saltelli et al. (2000) recognise should be between 1 and 5% over the nominal value of θ_i. Greater changes can alter the result for highly nonlinear models while smaller ones can lead to numerical difficulties due to very small differences between original and perturbed function values.

Equation (4.2) must be solved $n+1$ times to obtain sensitivity indices for n parameters. When central differences are being used, then $2n$ evaluations are needed.

Alternatively, differential sensitivity coefficients are calculated by differentiating equation (4.1) with respect to input parameter θ_i:

$$\frac{d}{dt}\frac{\partial y(t)}{\partial \theta_i} = J\frac{\partial y(t)}{\partial \theta_i} + \frac{\partial f}{\partial \theta_i} \tag{4.3}$$

where J is matrix of the derivatives of f with respect to the output variables for which the sensitivities are calculated:

$$J = \frac{\partial f}{\partial y} \tag{4.4}$$

The sensitivities can be evaluated by integration of the system of original equations augmented with the sensitivity equations (Caracotsios and Stewart, 1985).

4.2.2 Overview of global methods

In global sensitivity methods, the effect of input parameter variation on output variables is measured. Input parameter definitions such as ranges and probability distribution functions are used. These methods have a higher computational cost than local methods. However, global methods are very useful to analyse the effect of parameter variation over wide ranges, as they give a better assessment of the system under study, particularly where nonlinearities are present. Another advantage of these methods, as mentioned by Saltelli et al. (2000), is their ability to analyse multidimensional problems. Their use allows the study of the effect of one input variable while the others are modified as well, in contrast to local analysis where all factors but one are kept constant. This is useful to calculate the value of total and individual sensitivity indices.

Global sensitivity analysis methods are based on a random or quasi-random sampling approach to generate input combinations for evaluation. The general steps in the global approach to sensitivity analysis are:

1. Identification of parameter ranges and/or probability distribution functions.

2. Parameter sampling.

3. Evaluation of sampled points.

4. Analysis of results through calculation of sensitivity indices.

Information on parameter ranges is available from Step 1 of the proposed methodology (model development and validation).

The most widely used sampling technique is the Monte Carlo approach in which a random number generator is used to sample the uncertain parameter space. However, different sampling techniques can be used to improve the efficiency of analysis, such as stratified and low-discrepancy sequences.

Global sensitivity analysis techniques are more suitable than local techniques for the analysis of highly nonlinear multi-parameter process models. A global sensitivity analysis is therefore used in this work and the relevant components (parameter sampling, evaluation of sampled points and sensitivity indices) are discussed in the following sections.

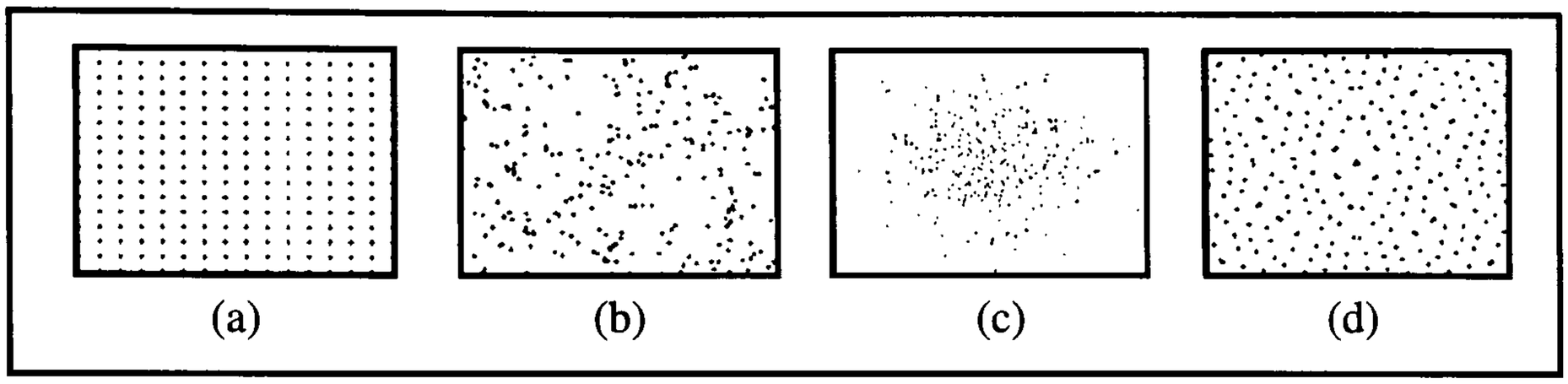


Figure 4.1: Two-dimensional sampling of 256 points using different methods (a) Uniform sampling, (b) Random sampling based on uniform distribution, (c) Random sampling based on normal distribution, (d) Sobol' sequence

4.2.3 Sampling methods

For any sampling method, the use of a large number of sample points increases the confidence in the results obtained. However, one is limited by computational resources. Therefore, efficient sampling methods are required to reduce the number of evaluations required during sensitivity analysis, especially when using complex models. Many methods are available, with widely varying results. To illustrate this diversity, Figure 4.1 shows four different sampling methods applied on a two-dimensional space with 256 points each.

Uniform or grid sampling.

This is one of the simplest sampling methods. For an n-dimensional problem, each parameter range is divided into a number of equal intervals to form an n-dimensional grid. Each grid point is used as a sample point. One disadvantage of the method is that many sample values in any one of the n dimensions overlap. For example, a uniform grid of 256 points which was generated by dividing each parameter range into 15 intervals is shown in figure 4.1(a). The overlapping can be seen when all the points are projected onto any of the axes: this results in only 16 points being sampled along each dimension.

Random sampling methods.

These techniques are applicable only when the parameters of interest follow a known probability distribution function. This pdf can then be used as the basis for sampling.

1. **Uniformly distributed sampling.** In this sampling technique, a series of points is generated randomly in the n-dimensional parameter space based on the uniform distribution. A disadvantage of this method is that, for small samples, some areas may have a higher concentration of points, while other areas could be left unexplored. This is seen in figure 4.1(b) for a two-dimensional sample of 256 points.

2. **Normal sampling.** This technique is based on the random sampling of a normal probability distribution, as shown in figure 4.1(c). High probability regions of the parameter space are sampled extensively, while other parameter regions are unexplored. This can result in low-probability but high-risk parameter realisations being ignored. When using a normal sampling method, a larger number of samples is needed to evaluate regions with low probability. This will be discussed further in the case study in Chapter 6.

3. **Stratified sampling.** This method relies on dividing the parameter space into different subspaces which are then randomly sampled using a uniform distribution. In this sampling, equal weight can be given to each subspace or specific weights assigned to each subspace to follow a specified probability distribution function. One of the advantages of the stratified sampling is that it improves the coverage of the parameter space when compared to conventional random sampling.

Low-discrepancy sampling methods.

These sampling techniques are quasi-random methods which ensure that the sample is *almost* uniformly distributed. Examples of low discrepancy sequences are the Halton, Sobol', Faure and Niederreiter sequences. A brief description of these methods can be found in Sobol' (1998).

1. **Sobol' method.** The Sobol' sampling technique (Sobol', 1976) is an efficient method to cover the uncertain parameter space (Antonov and Saleev, 1979; Sobol', 1998). In this method, each new sampled point is chosen by maximising its distance from all other previous points in the sequence. A property of the method is that the projection of any point onto any axis yields a unique value along this direction, so that no two points overlap. Therefore, if 256 points were generated in a two-dimensional case, there would be 256 different points on each axis. The

only disadvantage of the method is that it possesses the property of uniformity only when the number of sample points is a power of 2. Thus, increasing the samples size involves a doubling of the number of samples. A two-dimensional sample of 256 points is shown in figure 4.1(d).

2. **Sobol'-normal method.** An alternative to Sobol' sampling is the use of a number generator based on a given probability distribution. For instance, if the parameters are defined by a normal probability distribution function, a normal pdf sampling technique can be used. Because the normal pdf generator is based on Sobol' sampling, most of the properties of this technique are kept, while the points generated are normally distributed (Kucherenko et al., 2006).

Selection of sampling technique.

The selection of a sampling technique for this work depends on the statistical information available for the uncertain parameters and the scope of the analysis. The use of sampling techniques which make use of the known distributions (*e.g.* normal) yield results which already incorporate the underlying probabilities. However, this may prove computationally expensive if good space coverage is needed, for instance to assess feasibility. In such cases, a uniformly distributed (quasi-random or non-random) sampling may be a better option. Furthermore, these uniformly distributed sampling techniques can be used to represent non-uniformly distributed uncertain parameters if a weight factor is added to each point to reflect its probability.

The case study presented in chapter 6 illustrates the differences between the use of Sobol' sampling (quasi-random) and a sample based on the statistical definition of the uncertain parameters (*e.g.* normal distribution).

4.2.4 Point evaluation

Once points in the uncertainty space have been sampled, the performance of the process at those points must be calculated. In most sensitivity analysis approaches, a simulation-based method is used, in which the sampled point is evaluated while control variables remain unchanged. While this means each evaluation is relatively inexpensive as it requires the solution of a square system of nonlinear equations, it leads to a conservative assessment of the effect of the type of uncertainty we are dealing with in this work. Indeed, the use

of a simulation-based approach for sensitivity analysis in process design does not account for the system's ability to cope with uncertain conditions via control action .

The methodology proposed in this work relies on a different approach, which is referred to as "optimisation-based". This method exploits the system's flexibility when some variables in the model can be used to control and optimise the system's performance. Both the simulation-based and optimisation-based approaches are explained below in more detail.

Simulation-based approach.

In this approach, a simulation is used to evaluate every sampled point. For this purpose, design and control variables are fixed at their nominal values obtained in the deterministic optimisation step of the methodology (Step 2, chapter 3). The effect of the sampled parameters can be evaluated by analysing the change in process performance measures (KPIs) under fixed design and control conditions. Given process model (3.2), the simulation-based approach is represented by the following set of partial differential algebraic equations (PDAE):

$$\begin{aligned}
&\mathcal{P}(d^\star, u^\star, \theta^\star) = \Phi(d^\star, u^\star, y, \theta^\star) && (4.5)\\
&f(d^\star, u^\star, x(z), x_z(z), x_{zz}(z), \theta^\star) = 0 && \forall\, z \in \Omega\\
&h(d^\star, u^\star, x(z), x_z(z), x_{zz}(z), \theta^\star) = 0 && \forall\, z \in \Gamma(\Omega)\\
&y = \mathcal{Y}(d^\star, u^\star, x(z), x_z(z), x_{zz}(z), \theta^\star) && \forall\, z \in \Omega\\
&x \in X
\end{aligned}$$

The main key performance indicator (KPI), Φ, is evaluated for every sampled uncertain parameter point, $\theta^\star$, for fixed design and control variables, $d^\star$ and $u^\star$. The process model equations, *e.g.* mass and energy balances and equilibrium relationships, are represented by the vector of functions f, boundary conditions by h, while y represents additional process performance measures, x is the vector of state variables and z is the vector of spatial domains.

This evaluation is repeated at every sample point. One disadvantage of the simulation-based approach is its inability to easily take into account the operating constraints (g and bounds on y in process model (3.2)) to assess process performance. In a typical process design problem, there are usually constraints to ensure that quality, safety and operation limits are met. For example, consider a reactor where there is a maximum

allowed temperature described by an inequality constraint $g \leq 0$. The KPIs computed at every sample point, such as conversion or profitability, do not take into account the maximum temperature constraint, since it does not appear in the evaluated model.

Penalty term.

One way to remedy this problem and to take process constraints into account in the simulation-based approach is to add a penalty term to the performance objective:

$$\begin{aligned} & \mathcal{P}(d^\star, u^\star, \theta^\star) = \Phi(d^\star, u^\star, y, \theta^\star) - \Pi && (4.6) \\ & f(d^\star, u^\star, x(z), x_z(z), x_{zz}(z), \theta^\star) = 0 && \forall\, z \in \Omega \\ & h(d^\star, u^\star, x(z), x_z(z), x_{zz}(z), \theta^\star) = 0 && \forall\, z \in \Gamma(\Omega) \\ & y = \mathcal{Y}(d^\star, u^\star, x(z), x_z(z), x_{zz}(z), \theta^\star) && \forall\, z \in \Omega \\ & x \in X \end{aligned}$$

where

$$\Pi = s_1 \int \max(0, g(d^\star, u^\star, x(z), x_z(z), x_{zz}(z), \theta^\star))dz + s_2 \max(0, y^L - y, y - y^U) \quad (4.7)$$

where s_1 and s_2 are positive scaling factors chosen to match the order of magnitude of the values obtained for the main performance measure considered, Φ.

The penalty term Π in formulation (4.6) accounts for any model constraint violations, g, and any other process performance measure, y, falling out of the specified range $[y^L, y^U]$.

Although formulation (4.6) takes into account the effect of the uncertain parameters on model constraints, there is a further limitation to the simulation-based approach brought about by fixing the value of the control variables. The system's ability to cope with changes is eliminated by fixing these variables. An example of this is fixing the coolant flowrate in a reactor when analysing the effect of uncertain parameters. While it may be found that for a specific sample point, the maximum temperature constraint is violated, this could in fact be brought within allowable limits by simply changing the coolant flowrate. This clearly leads to an underestimation of system performance.

Optimisation-based approach.

The optimisation-based approach is an alternative method to overcome the limitation of fixing control variables in the sensitivity analysis. This method is based on treating the

LONDON UNIV.

performance evaluation at each sample point as an optimisation problem. The use of this approach allows to change the value of control variables to optimise process performance. while meeting process constraints. Therefore, different objective values may be obtained in the two approaches for the same uncertain parameter definition, and hence different sensitivities.

While a given uncertain parameter could be found to have a significant effect on performance in the simulation-based approach, its effect could be found to be insignificant in the optimisation-based approach if the process is flexible enough to counteract the impact of the parameter change by using the control variables.

The formulation of the optimisation problem for the evaluation of design $d^\star$ at a sample point $\theta^\star$ is as follows:

$$
\begin{aligned}
& \Phi(d^\star, \theta^\star) = \max_{u \in U} \Phi(d^\star, u, y, \theta^\star) && && (4.8)\\
\text{s.t.} \quad & f(d^\star, u, x(z), x_z(z), x_{zz}(z), \theta^\star) = 0 && \forall\, z \in \Omega \\
& h(d^\star, u, x(z), x_z(z), x_{zz}(z), \theta^\star) = 0 && \forall\, z \in \Gamma(\Omega) \\
& g(d^\star, u, x(z), x_z(z), x_{zz}(z), \theta^\star) \leq 0 && \forall\, z \in \Omega \\
& y = \mathcal{Y}(d^\star, u, x(z), x_z(z), x_{zz}(z), \theta^\star) && \forall\, z \in \Omega \\
& x \in X
\end{aligned}
$$

The methodology proposed in this work uses the optimisation-based approach for the sensitivity analysis step.

4.2.5 Analysis of results – Sensitivity indices

Once every sampled point has been evaluated, the results are processed to generate a sensitivity measure. The various global sensitivity methods differ in the way output information is processed. In the following sections, selected sensitivity measures are described in more detail. The Morris method is treated first. It is generally classified as a screening method due to its simplicity. Subsequent sections describe methods which can be classified in two categories: regression-based and variance-based global sensitivity measures. The methodology presented here makes use of the Sobol' method, which belongs to the variance-based class.

The sensitivity indices obtained in the different methods can be classified in first-order, higher-order and total sensitivity indices. First-order indices provide a measure of the

effect of a given parameter on the chosen output variable. This first-order index does not take into account effects of the interaction between the given parameter and the remaining parameters. Higher-order sensitivity indices measure the effect caused by the interaction of different parameters. For example, a second-order index measures the combined effect of two parameters, while a third-order index measures the effect of 3 parameters on the output variables. Finally, total sensitivity indices provide a measure of the combined effect of individual and higher-order interactions in which a given parameter appears.

The Morris method

The Morris method (Morris, 1991) uses a vector of n elements where n is the number of input factors or parameters in the model. In every element i, the value of at least one parameter is increased by Δ when compared to its value in the previous element $i-1$. The total effect, $S_i^{Tot}(\theta)$, of parameter θ_i, called the elementary effect, is defined as:

$$S_i^{Tot}(\theta) = \frac{[\Phi(\theta_1, \ldots, \theta_{i-1}, \theta_i + \Delta, \theta_{i+1}, \ldots, \theta_n) - \Phi(\theta)]}{\Delta} \tag{4.9}$$

In this way, the elementary effect estimates the individual contribution of factor θ_i plus higher-order contributions.

A number of independent vectors are evaluated for different values of θ and the average and standard deviation of the elementary effects are calculated. A high average value indicates a parameter with an important effect, while the standard deviation gives a measure of the parameter's interaction with the remaining parameters.

The method has a low computational cost, but it does not give a measure of specific parameter interactions. However, an improved Morris method by Campolongo and Braddock (1999) can give a measure of higher-order interactions. The new method uses the original Morris approach and adds calculations for second-order elementary effects. As with first-order elementary effects, the second-order calculation estimates the total effect, which is the sum of effects where the interacting parameters appear:

$$S_{ij}^{Tot}(\theta) = \frac{[f(\theta_1, \ldots, \theta_i + \Delta, \ldots, \theta_j + \Delta, \ldots, \theta_k) - f(\theta)]}{\Delta} \qquad (1 \leq i \leq j \leq k) \tag{4.10}$$

As in the original Morris method, a number of samples are used. The mean value of second-order elementary effects gives a measure of total second-order interactions while the standard deviation gives an estimate of third and higher-order interactions. Thus, when a

model has first-order interactions only, the method gives approximate values for the first-order effects and a standard deviation of zero, indicating no higher-order interactions. If the model has second-order interactions, the method of Campolongo and Braddock (1999) gives good estimates for second-order interactions, but the accuracy for first-order effects is reduced.

The disadvantage of the method is that it only provides accurate values for the highest-order interactions for which the standard deviation is zero. The accuracy is therefore reduced for lower parameter interactions. Furthermore, the work by Cropp and Braddock (2002) recognises the above disadvantage and detects a programming error in the previous work by Campolongo and Braddock (1999) which results in a poorer assessment of the method's efficiency.

Regression-based analysis

In regression-based methods, input-output information is used to map a relationship and analyse the system's sensitivity. The application of the technique generates a model, when working with data from experiments. When the results are obtained from another mathematical model, it generates a simplified model. In any case, the results must be used carefully as this regressed model does not necessarily represent the real or original system accurately.

Linear regression. One of the simplest methods is based on a linear regression for the input-output data:

$$y_k = b_0 + \sum_{j=1}^{n} b_j \theta_{kj} + \epsilon_k \tag{4.11}$$

where y_k is a function of n input parameters for sampled point k

$$y_k = f(\theta_{k1}, \ldots, \theta_{kn}), \tag{4.12}$$

b_j are the regression coefficients which can be calculated using a least-squares technique and ϵ_k is the residual value for point k.

The sensitivity coefficient obtained from this linear model is a standardised regression coefficient (SRC) which is defined as:

$$SRC = \frac{b_j \hat{s}_j}{\hat{s}} \tag{4.13}$$

where

$$\hat{s}_j = \left(\sum_{k=1}^{m} \frac{(\theta_{kj} - \bar{\theta}_j)^2}{m-1} \right)^{1/2} \tag{4.14}$$

$$\hat{s} = \left(\sum_{k=1}^{m} \frac{(y_k - \bar{y})^2}{m-1} \right)^{1/2} \tag{4.15}$$

$$\bar{\theta}_j = \sum_{k=1}^{m} \frac{\theta_{kj}}{m}, \qquad \bar{y} = \sum_{k=1}^{m} \frac{y_k}{m} \tag{4.16}$$

Another important measure used in linear regression analysis is the correlation coefficient R^2:

$$R^2 = \frac{\sum_{k=1}^{m} (\hat{y}_k - \bar{y})^2}{\sum_{k=1}^{m} (y_k - \bar{y})^2} \tag{4.17}$$

where $\hat{y}_k$ is the value obtained from the regressed model. The value of the coefficient R^2 is a measure of the proportion of variability between the y_k and $\hat{y}_k$. R^2 is bounded between 0 and 1 and as R^2 approaches 1, the regressed model shows a better performance.

The linearity assumption is one of the disadvantages of this simple method. For nonlinear models, the coefficient R^2 shows lower values, decreasing the confidence in the sensitivity results. An alternative method is Rank Transformation (Saltelli and Sobol', 1995), which can deal with nonlinearity, although the input-output relation has to be monotonic. As mentioned in Saltelli and Sobol' (1995), one of the disadvantages is that this approach increases the relative sensitivity of first-order terms, at the expense of higher-order terms.

Stepwise regression. This method (Helton, 1993) is useful when there are several input parameters and is based on building a series of models. In the first step, a model is built using only the most influential parameter. In the second step, a new parameter is added which is the most influential of the remaining parameters. Parameters are added sequentially when there is no change on the output effect with the remaining parameters.

Variance-based analysis

An alternative to regression methods are the measures-of-importance or variance-based methods. These methods use the variance of the model output obtained when fixing one or more parameters. This quantity is used to calculate the following correlation ratio:

$$\frac{Var_{X_j}[E(Y|X_j = x_j)]}{Var(Y)} \tag{4.18}$$

where the numerator is the variance over all possible values of X_j of the expected value of Y conditional on a fixed value of X_j.

The Sobol' method and Fourier amplitude sensitivity test (FAST) are the most representative of the variance-based methods. Both methods have similar definitions for first-order, higher-order and total sensitivity indices, but these are calculated in different ways. These sensitivities are estimated using no previous model assumption and are valid for monotonic and nonmonotonic models. The two methods are reviewed here.

Fourier amplitude sensitivity test (FAST) method The idea behind the FAST method (Cukier et al., 1973) is to transform the n-dimensional integral of the expected value of Φ into a one-dimensional one. This is done using the following G_i transformation functions to map the n-dimensional vector θ onto a single variable s:

$$\theta_i = G_i \sin(\omega_i s), \qquad i = 1, \ldots, n \tag{4.19}$$

where $s \in (-\pi, \pi)$ and ω_i is a set of integer frequencies. The one-dimensional integral for the expectancy is:

$$E(\Phi) = \frac{1}{2\pi} \int_{-\pi}^{\pi} f(s) ds \tag{4.20}$$

where

$$f(s) = f(G_1 \sin(\omega_1 s), \ldots, G_n \sin(\omega_n s)) \tag{4.21}$$

The variance of Φ is defined as:

$$\begin{aligned} Var(\Phi) &= \frac{1}{2\pi} \int_{-\pi}^{\pi} f^2(s) ds - [E(\Phi)]^2 \\ &\approx 2 \sum_{j=1}^{\infty} (A_j^2 + B_j^2) \end{aligned} \tag{4.22}$$

where

$$A_j = \frac{1}{2\pi}\int_{-\pi}^{\pi} f(s)\cos(js)ds \tag{4.23}$$

$$B_j = \frac{1}{2\pi}\int_{-\pi}^{\pi} f(s)\sin(js)ds \tag{4.24}$$

Finally, the FAST method sensitivity indices are calculated by:

$$S_i^{FAST} = \frac{Var(\Phi|\theta_i)}{Var(\Phi)} \tag{4.25}$$

The original FAST method only allows for the calculation of first and higher-order sensitivity indices. However, Saltelli et al. (1999) extended this method to include total sensitivity indices.

Sobol' sensitivity indices

The Sobol' method (Sobol', 2001a) is a variance-based approach for sensitivity analysis. In this method, similar indices to those from the FAST method are calculated: first-order, higher-order and total sensitivity indices.

ANOVA representation of a function. The Sobol' sensitivity indices are based on the analysis of variances (ANOVA) representation of the function $\Phi(\theta)$, where θ is an n-dimensional vector as shown in equation (4.26):

$$\Phi(\theta_1,\ldots,\theta_n) = \Phi_0 + \sum_{i=1}^{n}\Phi_i(\theta_i) + \sum_{i=1}^{n-1}\sum_{j=i+1}^{n}\Phi_{ij}(\theta_i,\theta_j) + \ldots + \Phi_{12\ldots n}(\theta_1,\theta_2,\ldots,\theta_n) \tag{4.26}$$

This is denoted more compactly by:

$$\Phi(\theta_1,\ldots,\theta_n) = \Phi_0 + \sum_{s=1}^{n}\sum_{i_1<\ldots<i_s}^{n}\Phi_{i_1\ldots i_s}(\theta_{i_1},\ldots,\theta_{i_s}). \tag{4.27}$$

For a function $\Phi(\theta)$, where θ is a 3-dimensional vector $(\theta_1,\theta_2,\theta_3)$ $(n = 3)$, the above representation becomes:

$$\Phi(\theta) = \Phi_0+\Phi_1(\theta_1)+\Phi_2(\theta_2)+\Phi_3(\theta_3)+\Phi_{12}(\theta_1,\theta_2)+\Phi_{13}(\theta_1,\theta_3)+\Phi_{23}(\theta_2,\theta_3)+\Phi_{123}(\theta_1,\theta_2,\theta_3) \tag{4.28}$$

where, for $s = 1$,

$$\sum_{i_1<\ldots<i_1}^{3} \Phi_{i_1\ldots i_1}(\theta_{i_1,\ldots,i_1}) = \Phi_1(\theta_1) + \Phi_2(\theta_2) + \Phi_3(\theta_3). \tag{4.29}$$

For $s = 2$,

$$\sum_{i_1<\ldots<i_2}^{3} \Phi_{i_1\ldots i_2}(\theta_{i_1},\ldots,\theta_{i_2}) = \Phi_{12}(\theta_1,\theta_2) + \Phi_{13}(\theta_1,\theta_3) + \Phi_{23}(\theta_2,\theta_3). \tag{4.30}$$

Finally, for $s = 3$,

$$\sum_{i_1<\ldots<i_3}^{3} \Phi_{i_1\ldots i_3}(\theta_{i_1},\ldots,\theta_{i_3}) = \Phi_{123}(\theta_1,\theta_2,\theta_3) \tag{4.31}$$

Integrals defining the Sobol' sensitivity indices. Assuming θ ranges between 0 and 1, Sobol' (2001a) showed that if:

$$\int_0^1 \Phi_{i_1\ldots i_s}(\theta_{i_1},\ldots,\theta_{i_s}) d\theta_{i_k} = 0, \qquad k = 1 \leq \ldots \leq s \tag{4.32}$$

then all the terms in equation (4.27) are orthogonal and:

$$\int_0^1 \Phi(\theta) \prod_{k=1}^{n} d\theta_k = \Phi_0 \tag{4.33}$$

$$\int_0^1 \Phi(\theta) \prod_{k\neq i} d\theta_k = \Phi_0 + \Phi_i(\theta_i) \tag{4.34}$$

$$\int_0^1 \Phi(\theta) \prod_{k\neq i,j} d\theta_k = \Phi_0 + \Phi_i(\theta_i) + \Phi_j(\theta_j) + \Phi_{ij}(\theta_i,\theta_j) \tag{4.35}$$

Squaring and integrating equation (4.27) results in:

$$\int_0^1 \Phi^2(\theta) d\theta - \Phi_0^2 = \sum_{s=1}^{n} \sum_{i_1<\ldots<i_s}^{n} \int_0^1 \Phi^2_{i_1\ldots i_s}(\theta_{i_1},\ldots,\theta_{i_s}) d\theta_{i_1} \ldots d\theta_{i_s}. \tag{4.36}$$

The total variance, D, is defined as:

$$D = \int_0^1 \Phi^2(\theta) d\theta - \Phi_0^2 \tag{4.37}$$

and the term variances, $D_{i_1 \ldots i_s}$, are:

$$D_{i_1 \ldots i_s} = \int_0^1 \Phi^2_{i_1 \ldots i_s}(\theta_{i_1}, \ldots, \theta_{i_s}) d\theta_{i_1} \ldots d\theta_{i_s}, \qquad \forall\, 1 \leq i_1 < \ldots < i_s \leq n \tag{4.38}$$

It can be shown that

$$D = \sum_{s=1}^{n} \sum_{i_1 < \ldots < i_s} D_{i_1 \ldots i_s} \tag{4.39}$$

Finally, the Sobol' sensitivity indices are defined by the following ratios:

$$S_{i_1 \ldots i_s} = \frac{D_{i_1 \ldots i_s}}{D} \tag{4.40}$$

From equation (4.39) it can be seen that the values of $S_{i_1 \ldots i_s}$ are bounded between 0 and 1. The significance of the sensitivity indices is that $S_i = 0$ when $\Phi(\theta)$ does not depend on θ_i. On the other hand, $S_i = 1$ when $\Phi(\theta)$ depends only on θ_i. The value of index S_i represents the sensitivity of the performance indicator Φ to parameter θ_i, when neglecting interactions of parameter θ_i with the remaining parameters.

From a computational point of view, when a model has several uncertain parameters, it may be easier to calculate indices for groups of parameters to do a preliminary evaluation, than calculate the indices for every parameter. Once a group is found with a significant impact, it can be decomposed into smaller subgroups or into individual parameters to calculate more detailed sensitivity index information. To illustrate this, let us define two subsets θ_Y and θ_Z:

$$\theta_Y = (\theta_1, \ldots, \theta_m), \qquad \theta_Z = (\theta_{m+1}, \ldots, \theta_n) \tag{4.41}$$

Then D_{θ_Y} and D_{θ_Z} are given by:

$$D_{\theta_Y} = \sum_{s=1}^{m} \sum_{(i_1 < \ldots < i_m) \in K} D_{i_1 \ldots i_m}, \tag{4.42}$$

$$D_{\theta_Z} = \sum_{s=m+1}^{n} \sum_{(i_{m+1} < \ldots < i_n) \in K} D_{i_{m+1}} \ldots i_n \tag{4.43}$$

The total variance of the subsets is given by:

$$D^{Tot}_{\theta_Y} = D - D_{\theta_Z} \tag{4.44}$$

$$D_{\theta_Z}^{Tot} = D - D_{\theta_Y} \tag{4.45}$$

and the total sensitivity indices by:

$$S_{\theta_Y} = \frac{D_{\theta_Y}}{D}, \qquad S_{\theta_Y}^{Tot} = \frac{D_{\theta_Y}^{Tot}}{D} \tag{4.46}$$

For example, for a 3-parameter function, $\Phi(\theta) = \Phi(\theta_1, \theta_2, \theta_3)$, the following groups

$$\theta_Y = (\theta_1), \qquad \theta_Z = (\theta_2, \theta_3) \tag{4.47}$$

result in the following individual and total sensitivity indices:

$$S_{\theta_Y} = S_1, \tag{4.48}$$

$$S_{\theta_Y}^{Tot} = S_1 + S_{12} + S_{13} + S_{123} = 1 - S_{23} \tag{4.49}$$

On the other hand, if $\theta_Y = (\theta_1, \theta_2)$:

$$\theta_Y = (\theta_1, \theta_2), \qquad \theta_Z = (\theta_3) \tag{4.50}$$

then, the corresponding individual and total sensitivity indices have the following definitions:

$$S_{\theta_Y} = S_1 + S_2 + S_{12}, \tag{4.51}$$

$$S_{\theta_Y}^{Tot} = S_1 + S_2 + S_{12} + S_{13} + S_{23} + S_{123} = 1 - S_3 \tag{4.52}$$

By looking at equation (4.52), it can be seen that individual indices for a given parameter, such as S_3, can be estimated from the total sensitivity index, $S_{\theta_Y}^{Tot}$, of the complementary parameters $\theta_Y = (\theta_1, \theta_2)$. In the numerical evaluation by sampling approximation, the above will be useful to estimate individual indices, as it can lead to a reduction in computational requirements.

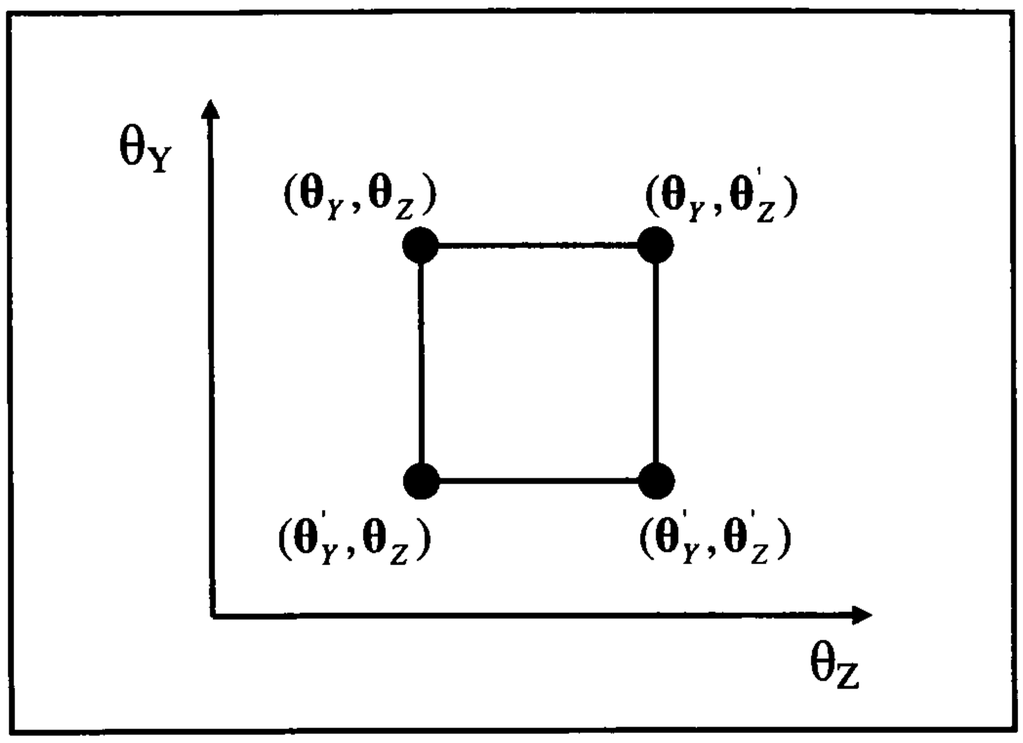


Figure 4.2: Points needed for a 2-dimensional sample or trial

Sampling-based approximation. The calculation of the Sobol' sensitivity indices can be performed by using a sampling-based approach to evaluate the integrals (4.37) and (4.38), as shown by Sobol' (2001a). Sample points can be obtained by any sampling method, such as random sampling or low-discrepancy sequences, as described in section 4.2.3. For each sample or trial, two independent points are needed, θ and θ':

$$\theta = (\theta_Y, \theta_Z) \qquad \theta' = (\theta'_Y, \theta'_Z) \tag{4.53}$$

which are combined to evaluate the process performance at three points:

$$\begin{aligned} &\Phi_1(\theta_Y, \theta_Z) \\ &\Phi_2(\theta_Y, \theta'_Z) \\ &\Phi_3(\theta'_Y, \theta_Z) \end{aligned} \tag{4.54}$$

For a two-dimensional space, the above points are shown in figure 4.2.

The Sobol' sensitivity indices are evaluated using the following approximations:

$$\lim_{N\to\infty} \frac{1}{N} \sum_{j=1}^{N} \Phi(\theta_{j_Y}, \theta_{j_Z}) = \Phi_0 \tag{4.55}$$

$$\lim_{N\to\infty} \frac{1}{N} \sum_{j=1}^{N} \Phi(\theta_{j_Y}, \theta_{j_Z}) \Phi(\theta_{j_Y}, \theta'_{j_Z}) = D_{\theta_Y} + \Phi_0^2 \tag{4.56}$$

$$\lim_{N\to\infty}\frac{1}{N}\sum_{j=1}^{N}\Phi^2(\theta_{jY},\theta_{jZ}) = D + \Phi_0^2 \tag{4.57}$$

$$\lim_{N\to\infty}\frac{1}{N}\sum_{j=1}^{N}\Phi(\theta_{jY},\theta_{jZ})\Phi(\theta'_{jY},\theta_{jZ}) = D_{\theta Z} + \Phi_0^2 \tag{4.58}$$

$$\lim_{N\to\infty}\frac{1}{2N}\sum_{j=1}^{N}[\Phi(\theta_{jY},\theta_{jZ}) - \Phi(\theta_{jY},\theta'_{jZ})]^2 = D_{\theta Z}^{Tot} \tag{4.59}$$

$$\lim_{N\to\infty}\frac{1}{2N}\sum_{j=1}^{N}[\Phi(\theta_{jY},\theta_{jZ}) - \Phi(\theta'_{Y},\theta_{jZ})]^2 = D_{\theta Y}^{Tot} \tag{4.60}$$

The sensitivity indices are:

$$S_{\theta_Y} = \frac{D_{\theta_Y}}{D} \tag{4.61}$$

$$S_{\theta_Y}^{Tot} = \frac{D_{\theta_Y}^{Tot}}{D} \tag{4.62}$$

and from equation (4.45), S_{θ_Y} is equivalently given by:

$$S_{\theta_Y} = 1 - \frac{D_{\theta_Z}^{Tot}}{D} \tag{4.63}$$

In practice, a finite number of evaluations is used and one of two stopping criteria can be used: a limit on the maximum number of sample points or a specified accuracy. The accuracy is defined as:

$$2\left|\frac{S_{k,i} - S_{k,i-1}}{S_{k,i} + S_{k,i-1}}\right| < \text{Required Accuracy}, \quad k = 1,\ldots,NS \tag{4.64}$$

where $S_{k,i}$ and $S_{k,i-1}$ are the estimates of sensitivity index S_k at "iterations" i and $i-1$ respectively and NS is the number of sensitivity indices being evaluated. An iteration is typically defined as the evaluation of a given number of sample points (*e.g.* 128 points).

As can be seen in the above approximation, the individual sensitivity indices are calculated by eliminating the interactions of the specified parameter with the remaining parameters. The calculated quantities are variances defined as follows:

$$D_{\theta_Y} = \text{Var}_{\theta_Y}[E_{\theta_Z}(\Phi(\theta_Y,\theta_Z)|\theta_Y = \theta_Y^\star)] \tag{4.65}$$

$$D = \text{Var}_{\theta_Y,\theta_Z}(\Phi(\theta_Y,\theta_Z) - \Phi_0) \tag{4.66}$$

Thus D_{θ_Y} is the variance, with respect to θ_Y, of the expected value, with respect to θ_Z, of function $\Phi(\theta_Y.\theta_Z)$. To evaluate the expected value of function $\Phi(\theta_Y,\theta_Z)$ with respect

to θ_Z, θ_Y is fixed to a given value: $E_{\theta_Z}(\Phi(\theta_Y, \theta_Z)|\theta_Y = \theta_Y^\star)$. Then, the variance of this expected value is obtained by calculating the expected value for different values of θ_Y. Finally, the value of D is the total variance of the function $\Phi(\theta_Y, \theta_Z)$.

While the Sobol' indices are used in this work, alternative indices such as those in the FAST method could be used instead. It is mentioned in Saltelli et al. (2000) that the FAST method is more efficient than the Sobol' method, since the former requires half the number of evaluations. However, recent work on the Sobol' method (Saltelli, 2002; Mauntz, 2002) has tried to reduce the number of evaluations required in the Sobol' method and to increase the information obtained from them. Two examples are used below to illustrate the Sobol' methodology.

Example 1. This first example shows the ANOVA decomposition and Sobol' index calculation for the following two-dimensional function:

$$\Phi(\theta_1, \theta_2) = \sin(\theta_1) + 0.1\ \theta_2^4 \sin(\theta_1) \tag{4.67}$$
$$-\pi \leq \theta_1, \theta_2 \leq \pi$$

which can be decomposed as:

$$\Phi(\theta_1, \theta_2) = \Phi_0 + \Phi_1(\theta_1) + \Phi_2(\theta_2) + \Phi_{12}(\theta_1, \theta_2) \tag{4.68}$$

The first three terms in (4.68) can be calculated using the integrals defined in equations (4.33-4.34):

$$\Phi_0 = \int_{-\pi}^{\pi}\int_{-\pi}^{\pi} \Phi(\theta_1, \theta_2) d\theta_1 d\theta_2 \tag{4.69}$$

$$\Phi_1(\theta_1) = \int_{-\pi}^{\pi} \Phi(\theta_1, \theta_2) d\theta_2 - \Phi_0 \tag{4.70}$$

$$\Phi_2(\theta_2) = \int_{-\pi}^{\pi} \Phi(\theta_1, \theta_2) d\theta_1 - \Phi_0 \tag{4.71}$$

while the last term, Φ_{12}, is given by:

$$\Phi_{12}(\theta_1, \theta_2) = \Phi(\theta_1, \theta_2) - \Phi_0 - \Phi_1(\theta_1) - \Phi_2(\theta_2) \tag{4.72}$$

The values of the different terms are then:

$$\Phi_0 = 0 \tag{4.73}$$

$$\Phi_1(\theta_1) = 0.04\pi^5 \sin(\theta_1) \tag{4.74}$$

$$\Phi_2(\theta_2) = 0 \tag{4.75}$$

$$\Phi_{12}(\theta_1, \theta_2) = (1 - 0.04\pi^5)\sin(\theta_1) + 0.1\ \theta_2^4 \sin(\theta_1) \tag{4.76}$$

The above results show that the average value, Φ_0, of function Φ for the given ranges of parameters is zero and the individual contribution of parameter θ_2 is also zero. Therefore, the ANOVA decomposition shows that the variation in Φ can be attributed to two factors: the individual effect of θ_1 and the interaction between θ_1 and θ_2.

The corresponding variances are defined as:

$$D = \int_{-\pi}^{\pi}\int_{-\pi}^{\pi} \left(\sin(\theta_1) + 0.1\,\theta_2^4 \sin(\theta_1)\right)^2 d\theta_1\, d\theta_2 - \Phi_0^2 \tag{4.77}$$

$$D_1 = \int_{-\pi}^{\pi} \left(0.04\pi^5 \sin(\theta_1)\right) d\theta_1 \tag{4.78}$$

$$D_2 = \int_{-\pi}^{\pi} 0\, d\theta_2 \tag{4.79}$$

$$D_{12} = D - D_1 - D_2 \tag{4.80}$$

and the index values are:

$$S_1 = 0.52 \tag{4.81}$$

$$S_2 = 0.00 \tag{4.82}$$

$$S_{12} = 0.48 \tag{4.83}$$

The sensitivity index S_1 indicates that 52% of the total variance of function $\Phi(\theta_1, \theta_2)$, for the given ranges, is due to parameter θ_1 individually and this contribution is quantified by Φ_1. On the other hand, parameter θ_2 has no individual contribution, but when its value is changed, the effect in $\Phi(\theta_1, \theta_2)$ is given by the interaction with θ_1, which corresponds to 48% of the overall variance within the given parameter ranges.

Example 2. This second example shows the application of the methodology to an isothermal CSTR described by a set of algebraic equations. The following two reactions take place:

$$2A \xrightarrow{k_1} B \qquad (1)$$

$$A + B \xrightarrow{k_2} C \qquad (2)$$

k_1 and k_2 are kinetic parameters for reactions (1) and (2) respectively, with units of $m^3/(kmol\ s)$. The objective in this second example is to investigate the effect of variations in the kinetic parameters k_1 and k_2 on the outlet flowrate of product B.

The set of algebraic equations describing the isothermal CSTR is given by:

$$F_{in}X_{in,i} - F_{out}\ X_i + V\sum_{j=1}^{2}\nu_{i,j}r_j = 0 \tag{4.84}$$

$$r_1 = k_1 C_A^2 \tag{4.85}$$

$$r_2 = k_2 C_A C_B \tag{4.86}$$

$$C_i = \frac{X_i P}{R\,T} \tag{4.87}$$

where F_{in} is the inlet flowrate (1 kmol/s), $X_{in,i}$ the inlet molar fraction for component i, F_{out} is the outlet flowrate in kmol/s, X_i the molar fraction of component i in the reactor, V is the reactor volume (1 m^3), $\nu_{i,j}$ the stoichiometric coefficient of component i in reaction j and r_j the rate of reaction j. C_i is the molar concentration of component i in kmol/m^3. P is the reactor pressure in kPa, R the gas constant in J/(mol K), and T the temperature in K. Here, the values P=101 kPa, T=298K and $X_{in} = (1, 0, 0)^T$ are used.

The analytical derivation of the ANOVA terms, like those developed in example 1, is complicated by the fact that the system is defined by a set of equations. Therefore, the sampling approximation described earlier in this section is used instead.

The nominal values of k_1 and k_2 are 1878.42 m^3/(kmol s) and 84.29 m^3/(kmol s) respectively. A deviation of 10% on either side of the nominal values is considered in this study. A uniform grid of 11×11 points is created in the two-dimensional space and the 121 points are used to approximate the value of the required integrals. The resulting Sobol' sensitivity indices are:

$$\begin{aligned} S_{k_1} &= 0.74 \\ S_{k_2} &= 0.26 \\ S_{k_1,k_2} &= 0.00 \end{aligned}$$

with a total variance, D, equal to 1.69×10^{-5} (kmol B/s)^2 and a mean value of 0.35 kmol B/s. These results show that the output flowrate of product B is affected only by first-order variation in the kinetic parameters, while the interaction between the parameters does not have any effect.

One of the advantages of global sensitivity indices when compared to local ones is that they differentiate between the individual effect of the specified parameter and its interactions with the other parameters.

4.3 Global Sensitivity/Feasibility Analysis and Risk Quantification

The Global Sensitivity/Feasibility Analysis, which is a key step of the methodology proposed in this work, is carried out by computing the Sobol' indices. Process performance is evaluated at each sampled point using the optimisation-based formulation of problem (4.8), described in Section 4.2.4, until convergence of the indices is achieved. The design variables are fixed to some value $d^\star$ in this formulation. The Sobol' sensitivity index framework was presented based on a single performance indicator, Φ, but this analysis can readily be extended to the case where several KPIs are of interest.

A large amount of information is gathered as problem (4.8) is solved repeatedly, often thousands of times, for different uncertain parameter realisations. One key piece of information is the expected value of the main performance measure (the objective function), denoted by $E_\theta[\Phi(d^\star)]$. In this section, we discuss how the results of this global analysis can be used to assess the impact of uncertainty on process feasibility, to quantify the inherent risk and to identify critical uncertain parameters.

4.3.1 Choice of sampling technique

As mentioned in Section 4.2.3, random and non-random sampling techniques can be used. During the construction of histograms for risk quantification and the calculation of metrics such as the expected value or variance of the KPIs, the values obtained must be adjusted to reflect the underlying uncertainty description rather than the sampling approach. For instance, if a non-random sampling technique is used, but the parameters are normally distributed, each sample point must be weighted by its probability of occurrence. One issue of concern in the context of risk analysis is the analysis of scenarios which carry low probability and high risk. If the uncertain parameters are defined by a non-uniform distribution, *e.g.* a normal pdf, the results obtained using a normal distribution may reflect accurately the behaviour of the system around the mean values, but give a poor representation of the tail ends of the probability distribution function. This can lead to an underestimate of the inherent risk.

A similar effect is seen in the feasibility analysis, although the purpose of the feasibility analysis is the identification of those regions within the uncertain parameter space which

are infeasible for the given problem. Therefore, a good sampling method to capture risk and infeasibility is one which results in a good coverage of the uncertainty space for a given number of sample points. In this case, a non-random method, such as Sobol' sampling, provides a better space coverage when compared to a random method, such as a normal pdf sampling.

The effect of sampling technique on the results is shown in the case studies in chapter 6. The following section describes the implementation of the global sensitivity/feasibility analysis and risk quantification.

4.3.2 Feasibility analysis

Feasibility analysis is made possible by the use of an optimisation-based approach to sensitivity analysis, which explicitly accounts for constraint violations. For some sampled points, problem (4.8) may not have a solution, indicating that design $d^\star$ cannot be operated for these parameter realisations. In this case, the point is not used in the calculation of the Sobol' sensitivity indices. The fact that an infeasible point has been found can nevertheless be used to calculate the infeasibility index, that is the probability that the process cannot be operated for the given uncertainty level. Furthermore, the infeasible points can be used to identify those parameters which have the most important impact on feasibility.

The estimation of the infeasibility index χ depends on the sampling approach used. If a non-random sample (*e.g.* Sobol') is used, the infeasibility index is

$$\chi = \frac{\sum_{k=1}^{N} \psi(\theta_k) y_k^f}{\sum_{k=1}^{N} \psi(\theta_k)} \tag{4.88}$$

where N is the number of sampled points; $\psi(\theta_k)$ is the probability of parameter realisation θ_k, which can be evaluated from the joint probability distribution of the uncertain parameters; and y_k^f is defined as

$$y_k^f = \begin{cases} 1 & \text{if } \theta_{\mathrm{k}} \text{ is infeasible} \\ 0 & \text{otherwise} \end{cases} \tag{4.89}$$

If the joint probability distribution of the uncertain parameters is sampled directly, the

infeasibility index is simply

$$\chi = \frac{\sum_{k=1}^{N} y_k^f}{N} \tag{4.90}$$

The parameters that most contribute to infeasibility can be identified by considering the ranges of parameter values over which infeasibility occurs. If, for a parameter θ_i, the process is found to be infeasible over the entire range of θ_i values, this indicates that the parameter has little effect on process feasibility. If, on the other hand, infeasible points are concentrated in one or several subintervals of the parameter range, this indicates that the parameter plays a significant role in feasibility. Those parameters are critical parameters. These subintervals can be identified graphically by projecting the infeasible points onto each parameter axis.

The results of the feasibility analysis can be used in the formulation of the scenario-based optimisation problem. One can attempt to find an improved design $d^{*\prime}$ by formulating a scenario-based optimisation problem that incorporates some infeasible scenarios (see Chapter 5), by modifying the control system, or by increasing the flexibility of downstream units.

4.3.3 Risk quantification

The solution of the many optimisations needed for the sensitivity analysis generates values of the objective function, other KPIs and control parameters. This information can be analysed to quantify the risk inherent in design d^*. The optimisation results can be translated into histograms of key performance indicators and summarised compactly in terms of an expected value and a variance. Once performance information has been gathered for each sample point, the analysis proceeds in one of two ways, depending on the sampling approach used.

If the Sobol' sampling technique has been used, the frequency $f_{\hat{\Phi}}$ of finding a profit between values Φ and $\Phi + \Delta\Phi$ is given by

$$f_{\hat{\Phi}} = \sum_{k=1}^{N} \psi(\theta_k) y_k^{\hat{\Phi}} \tag{4.91}$$

where

$$y_k^{\hat{\Phi}} = \begin{cases} 1 & \text{if} \hat{\Phi} \leq \Phi^*(\theta_k) < \hat{\Phi} + \Delta\Phi \\ 0 & \text{otherwise} \end{cases} \tag{4.92}$$

The use of $y_k^{\hat{\Phi}}$ automatically ensures that infeasible points are not counted in the generation of the histograms. The expected value $E_\theta[\Phi]$ is given by

$$E_\theta[\Phi] = \frac{\sum_{k=1}^{N} \psi(\theta_k)\Phi^*(\theta_k)y_k^f}{\sum_{k=1}^{N} \psi(\theta_k)y_k^f} \tag{4.93}$$

where y_k^f is used to ensure only feasible points are counted. Finally, the variance $\mathrm{Var}_\theta(\Phi)$ is given by

$$\mathrm{Var}_\theta(\Phi) = \frac{\sum_{k=1}^{N} y_k^f \psi(\theta_k)\left(\Phi^*(\theta_k) - E_\theta[\Phi]\right)^2}{\sum_{k=1}^{N} y_k^f \psi(\theta_k)} \tag{4.94}$$

If the parameters are uniformly distributed, the expected value and the variance are simply Φ_0 and D in the Sobol' sensitivity index formalism.

In the case where the sampling is carried out using the underlying distribution of the parameters (*e.g.* a normal pdf), the probability of each parameter realisation is inherently accounted for and can be removed from the equations. Thus, the frequency $f_{\hat{\Phi}}$ of finding a profit between values $\hat{\Phi}$ and $\hat{\Phi} + \Delta\Phi$ is simply given by

$$f_{\hat{\Phi}} = \sum_{k=1}^{N} y_k^{\hat{\Phi}} \tag{4.95}$$

where

$$y_k^{\hat{\Phi}} = \begin{cases} 1 & \text{if} \hat{\Phi} \leq \Phi^*(\theta_\mathrm{k}) < \hat{\Phi} + \Delta\Phi \\ 0 & \text{otherwise} \end{cases} \tag{4.96}$$

The expected value $E_\theta[\Phi]$ is given by

$$E_\theta[\Phi] = \frac{\sum_{k=1}^{N} \Phi^*(\theta_k)y_k^f}{\sum_{k=1}^{N} y_k^f} \tag{4.97}$$

Finally, the variance $\mathrm{Var}_\theta(\Phi)$ is given by

$$\mathrm{Var}_\theta(\Phi) = \frac{\sum_{k=1}^{N} \left(y_k^f \left(\Phi^*(\theta_k) - E_\theta[\Phi]\right)\right)^2}{\sum_{k=1}^{N} y_k^f} \tag{4.98}$$

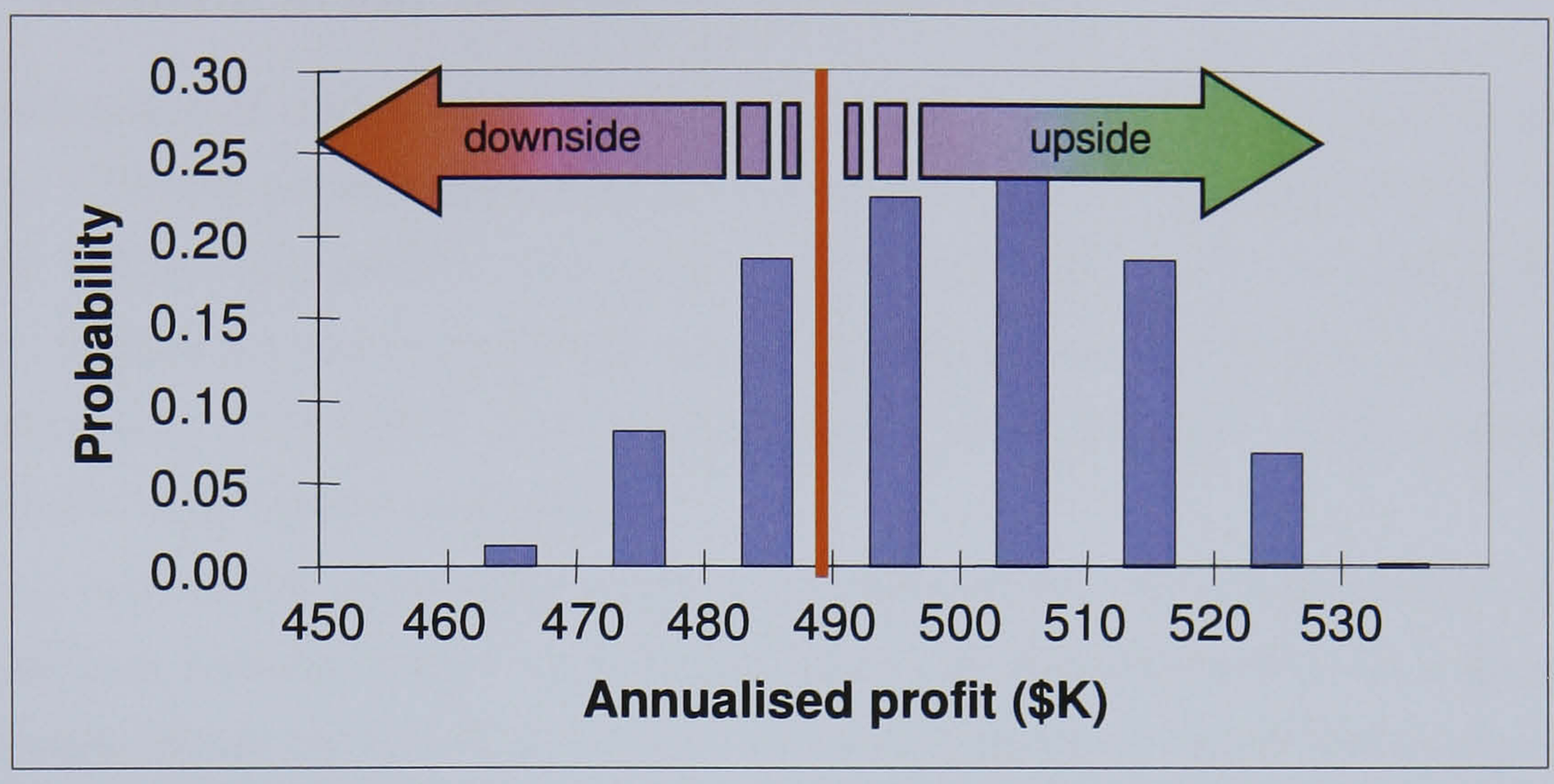


Figure 4.3: Probability for key performance indicator

The histograms present a good approximation of the full probability distribution functions of the KPIs. This graphical representation of the risk in key performance indicators can facilitate the decision-making process as it highlights important factors such as skewed distributions and large downsides. Figure 4.3 shows the probability distribution for a key performance indicator which, in this example, is defined as the annualised profit. The mean value or average is shown by the vertical line which can be used to define the upside and downside for the design used in the calculation. Furthermore, the histogram can be used to analyse the probability of observing a given performance. In this case, the most probable value of the profit is located in the upside region of the average annualised profit.

These histograms can be generated for any variable considered in the optimisation problems. Process-related decisions can be made with the above histograms, using the expected value and the variance. For example, histograms characterising the variation of control variables can be used to observe operating ranges and to ensure that control equipment can cope with the required range. The results can also be used to predict the effect of uncertainty on the performance of downstream units. The histograms of output stream conditions (*e.g.* concentration, temperature, flowrate) can be used as the basis for a risk assessment of downstream units. This serves to quantify the sensitivity of the downstream units to upstream variations and to identify the need for any mitigation units or design changes.

4.3.4 Identification of critical parameters

The identification of critical parameters contributing to infeasibility was discussed in Section 4.3.2. Critical parameters contributing to risk can also be determined. The global sensitivity indices are used for this purpose. For each KPI, the individual Sobol' global sensitivity indices are used to rank the individual input parameters in terms of their effect on the variability of the KPI. The combined effect of two or more input parameters can be considered with higher-order indices.

Given a ranked list of parameters, one can partition the set of parameters into critical and non-critical subsets, where the critical parameters are responsible for a large fraction of uncertainty. Since the Sobol' indices lie between 0 and 1, a cut-off value may be chosen to separate the two sets. Those parameters which have individual indices or joint indices above the cut-off should be classified as critical. The choice of a cut-off value is somewhat arbitrary, but a "natural" cut-off may occur in cases where there is a large gap between indices, with some values clustered near 1 and some near 0.

Alternatively, one can identify the critical parameters by considering how the Sobol' indices relate to the variance of the KPIs. As shown in eq. (4.40), the Sobol' indices are a *relative* measure since they quantify what proportion of the total variance of a given KPI over all parameters, D, is due to a specific parameter or set of parameters. Thus, the decision-maker can specify a target fraction of the variance (say, 80% of D) to be accounted for. The set of critical parameters is then the minimal set of parameters which accounts for the target fraction.

The calculation of Sobol' indices for subsets of parameters can be used to reduce the computational cost of global sensitivity analysis, especially when the number of uncertain parameters is high. For example, in a 3-parameter problem, the variance of the KPI $\Phi(\theta_1, \theta_2, \theta_3)$, two subsets can be defined as $\theta_Y = (\theta_1, \theta_2)$ and $\theta_Z = (\theta_3)$. The indices for the subsets are then:

$$\begin{aligned} S_{\theta_Y} &= S_1 + S_2 + S_{12} \\ S_{\theta_Z} &= S_3 \end{aligned}$$

Thus, S_{θ_Y} is a combined value. If S_{θ_Z} represents a sufficiently high proportion of the variance of Φ, θ_3 is the only critical parameter and further calculations are unnecessary. On the other hand, if S_{θ_Y} appears to be a critical subset, θ_1 and θ_2 can be classified as

critical parameters, or S_1 and S_2 can be calculated to determine whether θ_1 or θ_2 is in fact non-critical and can be removed from the critical set.

The critical parameters can be used to mitigate risk by indicating where R&D is required: experiments can be performed to reduce the uncertainty in the critical parameters and thus to reduce their effect on key performance indicators. Furthermore, the scenario-based design problem can be formulated in the reduced space of critical parameters. This option is discussed in Chapter 5.

4.4 GSFA Implementation

The Global Sensitivity/Feasibility Analysis using the sampling-based approximation for Sobol' indices described previously has been implemented as a C++ parallel code. The optimisation-based approach to performance evaluation is used and every optimisation problem is solved using gPROMS (Process Systems Enterprise, Ltd., 2006). The code has been parallelised using the MPI standard (The LAM/MPI Team, 2004) and has been tested on a Beowulf cluster with processors ranging from 1.79 to 3.29 GHz. The following sections show the structure of this code, explain how to generate the required input files and present some performance results.

4.4.1 Code structure

The structure of the code developed is shown in figure 4.4. This version was developed using a previous code created by Mauntz (2002) which calculates Sobol' sensitivity indices making use of gPROMS to solve a simulation-based problem. Mauntz's code is a gPROMS-based application (gBA) running on a single processor. It uses a different approximation of the integrals required in the evaluation of the Sobol' indices from that shown earlier in this chapter.

The version developed to implement the optimisation-based approach uses three unmodified subroutines found in Mauntz's code: PartOf.cpp, Urand.cpp and Sobol50.cpp. Subroutine PartOf.cpp is used to identify internal variables needed in the code which are chosen based on the sensitivity indices that are calculated. Urand.cpp and Sobol50.cpp are the random and Sobol' number generators, respectively. The random number algorithm is by Knuth (1981), while the Sobol' generator is from Sobol' (2001b).

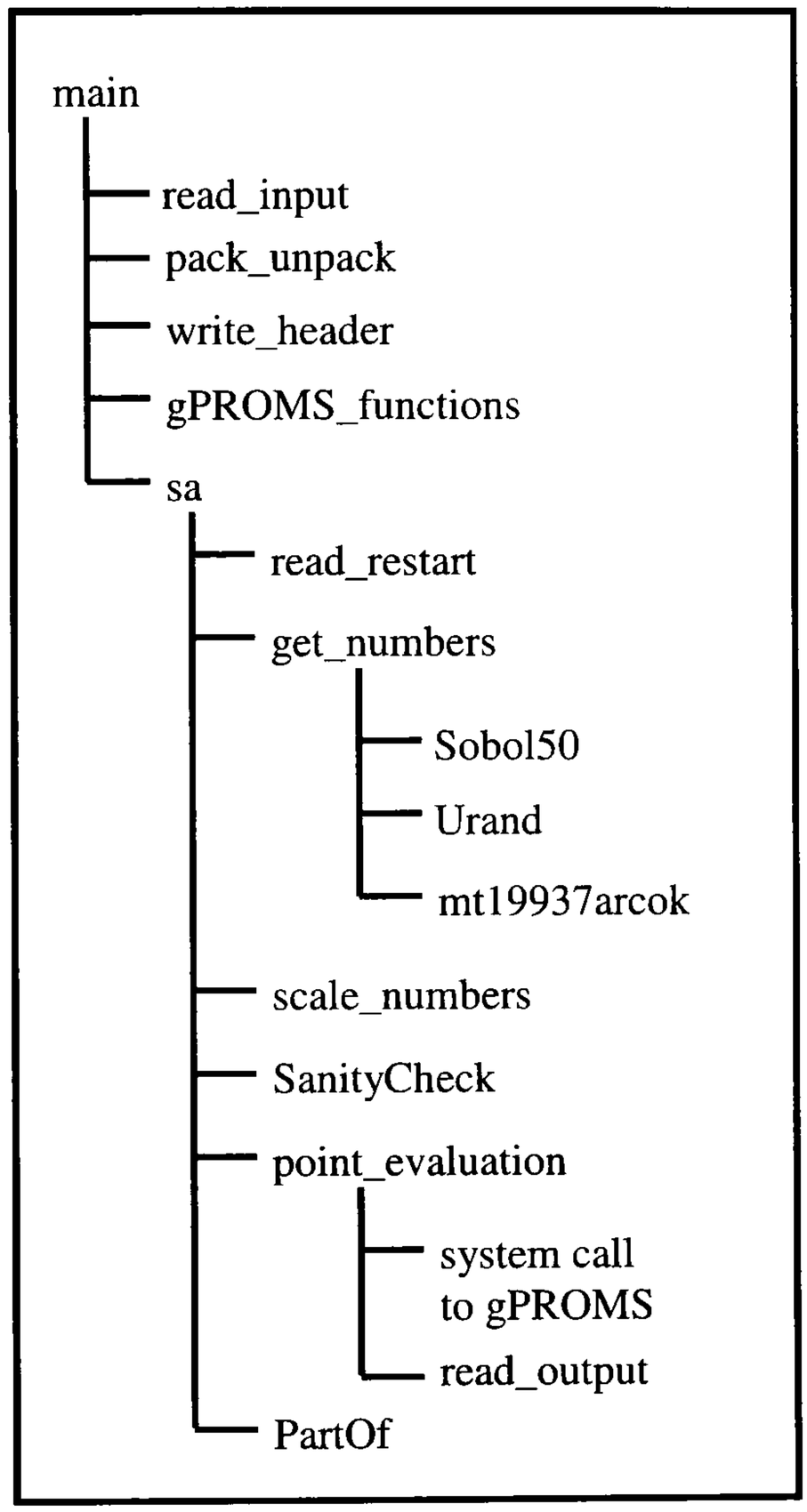


Figure 4.4: Code structure for GSFA implementation

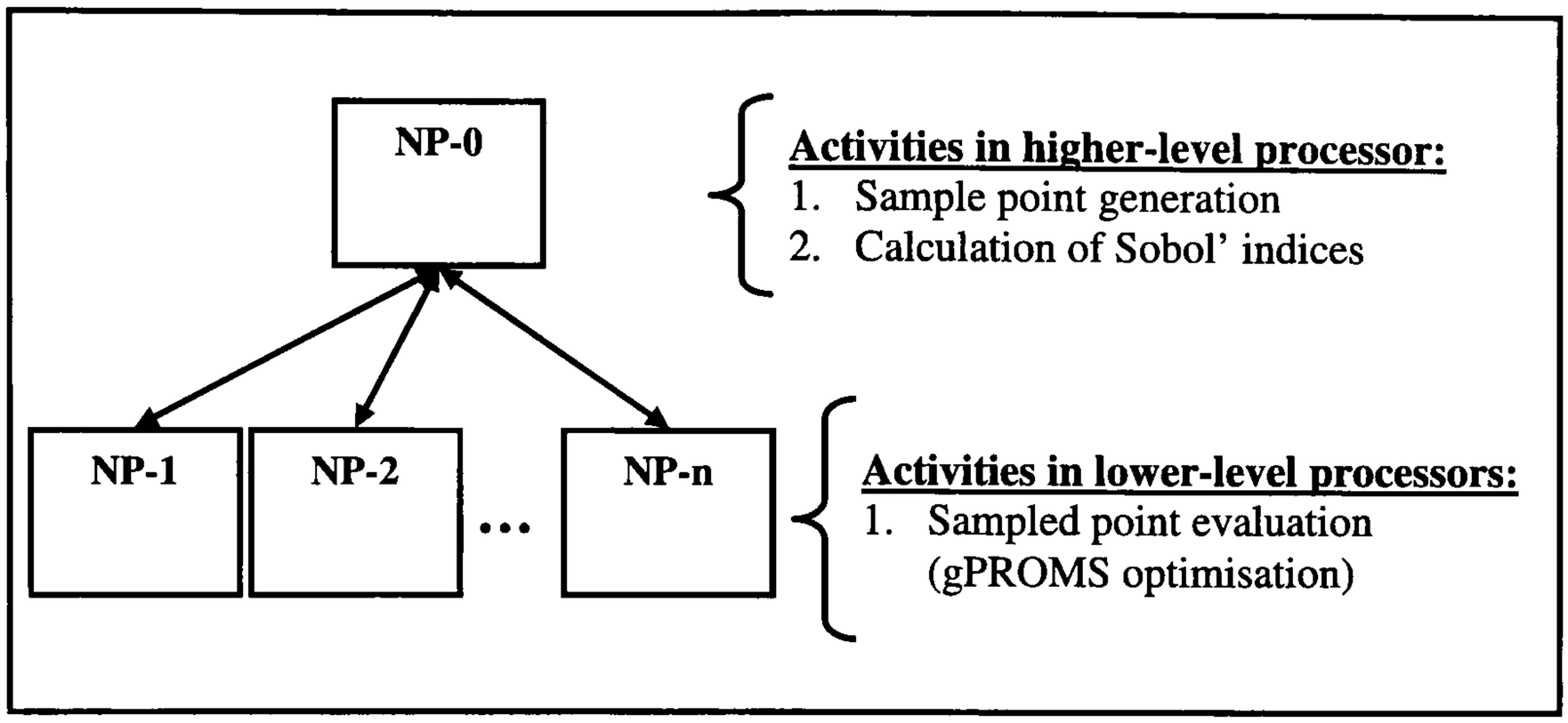


Figure 4.5: Parallel implementation structure

The new code has been developed to work in a parallel environment. Figure 4.5 shows the structure and the main activities performed in the higher and lower-level processing machines. There are n+1 nodes (NP-0, NP-1, ..., NP-n) specified on the command line when starting the application. Of these n+1 nodes, one is the higher-level processor (NP-0), and the remaining are the lower-level ones.

The program starts in node NP-0 with read_input by reading an input file (*input.txt*) which contains all the input information needed such as the names of the gPROMS files to be used, the names assigned to output files, the number of control variables and the number of uncertain parameters. This file also specifies the sensitivity indices to be estimated together with stopping criteria values such as accuracy and maximum number of sampled points, the type of sampling (random or Sobol') and the uncertain parameter ranges.

Once the input information is read, the remaining nodes are initialised and each node starts gPROMS as an external application. After this step, there is a continuous exchange of data between node NP-0 and the remaining nodes. The main processor, NP-0, generates the sampled points depending on the method chosen by the user and sends them to the remaining processors. The lower-level machines use gPROMS to solve the optimisation problem for the given sampled point and return the results to the main processor. The sensitivity indices are calculated every 128 points and the procedure terminates when sufficient accuracy has been achieved (in the case studies shown in this thesis, an accuracy of 1e-4 was used) or when the maximum number of sample points has been sampled.

To avoid initialisation problems and possible optimisation failures with the given sam-

pled points, the lower-level processors perform a series of calculations for each sampled point. Once the point is received, it is first evaluated as a steady-state simulation (SS1), with fixed values of the control variables. The results are saved in a file which is then used for the initialisation of the optimisation problem (Opt). If the optimisation solver fails to find a solution, a new series of calculations is performed, starting with a dynamic simulation (Dyn) to generate a new initial guess. This dynamic simulation is followed by a steady-state simulation (SS2) and a new optimisation (Opt2). If this last optimisation fails again, new initial guesses are generated for the optimisation variables and another optimisation is started. In each calculation the results are saved and then restored for the subsequent activities. This specific sequence was created for the case study shown in chapter 6. However, this series of activities can be modified in the code and be adapted to the complexity of the given problem. Some problems may need special initialisation sequences, while others could work directly on the optimisation. When all the simulations fail for a sample, it is classified as infeasible. All infeasible points are examined *a posteriori* to determine whether a different numerical method or starting point yields a solution. If not, the point is deemed infeasible.

4.4.2 Input files

The above implementation requires some specific files. An example of these files is given in appendix B and an explanation on naming and exporting gPROMS files is given here. The interaction between the gPROMS files and the code is through the use of *Foreign Objects*, which are explained in the gPROMS Advanced User Guide (PSE Ltd., 2004a). An example of how to call and use the simpleEventFOI foreign object in this context is given in appendix B. This is used to receive the sampled points for the different activities (simulation or optimisation).

The entities needed in the gPROMS file depend on the sequence of events required by the code. For the sequence explained above, 5 process and 2 optimisation entities are needed. The naming of the process entities should be as follows: *name_SS1*, *name_Opt*, *name_Dyn*, *name_SS2* and *name_Opt2*. And the naming of the optimisation entities as: *name_Opt* and *name_Opt2*. *name* is the gPROMS file name specified in the input file, *input.txt*. The project containing the set of entities needs to be exported, encrypted and named *nameX.gENCRYPT*. The password used for encryption is *moscow*.

Finally, the external gPROMS application to be called by every slave processor must be copied to the *code* folder. The main application will then be able to locate this file and copy it into every working directory.

4.4.3 Output files

The code generates four output files. The main output file, *output-file.csv*, where the name *output-file* is specified in the input file, contains a copy of the information specified in *input.txt* and displays the intermediate and final values for the calculated sensitivity indices. These indices are shown every 128 points.

The second file, *optimal.csv*, is used by every lower-level processor to record information related to the point being evaluated. This contains the number of the sample point, the values assigned to all the parameters and the respective values of the objective function and control variables. When no solution is found for a specific point, this is indicated in the file by showing *NOT FOUND* as the value for the objective function and control variables. New data are added as the different processors find a solution for their respective points.

The third output file, *optimal2.csv*, shows a list of the evaluated points in the order in which their solutions were received by the higher-level processor. This file records the values of the key performance indicators for the parameter combinations analysed, i.e. $\Phi(\theta_Y, \theta_Z)$, $\Phi(\theta_Y, \theta'_Z)$ and $\Phi(\theta'_Y, \theta_Z)$. Files *optimal.csv* and *optimal2.csv* can be used to identify infeasible points for the feasibility analysis. The data in those files are also used to generate histograms, expected values and variances for the risk analysis.

The last file, *temp_file.csv*, contains information needed to perform the sensitivity analysis in batches. Once a batch is completed, the file can be used at the start of the next batch by specifying a restart option in the input file. The file can be used only when the simulation finishes normally. Therefore, if the code fails to reach the specified maximum number of points or the desired accuracy, this file cannot be used and the analysis must be restarted from the previous completed analysis. The restart point was included to deal with any unexpected interruptions of the program (*e.g.* memory problems). In this case, only the calculations performed for the current batch are lost.

Table 4.1: Analytical values for Sobol' sensitivity indices of test functions.

Function	Measure	Values for measures at	
		n=2	n=10
Eq. (4.99)	$\frac{S_1}{S_1^{Tot}}$	0.99	0.95
	$\sum S_i$	0.99	0.97
Eq. (4.100)	$\frac{S_1}{S_1^{Tot}}$	0.75	0.89
	$\sum S_i$	0.86	0.89
Eq. (4.101)	$\frac{S_1}{S_1^{Tot}}$	0.51	6.7e-16
	$\sum S_i$	0.97	6.3e-13

4.4.4 Code performance

The implementation of the global sensitivity analysis has been tested using three functions for which there are known analytical expressions for the Sobol' sensitivity indices. These functions are:

$$\prod_{i=1}^{n} \frac{|4x_i - 2| + 6.52}{7.52} \qquad x \in [0,1]^n \tag{4.99}$$

$$\sum_{i=1}^{n} (-1)^i \prod_{j=1}^{i} x_j \qquad x \in [0,1]^n \tag{4.100}$$

$$\prod_{i=1}^{n} i \cos(i x_i) \qquad x \in [0,1]^n \tag{4.101}$$

Functions (4.99)–(4.100) are taken from Mauntz (2002). Two values were tested for n for each function: 2 and 10. The values of the Sobol' sensitivity indices obtained by evaluating the analytical expressions are shown in table 4.1.

The use of different sampling strategies is first investigated. The sensitivity indices for function (4.99) are calculated using random uniform sampling and Sobol' sampling with a value of n equal to 2. A comparison of the results is shown in figures 4.6 and 4.7 where it is seen that stable values are reached much sooner with the Sobol' sampling.

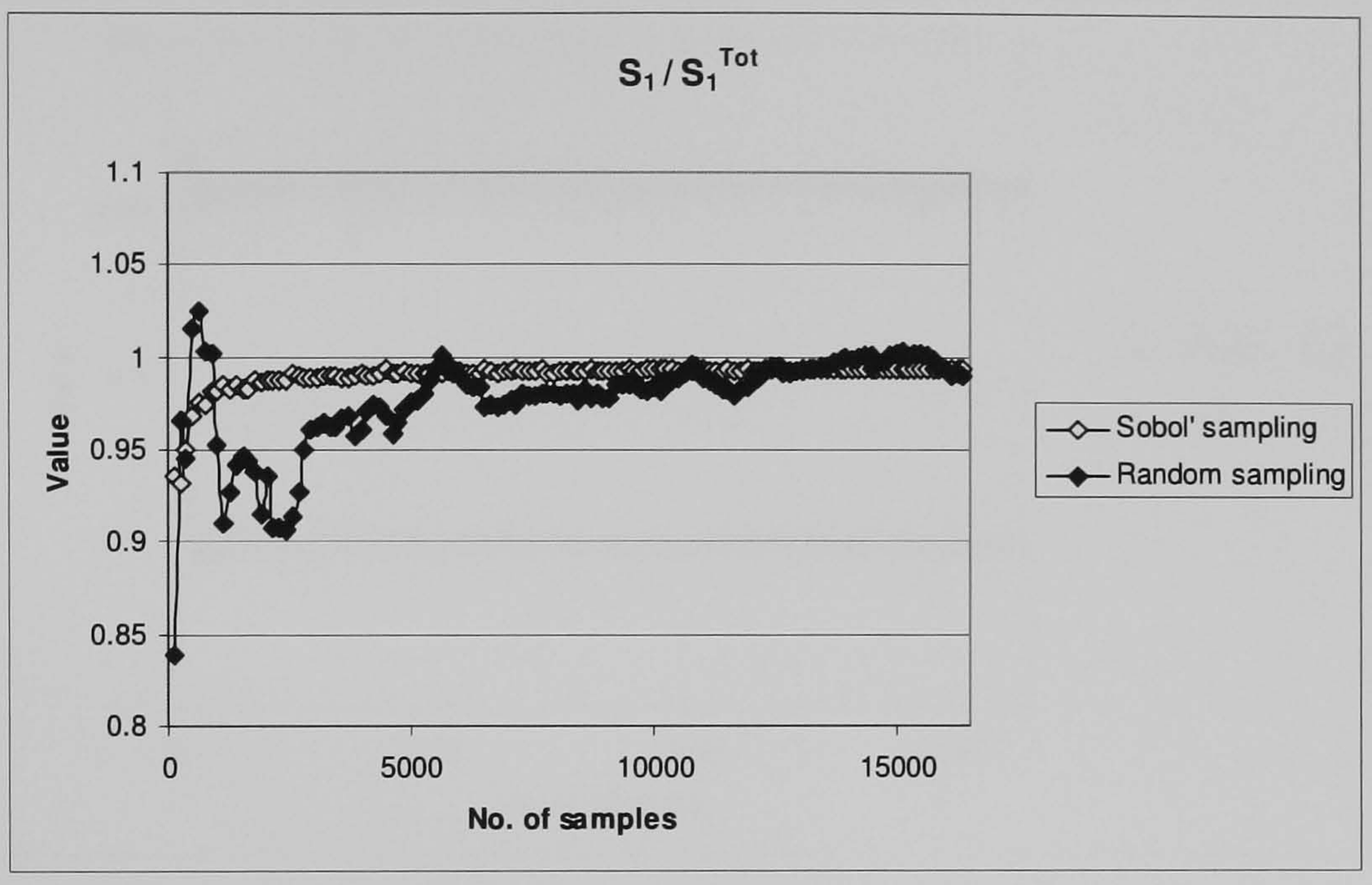


Figure 4.6: Convergence of S_1/S_1^{Tot} to the value of 1 as a function of the number of sample points for Sobol' and uniform random sampling for function (4.99), n=2

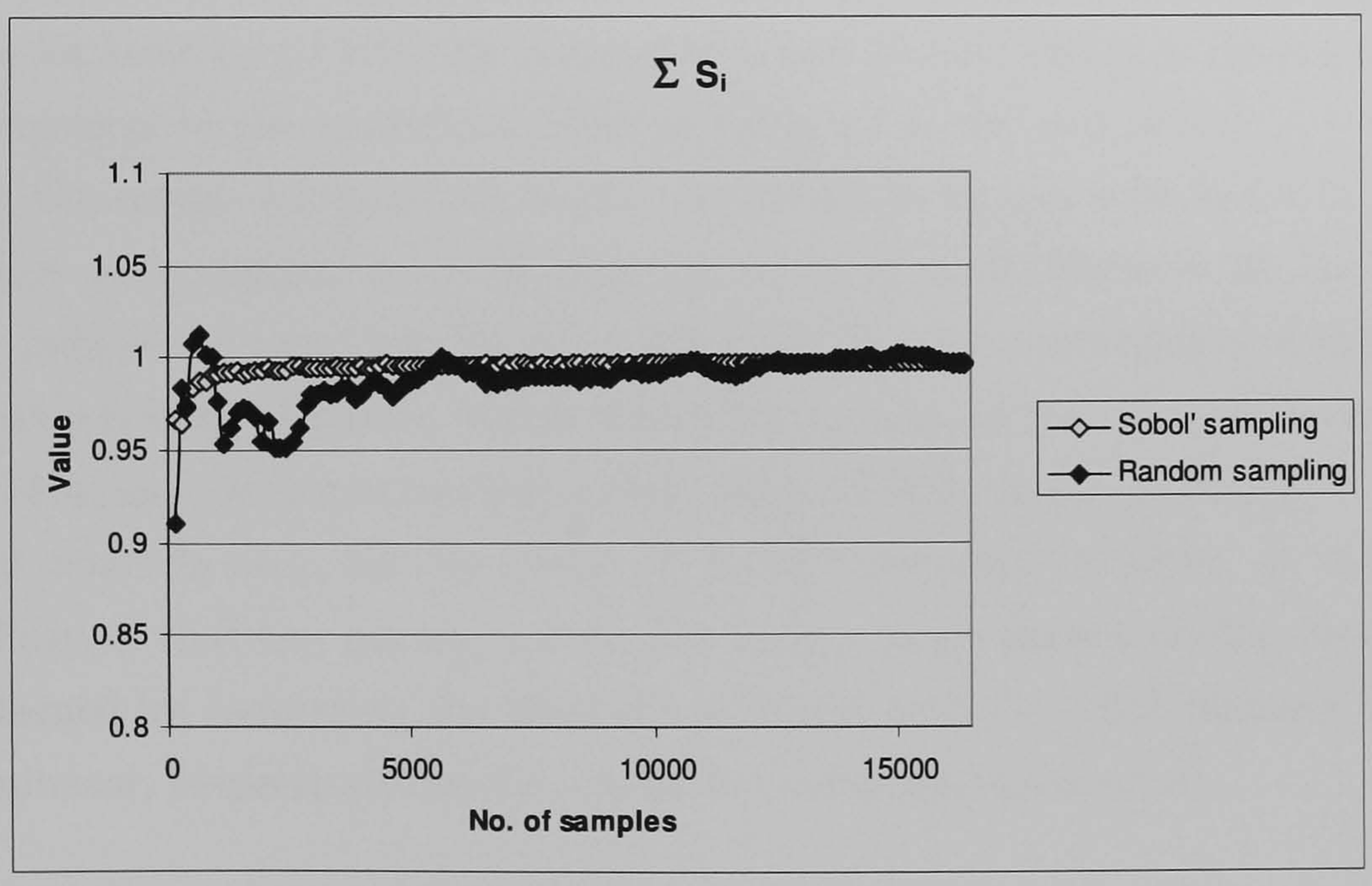


Figure 4.7: Convergence of $\sum S_i$ to the value of 1 as a function of the number of sample points for Sobol' and uniform random sampling for function (4.99) for n=2

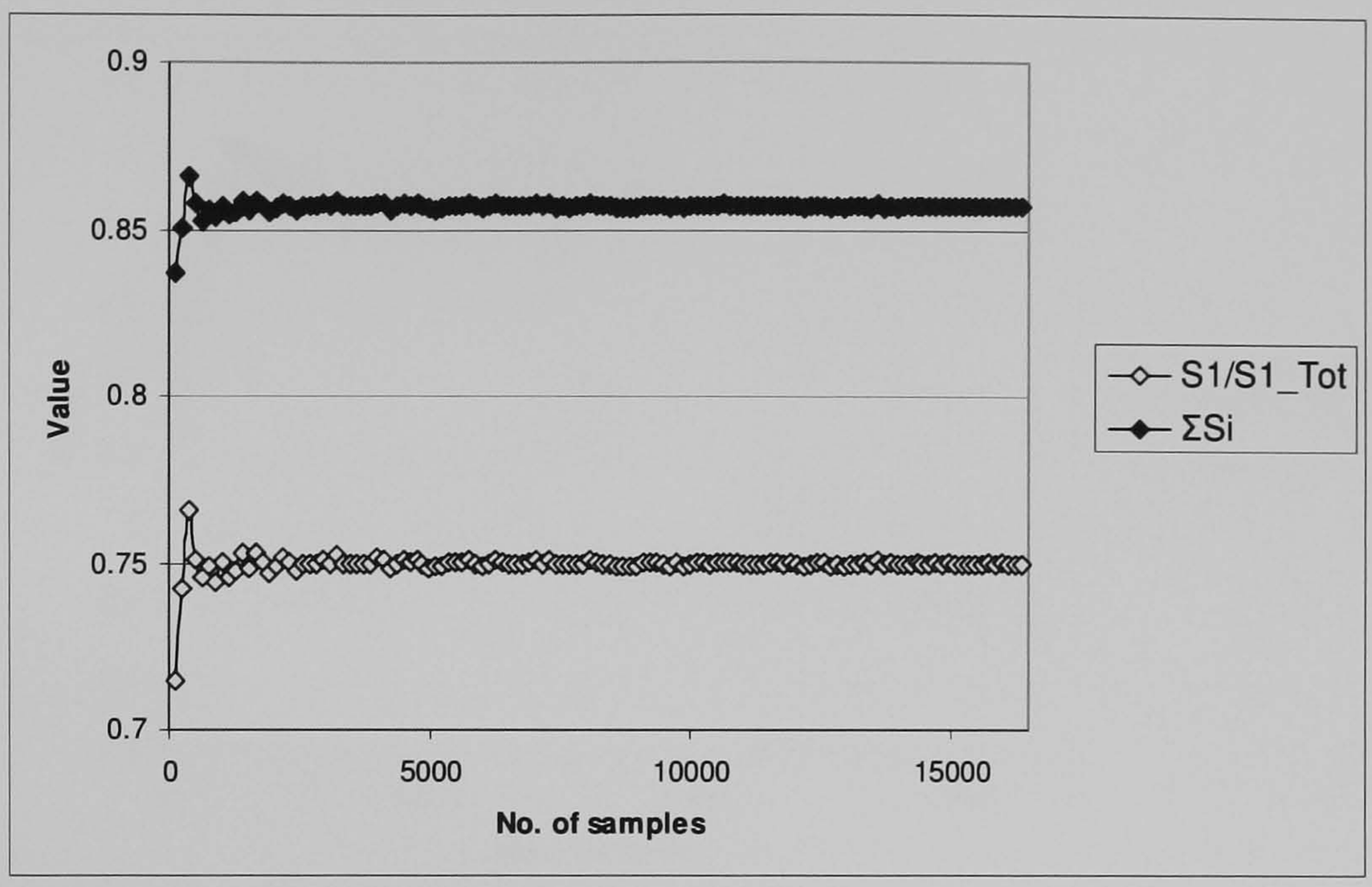


Figure 4.8: Convergence of S_1/S_1^{Tot} and $\sum S_i$ to analytical values for function (4.100) for n=2

Based on these results, the remaining tests are carried out using Sobol' sampling only. The results for function (4.100), for n equal to 2 and 10, are shown in figures 4.8 and 4.9. The runs converge to the analytical values in table 4.1 at an early stage.

Finally, the results for function (4.101) are shown in figures 4.10 and 4.11. The analytical values are estimated correctly only for values of n=2. For $n = 10$, the individual sensitivity indices are very low ($\sum S_i < 6.3 \times 10^{-13}$) and convergence of the sampling approximation is slower than for higher sensitivity indices, as the calculations involve very small numbers, introducing numerical errors. After 13,000 sample points, $\sum S_i$ is starting to converge towards zero, but the value of S_1/S_1^{Tot} remains unstable. In this case, an earlier indication that the parameters do not have a large impact on the function value can be obtained by comparing the absolute variances with the total variance (numerator and denominator, respectively, in the sensitivity index approximation).

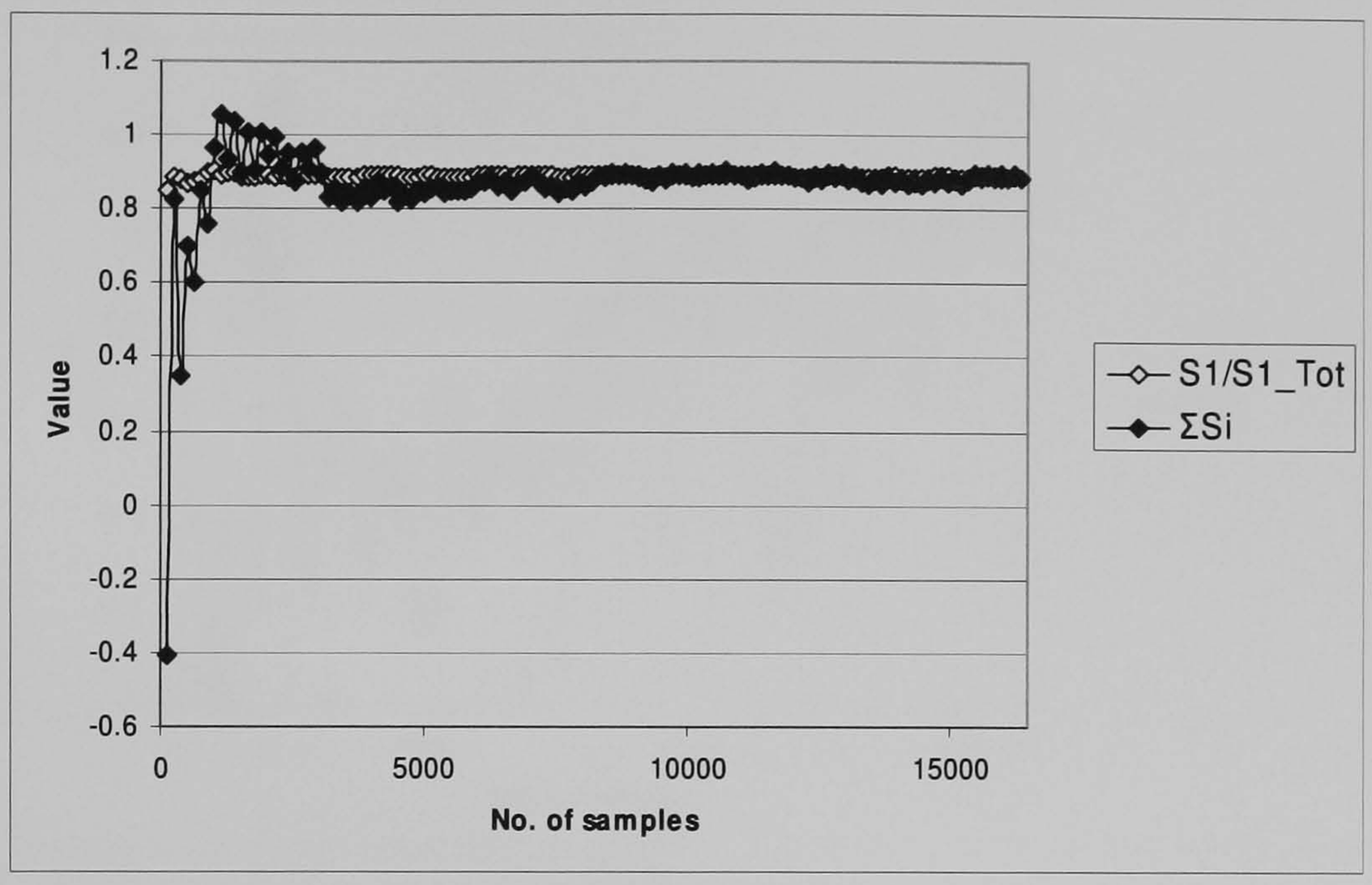


Figure 4.9: Convergence of S_1/S_1^{Tot} and $\sum S_i$ to analytical values for function (4.100) for n=10

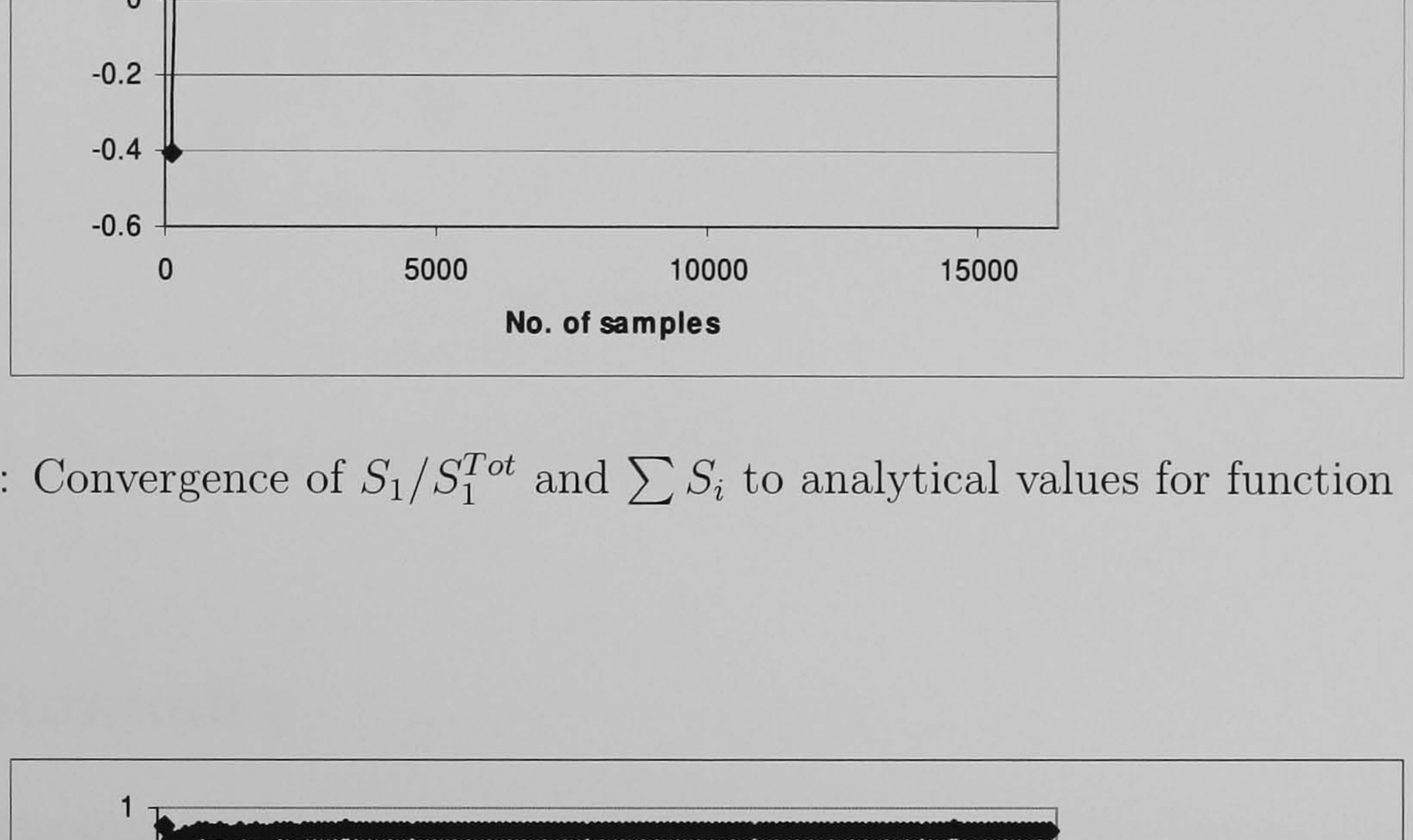


Figure 4.10: Convergence of S_1/S_1^{Tot} and $\sum S_i$ to analytical values for function (4.101) for n=2

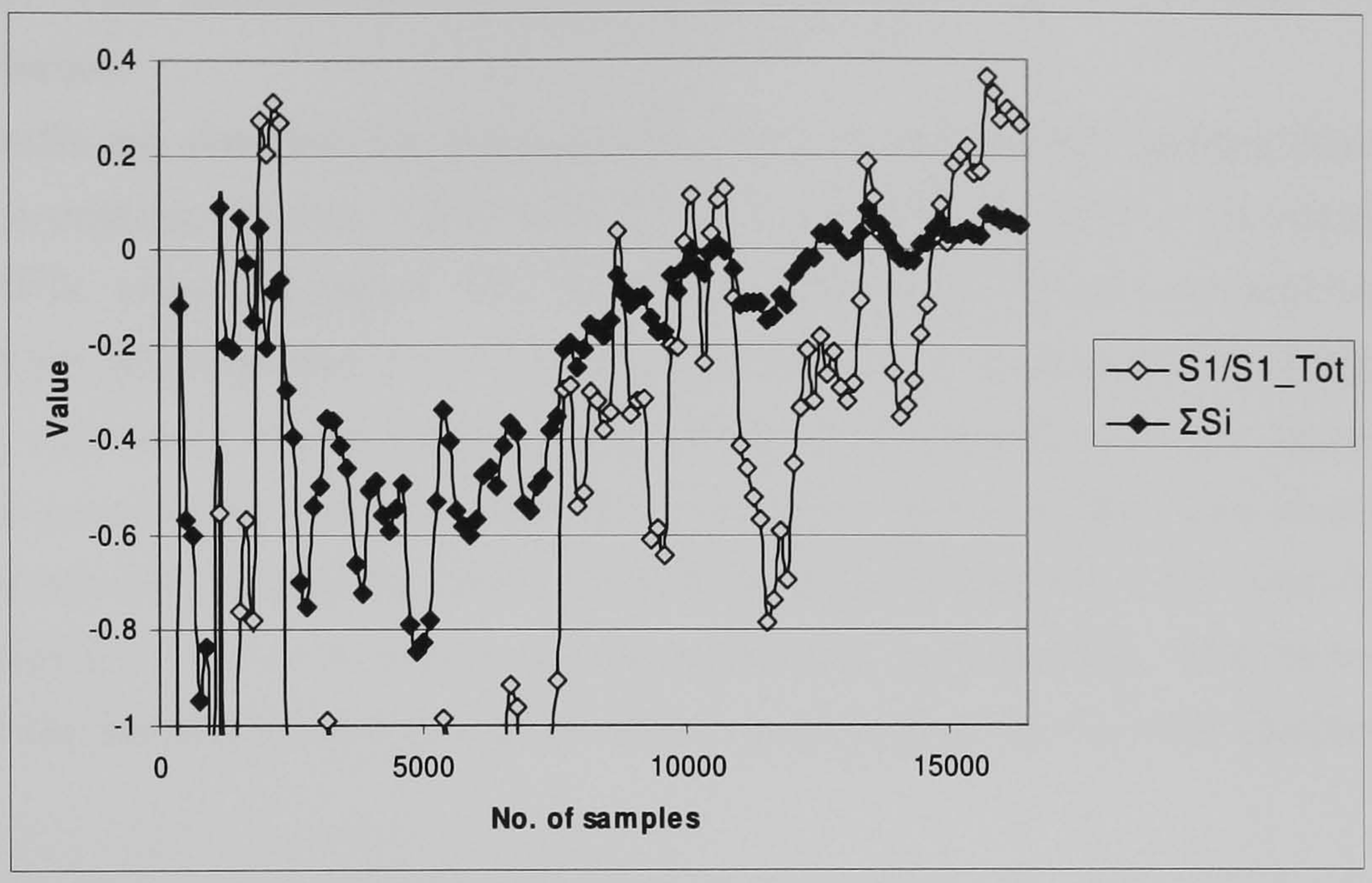


Figure 4.11: Convergence of S_1/S_1^{Tot} and $\sum S_i$ to analytical values for function (4.101) for n=10

4.5 Summary

The global sensitivity/feasibility analysis step of the methodology proposed in this thesis was described in this chapter. Sobol' sensitivity indices are estimated using a sampling approximation to evaluate the integrals defining those indices. A key feature of the approach is that it makes use of the system's flexibility, by solving an optimisation problem to evaluate performance at each sampled point. Further analysis of these results are used to perform a risk quantification and feasibility analysis.

The approach was implemented as a gPROMS-based application (gBA) written in C++, so that the optimisation problems are solved in gPROMS. The code was developed for a parallel environment and this was tested on a Beowulf cluster. A series of performance tests was carried out using functions for which the analytical values of the Sobol' indices were known. The results show good performance when using Sobol' sampling, except in cases where all the sensitivity indices have low values.

Based on the sampling results, a feasibility analysis has been proposed to compute an infeasibility index and to identify regions for which a given design is not feasible. Further analysis of the regions can be performed to identify those parameters causing the

infeasibility. This information can then be used to take further decisions to tackle the feasibility issues.

The results are also used for risk quantification, to provide information that facilitates the decision-making process. This information is given in the form of histograms for the different KPIs, expected values and variances. This then informs managerial decisions (*e.g.* is further R&D needed?) or technical decisions (*e.g.* control system design).

Finally, the use of the proposed global sensitivity/feasibility analysis allows the identification of parameters that have an important effect on the model. The identification of this critical subset is helpful to direct effort in subsequent phases of the overall methodology, be it further R&D or re-design via scenario-based optimisation. The formulation and solution of the scenario-based design problem are presented in the next chapter.

Chapter 5

Scenario-Based Optimisation

5.1 Introduction

The approach proposed to formulate and to solve scenario-based problems is discussed in this chapter. This method is used when a new design is needed within the methodology (step 3b in section 3.3.3). The dimensionality of the uncertain parameter space is reduced using the results from the sensitivity/feasibility analysis and risk quantification. A series of scenarios is generated by sampling the reduced parameter space. The objective is to find a design which is feasible over the given scenarios and which optimises the expected value of the process. A new approach is presented to deal with numerical difficulties associated with scenario-based problems and complex models.

The problem of finding a feasible and optimal design within a given uncertain parameter space Θ is defined by the following stochastic optimisation formulation:

$$\begin{aligned} v^\star = \quad & \max_{d} \quad E_{\theta\in\Theta}\left\{\Phi_{max}(d,\theta)\right\} \\ & s.t. \quad d \in D \end{aligned} \tag{5.1}$$

where E denotes the expected value operator and

$$\begin{aligned}
\Phi_{max}(d,\theta) = \max_{u} \quad & \Phi(d,u,y,\theta) \\
s.t \quad & f(d,u,x(z),x_z(z),x_{zz}(z),\theta) = 0 && \forall\ z \in \Omega \\
& h(d,u,x(z),x_z(z),x_{zz}(z),\theta) = 0 && \forall\ z \in \Gamma(\Omega) \\
& g(d,u,x(z),x_z(z),x_{zz}(z),\theta) \leq 0 && \forall\ z \in \Omega \\
& y = \mathcal{Y}(d,u,x(z),x_z(z),x_{zz}(z),\theta) && \forall\ z \in \Omega \\
& y \leq \overline{y} \\
& u \in U, x \in X
\end{aligned}$$

Other symbols are as previously defined.

A problem commonly encountered in solving this type of formulation is the calculation of the expected value. This calculation is defined as a multidimensional integral over the uncertain parameter space, Θ. Depending on the type of functions involved, the expected value can be difficult or even impossible to calculate exactly. An alternative way to formulate stochastic problems is to approximate the expected value using a scenario-based approach approach, as discussed in Chapter 2:

$$\begin{aligned}
\hat{v}_N = \max_{d} \frac{1}{N} \sum_{i=1}^{N} \{\Phi_{max}(d,\theta_i)\} \\
d \in D
\end{aligned} \tag{5.2}$$

where $\theta_i \in \Theta$ denotes scenario i and

$$\begin{aligned}
\Phi_{max}(d,\theta_i) = \max_{u_i} \quad & \Phi(d,u_i,y,\theta_i) \\
s.t. \quad & f(d,u_i,x(z),x_z(z),x_{zz}(z),\theta_i) = 0 && \forall\ z \in \Omega, i = 1,\ldots,N \\
& h(d,u_i,x(z),x_z(z),x_{zz}(z),\theta_i) = 0 && \forall\ z \in \Gamma(\Omega), i = 1,\ldots,N \\
& g(d,u_i,x(z),x_z(z),x_{zz}(z),\theta_i) \leq 0 && \forall\ z \in \Omega, i = 1,\ldots,N \\
& y = \mathcal{Y}(d,u_i,x(z),x_z(z),x_{zz}(z),\theta_i) && \forall\ z \in \Omega, i = 1,\ldots,N \\
& y \leq \overline{y} \\
& u \in U, x \in X
\end{aligned}$$

In the scenario-based approach, the quality of the estimate of the expected values improves as the number of samples, N, is increased:

$$E_{\Theta}\{\Phi(\theta)\} = \lim_{N\to\infty} \frac{1}{N} \sum_{i=1}^{N} \Phi(\theta_i) \tag{5.3}$$

However, the accurate evaluation of the approximation is a difficult task, especially for systems with a large number of uncertain parameters, since a large number of points or scenarios is needed to obtain acceptable results. Furthermore, an additional difficulty is associated with the use of complex models. A good initial guess is required for every scenario to avoid numerical problems during the solution of every point.

Therefore, the main issues to address in any scenario-based approach aimed at managing technological risk using complex models are:

- How can we ensure numerical robustness for large nonlinear models?
- How can we reduce the number of scenarios?

The following sections address these issues. The next section introduces a pseudo-dynamic approach which is used to overcome initialisation difficulties and ensures numerical robustness in the scenario-based methodology. The last section deals with scenario generation and shows how to make use of first-order and higher-order sensitivity indices to reduce the number of scenarios.

5.2 Pseudo-Dynamic Approach

As mentioned earlier, a large number of sample points is needed to obtain a good estimate of the expected value in problem (5.2). In the traditional approach to formulating and solving scenario-based problems, the size increases linearly with the number of scenarios. If a given deterministic problem has m variables and n scenarios are used, the number of variables in the scenario-based formulation is $m \times n$, as illustrated in figure 5.1. To handle the different scenarios simultaneously, different initial guesses are usually required, particularly for large nonlinear models. It is non-trivial to provide such guesses and this increases the complexity of solving the problem.

The maximum number of scenarios is usually limited by the available computing tools rather than by the desired accuracy. This can be a significant disadvantage, especially when using complex models like the ones this work deals with.

Some research work has been aimed at reducing the cost of the solution. For example, Paules and Floudas (1992) and Varvarezos et al. (1994) exploit the special block angular structure of these problems.

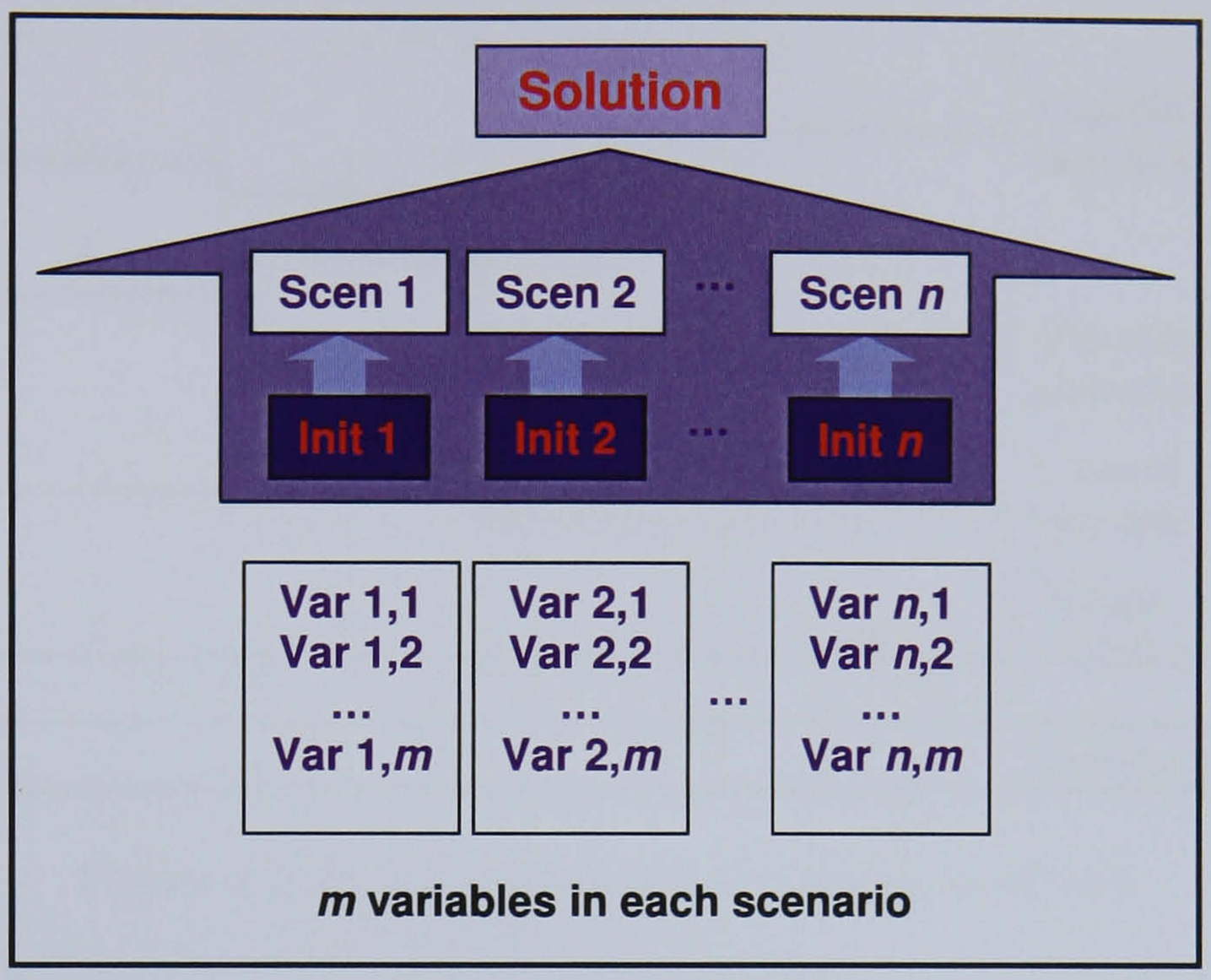


Figure 5.1: Graphical representation of the traditional scenario-based optimisation

In this section, we present an alternative approach to deal with scenario-based optimisation problems which avoids initialisation difficulties and allows a greater number of scenarios to be used. In this approach, the scenario-based problem is formulated as a dynamic optimisation problem. The uncertain parameters whose values change from scenario to scenario are treated as disturbances whose values change over a pseudo-time domain. The disturbances remain constant for a period of (pseudo-)time before changing to a new value which corresponds to a new scenario. In this way, one scenario follows another "dynamically". This results in a dynamic optimisation problem similar to an optimal control problem.

This approach has two benefits in terms of computational performance. Firstly, as with techniques which exploit the problem structure, for a given choice of design variables, n problems (one for each time period) of size $m \times q$ are solved rather than one large $n \times m \times q$ problem, where q is the number of constraints. Secondly, the system can be moved continuously from scenario to scenario as pseudo-time proceeds. This implies that only one initial guess is needed for the solution of the first scenario at the initial time, rather than one set for every scenario.

A few considerations related to the optimisation variables and constraints must be

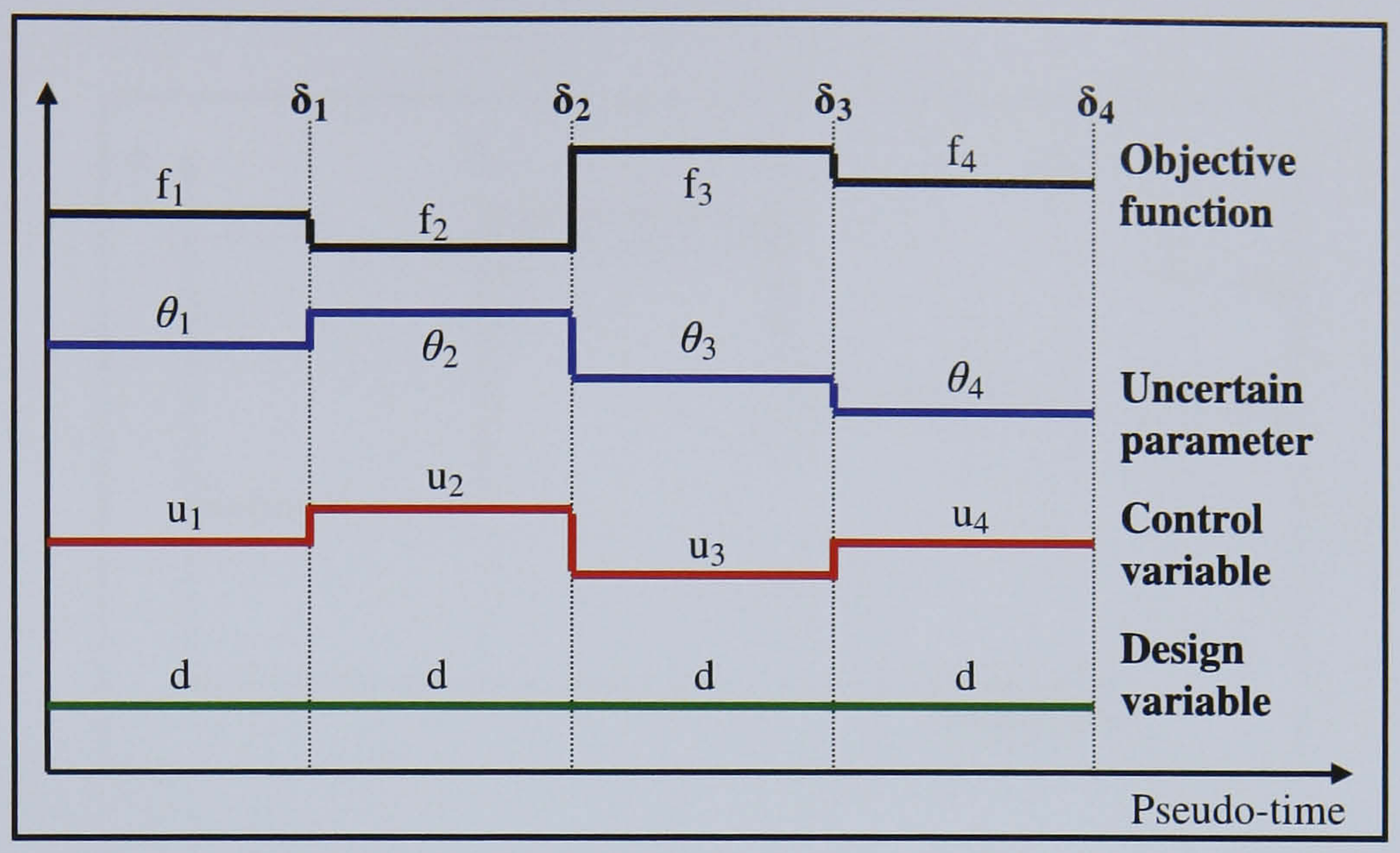


Figure 5.2: Pseudo-dynamic optimisation approach

taken into account when formulating a pseudo-dynamic problem. First, the design variables must remain constant for all different scenarios and therefore they are *time-invariant* variables. On the other hand, the control variables are allowed to change from one scenario to another. For steady-state process models, the control variables must remain constant during each scenario and are therefore known as *piecewise constant* variables. This is illustrated in figure 5.2.

In dynamic optimisation, two types of constraints are used: *end-point* and *interior-point constraints*. End-point constraints are used to specify limits or restrictions to be met at the end of the time, or pseudo-time, horizon. These constraints are typically used for key performance indicators such as product quality or final temperature. On the other hand, interior point constraints are used to specify limits or restrictions that must be met at some specific points within the time, or pseudo-time, horizon. These constraints are used to restrict the operation within specified limits at certain times before the end of the operation, *e.g.* by setting a maximum temperature limit at the end of a cooling phase.

In the proposed approach, all the constraints listed in stochastic problem (5.1) must be met in all scenarios. The performance of the process under each scenario is evaluated at the end of the time period corresponding to that scenario. Thus, to ensure that the "interior" scenarios meet the constraints, it suffices to impose those constraints at the end of the time period for each scenario. Therefore, interior-point constraints should be used.

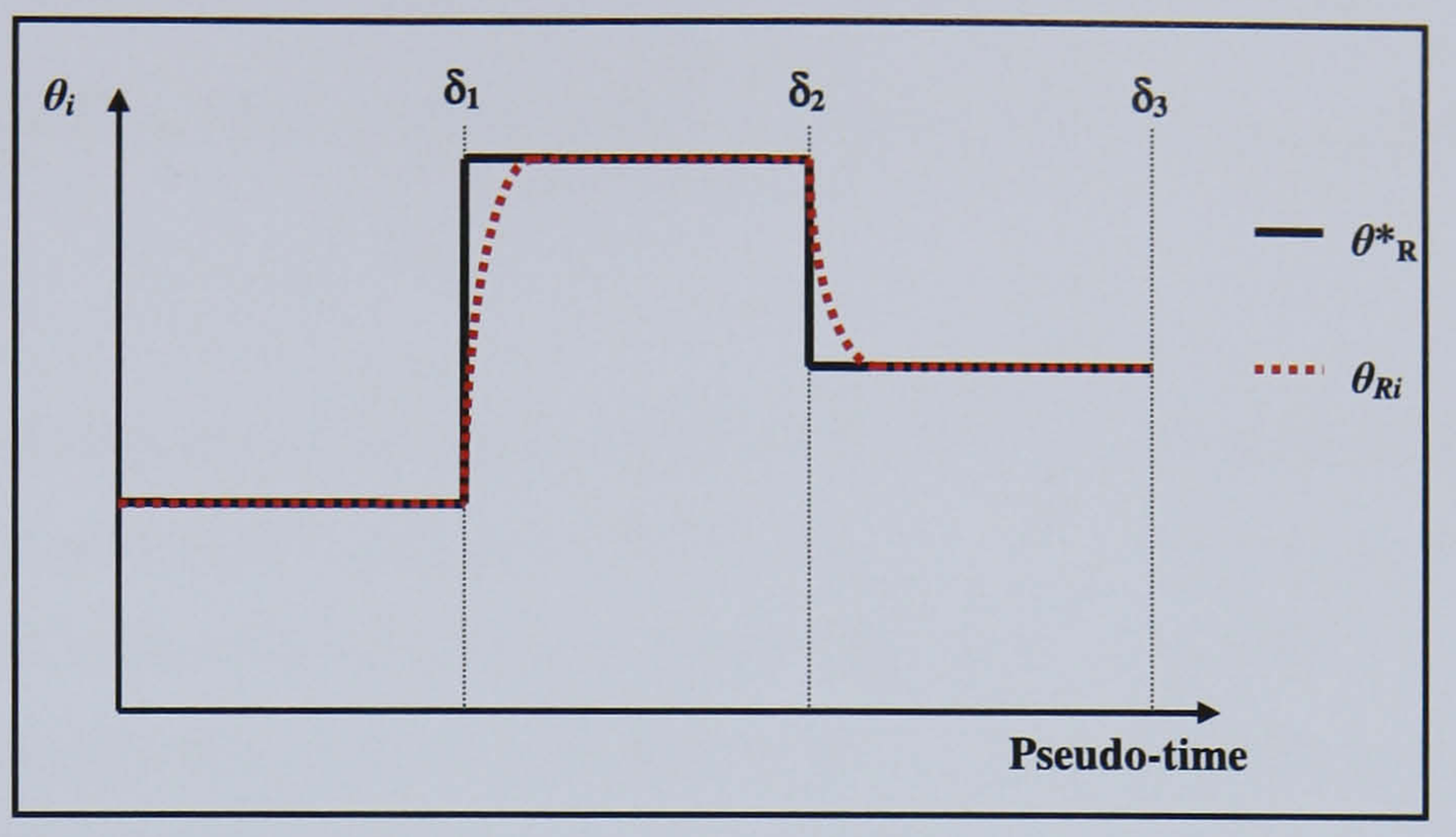


Figure 5.3: Homotopy approach

The pseudo-dynamic approach facilitates problem initialisation by allowing a single set of initial guesses to be used for all scenarios. However, the step changes in parameter values between two adjacent scenarios could give rise to numerical problems similar to those encountered in the standard formulation (5.2). These numerical difficulties can be avoided by using a homotopy or continuation technique to vary the value of the uncertain parameter θ_j from a value $\theta_{j,i-1}$ at time δ_i to a value $\theta_{j,i}$ at time δ_i:

$$\begin{aligned} k\frac{d\theta_j}{dt} &= \theta_{j,i} - \theta_j(t), \quad t \in (\delta_{i-1}, \delta_i] \\ \theta_j(t = \delta_{i-1}) &= \theta_{j,i-1} \end{aligned} \tag{5.4}$$

The continuation technique allows smooth transitions between the scenarios. k is a constant defining how fast θ_j follows the "set-point" value, $\theta_{j,i}$. The length of each interval is chosen to be large enough so that all the parameters and variables have converged to constant values by the end of the interval. Figure 5.3 illustrates this approach graphically.

The mathematical formulation of the pseudo-dynamic optimisation problem is shown

below:

$$\max_{d,u} E_{\theta\in\Theta}\left\{\Phi(d,u,\theta)\right\} \approx \max_{d,u(t)} \frac{1}{\tau}\int_0^{\tau} \Phi(d,u(t),x(z),x_z(z),x_{zz}(z),\theta(t))\,dt \tag{5.5}$$

s.t.

$$\begin{aligned}
&f(d,u(t),x(z),x_z(z),x_{zz}(z),\theta(t)) = 0, && \forall\, t\in[0,\tau], \forall z\in\Omega\\
&h(d,u(t),x(z),x_z(z),x_{zz}(z),\theta(t)) = 0, && \forall\, t\in[0,\tau], \forall z\in\Gamma(\Omega)\\
&C(d,u(0),x(z),x_z(z),x_{zz}(z),\theta(0)) = 0, && \forall z\in\Omega\\
&g(d,u(t),x(z),x_z(z),x_{zz}(z),\theta(t)) \le 0, && \forall\, t\in[0,\tau], \forall z\in\Omega\\
&g_i(d,u(\delta_i),x(z),x_z(z),x_{zz}(z),\theta(\delta_i)) \le 0,\\
&\qquad i=1\ldots N,\ \forall\,\delta_i\in[0,\tau], \forall z\in\Omega\\
&y = \mathcal{Y}(d,u(t),x(z),x_z(z),x_{zz}(z),\theta(t)) && \forall\, t\in[0,\tau], \forall z\in\Omega\\
&\theta(\delta_i) = \theta(t), && i=1\ldots N\\
&0\le\delta_{i-1}\le\delta_i\le\delta_N=\tau, && i=1\ldots N\\
&u^{min}(d)\le u(t)\le u^{max}(d), && \forall\, t\in[0,\tau]\\
&d^{min}\le d\le d^{max}\\
&k\frac{d\theta}{dt} = \theta^{\star}-\theta\\
&d\in D,\ u\in U,\ x\in X
\end{aligned}$$

The equality constraints describing the mass and energy balances for the process, f, are usually a mixed system of partial differential and algebraic equations. The use of partial and differential equations requires boundary and initial conditions which are specified by h and C, respectively, where $\Gamma(\Omega)$ represents the boundary limit for the spatial domain. Inequality constraints, g, define *end-point* or *path* constraints, providing limits or restrictions on the process, which must be met at the end of the operation and at all points in the pseudo-time domain, [0,τ]. The *interior-point* constraints, g_i, need to be met only at discrete points δ_i within the pseudo-time domain τ. The uncertain parameters, $\theta(t)$, have a profile in the "pseudo-time" domain corresponding to the sample points, $\theta(\delta_i)$. Each "pseudo-time" interval is bounded by the discrete time δ_{i-1} and δ_i. Finally, the bounds for the control variable vector, u, can be dependent on the design variables, d.

The objective function is defined as the average of function Φ over the pseudo-time domain $[0,\tau]$. The duration of each scenario and the value of k must be chosen to ne-

glect the transient periods between scenarios in the calculation of the objective function. Systems with a slow transition need a longer scenario duration.

The solution of this problem requires two steps: the solution of the PDAE system and the optimisation of the dynamic problem. A brief review of these methods can be found in appendix A. It yields the optimal values of the design variables and, for each scenario, of the control variables which maximise the approximation of the expected value of the objective function.

The use of the pseudo-time representation leads to a natural decomposition of the problem. It provides a robust initialisation strategy to assess the performance of the process for different uncertain parameter realisations. The use of this technique ensures numerical robustness when tackling large nonlinear problems. Nevertheless, the number of scenarios that can be employed is still limited by the available computational resources. Therefore, a good sampling approach is necessary to maximise the accuracy of the solution with a limited number of scenarios. The following section shows how to reduce the number of scenarios in the formulation using the GSFA results.

5.3 Scenario Generation

The objective function being considered is an expected value. Its calculation involves the solution of a multidimensional integral over the uncertain parameter space which is approximated through the generation of scenarios:

$$E_{\Theta}\{\Phi(\theta)\} = \lim_{N\to\infty} \frac{1}{N}\sum_{i=1}^{N}\Phi(\theta_i) \approx \frac{1}{N}\sum_{i=1}^{N}\Phi(\theta_i) \tag{5.6}$$

where the approximation on the right hand side improves as the number of samples is increased.

5.3.1 Reduction of scenarios using first-order sensitivity indices

It is assumed in equation (5.6) that the scenarios are obtained by sampling the full uncertain parameter space, Θ. However, the result of the GSFA can be used to reduce the dimensionality of this space. The first-order sensitivity indices give a measure of the relative importance of the uncertain parameters and therefore allows the identification of a subset of critical parameters, which most influence the KPIs and/or the feasibility of the

process. A reduced uncertain space, Θ_R, can be constructed using the subset of critical parameters. Parameters that are not critical can be fixed at their nominal values and the expected value of the objective function can be computed over the reduced parameter space: $E_{\Theta_R}\{\Phi(\theta)\}$. The objective function for the pseudo-time dynamic optimisation problem can then be re-defined as follows:

$$\frac{1}{\tau}\int_0^{\tau} \Phi(d, u(t), x(z), x_z(z), x_{zz}(z), \theta_R(t))\, dt \tag{5.7}$$

Even with a reduction of the uncertain parameter space, the number of scenarios remains a limiting factor in the scenario-based optimisation. Therefore, special care must be taken to select representative scenarios from the uncertain parameter space. To illustrate this problem, consider the case where a normal distribution is used to generate scenarios. More points are taken in the vicinity of the most probable value. With a limited number of scenarios, especially when there is a large number of uncertain parameters, regions with lower probability may not be explored at all, reducing the confidence in the scenario-based optimisation results. In the worst case, an infeasible region or a region of very poor performance could exist in the unexplored area, and not taking this into account would generate misleading results. With the proposed methodology, this problem would be identified during the course of GSFA for the optimal stochastic design. A new design would then need to be generated by formulating and solving another scenario-based problem. Hence, although the problem can be rectified through further iterations of Step 3 of the methodology, a poor choice of scenarios can result in significant computational effort being wasted.

It is therefore important to use efficient sampling techniques when the number of scenarios is limited to have a good coverage of the uncertain parameter space. As explained in section 4.2.3, the uniform and low discrepancy sequences are good options in terms of space coverage. They can be used to achieve a given accuracy in the estimation of the expected value with fewer scenarios than random sampling techniques. However, statistically, they only represent parameters with uniform probability distribution functions. This limitation can be overcome by introducing a weight factor, w_i, when using these sampling techniques. This weight factor is the probability of the scenario according to the relevant probability distribution function:

$$\sum_{i=1}^{N} w_i \Phi(\theta_{R_i}) = \int_0^{\tau} w(t)\Phi(\theta_R(t))dt \tag{5.8}$$

So far, a reduction of the size of the scenario-based problem has been achieved with two methods. Firstly, the scenarios are generated from a reduced critical parameter space, Θ_R, identified in the global sensitivity/feasibility analysis. Secondly a broad exploration of the uncertain space is obtained with few scenarios by combining a low discrepancy sequence and weight factors.

5.3.2 Reduction of scenarios using higher-order sensitivity indices

In some cases, a further scenario reduction can be achieved with additional information obtained in the GSFA. This reduction is possible in systems where parameter interactions have no or little effect on the key performance indicators.

To illustrate this, suppose we want to calculate the expected value of a two-parameter function $\Phi(\theta_1, \theta_2)$. Its ANOVA representation is given as follows:

$$E_\Theta \{\Phi(\theta_1, \theta_2)\} = E_\Theta \{\Phi_1(\theta_1) + \Phi_2(\theta_2) + \Phi_{12}(\theta_1, \theta_2)\} \tag{5.9}$$

If the combined effect of parameters θ_1 and θ_2 is negligible, the last term in equation (5.9), Φ_{12}, can be eliminated without any significant effect on the expected value of Φ:

$$E_\Theta \{\Phi(\theta_1, \theta_2)\} \approx E_\Theta \{\Phi_1(\theta_1) + \Phi_2(\theta_2)\} \approx E_\Theta \{\Phi_1(\theta_1)\} + E_\Theta \{\Phi_2(\theta_2)\} \tag{5.10}$$

Due to this low interaction we can use a reduced sampling approach to evaluate the expected value of the above function. This can be seen graphically in figure 5.4. Figure 5.4a shows a 6×6 uniform grid of points which could be used to evaluate the expected value. Taking advantage of the low parameter interaction, we could reduce this grid of 36 points to a sampling sequence of 11 points, as shown in figure 5.4b. This approach samples the space along each parameter domain independently.

The GSFA step, described in the previous chapter, can be used to calculate higher-order interactions. In many cases, the GSFA will show no higher-order effects and the critical uncertain parameters can be sampled independently as shown in the above example. In some other cases, there may be important interactions, which exist only between some of the critical parameters. In the worst case, all interactions between critical uncertain parameters will need to be considered.

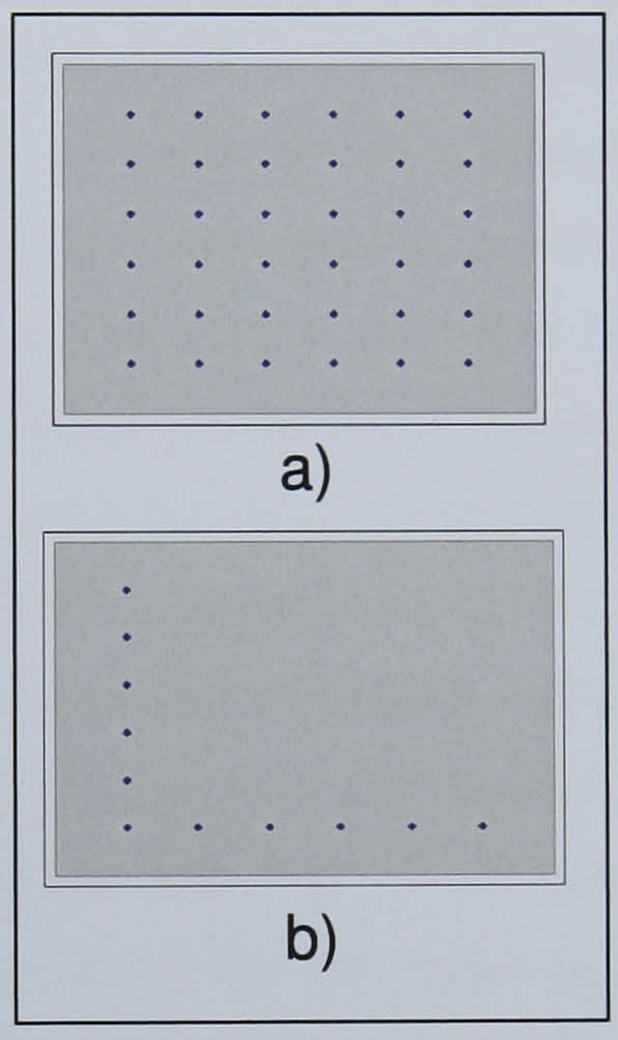


Figure 5.4: Representation of scenario reduction in a 2-dimensional space: a) a uniform grid is used to capture interactions between parameters; b) the number of sample points is reduced when a second-order sensitivity index calculation indicates there is no interaction between parameters.

5.4 Summary

The algorithm presented in this chapter is an alternative scenario-based optimisation approach which allows large dimensional problems to be tackled. It can be used in cases where the complexity of the problem and/or available resources limit the number of sample points that can be used. The algorithm is a combination of different approaches which help to reduce the complexity of the problem.

The first idea is based on the formulation of a pseudo-dynamic optimisation problem. This approach is useful to achieve the numerical robustness needed in complex problems. Its use means a single initialisation point is needed, whereas in the traditional approach up to n sets of initial points may be required for n scenarios.

The results of the GSFA step are then used to generate a reduced number of sample points. The global sensitivity indices give a measure of the relative importance of the different uncertain parameters. Based on these results, a subset of critical parameters can be identified. The sampling can then be done on the reduced uncertain space.

Based also on results of the GSFA, specific sampling patterns can be generated to reduce the number of scenarios in the pseudo-dynamic approach in the absence of parameter interactions. Furthermore, since the maximum number of scenarios is limited, a Sobol' sampling is proposed to generate the different scenarios. This sampling has a better coverage of the uncertain parameter space for the same number of points than many other sampling techniques (*e.g.* random, uniform or normal). It also improves the evaluation of the expected values when using *quasi*-Monte Carlo techniques. To map the statistical definition of the uncertain parameter space when using this low-discrepancy sequence, a weight factor is introduced in the problem formulation.

Chapter 6

Case Study

6.1 Overview

A case study was selected to apply the methodology described in the previous chapters and identify the key issues in decision-making under technological risk. This case study consists of a phosgene reactor design problem in which the main objectives are:

- to quantify the inherent risk for a given parameter uncertainty,
- to identify critical parameters affecting key performance indicators,
- to find the design that maximises profit for a given parameter uncertainty.

Two different cases are studied by changing the uncertain parameter distributions (uniform and normal). The problem definition and the results obtained after applying the proposed methodology are shown in the following sections.

6.2 Catalytic Tubular Reactor

Phosgene is a raw material in the manufacture of diisocynates which are widely used in the polyurethane industry. It is produced industrially by passing carbon monoxide and chlorine over an activated carbon bed in a tubular reactor (figure 6.1). The reaction is highly exothermic and heat is removed by water or another cooling agent. The process pressure is atmospheric, with a temperature at the inlet of around 673 K which then

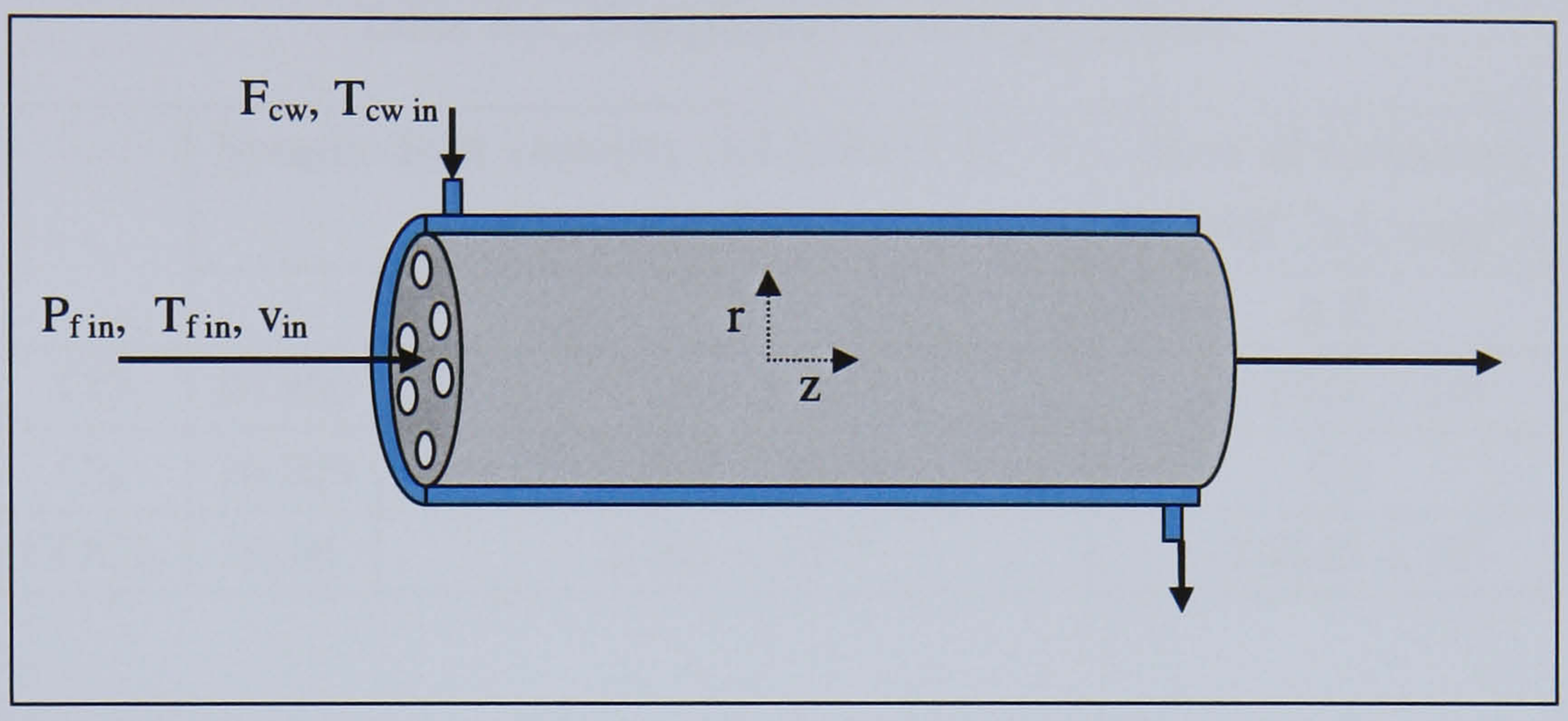


Figure 6.1: Schematic of catalytic tubular reactor

falls to around 313 - 423 K at the reactor exit (Schneider and Diller, 2002; Ministry of Munitions, 1920; Jacqué, 1928).

6.2.1 Description and data

The reaction carried out in the gas phase within a jacketed tubular reactor, as depicted in figure 6.1, is:

$$CO_{(g)} + Cl_{2(g)} \rightarrow COCl_{2(g)} \tag{6.1}$$

Physical properties

The physical properties of the species in the system are shown in table 6.1.

Reaction kinetics

The reaction rate, *Rate* (in kmol kg-catalyst^{-1} h^{-1}), is described by a kinetic expression of the form:

$$Rate = \frac{k_r K_{CO} K_{Cl_2} pp_{CO} pp_{Cl_2}}{(1 + K_{CO} pp_{CO} + K_{Cl_2} pp_{Cl_2} + K_{COCl_2} pp_{COCl_2})^2} \tag{6.2}$$

where pp_i denotes the partial pressure of species i (in kPa). The rate and equilibrium constants, k_r and K_i respectively, follow an Arrhenius-type relationship with respect to

Table 6.1: Gas-phase physical properties

	Specific heat capacity (kJ kmol^{-1} K^{-1}) $C_p = \alpha + \beta T$		Heat of formation @ 298K (kJ kmol^{-1})
	α	β	ΔH_f
CO	30.869	-1.285×10^{-2}	-1.1044×10^5
Cl_2	26.929	3.883×10^{-2}	0.0
$COCl_2$	60.66	2.463×10^{-2}	-2.2285×10^5

Table 6.2: Reaction kinetics

	A (kmol kg-catalyst^{-1}h^{-1})	Ek (kPa m^3 kmol^{-1})
k_r	0.127521	57686.3
K_{CO}	100	20000
K_{Cl_2}	100	-26233.3
K_{COCl_2}	141.819	6000

temperature, T, of the form $A \cdot exp(-Ek/RG \cdot T)$, where RG is the universal gas constant. The constants A and Ek are given in table 6.2. The physical properties and reaction kinetics described above were chosen arbitrarily.

Due to noticeable phosgene decomposition at high temperatures (Gordon and Goland, 1957), the maximum temperature allowed inside the reactor is 673 K.

Reactor characteristics and operating conditions

The following data is taken from Perry and Green (1997), unless otherwise indicated. The reactor contains a fixed catalyst bed with a density, ρ_{Bed}, of 800 kg m^{-3} and a specific heat capacity, C_{pBed}, of 0.85 kJ kg^{-1}K^{-1}. Carbon monoxide and chlorine gas at 293 K are fed to the reactor at a velocity, Vel, of 0.02 m s^{-1} and partial pressures of 80 and 40 kPa, respectively. The carbon monoxide is fed in excess to serve as a heat sink to avoid high temperatures in the reactor. The high temperature is the result of the high heat of formation for phosgene. For simulation purposes, the reactor is initially at 293 K and contains only carbon monoxide at 120 kPa. Further data are listed in table 6.3.

Table 6.3: Data for the gas stream

Axial and radial thermal dispersion coefficients (kz, kr) $kWm^{-1}K^{-1}$	5×10^{-2}
Radial dispersion coefficient (Dr) m^2s^{-1}	1×10^{-3}
Axial dispersion coefficient (Dz) m^2s^{-1}	1×10^{-2}
Void fraction (ϵ)	0.35

Temperature control system

A water jacket is used to add thermal stability to the reactor. The temperature of the reactor can be manipulated by controlling the flowrate of the cooling water, F_{cwin}, through the jacket. Water is available on site at a temperature of 293 K. The overall heat transfer coefficient, U, between the tubular reactor and the cooling jacket is 96 J $m^{-2}K^{-1}$. The volume of the cooling jacket, V_{cw}, is $0.4m^3$ and the mass flowrate of water through the jacket is 1 kg s^{-1}. The density, ρ_{cw}, is 1000 kg m^{-3} and the specific heat capacity, $C_{p_{cw}}$, is 4.2 kJ $kg^{-1}K^{-1}$. The axial thermal dispersion coefficient, kz_{cw}, is 6 x 10^{-4} kW $m^{-1}K^{-1}$.

Cost evaluation

The objective function for the optimisation is the maximisation of annualised profit. Profit is evaluated by taking into account the product sales revenue and annualised reactor, raw material and cooling water costs, as shown in table 6.4. When calculating raw material costs, it is assumed that unreacted material is recycled to the reactor. The raw material expenses include cost incurred for recycling unreacted material at 50% of the raw material cost, see equation (C.22).

$$Profit = Revenue - Cost_{reac} - Cost_{Raw\ material} - Cost_{Cooling\ water} \tag{6.3}$$

The PDAEs describing the reactor shown in figure 6.1 can be found in appendix C. The analysis was done on the steady-state operation and ideal gas behaviour is assumed.

6.2.2 Description of the uncertainty

The uncertain parameters are defined in table 6.5. Two cases are considered: in the uniform case, all parameters vary uniformly within a set range of ±10% or ±1%; in the

Table 6.4: Cost data

Reactor cost (MUSD/yr)	$100V_{reac}^{0.6}$
Cooling water cost	0.001 USD kg^{-1}
Product price	1.0 USD kg^{-1} $COCl_2$
Carbon monoxide cost	0.016 USD kg^{-1} CO
Chlorine cost	0.051 USD kg^{-1} Cl_2

Table 6.5: 8 Uncertain parameters

Parameter	Mean	Range % (uniform)	Std Dev % (normal)
$\Delta H_{f(CO)}$ (kJ $kmol^{-1}$)	-110440	± 10	3.0
$\Delta H_{f(COCl_2)}$ (kJ $kmol^{-1}$)	-222850	± 10	3.0
Ek_r (kPa m^3 $kmol^{-1}$)	57686.3	± 10	3.0
kr (kW $m^{-1}K^{-1}$)	0.05	± 10	3.0
kz (kW $m^{-1}K^{-1}$)	0.05	± 10	3.0
U (kJ $m^{-2}K^{-1}$)	0.096	± 10	3.0
T_{cwin} (K)	293	± 1	0.3
T_{in} (K)	293	± 1	0.3

normal case, all the parameters are normally distributed with the standard deviations listed in the table. The mean parameter values are the same for both cases. In the normal case, the range used to define the parameter space for the purpose of sampling was $\pm 3\sigma$, in order to cover 99% of the uncertainty range.

It can be seen that the first six parameters are model-related and their uncertainty could be reduced by spending in further R&D. Process-related parameters, the feed stream inlet temperature, T_{in}, and the cooling water inlet temperature, T_{cwin}, are shown in the last two rows for which the uncertainty could be reduced by additional control equipment.

All the simulations and optimisation problems were solved using gPROMS v2.3.6 (Process Systems Enterprise Ltd.), which is an equation-oriented modelling tool. The set of PDAEs was solved by discretising the distributed equations with respect to the spatial do-

mains using the method-of-lines (Schiesser, 1991). The spatial discretisation used for the axial and radial domains was the Centre Finite Difference Method (CFDM) with a second-order approximation. The number of partition elements was 50 for the axial direction and 5 for the radial direction.

In the following sections, two iterations of the overall approach presented in figure 3.1 are considered.

6.3 Iteration I

6.3.1 Deterministic optimisation

In this first step the values of the uncertain parameters are fixed to their nominal or mean values and a set of performance constraints is added to the model. The upper and lower bounds on the product flowrate are 600 and 480 MT/yr of phosgene respectively. The maximum temperature allowed along the reactor wall is 673 K. The outlet stream temperature should be less than 323 K while the cooling water outlet temperature should not exceed 323 K. The ratio of the cooling jacket to reactor diameter should be between 1.05 and 3. The pp_{inCO} to pp_{inCl_2} ratio should be between 1.0 and 1.5, and the inlet pressure range is 100 to 150 kPa. The annual operating time is 8000 hours.

The control variables to be determined in the optimisation are the feed stream velocity (Vel), cooling water flowrate (F_{cw}), and partial pressures of raw material (pp_{in1} and pp_{in2}). The design variables are the reactor length RZ, reactor radius RZ and cooling jacket radius RCW.

Due to the complexity of the model, an initialisation file is needed in the optimisation algorithm. This file is generated running a dynamic simulation of the model since, numerically speaking, it is easier to run a dynamic model than a steady state. The values chosen for the reactor length and diameter in this simulation are 5 m and 0.4 m respectively.

The results for the deterministic optimisation are obtained after 19 NLP iterations with a CPU time of 50 seconds on a 3.0 GHz Pentium 4 processor. There are 56 equations. However, some of these equations are distributed over the axial and radial domains and, therefore, the total number of equations for the chosen number of partition elements is 5897. The optimisation solver used in gPROMS is CVP_SS, with DASOLV for solving differential-algebraic equations (PSE Ltd., 2004b). The value of the objective function is

Table 6.6: Optimal design and control variables in nominal design for Iteration I

Variable	Value	Lower bound	Upper bound
RZ (m)	1.403	0.5	5
RR (m)	0.357	0.05	2
RCW (m)	0.375	0.05	3
F_{cw} (kg/s)	0.379	0.0	10.0
Vel (m/s)	0.0256	0.001	5.0
pp_{CO} (kPa)	50	10	100
pp_{Cl_2} (kPa)	50	10	100

489,590 USD/yr. The values of the design and control variables are shown in table 6.6.

The above results show the local optimal performance of the reactor in the absence of uncertainty in the parameters. While this result is optimal for the given nominal values, it may not provide the optimal design and operation for the given uncertainty. These results are now used as a starting point for the remaining steps of the methodology.

6.3.2 First stochastic design - GSFA

The first stochastic design step is now undertaken, as shown in figure 3.2. This begins with a global sensitivity/feasibiligy analysis (GSFA) of the current design. It is applied to deterministic design for the case study as explained in chapter 4. The results obtained after applying a simple one-at-a-time parameter analysis using a simulation-based approach are shown in the first section. These results are then compared in the second section to those obtained with the global sensitivity analysis using the proposed optimisation-based approach.

Simulation-based global sensitivity analysis

The one-at-a-time global sensitivity analysis was performed by changing the value of one uncertain parameter while fixing the rest at their nominal values. The sampled points were generated using a Sobol' sampling technique and every point was simulated in gPROMS. The objective function was penalised by adding various terms corresponding to the viola-

Table 6.7: One-at-a-time sensitivity analysis results for simulation-based approach

Parameter	Mean value of penalised profit, × 1000 USD/yr	Std. dev. × 1000 USD/yr	Rank
$\Delta H_{f(CO)}$	489.578	0.0107	4
$\Delta H_{f(COCl_2)}$	489.463	0.1689	2
Ek_r	489.550	0.0159	3
kr	489.584	0.0008	7
kz	489.581	0.0070	5
U	489.583	0.0013	6
T_{cwin}	489.585	0.0	8
T_{in}	489.615	0.1756	1

tions of the different process constraints (eq. 6.4). The analysis was done for 1024 Sobol' points for each parameter and the results can be seen in table 6.7.

$$
\begin{aligned}
Profit &= Revenues - C_{reactor} - C_{raw\ material} - C_{cw} - T_{max} - T_{maxend} - T_{cwend} \\
T_{max} &= \int_0^{RZ} max(0,\ T(z,1) - 673)\ dz \\
T_{maxend} &= max(0,\ T(RZ,0) - 323) \\
T_{cwend} &= max(0,\ T_{cw}(RZ) - 323)
\end{aligned}
\tag{6.4}
$$

The simulation-based sensitivity analysis shows that the feed stream temperature is the parameter which affects the penalised profit most, followed by the phosgene heat of formation.

This effect can be explained as follows. The feed stream temperature, T_{in}, has a direct effect on the initial concentration, $C_{i_{in}}$, for a given initial partial pressure, as shown in equation (C.12). The lower the inlet temperature the higher the initial concentration for a fixed feed partial pressure, $pp_{i_{in}}$. Due to the rapid and highly exothermic reaction taking

place, more raw material available for the reaction means higher production rate and more heat generated. Therefore there is an impact on the objective function in the form of raw material costs, revenues for product sales and the penalty incurred by violation of the maximum temperature constraint.

The heat of formation of phosgene, ΔH_{fCOCl_2}, is the second parameter most affecting the objective function. This parameter changes the term penalising the maximum allowed temperature inside the reactor, T_{max}, as it is the main contributor in this constraint. At the nominal solution, the constraint is active. Any value of ΔH_{fCOCl_2} greater than the nominal value (-222850 kJ kmol^{-1}) leads to constraint violation.

A similar effect can be observed in the heat of formation of carbon monoxide, ΔH_{fCO}. This parameter also affects the maximum allowed temperature inside the reactor, but with the opposite effect when compared to the phosgene heat of formation, since carbon monoxide is a reactant. The value of T_{max} increases for absolute parameter values below the mean (-110440 kJ kmol^{-1}).

If these results were to be used to identify ways in which the impact of uncertainty may be reduced, the decision may be to target the uncertainty in the feed stream temperature to reduce the range of the performance measure. However, the results show that the variation obtained for the different uncertain parameter values is negligible, with a standard deviation less than 175.6 USD/yr.

The simple one-at-a-time analysis does not include the analysis of parameter interactions. Every sampled point deviates from the nominal value by the value of one parameter only. Furthermore, the values of the control variables were fixed at the optimal values obtained in the deterministic optimisation. This may not be the best approach since the reactor's flexibility is not being used. Clearly, the effect of variations in the feed stream temperature could be controlled by a combination of actions in the control variables. The following section shows the results obtained after using the proposed optimisation-based approach, which addresses some of these issues.

Optimisation-based global sensitivity/feasibility analysis and risk quantification

The global sensitivity analysis with the optimisation-based approach presented in chapter 4 is used to quantify the risk and rank the different uncertain parameters in terms of their influence on the profit and KPIs. The analysis makes use of the reactor's flexibility by

Table 6.8: GSFA results for first-order Sobol' indices for the nominal design in iteration I (uniform case)

Parameter	Individual sensitivity indices, S_i	Total sensitivity indices, S_i^{Tot}	Rank
$\Delta H_{f(CO)}$	0.0842	0.3199	2
$\Delta H_{f(COCl_2)}$	0.5555	0.8656	1
Ek_r	-0.0269	0.0134	6
kr	-0.0687	0.0295	5
kz	-0.0296	0.0763	3
U	-0.0247	0.0587	4
T_{cwin}	-0.0307	0.0073	7
T_{in}	-0.0275	0.0031	8

allowing the control variables to best deal with the parameter values at the point being analysed.

The problem solved for every sampled point was similar to that specified for the deterministic optimisation. The sensitivity analysis was done using the parallel implementation running on a Linux Beowulf cluster.

Uniform case The results for the first-order individual and total sensitivity indices can be seen in table 6.8. They were obtained after running 4096, or 2^{12}, Sobol' points. This number was chosen since the index values had converged at this stage. The next iteration would have required 2^{13} or 8192 points, doubling computation time. As mentioned in section 4.4, the total number of optimisation problems to solve depends directly on the number of sensitivity indices. For this case study a total of 69,632 problems were solved ($4096\times(2\times8+1)$). The computational time required was 62 hours and 9 minutes on 17 Linux machines ranging from 1.79 to 3.39 GHz.

As shown in tables 6.7 and 6.8, the ranking of the uncertain parameters with this approach is different from the one obtained in the simulation-based analysis. The ranking is based on the value of the total sensitivity indices. It can be seen that the feed stream temperature, which was ranked first in the simulation-based analysis, is now the least

Table 6.9: GSFA results for higher-order Sobol' indices for the nominal design in iteration I

Parameter i	Group sensitivity index, S_i^g	Total group sensitivity index, S_i^{Tot}
$\Delta H_{f(CO)}$-$\Delta H_{f(COCl_2)}$	0.8532	0.9883

important parameter. This new ranking is the result of the control variable values being modified to optimise the operation and to meet the specified constraints. This result means that the variation in the feed stream temperature can be controlled by the selected control variables and has no effect on the annualised profit.

The individual sensitivity indices in table 6.8 are negative for six parameters. As mentioned in chapter 4, the approximation used looses accuracy for values close to 0, which results in these negative values. The corresponding total sensitivity indices, which account for interactions with other parameters as well as the individual indices, also show low, but positive, values. In general, the total indices are easier to approximate since they are the accumulated effect of the given parameter and its higher-order interactions, which is usually a higher value than the individual index.

If the individual indices are compared to the total ones, it is seen that there is a significant higher-order effect for the heats of formation of carbon monoxide and phosgene. This higher-order effect can be easily calculated by the difference between the individual and total index values. However, to determine which parameters are involved in this interaction, a new sensitivity analysis is needed. Rather than considering all possible binary contributions of the parameters, the new analysis is performed to calculate the second-order interaction between the heat of formations, since these have the highest higher-order indices.

The calculation was carried out for 4096 Sobol' points, requiring the solution of 12,288 optimisation problems ($4096\times(2\times1+1)$). The results are shown in table 6.9. Seventeen parallel processes were used and the computational time was 12 hours and 12 minutes.

The total group index shown in table 6.9 includes all the contributions in which the heat of formation parameters appear. The group index value for $\Delta H_{f(CO)}$-$\Delta H_{f(COCl_2)}$ is the cumulative effect of the individual indices for $\Delta H_{f(CO)}$ and $\Delta H_{f(COCl_2)}$ plus the

interaction between them. Therefore, the second-order sensitivity index has a value of:

$$S_{\Delta H_{f(CO)}-\Delta H_{f(COCl_2)}} = S_i^g - \sum S_i = 0.2135$$

which shows a significant effect given by this interaction. The value for the total group sensitivity index (0.9883) shows that the profit is affected mainly by these two parameters. The main contribution is attributed to the individual effect of the heat of reaction of phosgene (0.5555), followed by its interaction with the heat of formation of carbon monoxide (0.2135) and finally, the individual contribution of the latter one (0.0842).

So far, the values obtained from the global sensitivity analysis provide a way to rank the effect of the individual uncertain parameters and their interactions. However, these values, defined as the ratio of the individual or interacting variance to the total variance, only provide a relative measure. One may need additional information to quantify the absolute effect of the uncertain parameters on the key performance indicators. One such measure can be given by the total variance, D, which is the denominator in the calculation of all sensitivity indices. In this case, the value of the variance is 1,133,896 $(\text{USD/yr})^2$, corresponding to a standard deviation of 33,670 USD/yr.

A more refined analysis can be obtained based on the results of the thousands of optimisation problems solved. The sampling and evaluation of nearly 70,000 points for the individual indices and 12,000 points for the higher-order index is a good exploration of the uncertain parameter space. The solution at every point, if it is feasible, provides the value of the key performance indicators and the control variables. A risk evaluation can be performed by analysing the histograms for the different KPIs.

The probability distribution for the annualised profit is shown in figure 6.2. The mean annualised profit is 467,810 USD/yr, with a standard deviation of 34,390 USD/yr, which is in reasonable agreement with the value of 33,670 USD/yr calculated in the sensitivity analysis. There is a high probability that the expected profit will fall in a range between 485,000 and 495,000 USD/yr as shown in the graph. There is also, however, a long tail of low profit values with a large cumulative probability. This can be predicted based on mean and standard deviation only and highlights the usefulness of the histograms.

Similar graphs can be plotted for the different control variables and any other key performance indicators. Figures 6.3 to 6.6 show histograms for these four control variables. This information can be useful to analyse the impact on the design of control equipment. The mean value and standard deviation of the KPIs are shown in table 6.10.

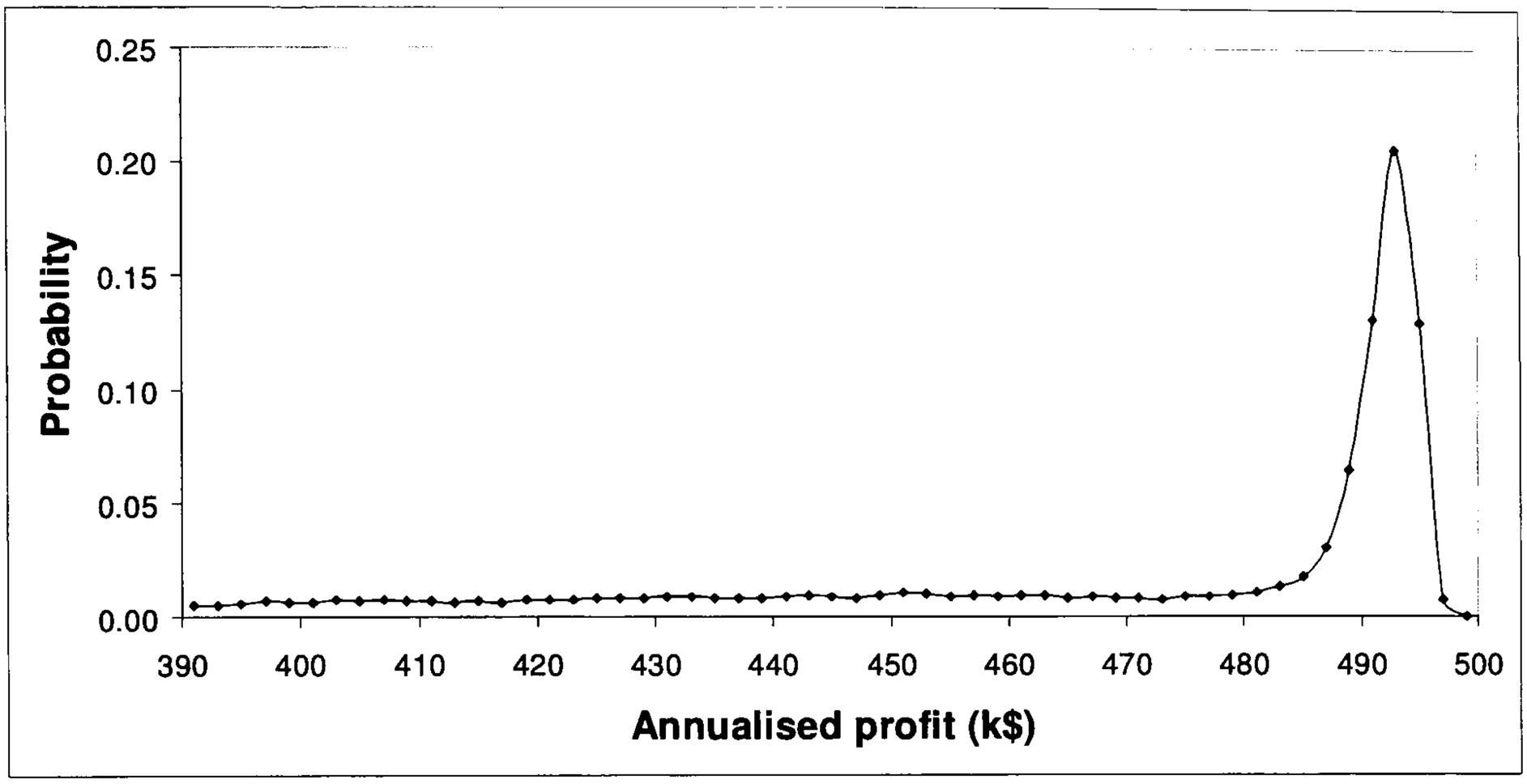


Figure 6.2: Annualised profit probability distribution for the nominal design in iteration I (uniform case)

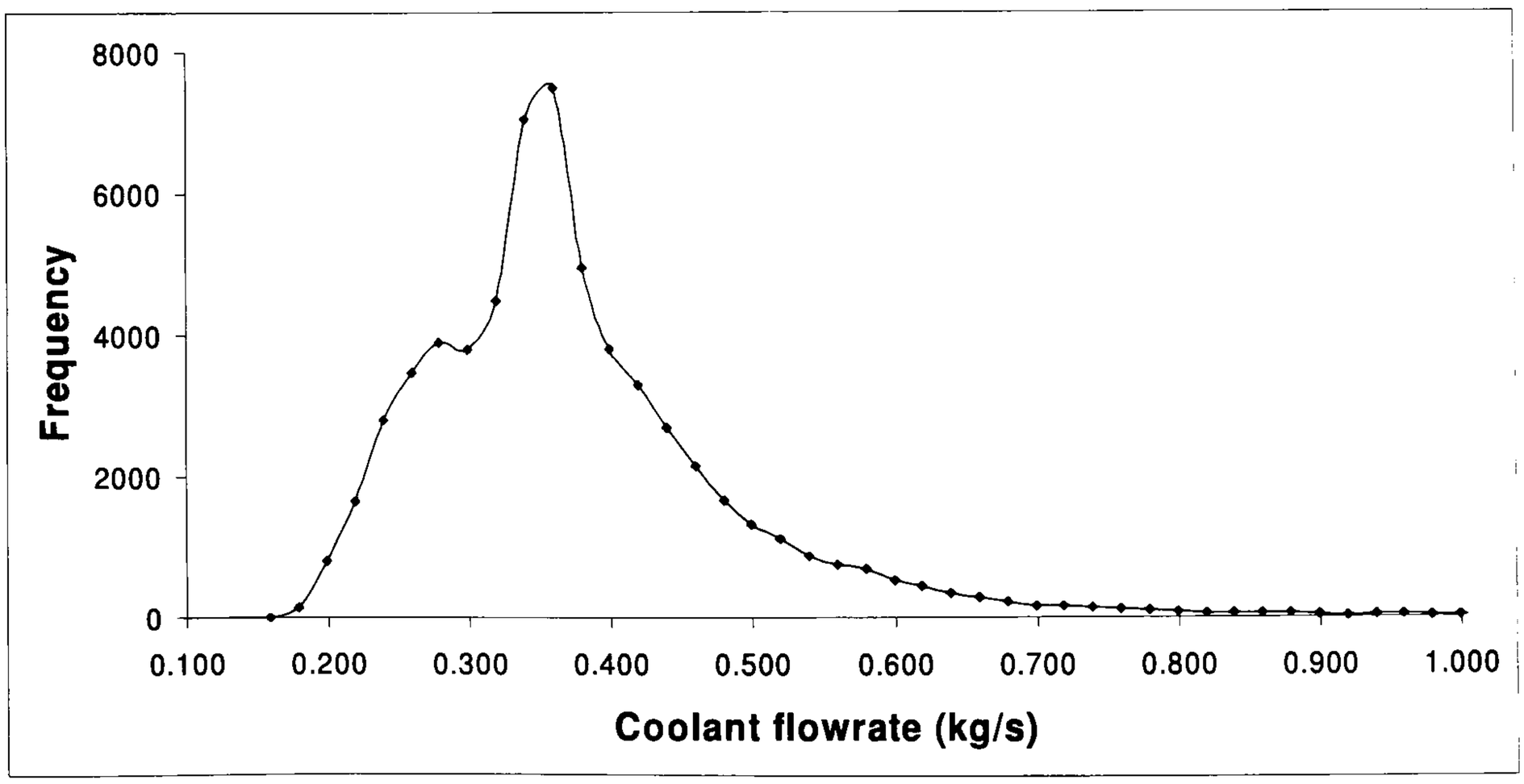


Figure 6.3: Coolant flowrate histogram for the nominal design in iteration I (uniform case)

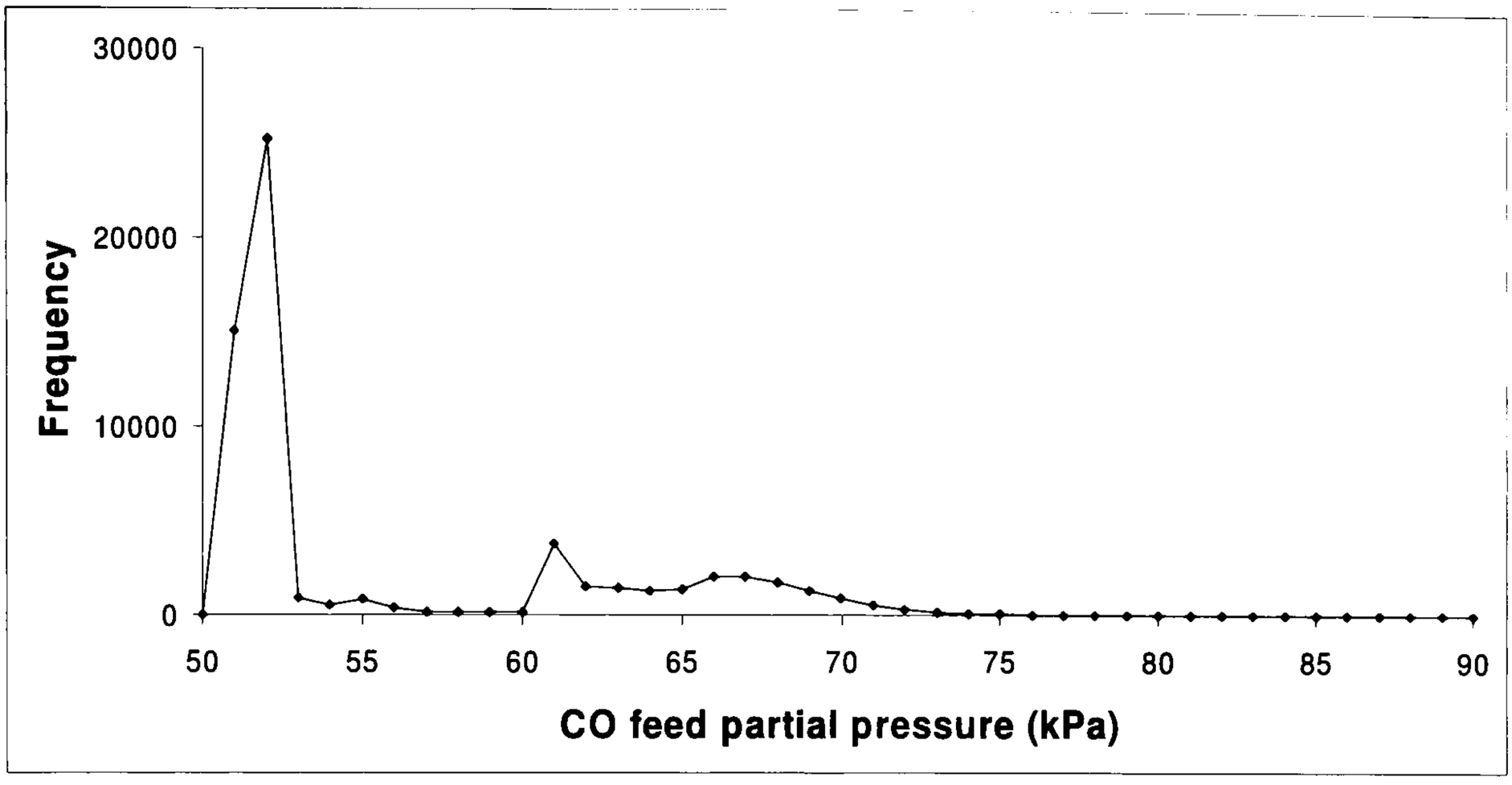


Figure 6.4: Carbon monoxide feed partial pressure histogram for the nominal design in iteration I (uniform case)

Figure 6.5: Chlorine feed partial pressure histogram for the nominal design in iteration I (uniform case)

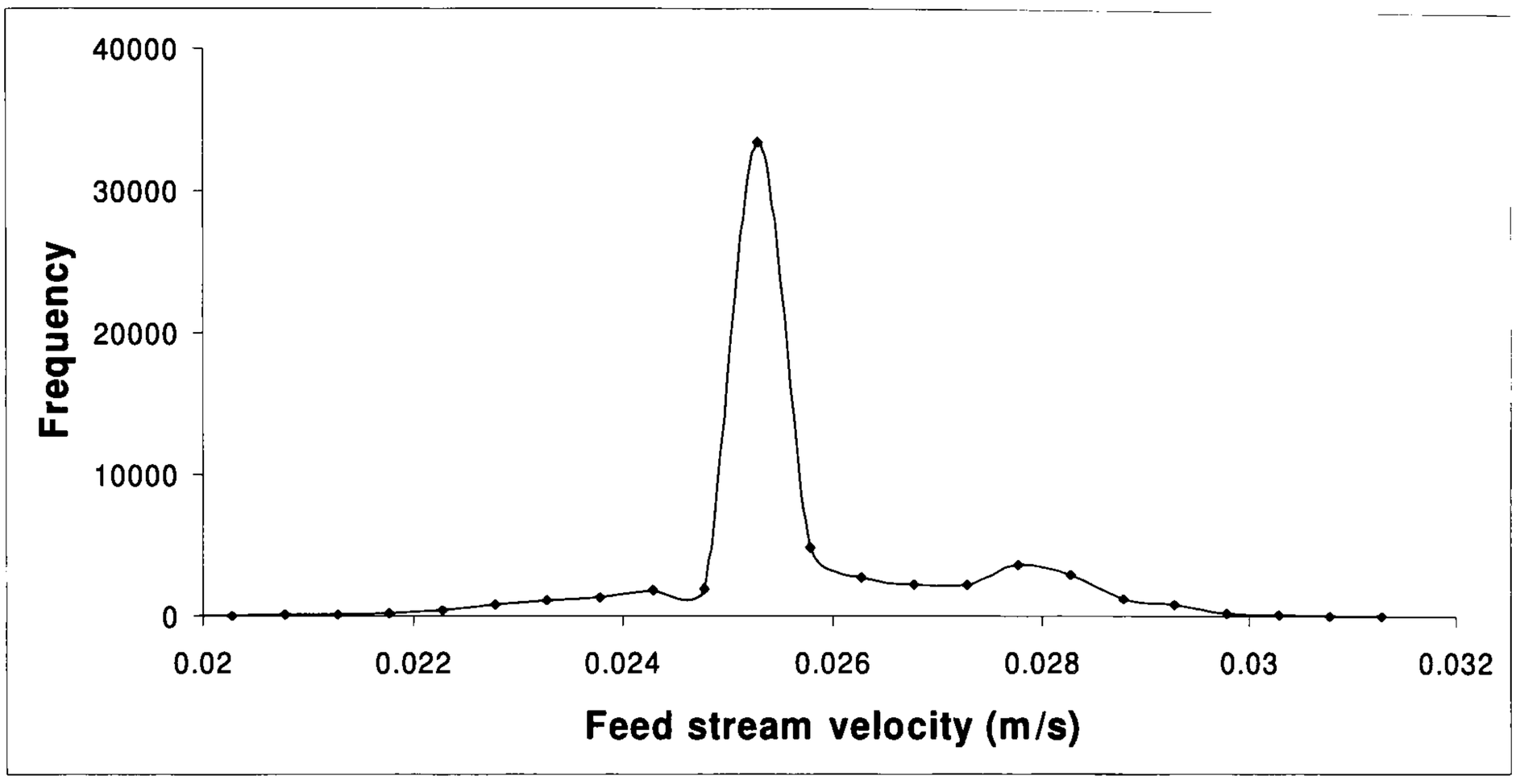


Figure 6.6: Feed stream velocity histogram for the nominal design in iteration I (uniform case)

Table 6.10: Mean value and standard deviation for profit and control variables for the nominal design in iteration I (uniform case)

	Sobol' sampling	
Parameter	Mean	Std. Dev.
Profit (USD/yr)	467,810	34,390
F_{cw} (kg/s)	0.371	0.204
Vel (m/s)	0.026	0.001
pp_{CO} (kPa)	55.3	6.6
pp_{Cl_2} (kPa)	48.4	3.6

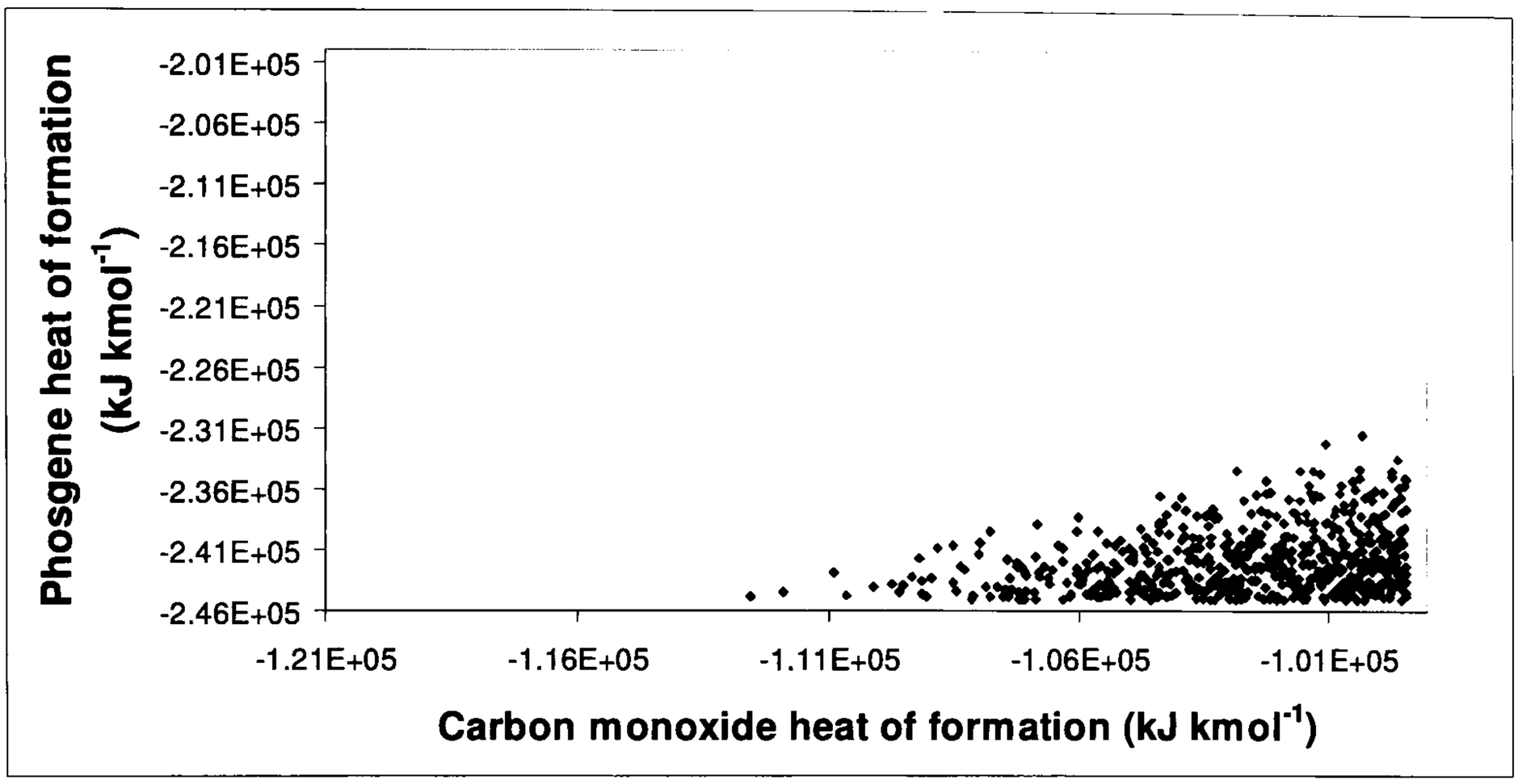


Figure 6.7: Infeasible points for the nominal design in iteration I using Sobol' sampling

Finally, some additional information can be obtained from analysing the results of the several sampled points regarding the feasibility of the design. In this case, 1,340 out of 69,632 sampled points were found infeasible for the given design. Therefore, an estimate of the infeasibility probability is around 1.92%. A further analysis of the infeasible points can be performed by plotting the feasible and infeasible points for the parameter values tested. If the feasible and infeasible points are randomly distributed over the parameter range, the parameter does not play a significant part in the infeasibility. If the infeasible values are grouped in a particular area, the parameter does have an impact on process feasibility, as explained in section 4.3.2. This analysis shows that most infeasibilities are caused by two parameters only: $\Delta H_{f(CO)}$ and $\Delta H_{f(COCl_2)}$. Figure 6.7 shows the infeasible points plotted over the uncertain parameter space for $\Delta H_{f(CO)}$ and $\Delta H_{f(COCl_2)}$.

With the above information, such as histograms, sensitivity indices and infeasibility index, decisions can be taken based on their quantitative risk profiles for the given design. On one hand, graphs such as the profit probability distribution can be used for managerial decisions. Information such as mean, probabilities and upside/downside are easily visualised and available reliably thanks to the thorough exploration of the uncertain parameter space. On the other hand, similar information can be extracted for control variables and key performance indicators and thus guide technical decisions. This information can be

useful to predict operating ranges for the specification of the process controllers. Furthermore, the analysis of the different key performance indicators can be a helpful starting point to analyse the effect on downstream units.

The first decision to be made is whether the proposed design is deemed feasible for the given parameter uncertainty. The points in the infeasible region shown in figure 6.7 violate the maximum allowed temperature constraint inside the reactor. Analysis of some of these points shows that, if the uncertain parameters fall in this infeasible region, the reaction will generate more heat leading to a violation of the constraint. If less material is fed to the reactor, the temperature can be reduced. However, the lower bound on production is reached before the temperature is brought back within the required limits. Other combinations of the control variables have a similar effect.

An infeasibility probability of 1.92% and the long tail of poor performance seen in the profit histogram may be considered too risky. An alternative design will be sought for the uniform case.

Normal case When the uncertain parameters follow normal distributions, two approaches to GSFA can be followed. In the first approach, the Sobol'-normal sampling of Kucherenko et al. (2006) is used. This means that the more probable a parameter realisation, the more likely it is to be sampled. In the second approach, Sobol' sampling is used and a re-weighting is applied to calculate the risk metrics, as described in section 4.3. The benefit of this latter approach is that it offers a good coverage of space, so that important but low-probability points, which could be infeasible points, are more likely to be identified.

The results using the Sobol'-normal sampling technique are shown in table 6.11. The sensitivity index values are similar to the ones obtained with the Sobol' sampling. However, the use of the normal parameter probability distribution slightly increases the values for the heat of formation indices, while reducing the effect caused by the interaction between these parameters. After performing the analysis for the higher-order indices, for the interaction between the heats of formation, the value of the group sensitivity index is 0.8867, which means that the index for the interaction between the heats of formation is $0.8867 - 0.6661 - 0.1322 = 0.0884$. The CPU time taken for the first-order SI calculation was approximately 40 hours and 47 minutes using 16 Linux machines, while the higher-order SI evaluation took 6 hours and 23 minutes using 17 parallel processes.

Table 6.11: GSFA results for first-order Sobol' indices for the nominal design in iteration I (normal case) using Sobol'-normal sampling

	Sobol'-normal sampling	
Parameter	S_i	S_i^{Tot}
$\Delta H_{f(CO)}$	0.1322	0.2690
$\Delta H_{f(COCl_2)}$	0.6661	0.8089
Ek_r	0.0131	0.0260
kr	0.0079	0.0111
kz	0.0147	0.0548
U	0.0185	0.0454
T_{cwin}	0.0027	0.0076
T_{in}	0.0010	0.0042

The profit probability and control variable histograms generated with the Sobol'-normal sampling method are shown in figures 6.8 to 6.12. It can be seen that the results obtained with the Sobol'-normal sampling have a higher frequency/probability around the mean value thus reducing the standard deviation for the annualised profit and most control variables as shown in table 6.12.

The number of infeasible points found for the 69,632 optimisation problems was 19 in the Sobol'-normal sampling, compared to 1,340 in the Sobol' sampling. As mentioned before, the advantage of the Sobol' sampling is the good space coverage it offers for a given number of points. Figure 6.13 shows graphically the different infeasible points found by each sampling technique, showing the advantage of the Sobol' sampling. The infeasibility probability using the Sobol'-normal sampling is 19/69,632 = 0.027%.

The use of Sobol' sampling and weight factors is considered next to calculate the mean value and standard deviation of the profit and control variables and the infeasibility index. A weight factor is calculated for every sampled point using the normal probability distribution definition for each parameter. The values are normalised to add up to one. These results are shown in table 6.13 and compared with the results of the Sobol'-normal sampling method. It can be seen that the standard deviation for the profit and control variables using the Sobol' sampling with the weight factor is lower than those values

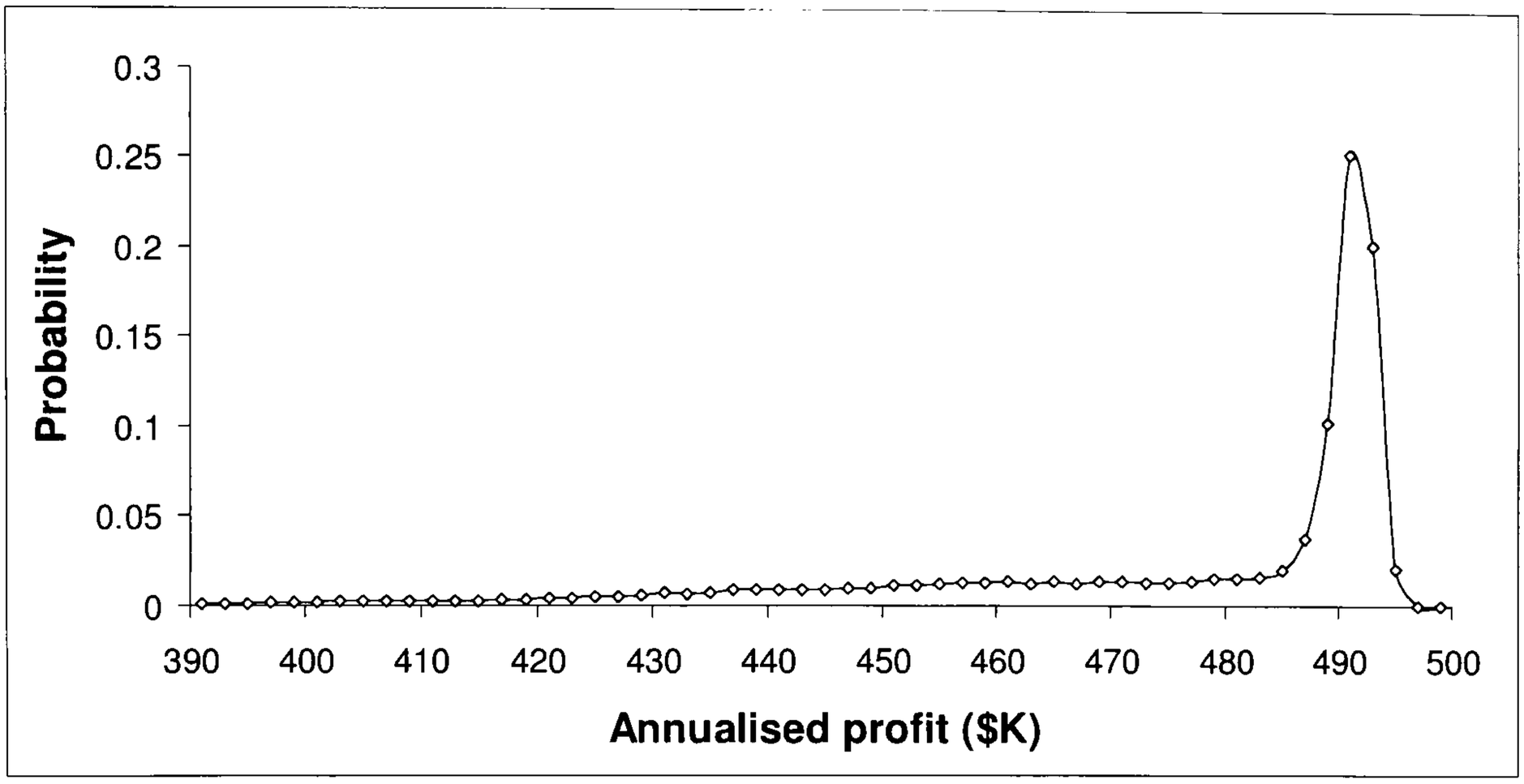


Figure 6.8: Annualised profit probability distribution for the nominal design in iteration I using Sobol'-normal sampling

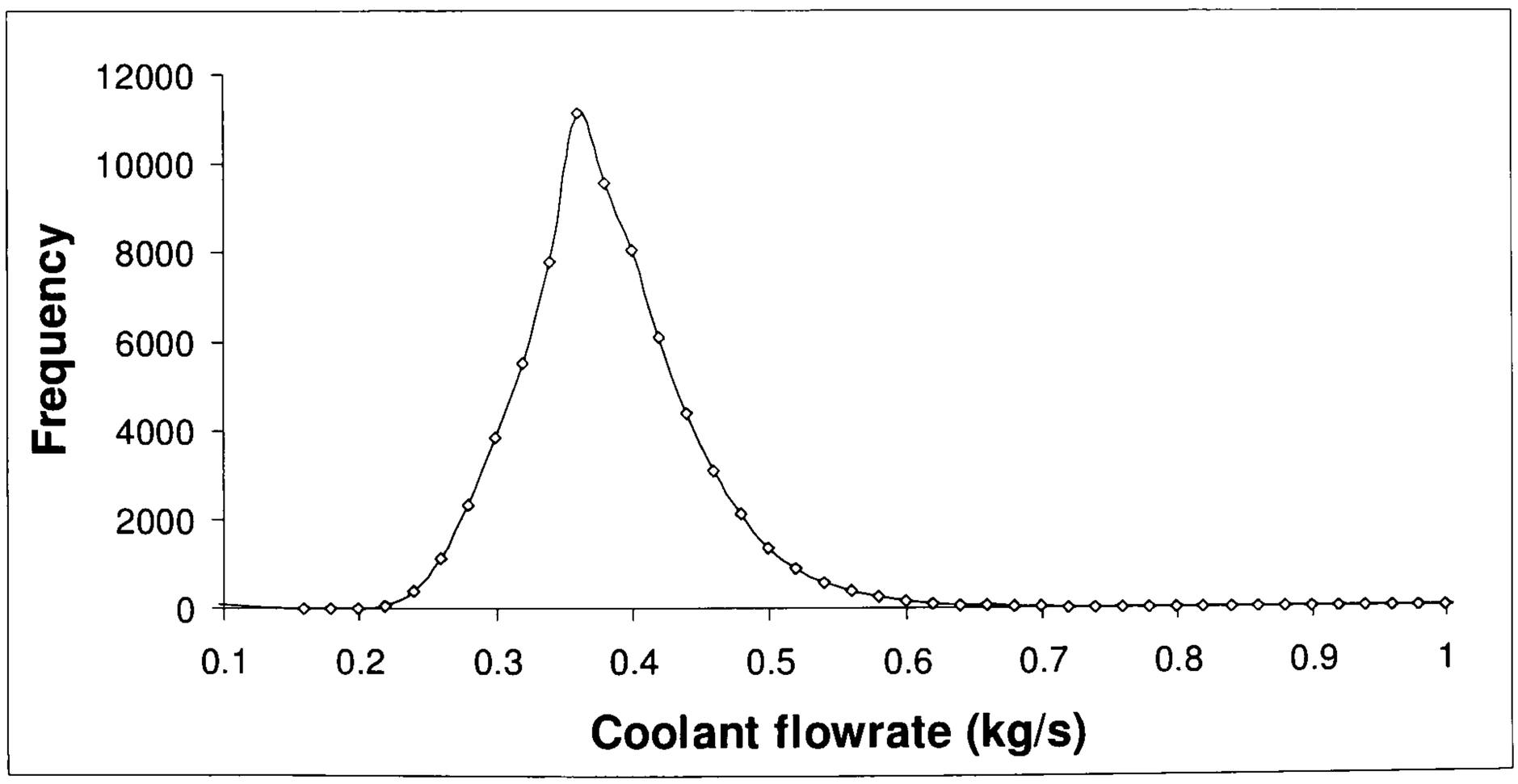


Figure 6.9: Coolant flowrate histogram for the nominal design in iteration I using Sobol'-normal sampling

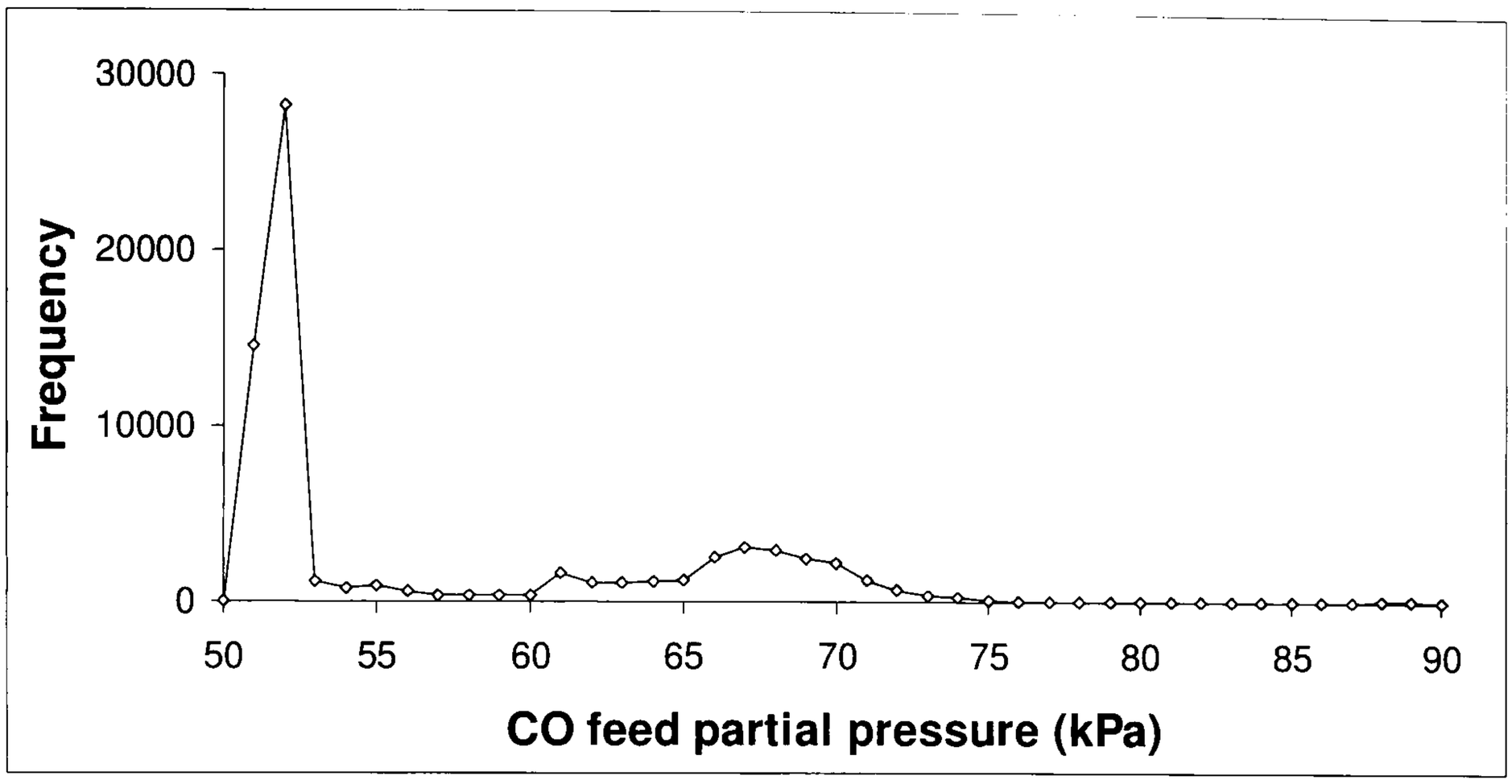


Figure 6.10: Carbon monoxide feed partial pressure histogram for the nominal design in iteration I using Sobol'-normal sampling

Figure 6.11: Chlorine feed partial pressure histogram for the nominal design in iteration I using Sobol'-normal sampling

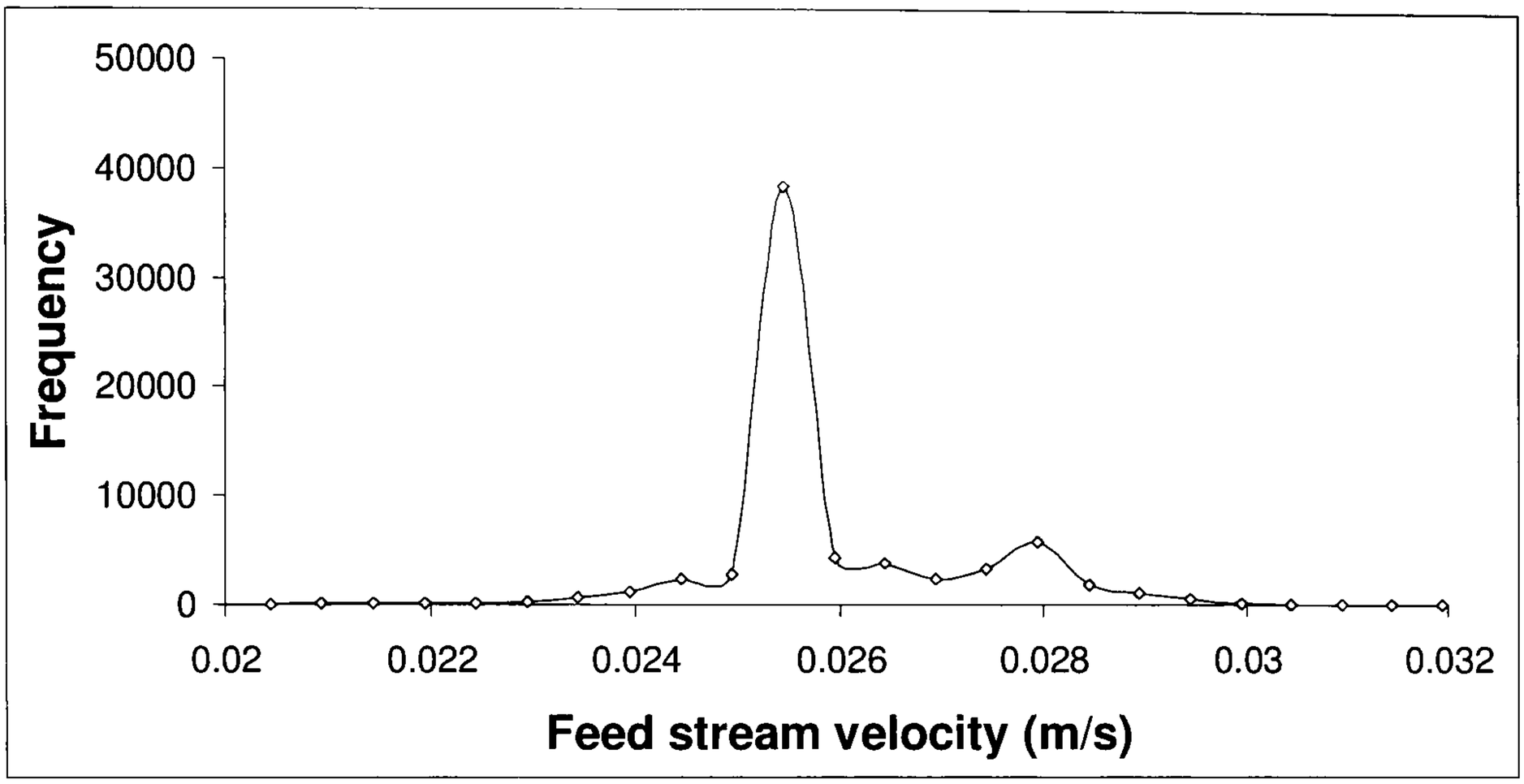


Figure 6.12: Feed stream velocity histogram for the nominal design in iteration I using Sobol'-normal sampling

Table 6.12: Mean value and standard deviation for profit and control variables for the nominal design in iteration I using Sobol'-normal sampling

	Sobol'-normal sampling	
Parameter	Mean	Std. Dev.
Profit (USD/yr)	476,110	23,020
F_{cw} (kg/s)	0.372	0.075
Vel (m/s)	0.026	0.001
pp_{CO} (kPa)	56.2	7.5
pp_{Cl_2} (kPa)	48.8	3.0

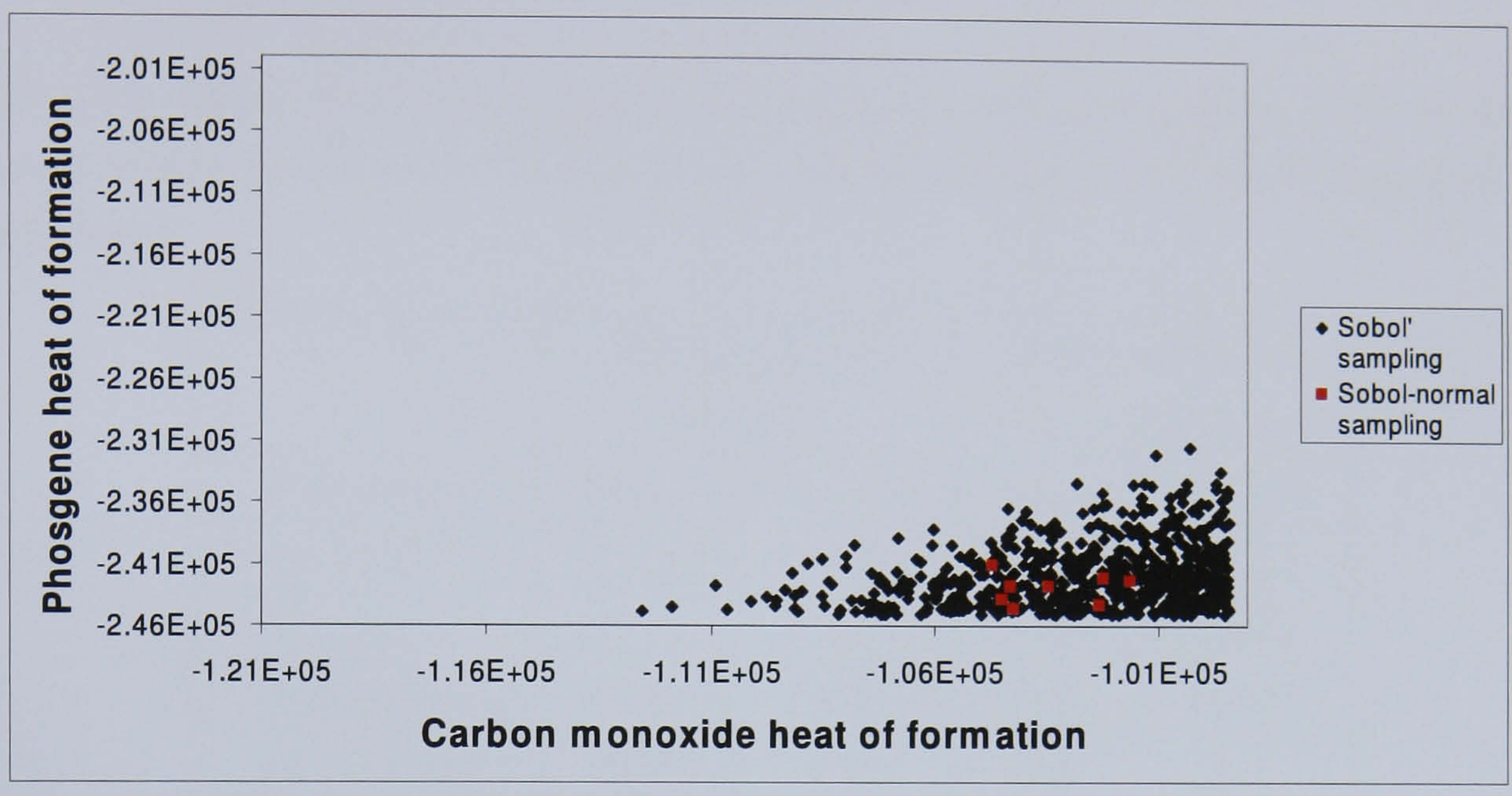


Figure 6.13: Comparison of infeasible points found by Sobol' and Sobol'-normal sampling for the nominal design in iteration I

obtained using the Sobol'-normal sampling. This is due to assigning higher weight factors to values close to the mean value and lower weights to those points away from the mean.

The mean profit value is higher than the mean obtained using the Sobol'-normal sampling method. This difference is related to the samples used in the evaluation. While the Sobol' sampling with weight factors has a better space coverage for the given uncertain parameter region, the Sobol'-normal sampling uses more points around the mean values of the uncertain parameters. Therefore, it is expected that a better evaluation can be obtained using the Sobol' sampling with weight factors as the uncertain parameter space is better explored for a given number of points than when using the Sobol'-normal sampling. The histograms for the KPIs can be seen in figures 6.14 to 6.18.

The results for the infeasibility probability calculation are shown in table 6.14. The infeasibility probability is 0.027%, when using the Sobol'-normal sampling, and 0.0034%, when using the Sobol' sampling with weight factors. The Sobol' sampling with weight factors is a better estimate as this is the result of finding 1,340 infeasible points (out of 69,632 samples) and applying a weight factor to them. On the other hand, the use of the Sobol'-normal sampling takes into account only 19 infeasible points out of 69,632 samples. Therefore, the result obtained using the Sobol'-normal sampling is overestimating the

Table 6.13: Mean value and standard deviation for profit and control variables for the nominal design in iteration I using Sobol'-normal sampling and Sobol' sampling with weight factor

	Sobol'-normal sampling		Sobol' sampling with weight factor	
Parameter	Mean	Std. Dev.	Mean	Std. Dev.
Profit (USD/yr)	476,110	23,020	482,160	17,830
F_{cw} (kg/s)	0.372	0.075	0.374	0.062
Vel (m/s)	0.026	0.001	0.026	0.001
pp_{CO} (kPa)	56.2	7.5	55.5	6.3
pp_{Cl_2} (kPa)	48.8	3.0	48.5	3.4

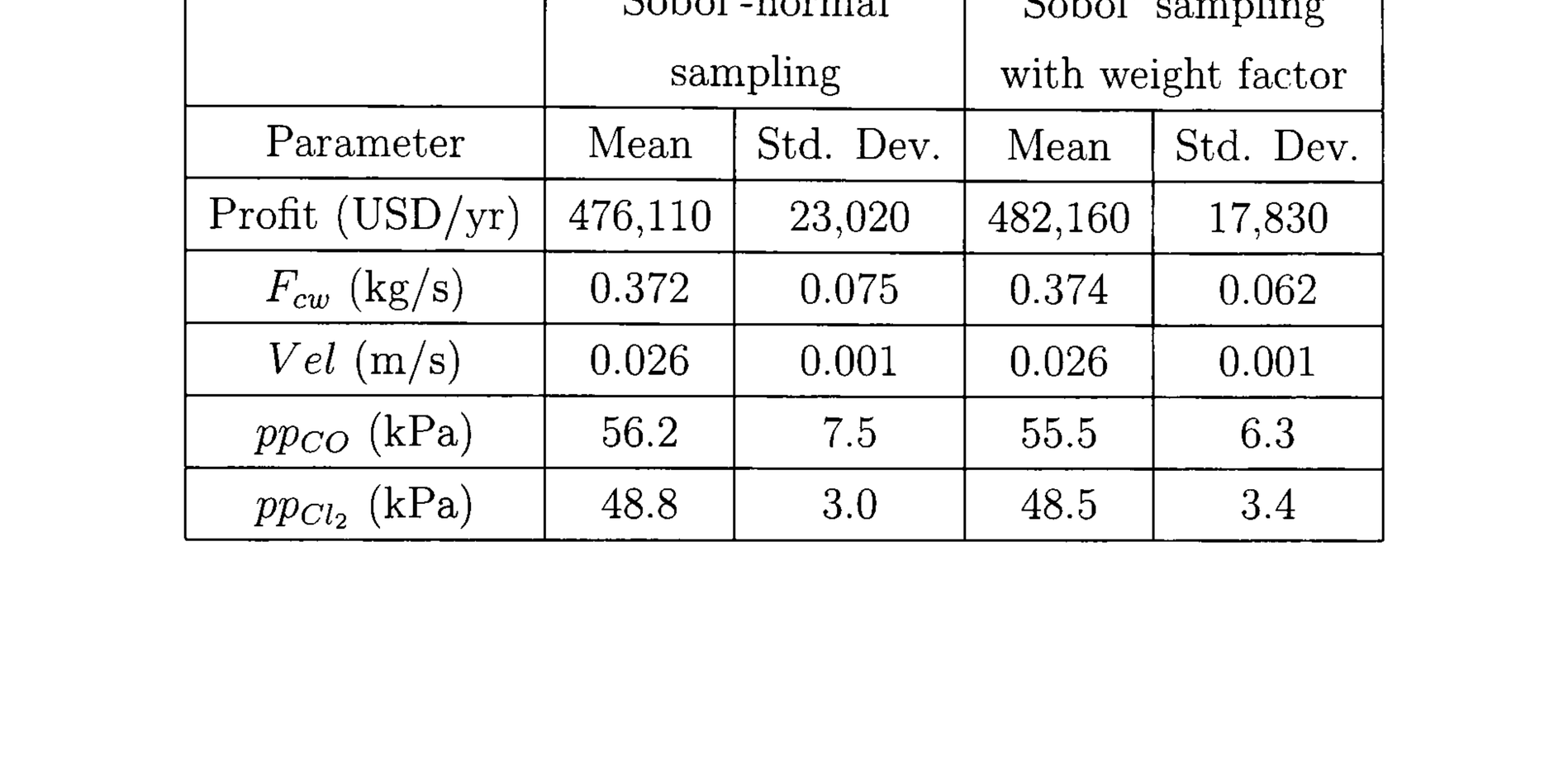


Figure 6.14: Annualised profit probability distribution for the nominal design in iteration I using Sobol' sampling with weight factors

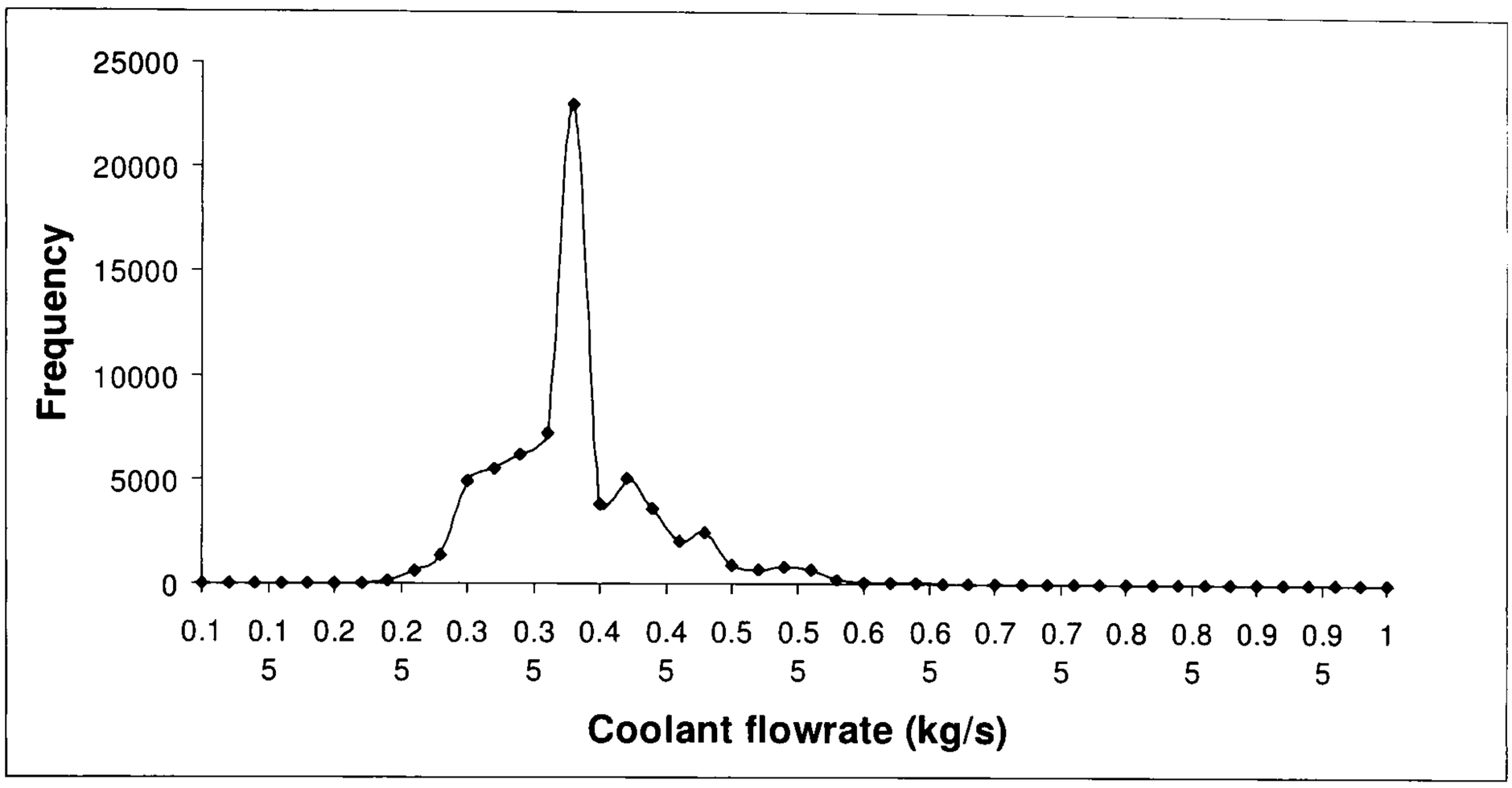


Figure 6.15: Coolant flowrate histogram for the nominal design in iteration I using Sobol' sampling with weight factors

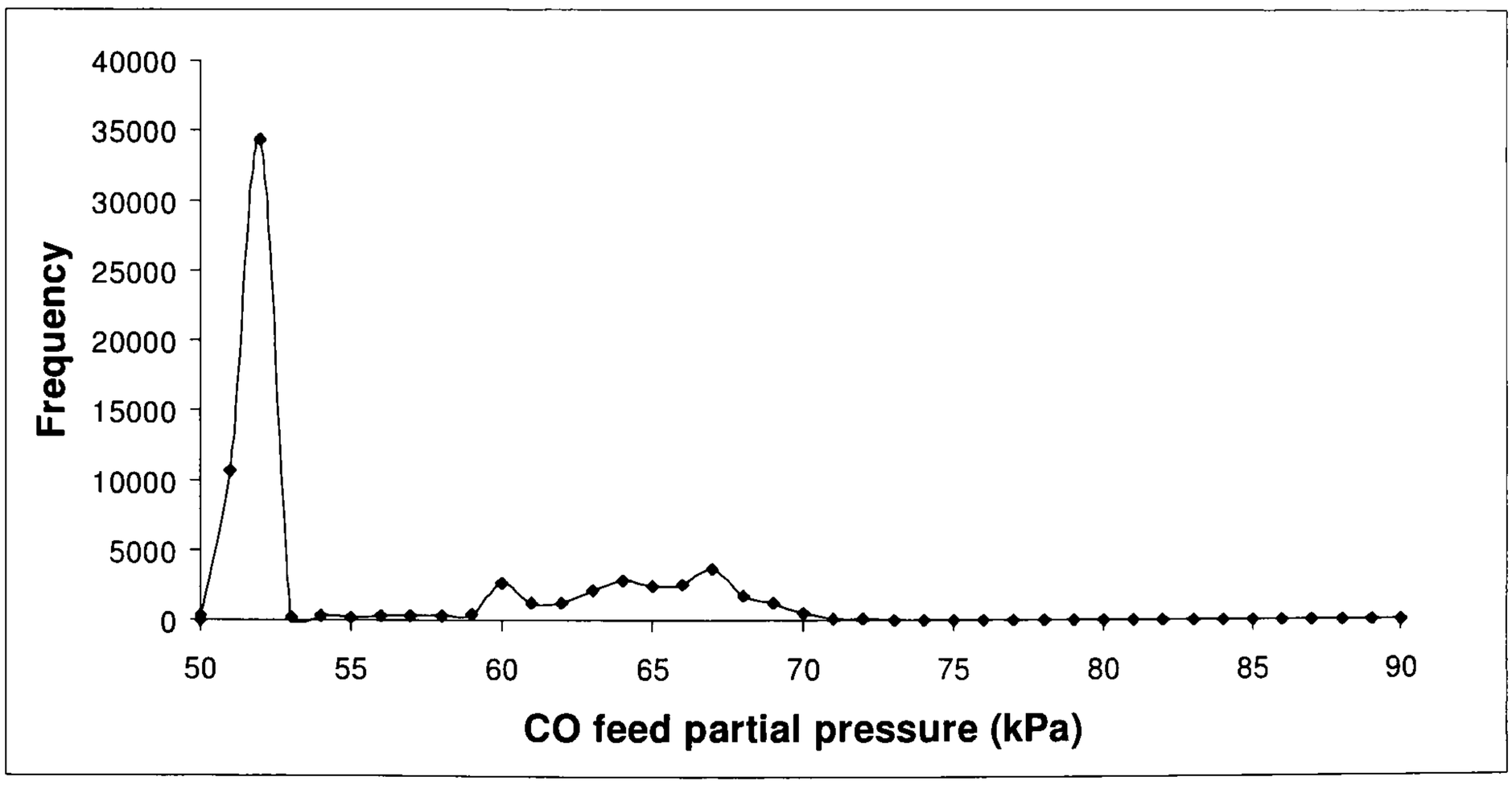


Figure 6.16: Carbon monoxide feed partial pressure histogram for the nominal design in iteration I using Sobol' sampling with weight factors

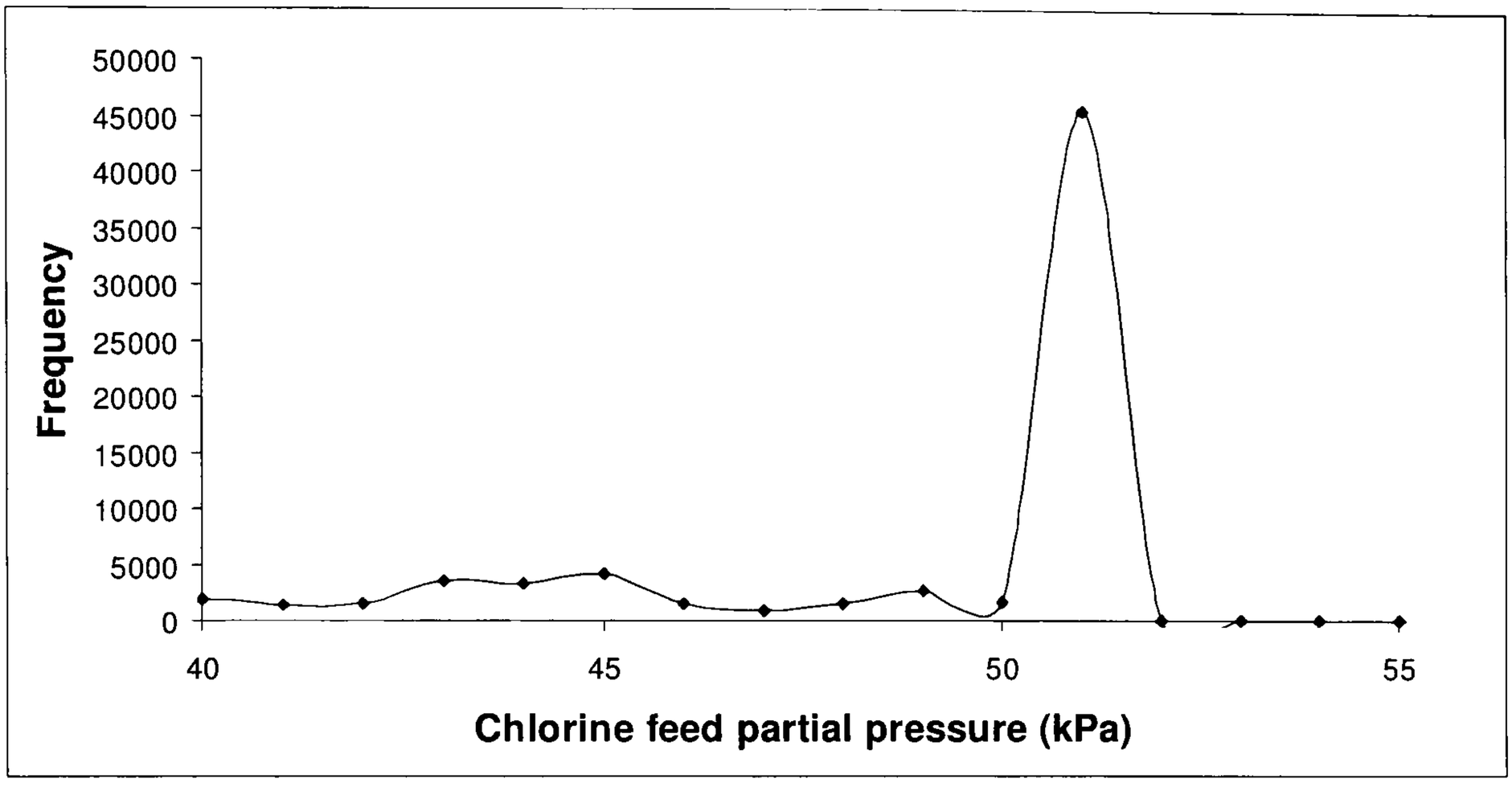


Figure 6.17: Chlorine feed partial pressure histogram for the nominal design in iteration I using Sobol' sampling with weight factors

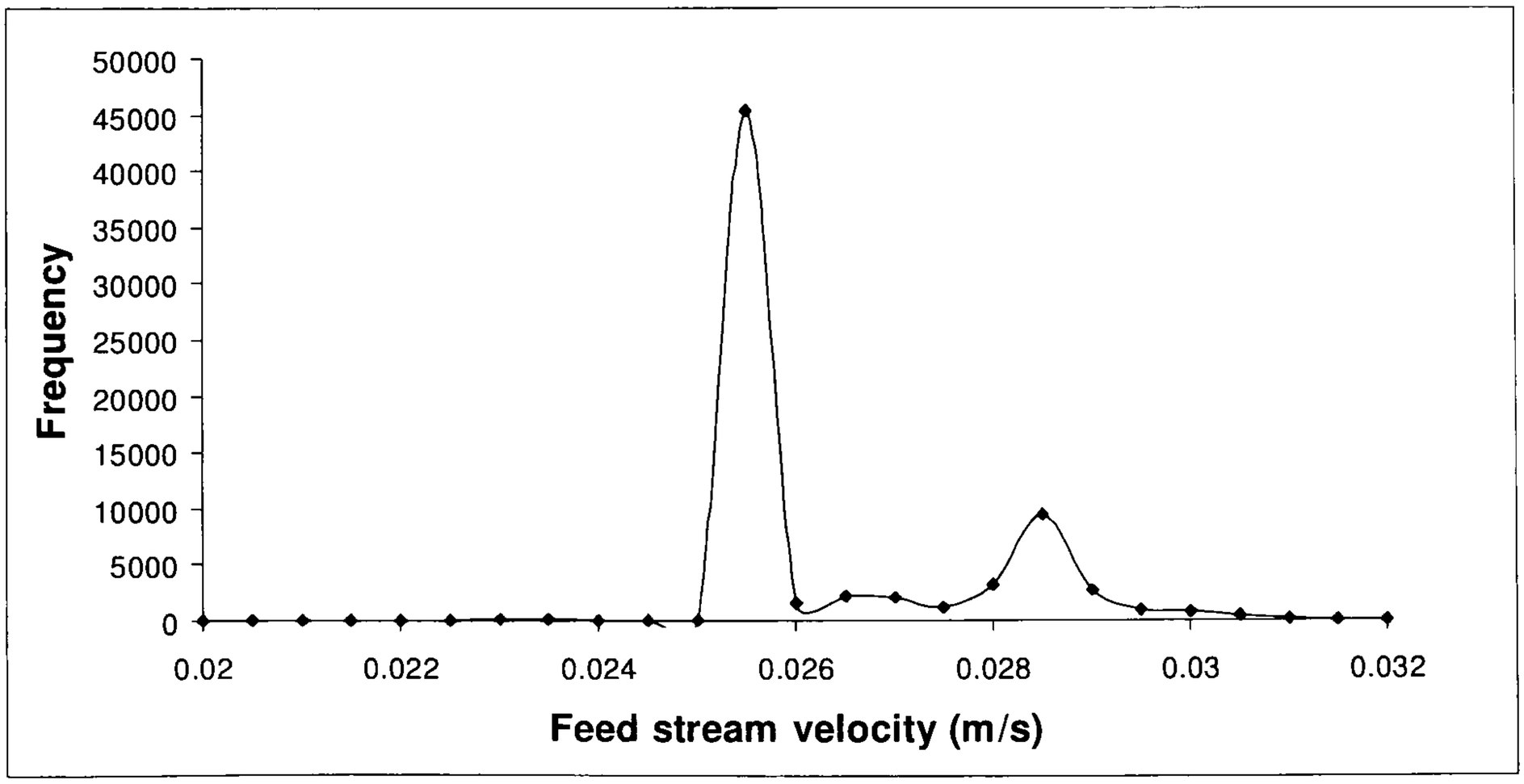


Figure 6.18: Feed stream velocity histogram for the nominal design in iteration I using Sobol' sampling with weight factors

Table 6.14: Infeasibility index for the nominal design in iteration I using Sobol'-normal sampling and Sobol' sampling with weight factor approach

	Sobol'-normal sampling	Sobol' sampling with weight factor
Infeasibility index	0.027%	0.0034%

actual infeasibility probability value.

The above results show an advantage in the use of the Sobol' sampling with weight factors over the use of a Sobol'-normal sampling. The main difference is that, for a given number of points, the first method has a better coverage of the uncertain parameter space than the Sobol'-normal sampling. A better space coverage allows a better evaluation of the uncertain region as more infeasible points can be found and low probability regions are evaluated at the same frequency as high probability regions.

Once these results are available, the infeasibility probability together with the risk quantification must be deemed as acceptable or unacceptable. If found acceptable, the deterministic design, used in the previous GSFA evaluation, can be used. However, this design was found using the nominal or most probable values for the uncertain parameters. A scenario-based optimisation problem can be formulated to find an optimal design for the specified parameter range and not only for the most probable values.

On the other hand, if the infeasibility probability and risk quantification are regarded as unacceptable, the infeasibility issue and/or resulting risk must be addressed. A new robust design has to be obtained for the given parameter ranges. In this case, a scenario-based optimisation is undertaken with the objective of finding a feasible design for the given parameter ranges.

The steps for both cases, acceptable and unacceptable results, are illustrated in the next section.

6.3.3 First stochastic design - Scenario-based optimisation

The objective of the scenario-based optimisation is to find an optimal design for a given set of samples or scenarios. The results obtained in the previous section identified two critical uncertain parameters: $\Delta H_{f(CO)}$ and $\Delta H_{f(COCl_2)}$. These parameters are used to generate

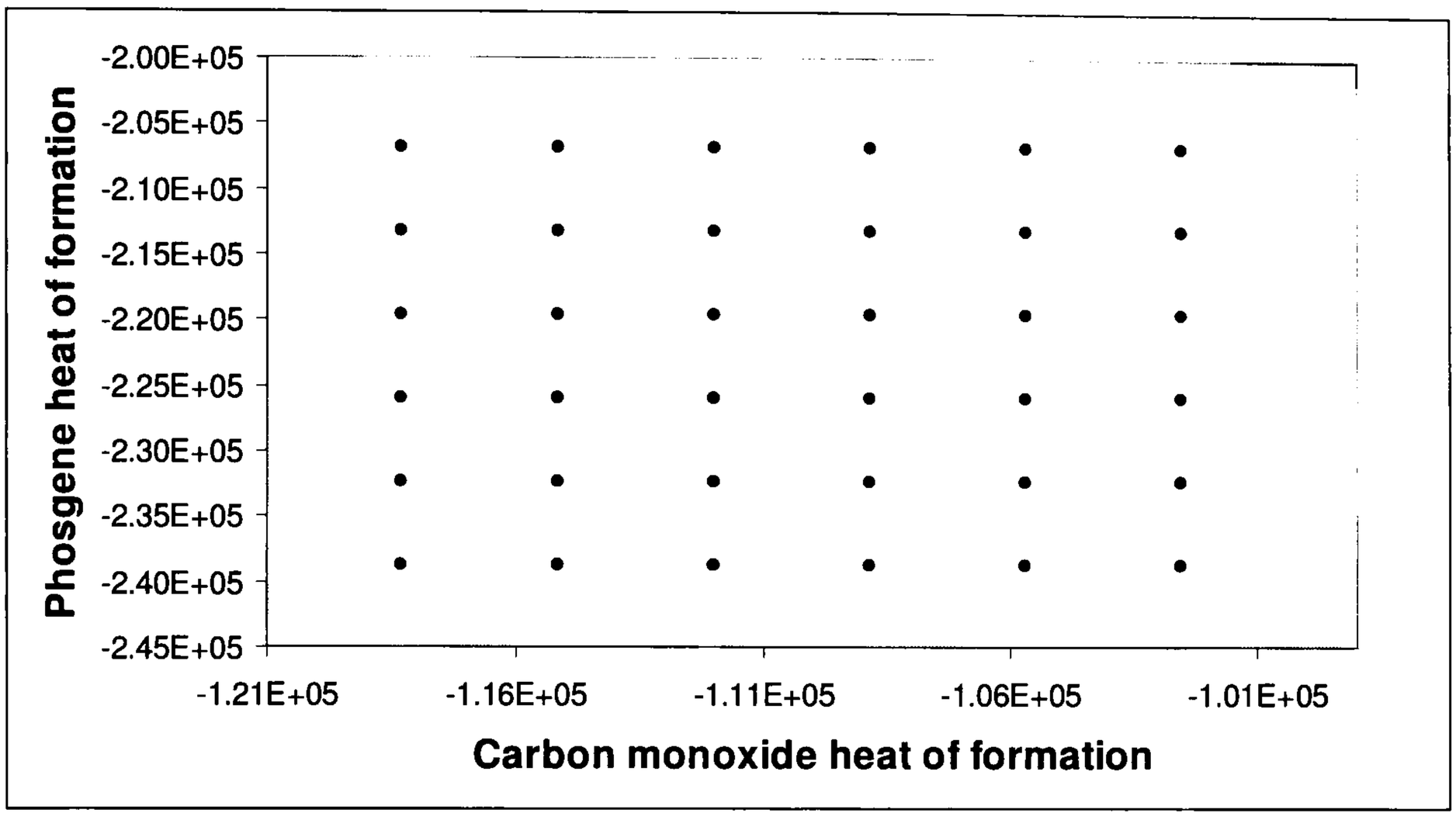


Figure 6.19: 36 scenarios generated from the 2-dimensional space of critical parameters

the set of scenarios to be used in the following two scenario-based optimisation problems. The first one is based on treating the infeasibility probability as acceptable and aims at finding an optimal design in terms of expected performance for the given parameter range. The second problem, based on treating the infeasibility probability as unacceptable, has as objective to find a new feasible design for the given uncertainty parameter range. In this study, the parameters are assumed to be uniformly distributed.

First problem: infeasibility probability acceptable

A series of 36 scenarios is generated by sampling the 2-dimensional region of critical parameters. Figure 6.19 shows the generated uniform grid of 36 scenarios. The 36 scenarios were given the same weight because the uniform case is considered.

The 36-scenario problem was solved using the pseudo-dynamic optimisation approach presented in chapter 5. A new set of equations was included for the homotopy/continuation

approach to smooth the transitions between the given scenarios:

$$k\frac{d\Delta H_{f(CO)}}{dt} = \Delta H^{\star}_{f(CO)} - \Delta H_{f(CO)} \tag{6.5}$$

$$k\frac{d\Delta H_{f(COCl_2)}}{dt} = \Delta H^{\star}_{f(COCl_2)} - \Delta H_{f(COCl_2)} \tag{6.6}$$

$$k\frac{dVel}{dt} = Vel^{\star} - Vel \tag{6.7}$$

$$k\frac{dF_{cw}}{dt} = F^{\star}_{cw} - F_{cw} \tag{6.8}$$

$$k\frac{dpp_{CO}}{dt} = pp^{\star}_{CO} - pp_{CO} \tag{6.9}$$

$$k\frac{dpp_{COCl_2}}{dt} = pp^{\star}_{COCl_2} - pp_{COCl_2} \tag{6.10}$$

The value of k was 10^{-4} and the *set-point* variables are marked with a $\star$. The *set-point* variables for the heats of formation were used to define each scenario, while the remaining set points become the optimisation variables.

The objective function was modified to maximise the average profit over the 36 scenarios as follows:

$$\text{Average Profit} = \frac{1}{\tau}\int_0^{\tau} \text{Profit}\ dt \tag{6.11}$$

The pseudo-time domain was divided in 36 scenarios, each with a duration of 1 unit time. Therefore, the integration of the above equation is performed from 0 to τ=36.

The result has an expected annualised profit of 470,000 USD/yr for a reactor length of 1.403 m, a reactor diameter of 0.714 m and a cooling jacket diameter of 0.750 m. The results were obtained after approximately 66.4 CPU hrs. This design is the same as that obtained in the deterministic optimisation. The result shows that the deterministic design is also the optimal design for the chosen 36 scenarios. If the optimal design for the 36 scenarios was different, a new GSFA would have to be done to estimate the expected mean and standard deviations for the KPIs. The next section presents further work on this case study to illustrate the procedure when the risk quantification and/or infeasibility probability is deemed as unacceptable.

Second problem: infeasibility probability unacceptable

The objective of this second problem is to find a new design which is feasible for the entire uncertain parameter space. In this case, 4 new scenarios are added to the previous 36

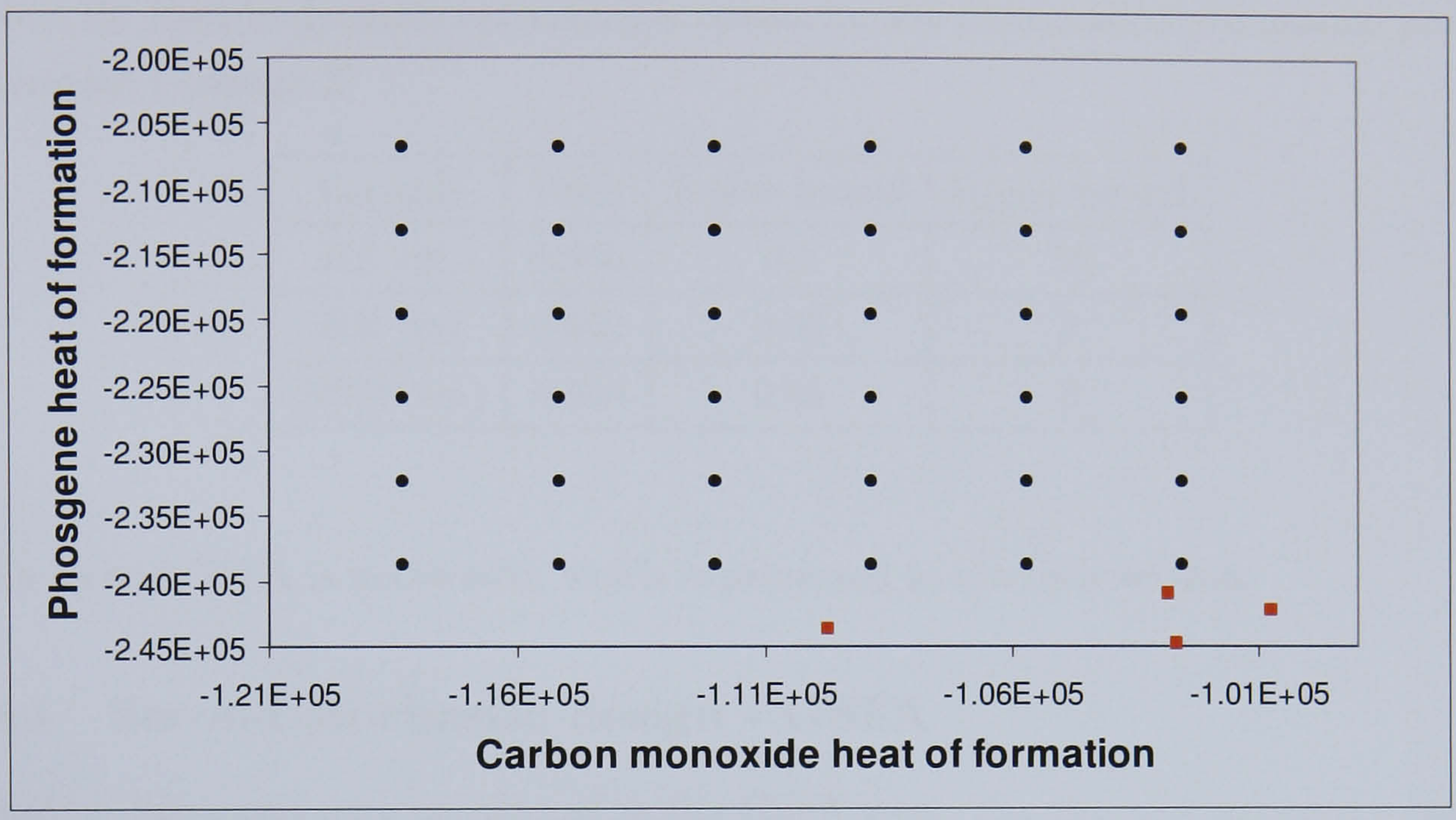


Figure 6.20: Scenarios used in the first stochastic design step of iteration I, when assuming that the infeasibility probability is unacceptable

scenario-based optimisation, all with the same weight. The 4 new scenarios are chosen from the list of infeasible points identified in the GSFA shown previously. The criteria to choose those scenarios is based on the Sobol' sampled point they represent. As mentioned in section 4.2.3, the Sobol' method covers the space uniformly for every 2^n sample points. Since every infeasible point represents a sampled point in the Sobol' sequence, the points are chosen based on their number in this Sobol' sequence, starting with the lowest number. In this case, the Sobol' numbers are 11, 19, 30 and 121. These new scenarios are shown in figure 6.20 as red dots on top of the original 36 scenarios.

The solution of the new scenario-based optimisation problem was obtained using the pseudo-dynamic approach using gPROMS, which required approximately 51 hours and 40 minutes. The value of the objective function is 362,963 USD/yr and the design (design 2) is shown in table 6.15.

It can be seen that, to meet the given process constraints, a longer reactor, 6.456 m, is found. This increases the heat transfer area to bring the temperature within the required operational limits and meet the remaining constraints.

The next step is a new analysis of this new design to quantify the inherent risk. There-

Table 6.15: Pseudo-dynamic optimisation results for the 40-scenario optimisation problem in iteration I (design 2)

Variable	Value	Lower bound	Upper bound
RZ (m)	6.456	0.5	15
RR (m)	0.342	0.05	2
RCW (m)	0.359	0.05	3

fore a second GSFA is performed, which is presented in the next section.

6.3.4 Second stochastic design - GSFA

As before, two cases were considered in the GSFA step. The first one assumes a uniform distribution and uses the Sobol' sampling, while the second one is based on a normal pdf. In this latter case, Sobol' sampling with weight factors is used in the analysis.

Uniform case The GSFA is performed on the new design found with the 40-scenario-based optimisation to identify critical uncertain parameters and any infeasible points. The results for the first-order Sobol' indices are shown in table 6.16. A Sobol' sample with 4096 points was used, aiming to find new infeasible points. The approximate CPU time was 61 hours and 14 minutes using 33 parallel processes.

The new GSFA results show that the total sensitivity indices for the heats of formation have increased compared to those for the nominal design. This indicates that, for this new design, the higher-order interactions are becoming relevant and that they can be mainly attributed to interactions involving the heats of formation. These relevant second-order sensitivity indices are shown in table 6.17. 4096 Sobol' points were used and the CPU time was 43 hours and 36 minutes using 35 parallel processes.

The mean and standard deviation values for the profit and control variables are shown in table 6.18. The first point to notice is the decrease in the expected profit from 467,810 to 369,390 USD/yr. This is the result of increasing the reactor's length to deal with the infeasible points. This profit loss of around 100,000 USD/yr can be seen as the penalty arising from the uncertainty in the parameters and the need to find a feasible design for the given conditions. The histograms for the profit and standard deviation can be seen

Table 6.16: GSFA results for first-order Sobol' indices for design 2 in iteration I

Parameter	Individual sensitivity indices, S_i	Total sensitivity indices, S_i^{Tot}	Rank
$\Delta H_{f(CO)}$	0.0649	0.3736	2
$\Delta H_{f(COCl_2)}$	0.5616	0.8892	1
Ek_r	-0.0219	0.0624	5
kr	-0.0277	0.0521	6
kz	-0.0506	0.1516	3
U	-0.0195	0.0958	4
T_{cwin}	-0.0260	0.0429	7
T_{in}	-0.0414	0.0371	8

Table 6.17: GSFA results for second-order Sobol' indices for design 2 in iteration I

Parameter	Second-order sensitivity indices, S_i
$\Delta H_{f(CO)}$-$\Delta H_{f(COCl_2)}$	0.1505
kz-$\Delta H_{f(CO)}$	0.0984
kz-$\Delta H_{f(COCl_2)}$	0.0671

Table 6.18: Mean value and standard deviation for profit and control variables in iteration I for design 2 (uniform case)

	Sobol' sampling	
Parameter	Mean	Std. Dev.
Profit (USD/yr)	369,390	34,290
F_{cw} (kg/s)	0.250	0.181
Vel (m/s)	0.026	0.003
pp_{CO} (kPa)	56.2	4.4
pp_{Cl_2} (kPa)	50.8	6.5

in figures 6.21 to 6.25. Figures 6.22 to 6.24 show at least 2 distinct peaks which can be attributed to different operating regions for the new design and given constraints. This could lead to important considerations to take into account during the operation of the reactor.

Addressing the issue of feasibility, the new design still has some infeasible points. Whereas in the original design the number of infeasible points was 1,340, in this new design there are 1,002 infeasible points. As in the previous case, the main parameters responsible for the infeasibility are the heats of formation. A plot of the 1002 infeasible points is shown in figure 6.26. The 1,002 infeasible points identified are equivalent to an infeasibility probability of 1.44%, for the uniform case. As expected, the infeasibility probability has been reduced compared to the deterministic or nominal design. The new infeasibility probability is low, but further improvements are desirable. Therefore, a new scenario-based optimisation problem will be solved.

Normal case The results from the uniform case can readily be converted to the normal case by introducing appropriate weight factors, since Sobol' sampling can be used for both cases. The recalculated means and standard deviations for the KPIs are shown in table 6.19. As in the uniform case, there is a reduction in the annualised profit from 476,110 to 382,910 USD/yr, which is the result of the increase in the reactor length.

The histograms for the annualised profit and control variables are shown in figures 6.27

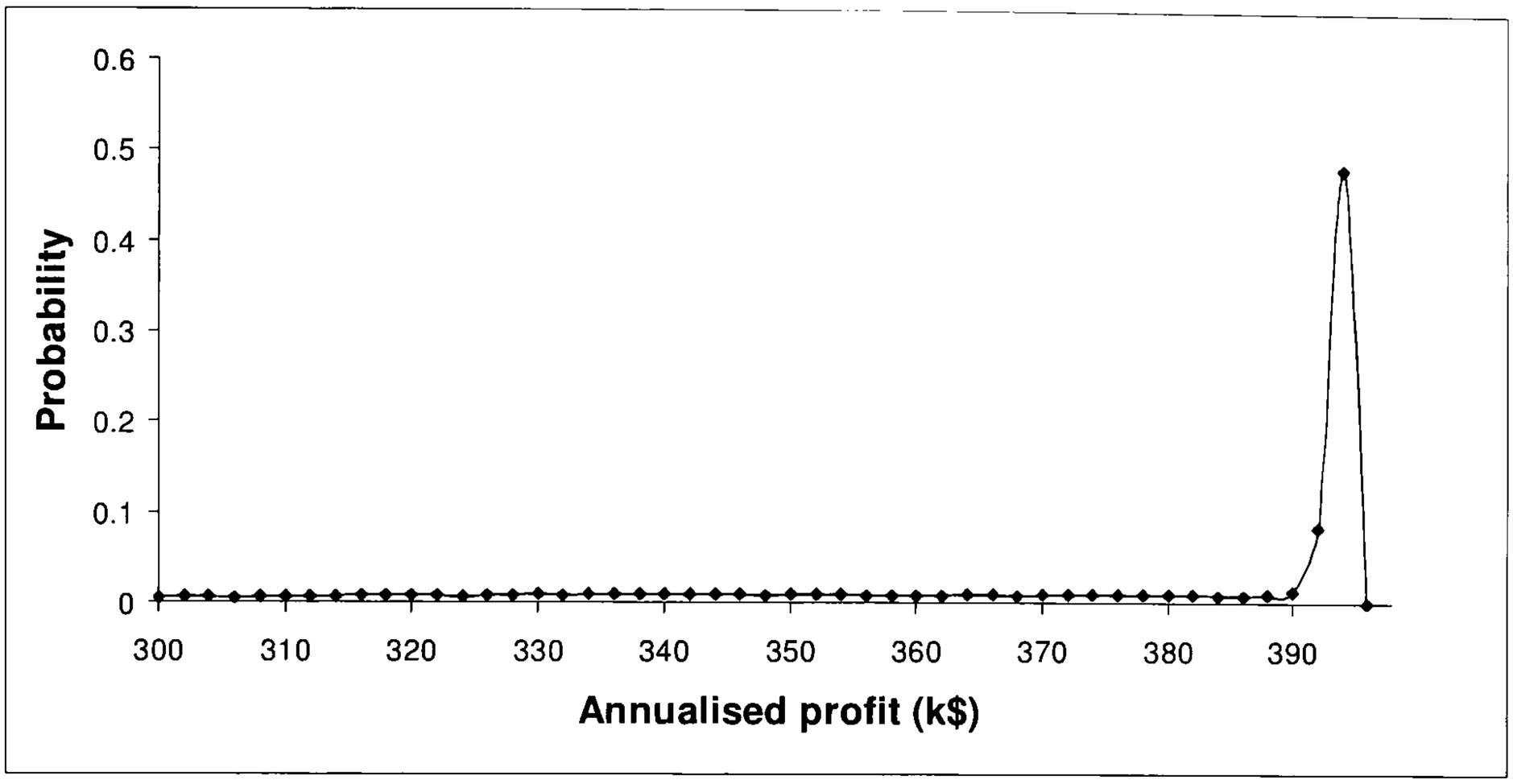


Figure 6.21: Annualised profit probability distribution for design 2 in iteration I (uniform case)

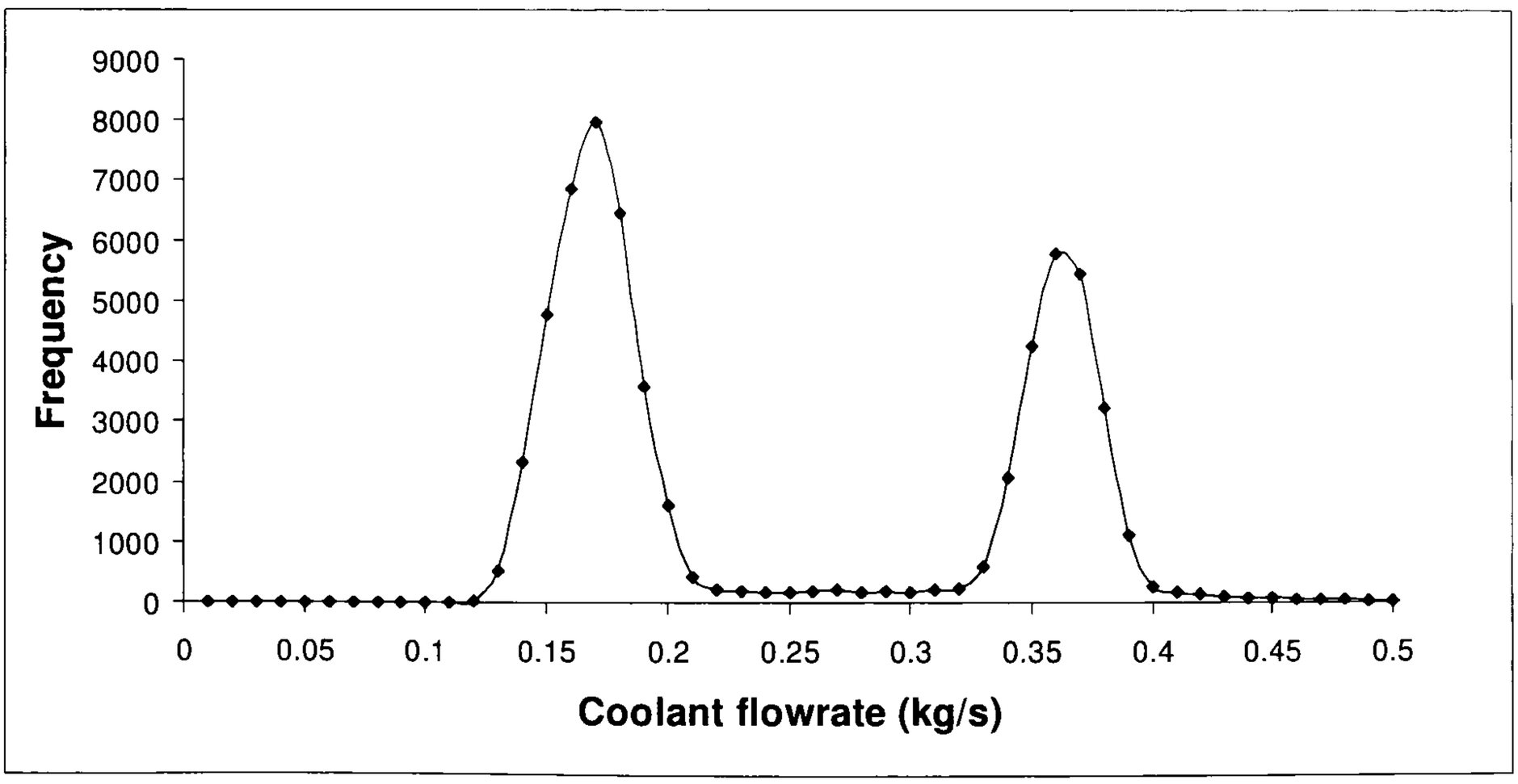


Figure 6.22: Coolant flowrate histogram for design 2 in iteration I (uniform case)

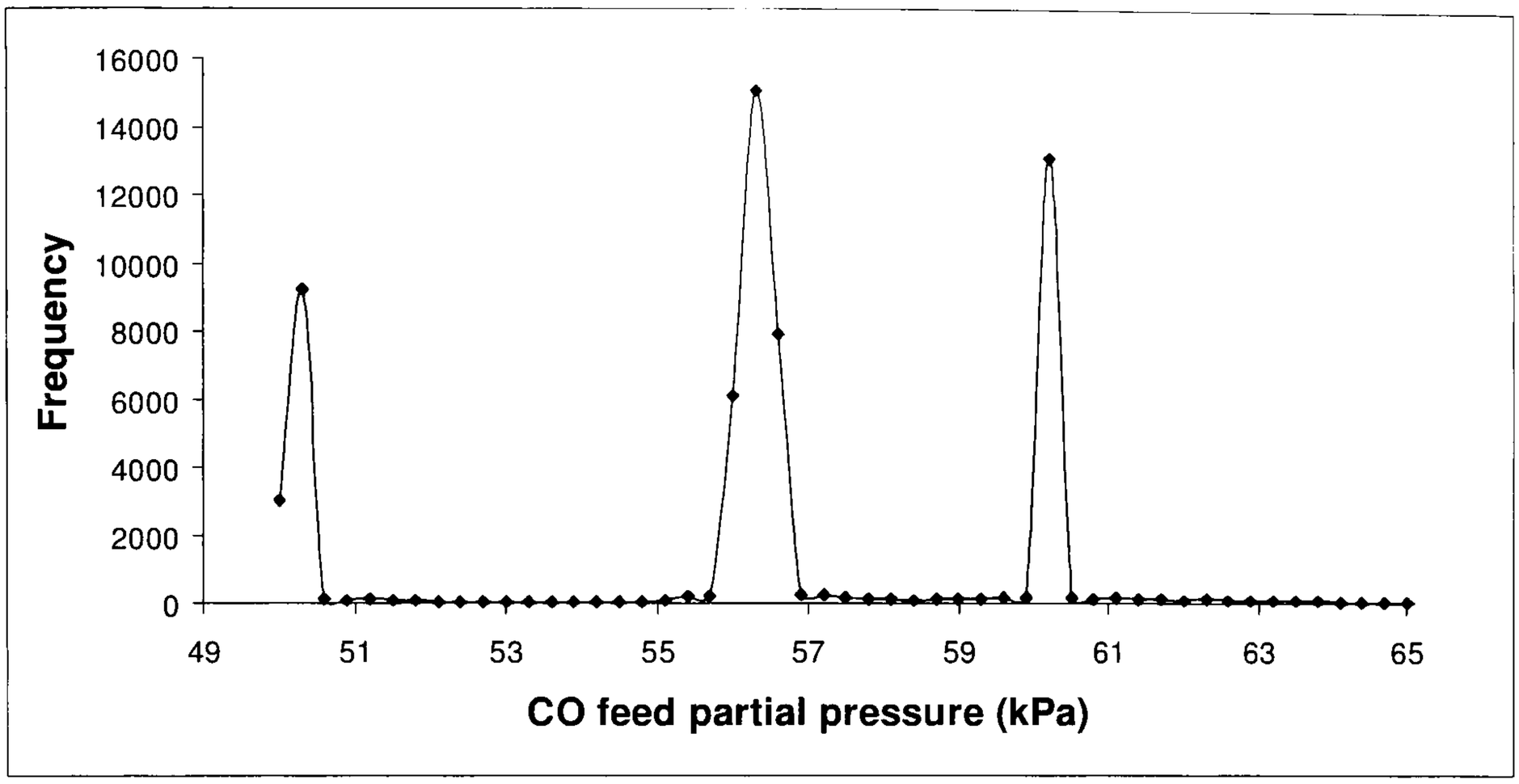


Figure 6.23: Carbon monoxide feed partial pressure histogram for design 2 in iteration I (uniform case)

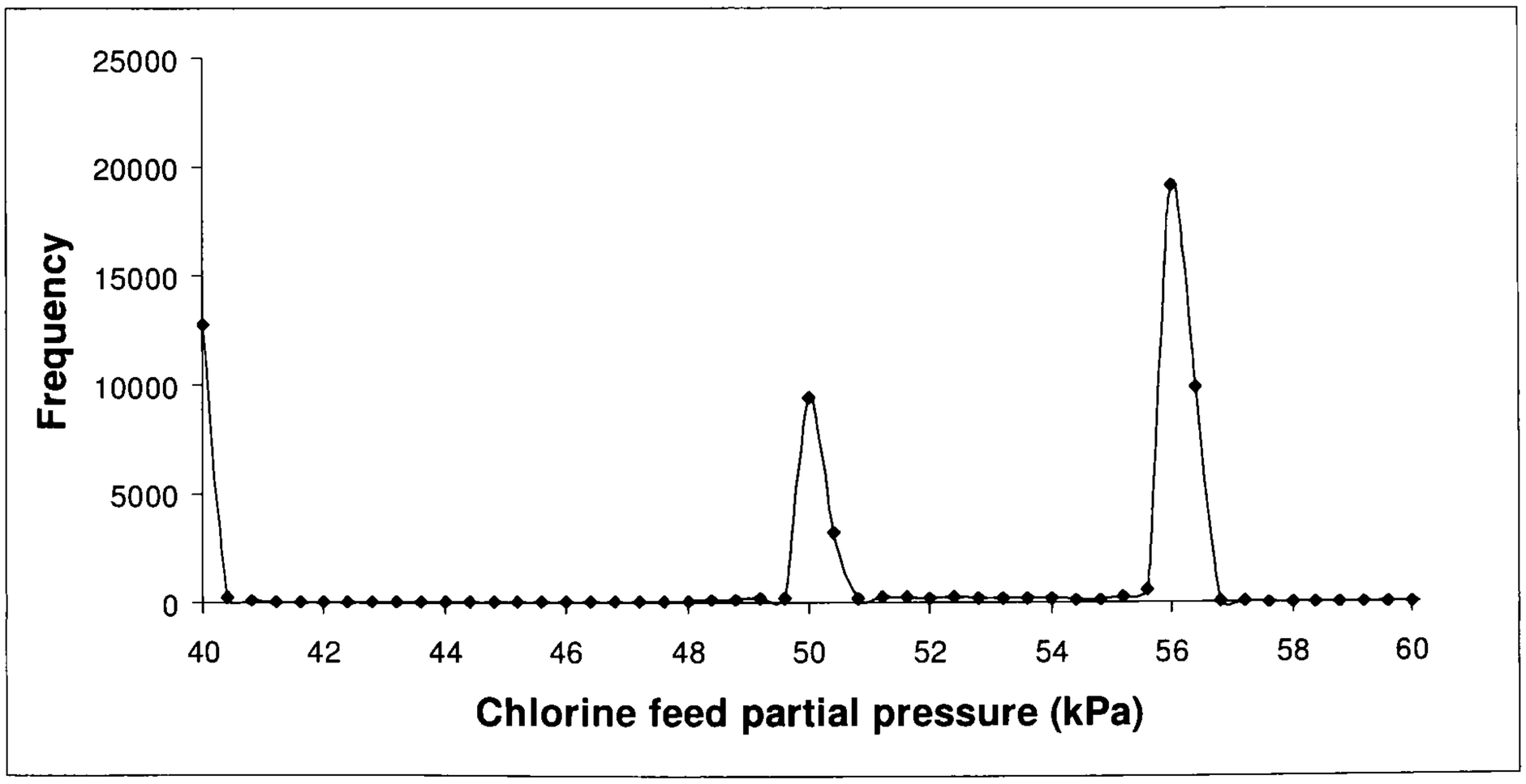


Figure 6.24: Chlorine feed partial pressure histogram for design 2 in iteration I (uniform case)

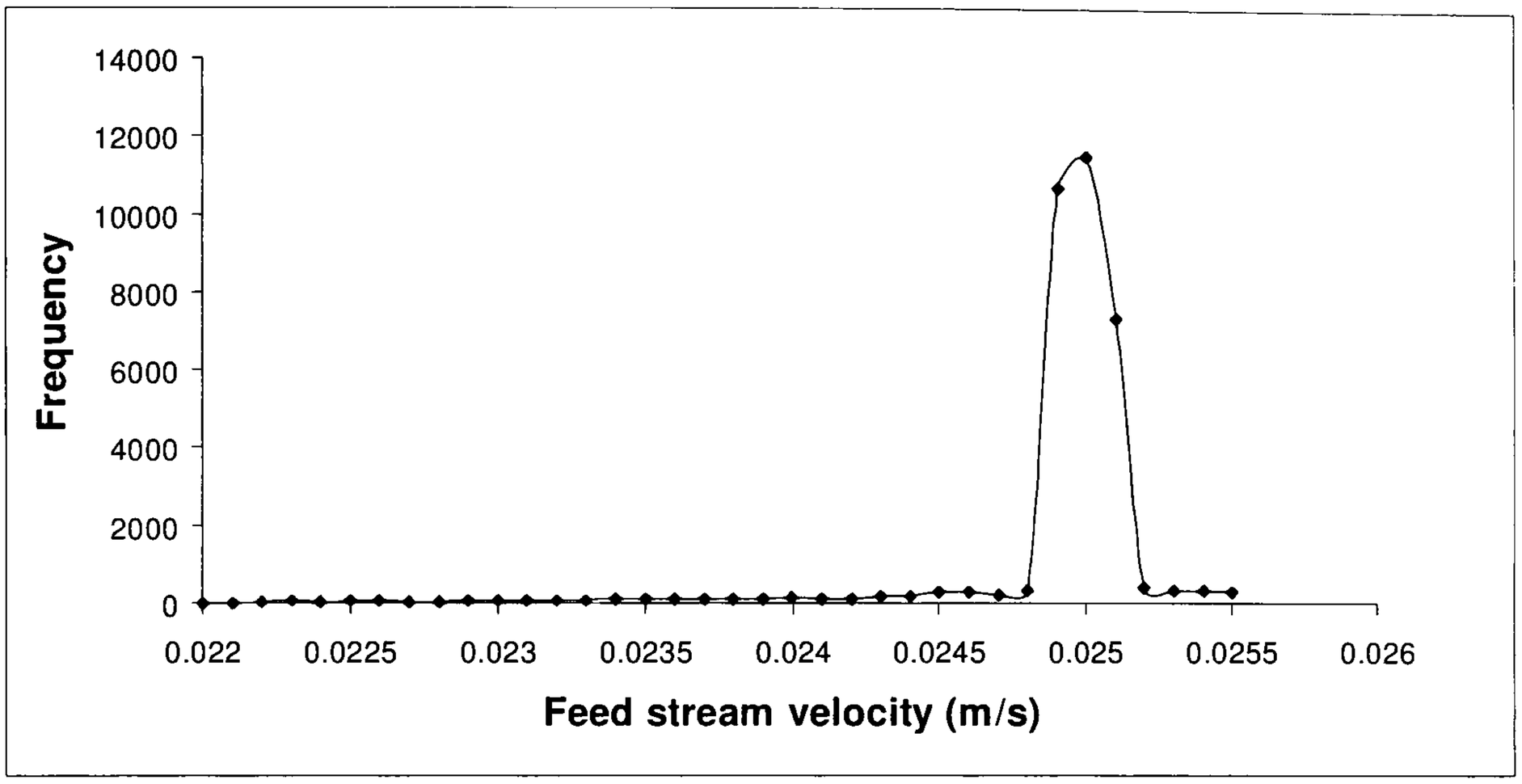


Figure 6.25: Feed stream velocity histogram for design 2 in iteration I (uniform case)

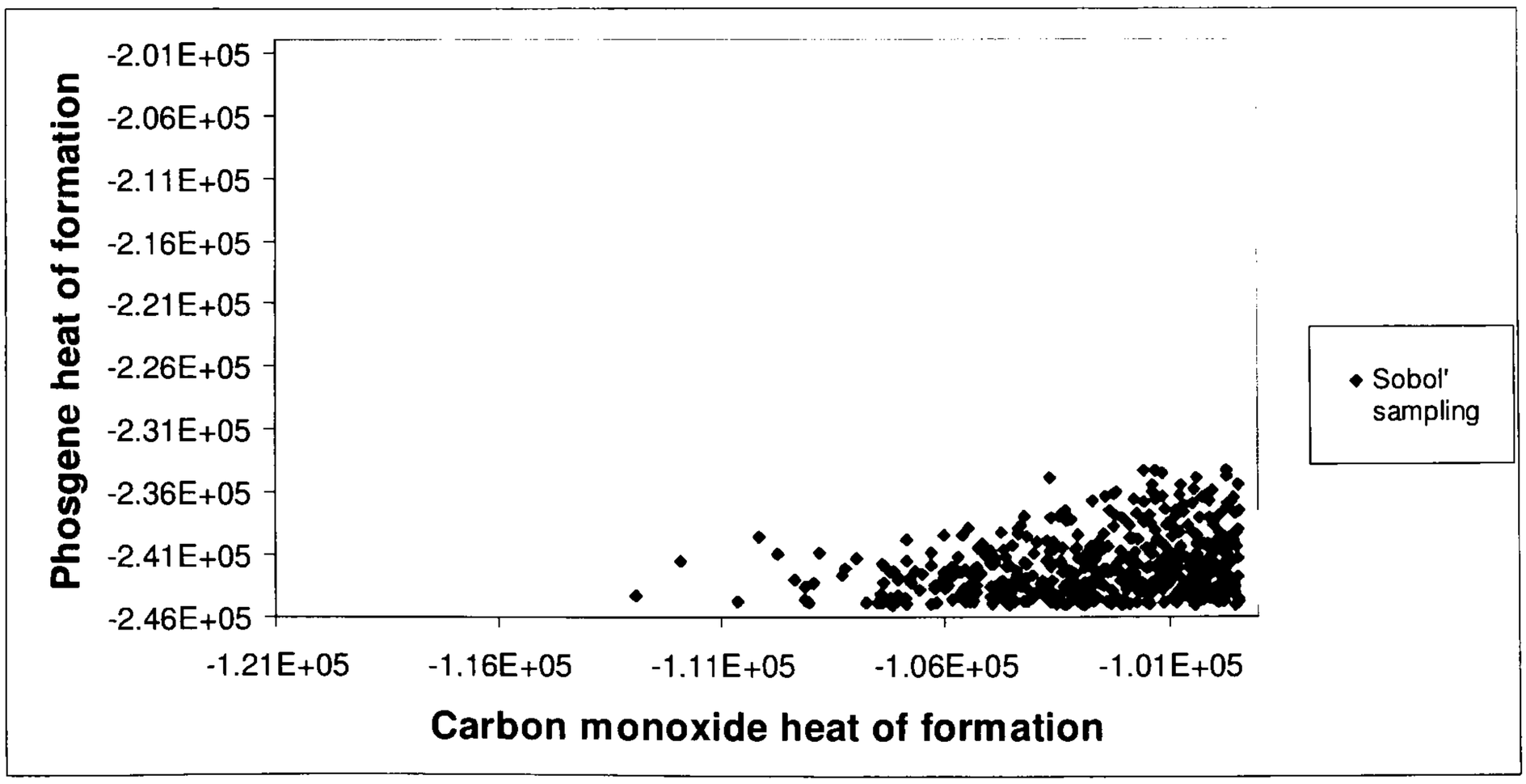


Figure 6.26: Infeasible points identified in the second GSFA for new design in iteration I

Table 6.19: Mean value and standard deviation for profit and control variables in iteration I for design 2 using Sobol' sampling with weight factors

	Sobol' sampling with weight factor	
Parameter	Mean	Std. Dev.
Profit (USD/yr)	382,910	19,370
F_{cw} (kg/s)	0.226	0.086
Vel (m/s)	0.027	0.003
pp_{CO} (kPa)	57.6	5.1
pp_{Cl_2} (kPa)	51.2	5.4

to 6.31.

The analysis identified 1,002 infeasible points which are equivalent to an infeasibility probability 0.0029% when using the normal parameter probability distributions.

6.3.5 Second stochastic design - Scenario-based optimisation

A similar approach to the previous case is followed when to generate the scenarios for the optimisation problem. Four new points are chosen from the list of infeasible points identified in the GSFA. These points, shown in blue, are plotted in figure 6.32 together with the previous points.

The solution of the 44-scenario based optimisation was obtained after approximately 71 hours and 51 minutes. The 44 points had the same weight. The value of the expected profit was 335,980 USD/yr and the new design (design 3) is shown in table 6.20. It can be seen that the reactor is longer than design 2 (6.456 m). This length is required to increase the cooling area and operate the reactor within the specified limits.

A new GSFA step is required to evaluate the risk and feasibility of design 3. This step is shown next.

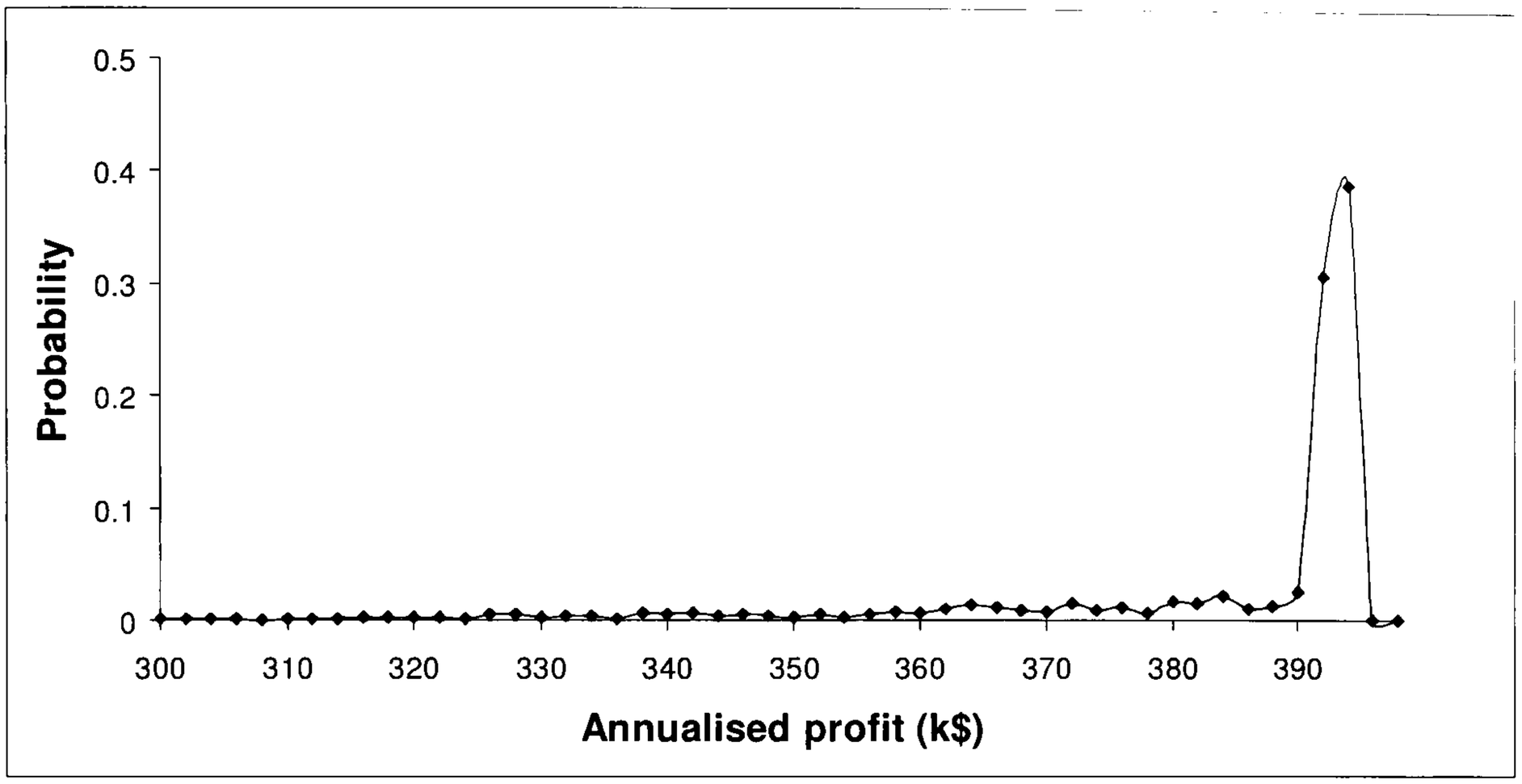


Figure 6.27: Annualised profit probability distribution for design 2 (normal case) in iteration I

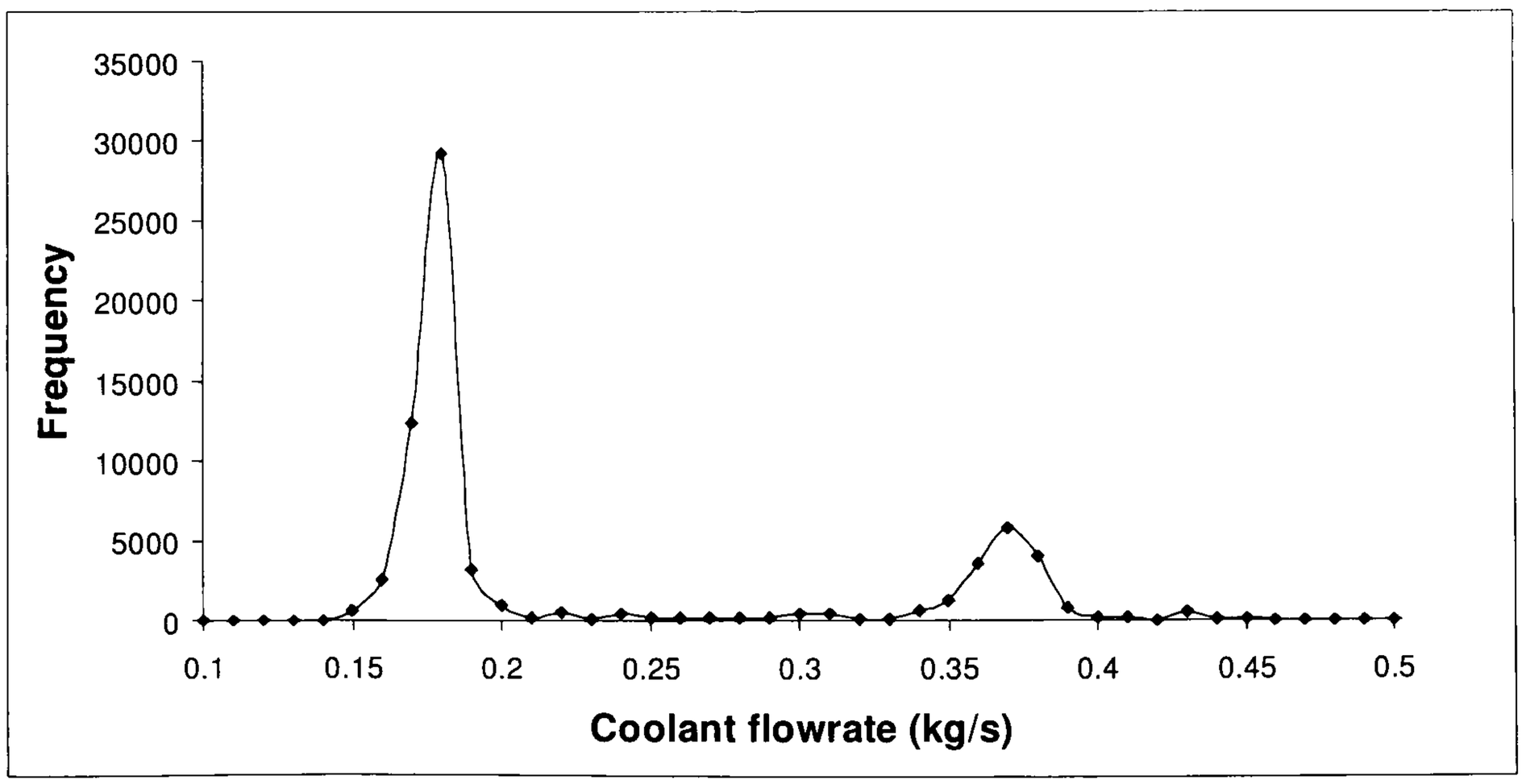


Figure 6.28: Normal coolant flowrate histogram for design 2 (normal case) in iteration I

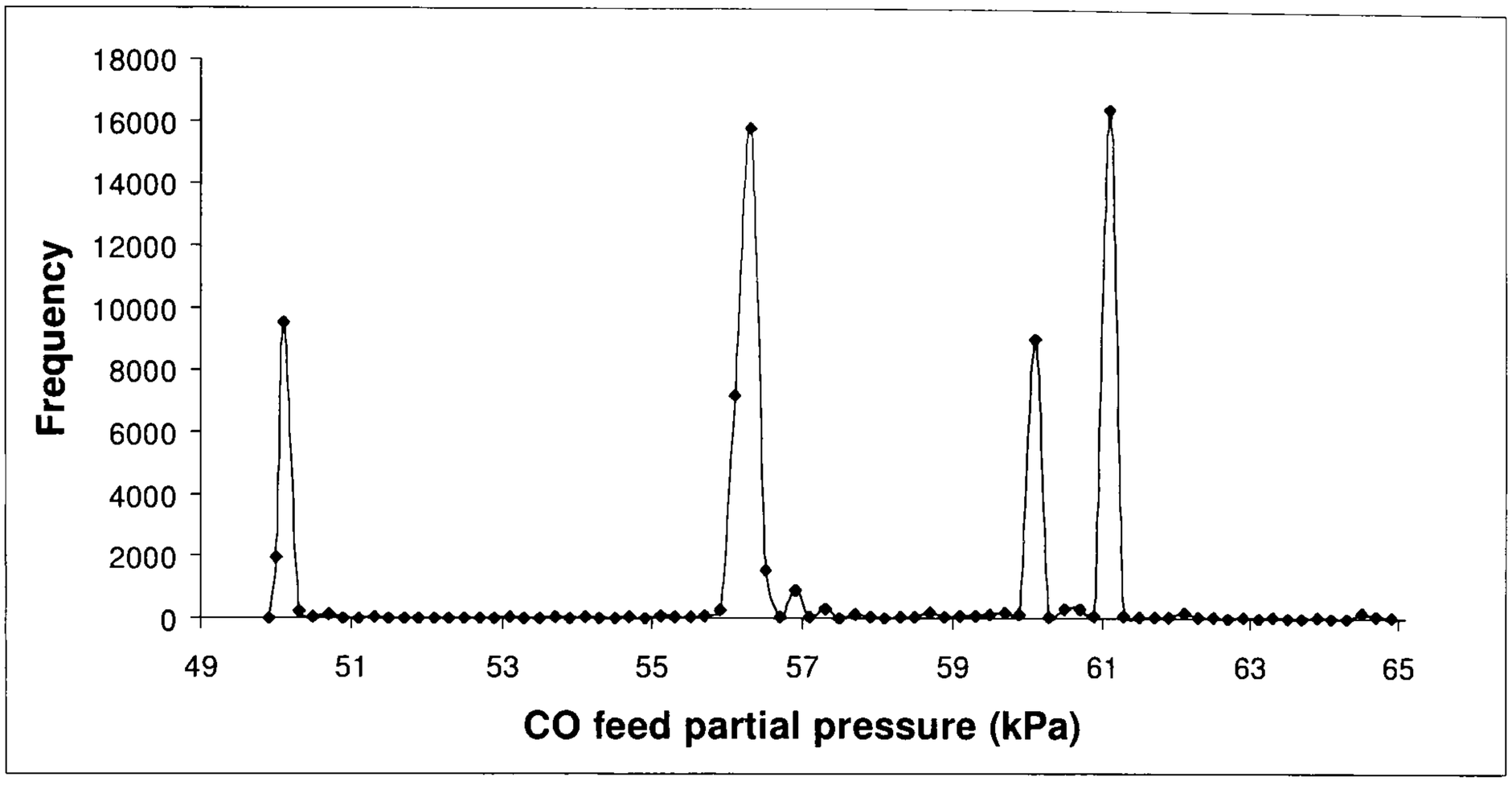


Figure 6.29: Carbon monoxide feed partial pressure histogram for design 2 (normal case) in iteration I

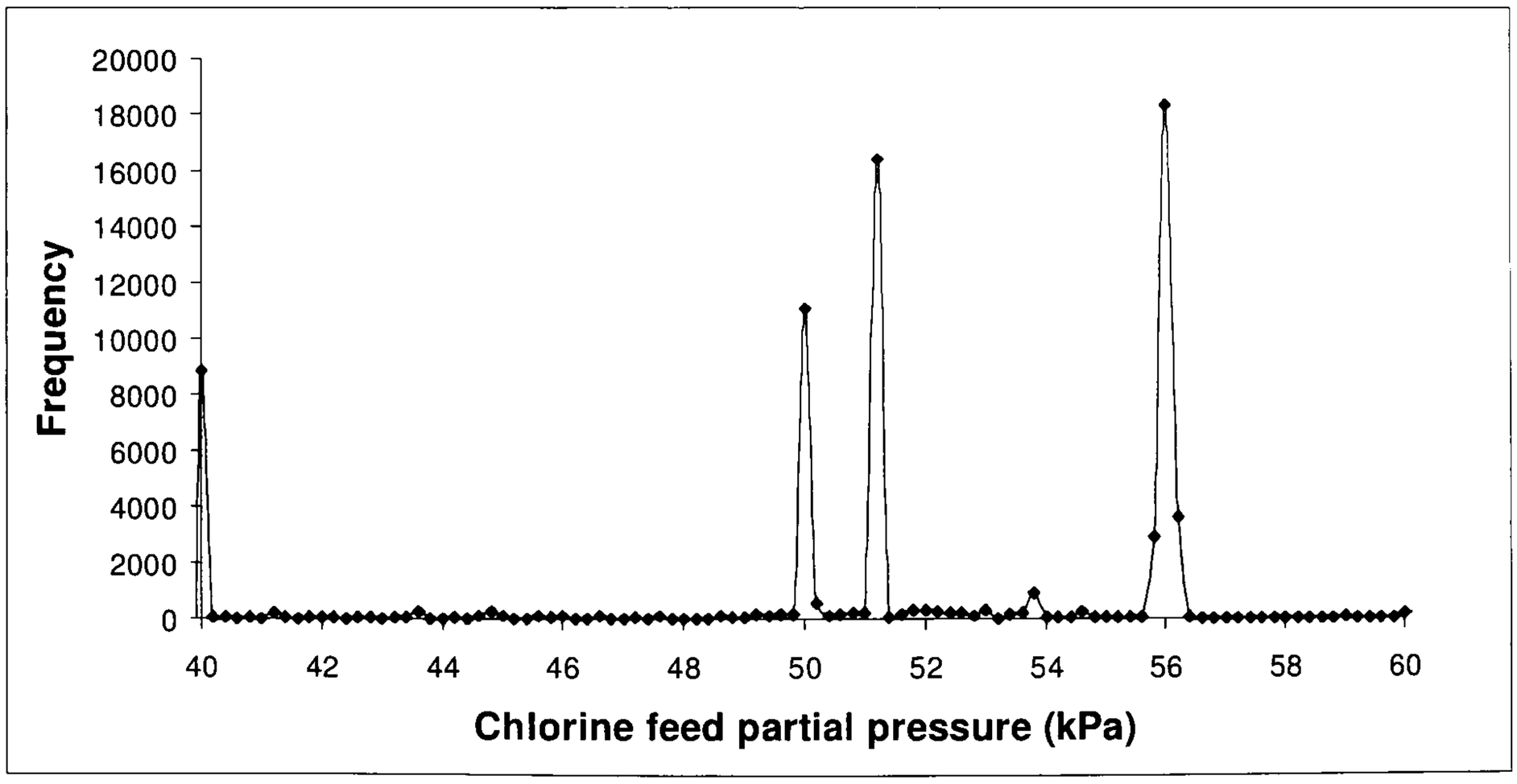


Figure 6.30: Chlorine feed partial pressure histogram for design 2 (normal case) in iteration I

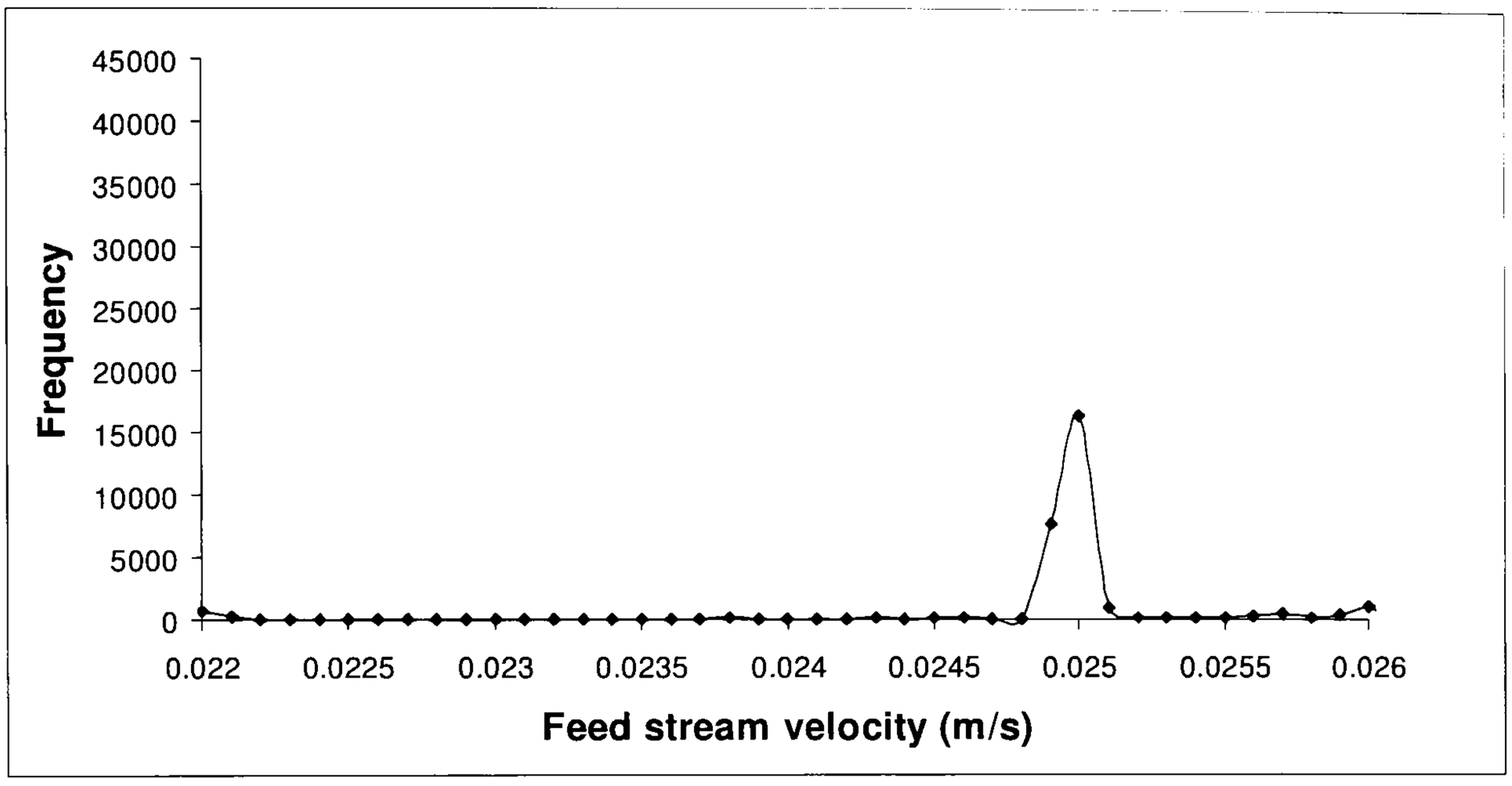


Figure 6.31: Feed stream velocity histogram for design 2 (normal case) in iteration I

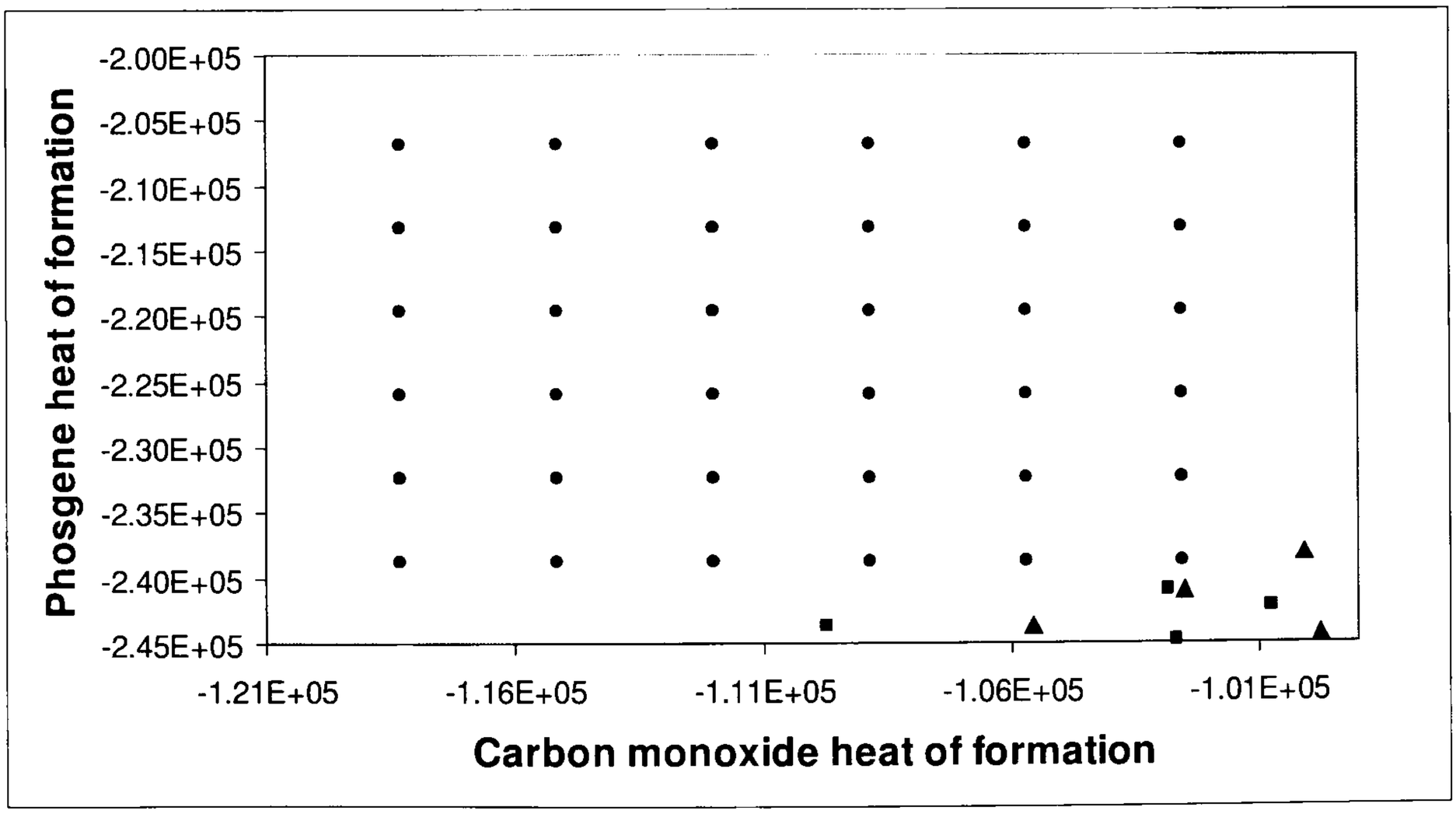


Figure 6.32: Sample points used for the scenario-based optimisation in the second stochastic design loop of iteration I

Table 6.20: Pseudo-dynamic optimisation results for the 44-scenario optimisation problem in iteration I (design 3)

Variable	Value	Lower bound	Upper bound
RZ (m)	8.062	0.5	20
RR (m)	0.342	0.05	2
RCW (m)	0.359	0.05	3

Table 6.21: GSFA results for first-order Sobol' indices for design 3 in iteration I

Parameter	Individual sensitivity indices, S_i	Total sensitivity indices, S_i^{Tot}	Rank
$\Delta H_{f(CO)}$	0.0362	0.4134	2
$\Delta H_{f(COCl_2)}$	0.4904	0.8612	1
Ek_r	-0.0268	0.0915	6
kr	-0.0380	0.0942	5
kz	-0.0803	0.1906	3
U	-0.0245	0.1474	4
T_{cwin}	-0.0434	0.0762	8
T_{in}	-0.0208	0.0874	7

6.3.6 Third stochastic design - GSFA

Uniform case A new GSFA was run for design 3. A Sobol' sampling of 4096 points was used and the results for the first order sensitivity indices are shown in table 6.21. These results show that the heats of formation are still the most relevant parameters. However, their value is decreasing, while the total sensitivity indices for all the parameters are increasing. This indicates that for this new design the higher order interactions are becoming relevant. The relevant second-order sensitivity indices are shown in table 6.22. The first order results were obtained after 72 hours and 18 minutes using 35 parallel processes. The second-order analysis was run in 35 machines after 57 hours and 56 minutes.

The mean and standard deviation of the profit and control variables can be seen in

Table 6.22: GSFA results for second-order Sobol' indices for design 3 in iteration I

Parameter	Second-order sensitivity indices, S_i
$\Delta H_{f(CO)}$-$\Delta H_{f(COCl_2)}$	0.2492
kz-$\Delta H_{f(CO)}$	0.0873
kz-$\Delta H_{f(COCl_2)}$	0.0793

Table 6.23: Mean value and standard deviation for profit and control variables in iteration I for design 3 (uniform case)

	Sobol' sampling	
Parameter	Mean	Std. Dev.
Profit (USD/yr)	349,330	31,180
F_{cw} (kg/s)	0.243	0.193
Vel (m/s)	0.028	0.003
pp_{CO} (kPa)	56.1	3.9
pp_{Cl_2} (kPa)	49.9	6.6

table 6.23. As seen with design 2, the further increase in reactor length for design 3 led to a lower annualised expected profit. The difference with respect to the deterministic design is around 120,000 USD/yr and the difference with respect to design 2 is around 20,000 USD/yr. Furthermore, the standard deviation has also been reduced when compared to the deterministic design and design 2. This indicates that the expected profit is less affected by the given uncertainty level in design 3 than when using the previous designs. The histogram for the annualised profit can be seen in figure 6.33, while those for the control variables are shown in figures 6.34 to 6.37.

The comparison between of expected profit between the nominal and final designs can be useful to determine the cost of reducing the infeasibility probability. In the final design, the number of infeasible points was 527 after analysing around 69,632 sample points. In the initial nominal design, it was shown that there is an infeasibility probability of 1.92%.

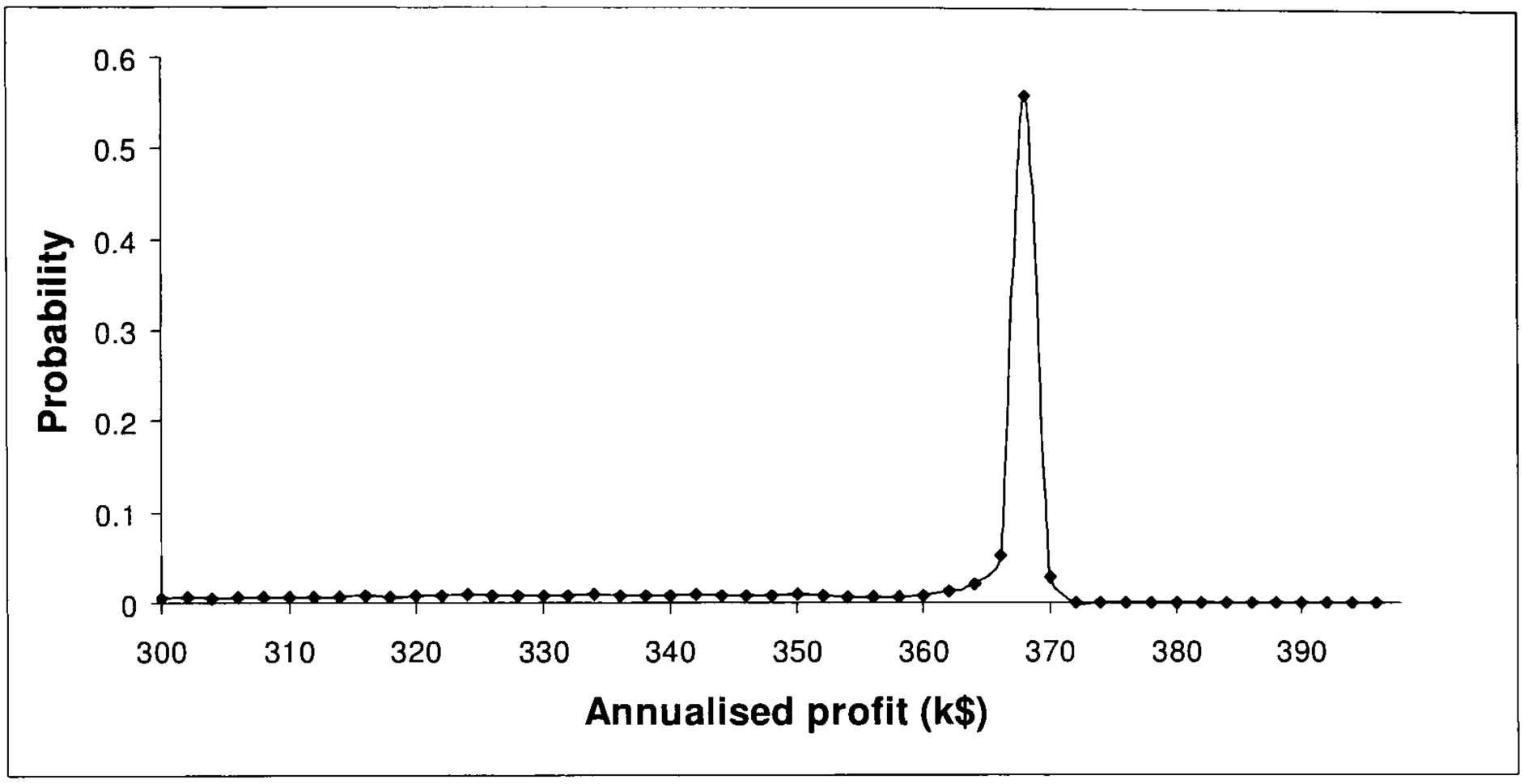


Figure 6.33: Annualised profit probability distribution for design 3 in iteration I (uniform case)

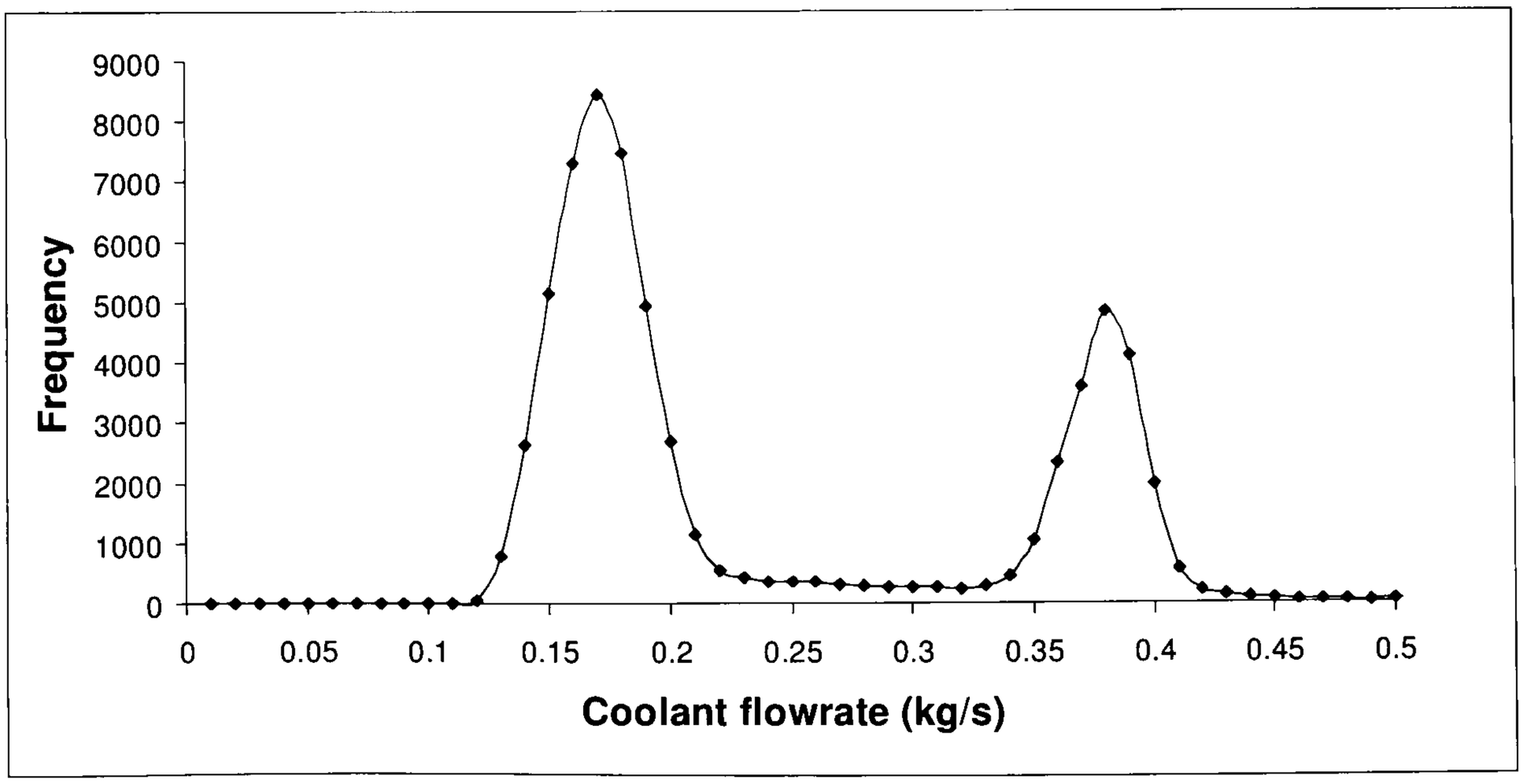


Figure 6.34: Coolant flowrate histogram for design 3 in iteration I (uniform case)

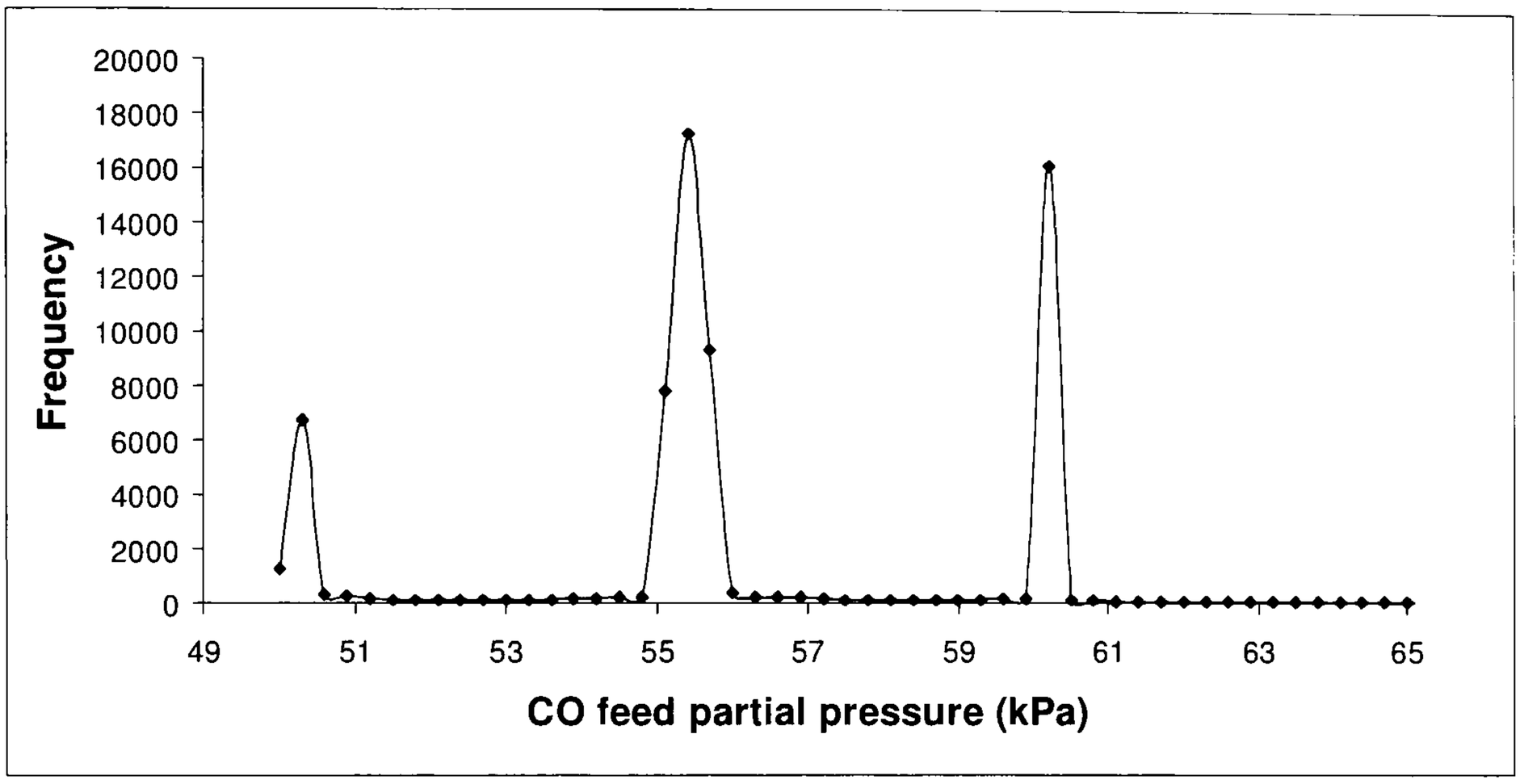


Figure 6.35: Carbon monoxide feed partial pressure histogram for design 3 in iteration I (uniform case)

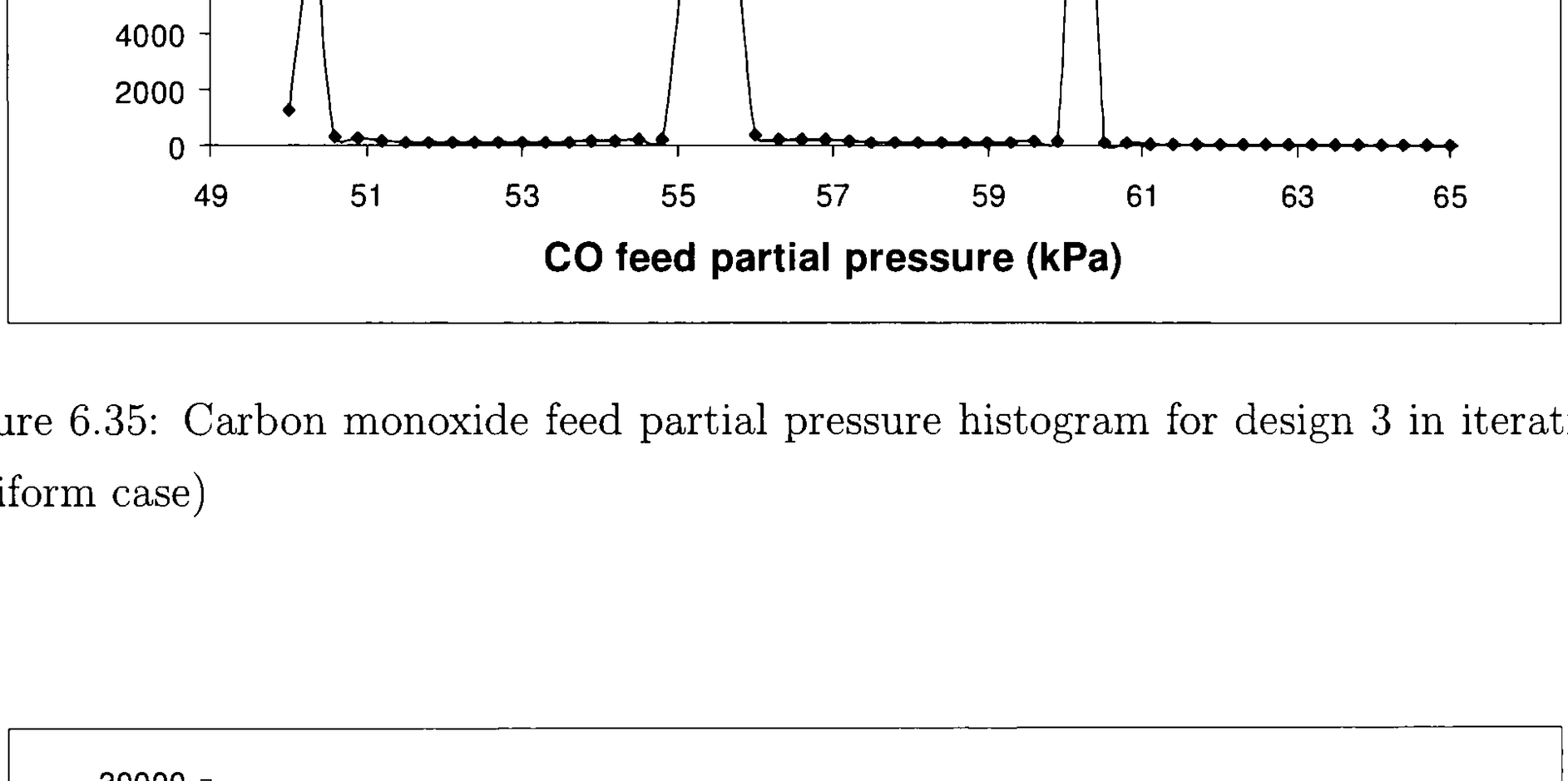


Figure 6.36: Chlorine feed partial pressure histogram for design 3 in iteration I (uniform case)

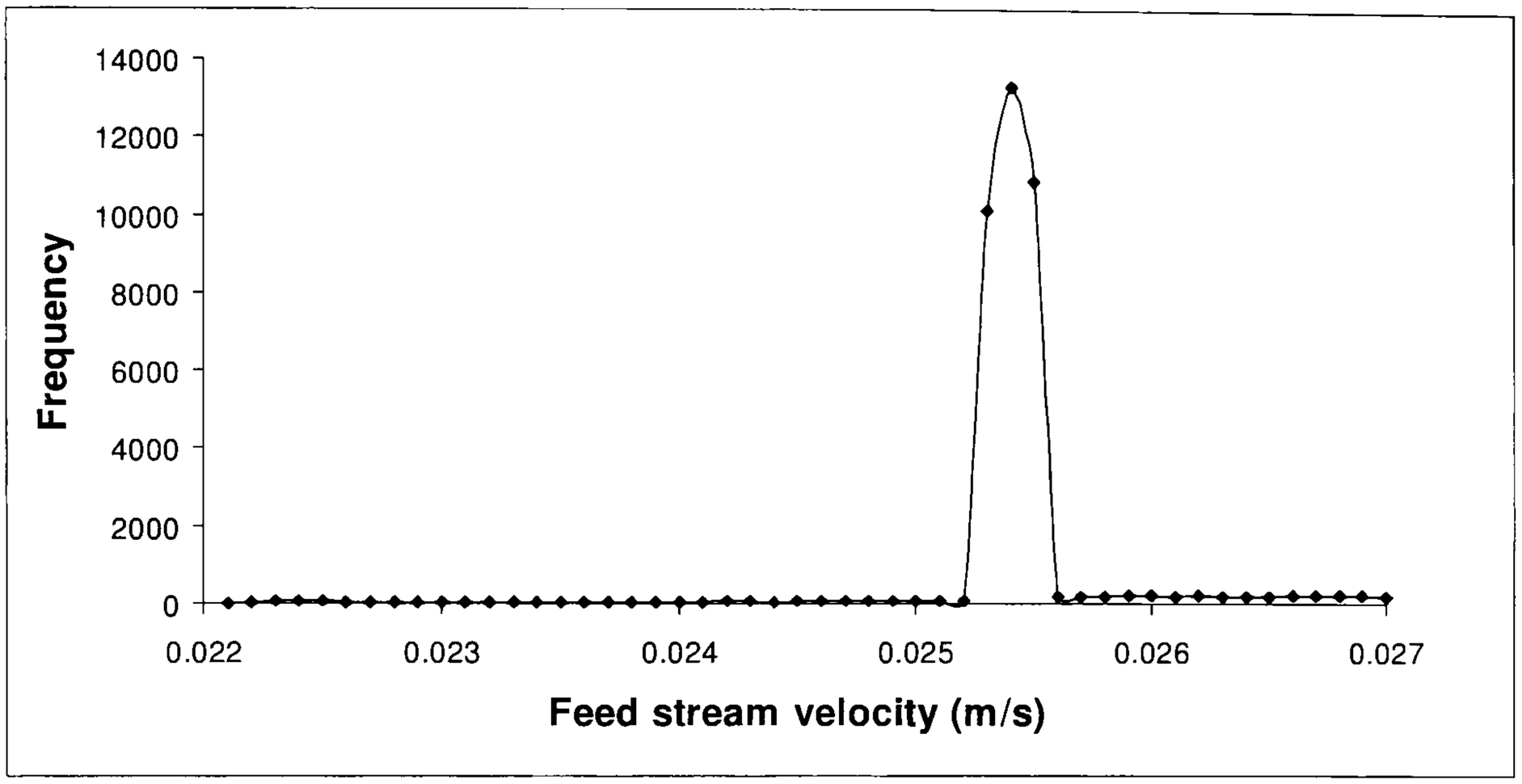


Figure 6.37: Feed stream velocity histogram for design 3 in iteration I (uniform case)

while the value for design 3 is 0.75%. Therefore, the annualised profit difference between the deterministic design and design 3, 120,000 USD/yr, can be seen as the cost of reducing the infeasibility probability to a value of 0.75%.

Normal case As before, the results of the uniform case were converted to a normal pdf by using weight factors. Table 6.24 shows the results of this conversion for the mean and standard deviation of the KPIs. The mean annualised difference between design 3 and the nominal design is around 120,000 USD/yr, and the difference with respect to design 2 is 20,000 USD/yr.

The histograms for the annualised profit and control variables are shown in figures 6.38 to 6.42.

A total of 527 infeasible points were identified during the GSFA using Sobol' sampling. Using the weight factors, the infeasibility probability for these 527 points is equivalent to a probability of 0.0007%.

With the given information, managerial and technical decisions can be made. A comparison of performance between the nominal and the updated designs can be made, together with the analysis on costs associated with the reduction on the infeasibility probability and deviations on the expected value of key performance indicators. A managerial

Table 6.24: Mean value and standard deviation for profit and control variables in iteration I for design 3 (normal case)

	Sobol' sampling with weight factor	
Parameter	Mean	Std. Dev.
Profit (USD/yr)	361,750	14,020
F_{cw} (kg/s)	0.212	0.078
Vel (m/s)	0.027	0.003
pp_{CO} (kPa)	55.2	3.2
pp_{Cl_2} (kPa)	51.9	5.2

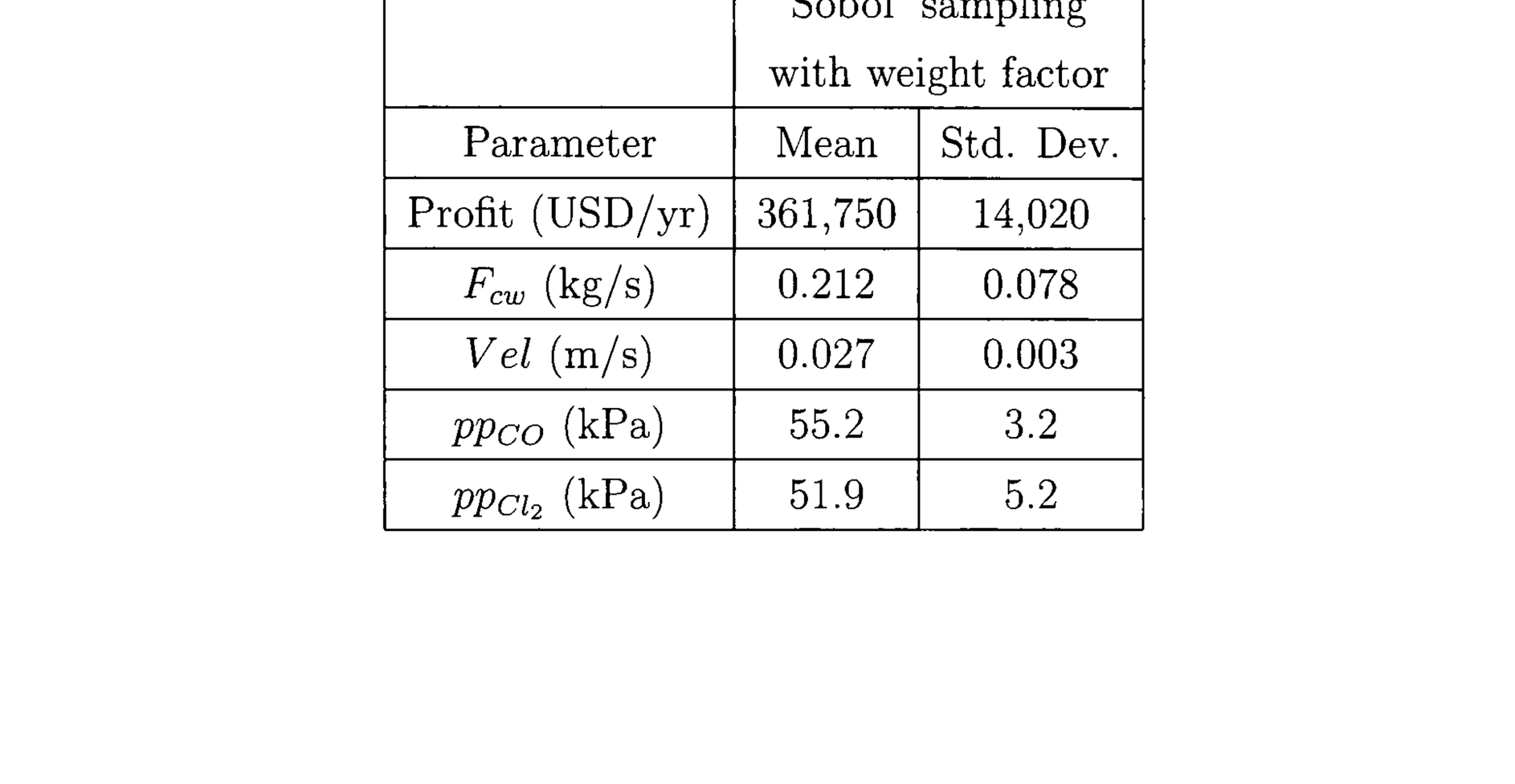


Figure 6.38: Annualised profit probability distribution for design 3 (normal case) in iteration I

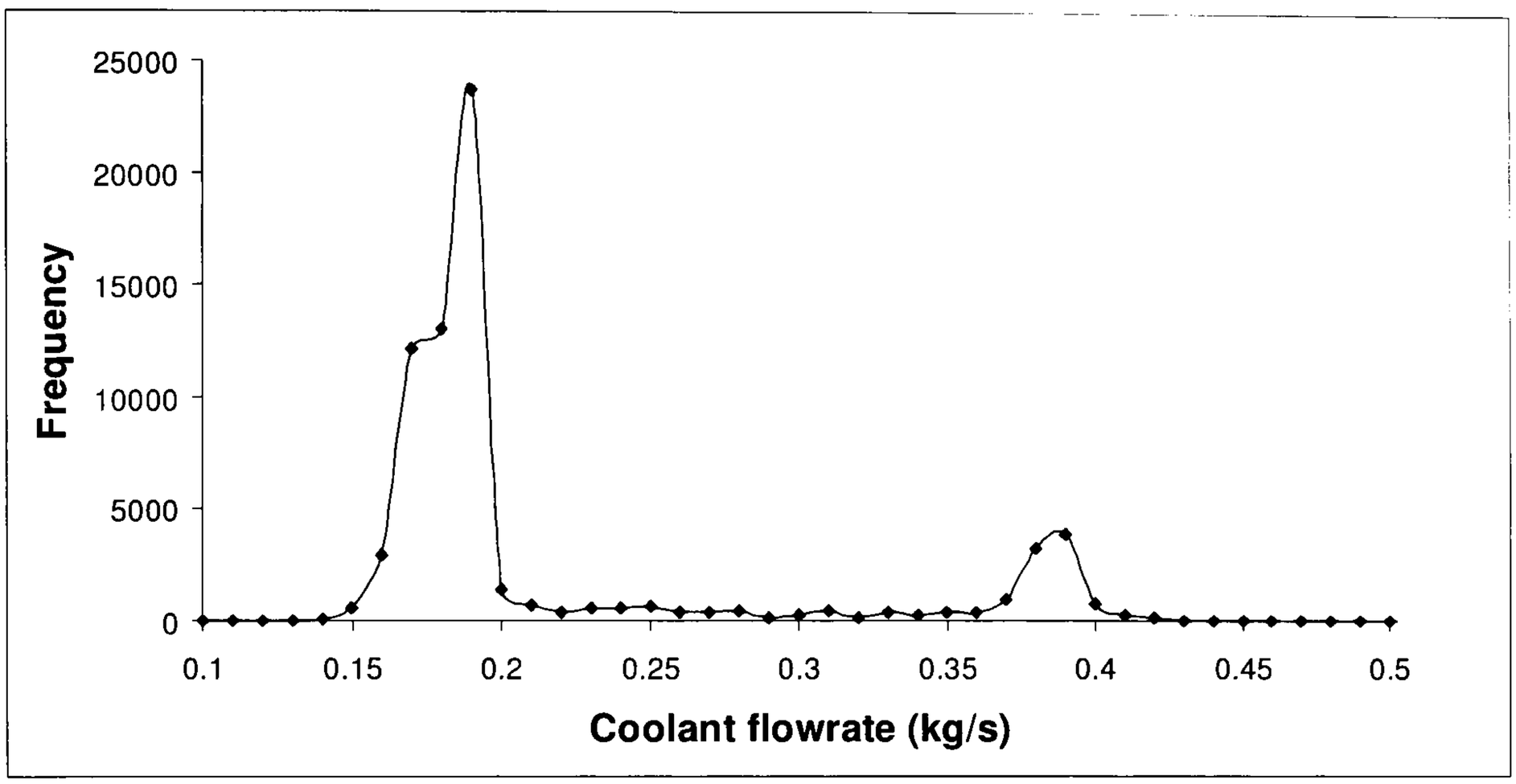


Figure 6.39: Normal coolant flowrate histogram for design 3 (normal case) in iteration I

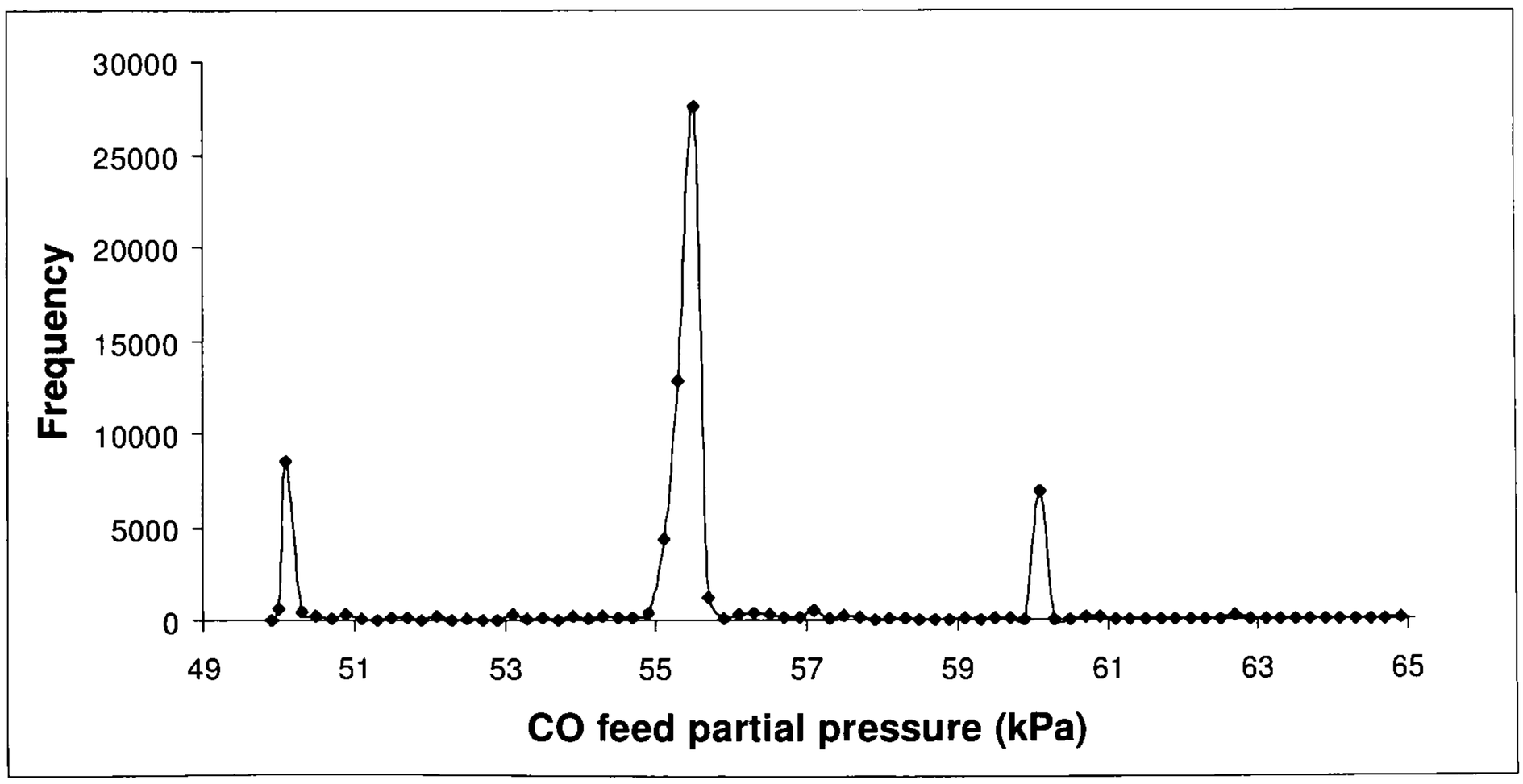


Figure 6.40: Carbon monoxide feed partial pressure histogram for design 3 (normal case) in iteration I

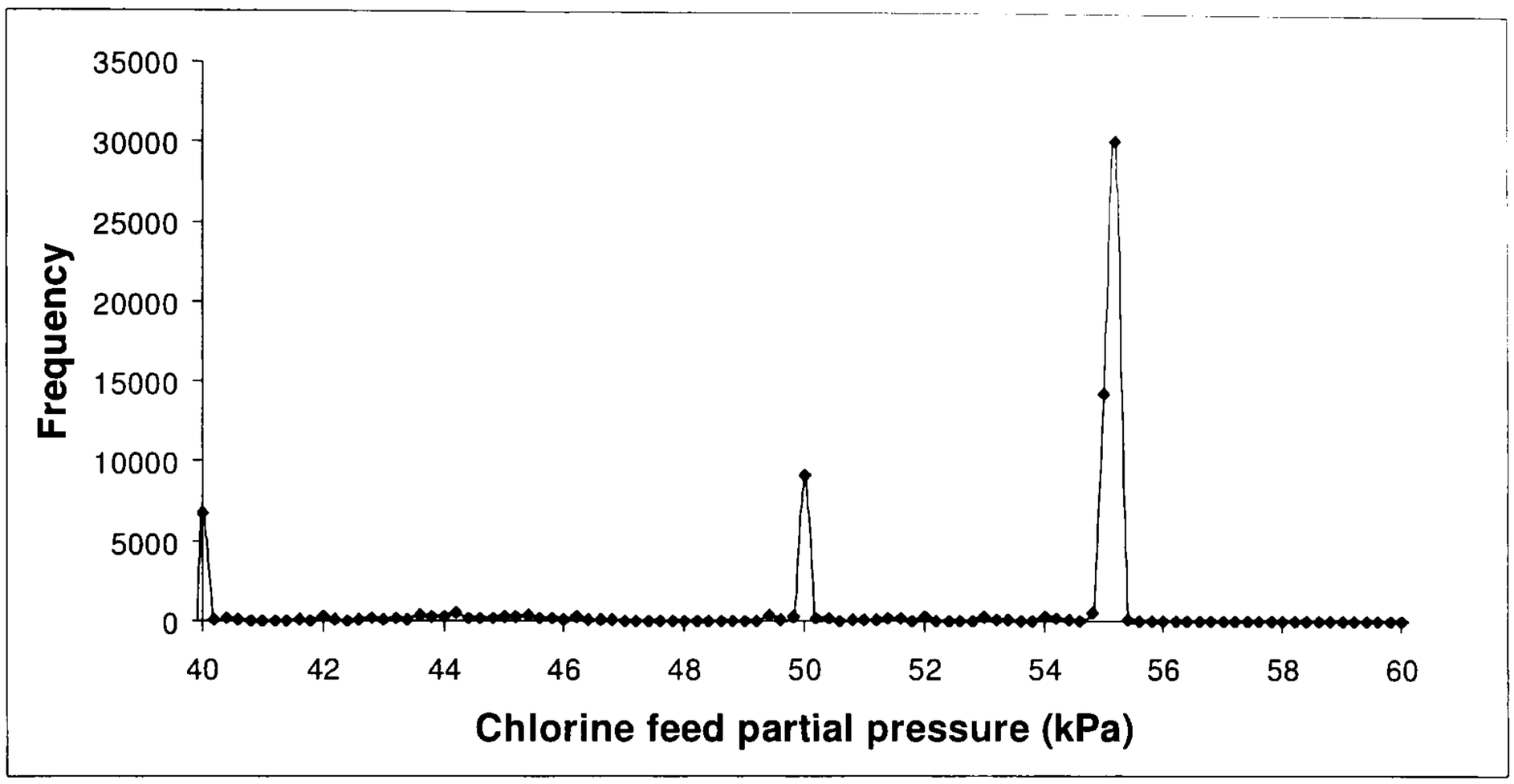


Figure 6.41: Chlorine feed partial pressure histogram for design 3 (normal case) in iteration I

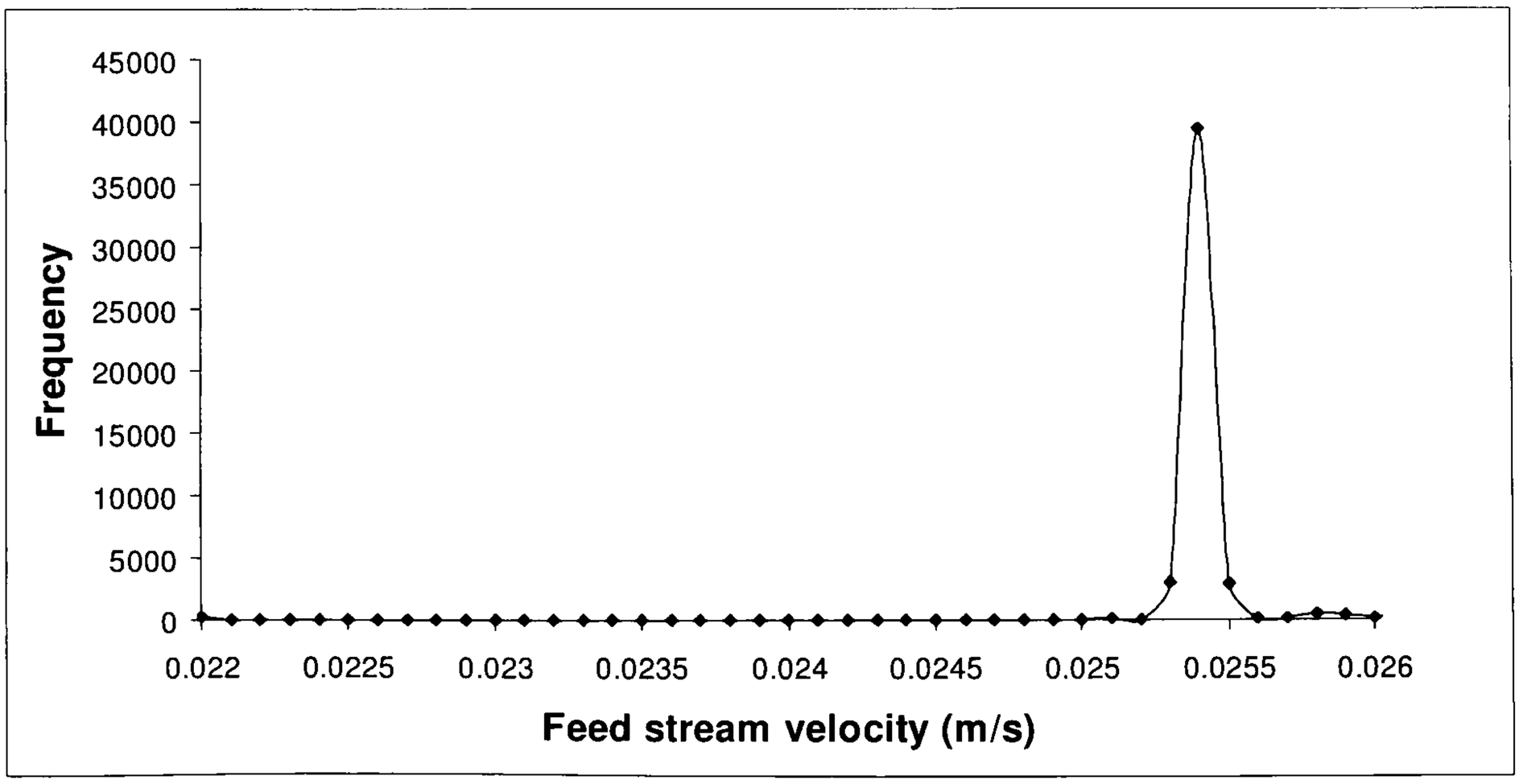


Figure 6.42: Feed stream velocity histogram for design 3 (normal case) in iteration I

decision may be made on which design to use based on the infeasibility probability and the associated cost to reduce it. On the other hand, technical decisions can be focused on acceptable ranges for control variables, expected operating conditions or output stream conditions which may have an effect on downstream units.

A decision regarding the parameter uncertainty can also be taken. If the risk is still considered unacceptable, even for a low infeasibility probability, the decisions can be focused on reducing the parameter uncertainty. The decision will depend on the expected costs required to reduce it. In some cases, this may be a cheaper and/or quicker option to take than going for a more expensive design which deals with the given uncertainty range.

The results obtained illustrate the use of the proposed methodology to quantify the risk in cases where uncertainty is present. The expected performance and risk of the nominal design was analysed and the infeasible regions were identified. If the risk is deemed as unacceptable, the methodology was used to generate a feasible design and compare the inherent risk and expected performance between the new and nominal designs. The information generated can be used to facilitate the decision-making process, where managerial or technical decision are involved.

In the following section, it is assumed that R&D has been undertaken in view of the high cost of uncertainty.

6.4 Iteration II

One of the decisions that can be taken after obtaining the results of iteration I is to focus R&D resources to reduce the uncertainty level of the critical parameters. In iteration II, the effect of uncertainty reduction is investigated. It is assumed the uncertainty in the parameters has been reduced to the levels shown in table 6.25.

The nominal design, obtained in the deterministic optimisation step, is the same as that obtained for iteration I since the nominal values are assumed to remain unchanged and only their ranges/standard deviations are affected.

The next step in the proposed methodology is stochastic design, starting with GSFA.

Table 6.25: Uncertain parameters for iteration II

Parameter	Mean	Range % (uniform)	Std Dev % (normal)
$\Delta H_{f(CO)}$ (kJ kmol^{-1})	-110440	±1	0.33
$\Delta H_{f(COCl_2)}$ (kJ kmol^{-1})	-222850	±1	0.33
Ek_r (kPa m^3 kmol^{-1})	57686.3	±10	3.33
kr (kW m^{-1}K^{-1})	0.05	±3.34	1.67
kz (kW m^{-1}K^{-1})	0.05	±3.34	1.67
U (kJ m^{-2}K^{-1})	0.096	±3.34	1.67
T_{cwin} (K)	293	±1	0.33
T_{in} (K)	293	±1	0.33

6.4.1 First stochastic design - GSFA

Uniform case

The analysis was run for 4096 Sobol' points for the 8-dimensional space defined by the uncertain parameters. The results for the first-order Sobol' sensitivity indices are shown in table 6.26 and the values are compared to those obtained in iteration I. The number of optimisation problems solved was 69,632 equal to (4096×(2×8+1)). The computational time needed was approximately 23.5 hours using 30 parallel machines on Linux cluster with machines ranging from 1.79 - 3.39 GHz.

Table 6.26 shows that the heat of formation of phosgene is still the parameter affecting the most the annualised profit. However, its sensitivity index value is not as high as that in iteration I (0.5555 vs. 0.1575) and the higher-order indices have also decreased, see table 6.27. On the other hand, values such as the kinetic parameter, Ek_r, the axial heat transfer coefficient, kz, and the overall heat transfer coefficient, U, have their values increased. Overall, the sensitivity is been distributed over the different uncertain parameters.

The calculation of the 6 second-order sensitivity indices was done for 4096 Sobol' points, requiring 53248, (4096×(2×6+1)), optimisation problems. 11 parallel computers were used ranging from 1.79 - 3.39 GHz with a total CPU time of approximately 40.5 hours.

Table 6.26: Comparison of GSFA results for first-order Sobol' indices for nominal design between iterations I and II

	Iteration I, nominal design		Iteration II, nominal design	
Parameter	S_i	S_i^{Tot}	S_i	S_i^{Tot}
$\Delta H_{f(CO)}$	0.0842	0.3199	0.0326	0.1117
$\Delta H_{f(COCl_2)}$	0.5555	0.8656	0.1575	0.3464
Ek_r	-0.0269	0.0134	0.1234	0.3398
kr	-0.0687	0.0295	0.0262	0.0599
kz	-0.0296	0.0763	0.1016	0.3237
U	-0.0247	0.0587	0.1390	0.2857
T_{cwin}	-0.0307	0.0073	0.0829	0.1187
T_{in}	-0.0275	0.0031	0.0008	0.0218

Table 6.27: GSFA results for higher-order Sobol' indices for nominal design in iteration II

Parameter	Second-order sensitivity index, S_i^{2nd}	Group sensitivity index, S_i
k_z-U	0.0308	0.2714
$\Delta H_{f(COCl_2)}$-k_z	0.0299	0.2889
k_z-Ek_r	0.0419	0.2669
$\Delta H_{f(COCl_2)}$-U	0.0078	0.3042
U-Ek_r	0.0063	0.2686
$\Delta H_{f(COCl_2)}$-Ek_r	0.0229	0.3038

Table 6.28: Mean value and standard deviation for profit and control variables for nominal design in iteration II using Sobol' sampling

	Sobol' sampling	
Parameter	Mean	Std. Dev.
Profit (USD/yr)	486,500	6,110
F_{cw} (kg/s)	0.391	0.065
Vel (m/s)	0.026	0.001
pp_{CO} (kPa)	54.1	6.2
pp_{Cl_2} (kPa)	50.0	1.4

The group sensitivity indices in table 6.27 are formed of the contributions of the parameters involved in the index. For example, the group sensitivity index for k_z-U is formed by the first-order sensitivity indices of k_z and U and the second-order sensitivity index of k_z-U. Therefore, it can be seen that first-order contributions are the main effects affecting the annualised profit.

The sensitivity indices on their own do not provide a complete analysis for the given problem, since they are relative values. The use of the variance can provide a better analysis to relate the indices to a base value and give a measure of how much are the uncertain parameters affecting the key performance indicator. The value of the total variance, D, for iteration I is 1,133,896 $(\text{USD/yr})^2$, corresponding to a standard deviation of 33,670 USD/yr. In comparison, the total variance in iteration II is 37,360 $(\text{USD/yr})^2$, for a standard deviation of 6,110 USD/yr. The mean and standard deviation values for the KPIs are shown in table 6.28.

These results illustrate the fact that the output uncertainty can be reduced by focusing effort in reducing the uncertainty in some parameters. In iteration I, the two parameters affecting the most the annualised profit were the heats of formation of carbon monoxide and phosgene. If the uncertainty in iteration I can be reduced from a range of $\pm 10\%$ to $\pm 1\%$ the observed variance is reduced considerably.

Furthermore, after solving approximately 122,000 optimisation problems, no infeasible points were found. Therefore, the nominal design can be regarded as acceptable for the existing uncertainty level.

Table 6.29: Comparison of GSFA results for first-order Sobol' indices using a Sobol'-normal sampling between iterations I and II (normal case, nominal design)

	Iteration I, nominal design		Iteration II, nominal design	
Parameter	S_i	S_i^{Tot}	S_i	S_i^{Tot}
$\Delta H_{f(CO)}$	0.1322	0.2690	0.0264	0.1228
$\Delta H_{f(COCl_2)}$	0.6661	0.8089	0.1024	0.3396
Ek_r	0.0131	0.0260	0.1559	0.5355
kr	0.0079	0.0111	0.0266	0.0797
kz	0.0147	0.0548	0.0686	0.3280
U	0.0185	0.0454	0.1167	0.3020
T_{cwin}	0.0027	0.0076	0.0975	0.1294
T_{in}	0.0010	0.0042	0.0028	0.0329

Normal case

A Sobol'-normal sampling method is used to generate 4096 points. The results for the first-order Sobol' indices are shown in table 6.29. It can be seen that the resulting ranking may change depending on the sampling method used. For instance, the uncertain parameter having the highest effect using the Sobol'-normal sampling is Ek_r, followed by U and $\Delta H_{f(COCl_2)}$. In comparison, the ranking using a Sobol' sampling method (see table 6.26) is $\Delta H_{f(COCl_2)}$, followed by U and Ek_r.

The second-order indices for the Sobol'-normal sampling are shown in table 6.30. It can be seen that second-order indices are relatively low, with the highest second-order index equal to 0.0669 corresponding to the interaction between k_z and Ek_r.

The standard deviation values for this iteration are compared to those obtained in iteration I using the nominal and final designs. These values are shown in table 6.31. When comparing the results for the nominal designs, it can be seen that the mean values of the annualised profit and control variables are similar. However, the effect of reducing the uncertainty level from iteration I to iteration II is observed as a decrease in the standard deviation.

The risk quantification for this iteration can be graphically seen in the histograms of

Table 6.30: GSFA results for higher-order Sobol' indices using Sobol'-normal sampling in iteration II

Parameter	Second-order sensitivity index, S_i^{2nd}	Group sensitivity index, S_i
k_z-U	0.0196	0.2048
$\Delta H_{f(COCl_2)}$-k_z	0.0086	0.1795
k_z-Ek_r	0.0669	0.2914
$\Delta H_{f(COCl_2)}$-U	0.0157	0.2348
U-Ek_r	0.0064	0.2789
$\Delta H_{f(COCl_2)}$-Ek_r	0.0582	0.3165

Table 6.31: Comparison of standard deviations for nominal designs using Sobol'-normal sampling in iterations I and II

	Iteration I, nominal design		Iteration I, design 3		Iteration II, nominal design	
Parameter	Mean	Std. Dev.	Mean	Std. Dev.	Mean	Std. Dev.
Profit (USD/yr)	476,110	23,020	361,750	14,020	488,350	3,000
F_{cw} (kg/s)	0.372	0.075	0.212	0.078	0.384	0.037
Vel (m/s)	0.026	0.001	0.027	0.003	0.025	0.000
pp_{CO} (kPa)	56.2	7.5	55.2	3.2	53.7	5.1
pp_{Cl_2} (kPa)	48.8	3.0	51.9	5.2	50.3	0.9

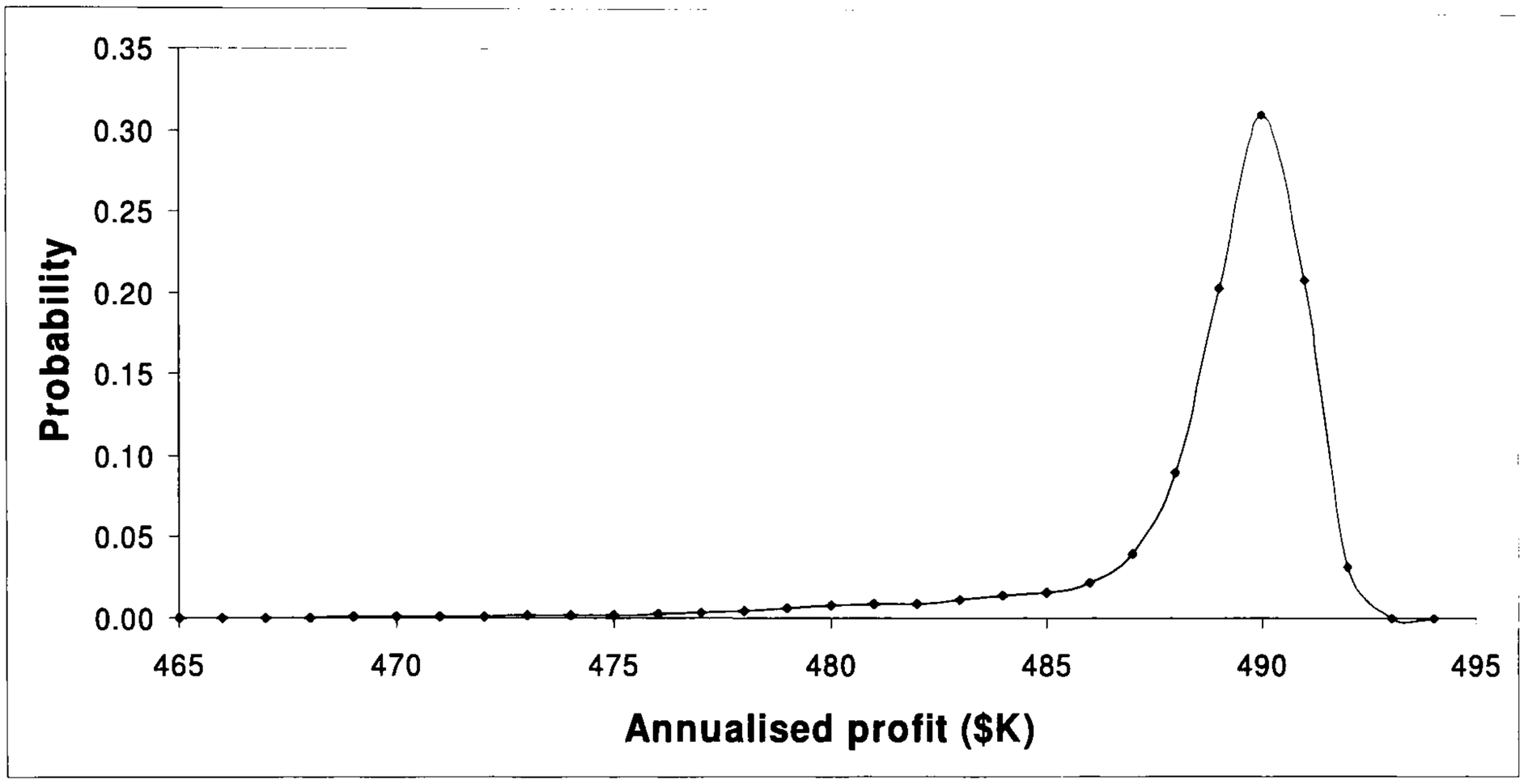


Figure 6.43: Profit probability using Sobol'-normal sampling for nominal design in iteration II

the key performance indicators. These graphs are shown in figures 6.43 to 6.47.

The comparison of histograms for key performance indicators between iterations I and II shows that a higher expected profit and less variation in the control variables can be obtained if the uncertainty is reduced to the levels shown in table 6.25. The difference between expected annualised profits in iterations I and II can be used to show the price that is paid by working under more uncertain conditions. If the uncertainty can be reduced to the levels of iteration II, the expected annualised profit is 488,350 USD/yr. If the results for the nominal design in iteration I are unacceptable, one solution is to modify the reactor design to a length of 8.062 m, which brings the expected profit down to 361,750 USD/yr. The difference is 126,600 USD/yr, which is nearly 26% of the expected profit in iteration II. However, no costs have been associated with the R&D activities. There is a trade-off to be taken into account between the cost associated to decreasing the uncertainty levels and the benefits of this reduction.

Therefore, this step could also be used to set targets for uncertainty reduction by analysing new uncertain parameter definitions until an acceptable result is obtained. Then, R&D teams can aim at achieving such uncertainty reductions and their associated costs could be included to find the optimal trade-off.

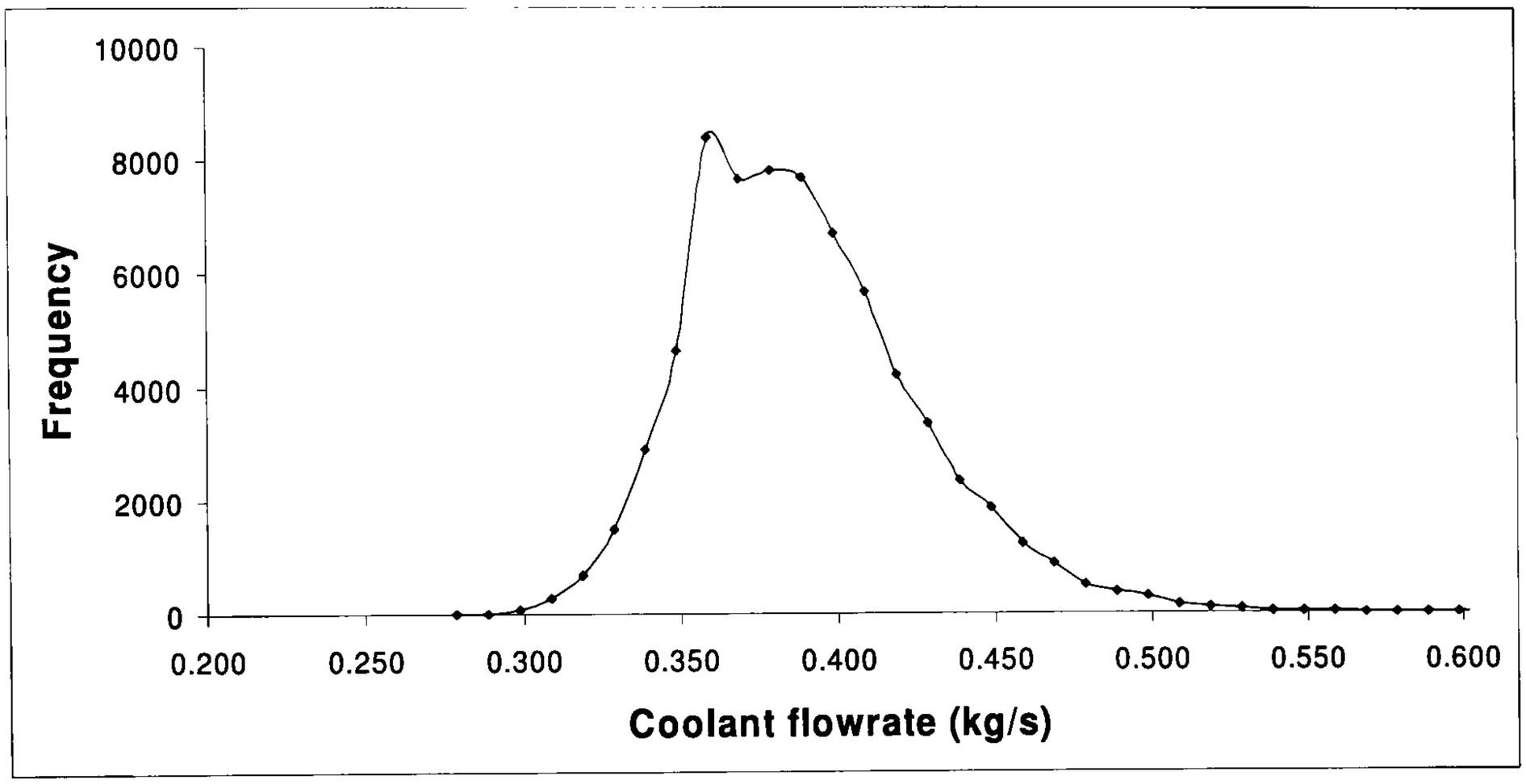


Figure 6.44: Coolant flowrate histogram using Sobol'-normal sampling for nominal design in iteration II

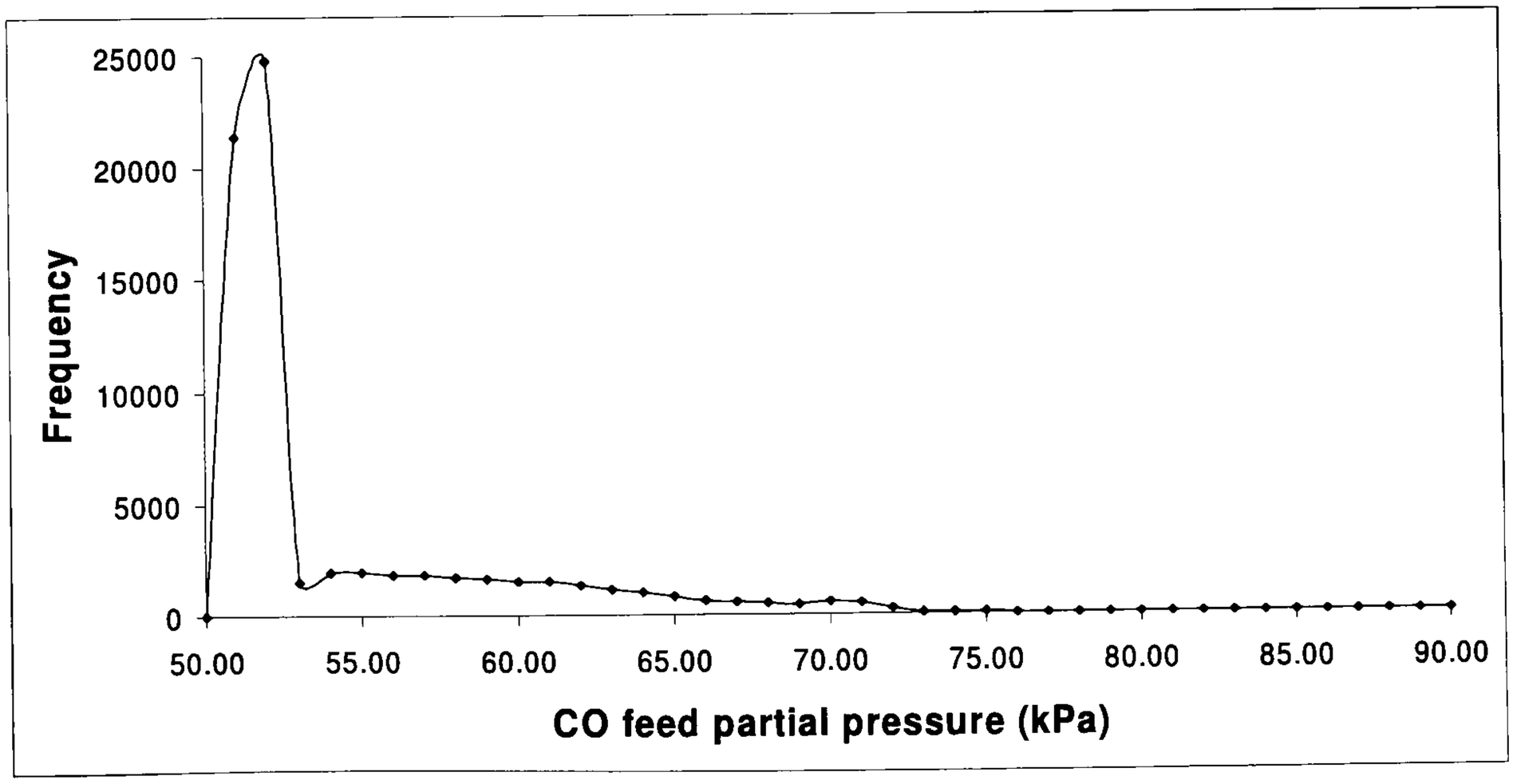


Figure 6.45: Carbon monoxide histogram using Sobol'-normal sampling for nominal design in iteration II

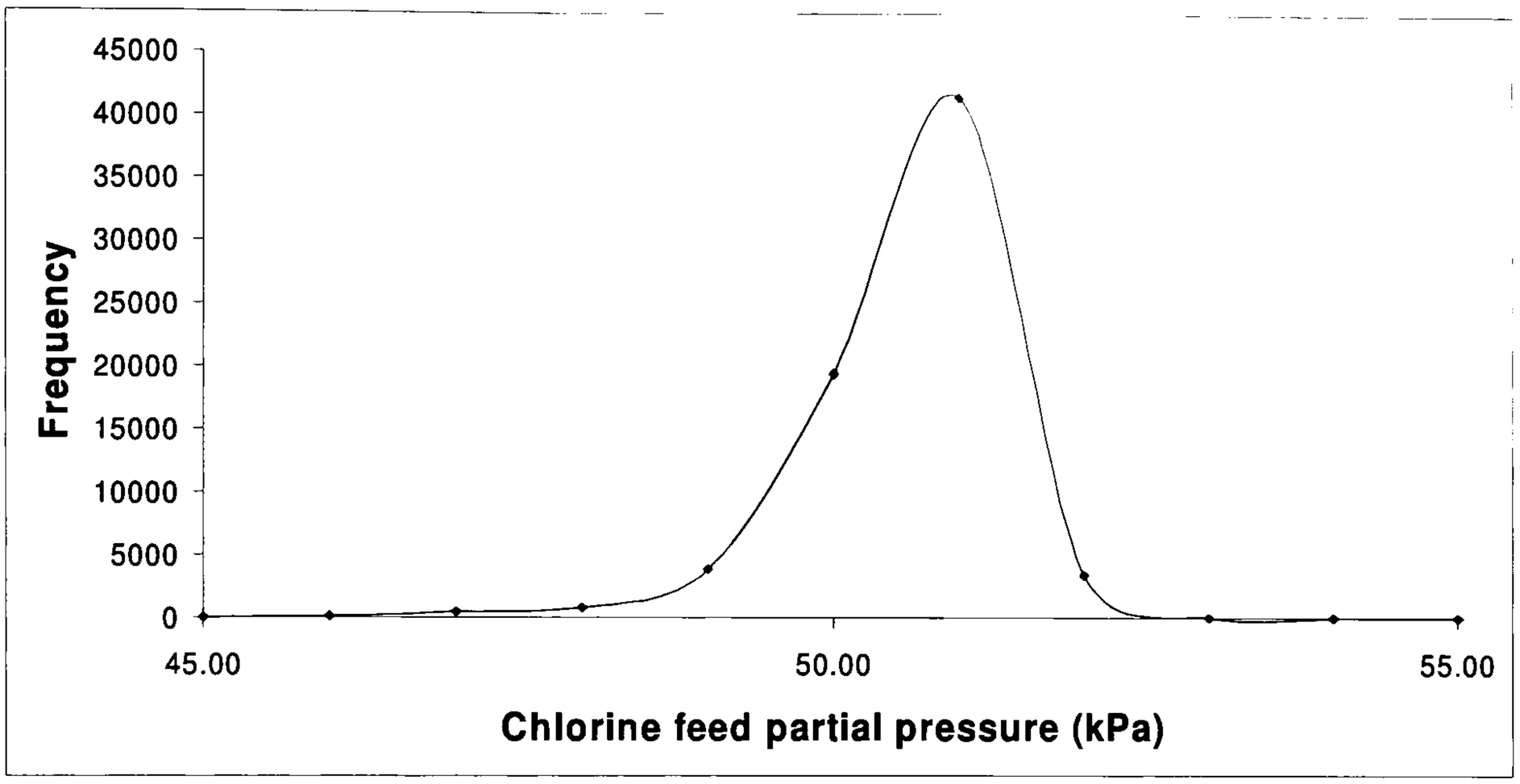


Figure 6.46: Chlorine histogram using Sobol'-normal sampling for nominal design in iteration II

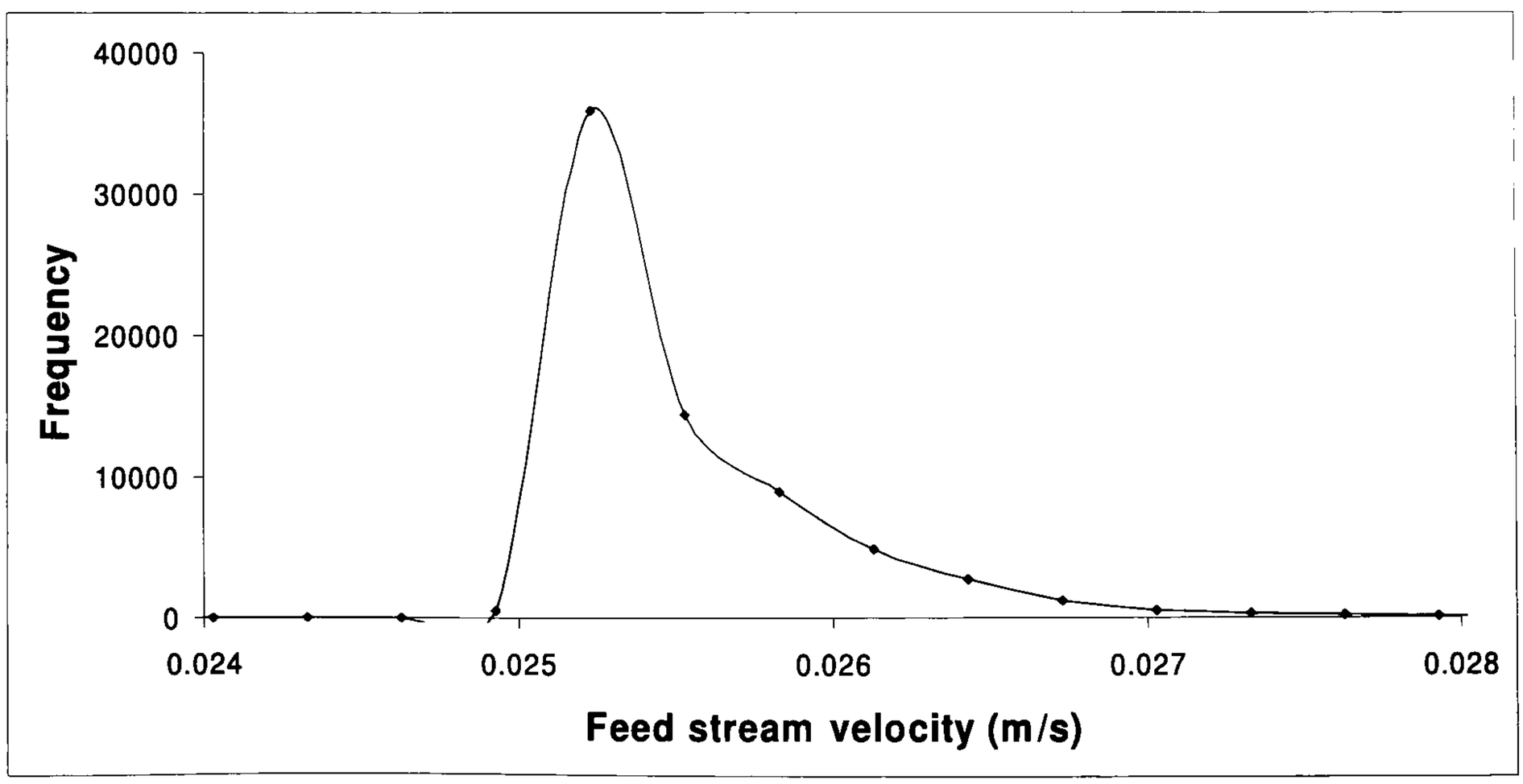


Figure 6.47: Feed stream velocity histogram using Sobol'-normal sampling in iteration II

6.5 Summary

The case study presented in this chapter illustrates the use of the methodology proposed in this work. Starting with a validated model and the uncertain parameter definition, a nominal design is obtained using the nominal values of the uncertain parameters.

A stochastic design step is then undertaken, which consists of several iterations between global sensitivity/feasibility analysis and scenario-based optimisation. A GSFA was first performed on the nominal design. The analysis was performed using Sobol' sampling for the case of uniformly distributed parameters and using two different sampling techniques for the case of normally distributed parameters. A Sobol'-normal sampling is used to account directly for the parameter distribution. In a second method, the results obtained with the Sobol' sampling were used together with a weight factor to convert the uniform distribution of this sampling to a normal distribution. This means a good coverage of the uncertain parameter space is obtained to identify any potential regions where infeasibility could be an issue. The results provide sensitivity index values and risk metrics such as an infeasibility probability, histograms and statistical information for the key performance indicators. The sensitivity indices are used to identify critical parameters, while the histograms facilitate the decision making process, which can be in the form of managerial and/or technical decisions.

Following the GSFA, the risk profile of the nominal design was found to be unacceptable and the pseudo-dynamic optimisation approach was used to find a new design by solving a scenario-based optimisation problem.

The GSFA and scenario-based design were repeated several times until a satisfactory design was identified.

Further R&D was assumed to have reduced the parameter uncertainty and a second iteration of the overall approach was undertaken. The results highlighted the potential benefits that could be obtained if the parameter variation can be reduced. These results were compared to those obtained in iteration I to quantify the cost of working under different uncertain conditions.

Chapter 7

Conclusions and future work

7.1 Conclusions

A systematic methodology to manage technological risk in process design has been presented in this thesis. The risk arises from limitations in the available understanding of the behaviour of new technology and is a natural and unavoidable consequence of innovation. Because details are often the source of uncertainty, the proposed approach is based on mathematical models which are sufficiently detailed to quantify the risk arising from a new technology. This is in contrast to most academic work in the area of process design under uncertainty, where fairly simple models are usually used.

The approach, as described in Chapter 3, consists of a series of steps which include model building and validation, a deterministic optimisation to obtain a nominal design and a stochastic design step. Using the information generated in the stochastic design step on the risk associated with the current design, decisions can be made to undertake further R&D or not, and to proceed with the project or not. If R&D activities are pursued to reduce the level of uncertainty, the entire procedure can be re-iterated to obtain a risk assessment and possibly a better design. The stochastic design step is at the heart of the approach and consists of two steps: a global sensitivity/feasibility analysis (GSFA) and a scenario-based design step.

The global sensitivity/feasibility analysis and risk quantification allows, for a given design, the identification of critical parameters affecting the key performance indicators (KPI), the determination of infeasible operating regions and the probability of infeasible operation and the probability distributions of the KPIs. An approach to obtain this

information is described in Chapter 4. The uncertain parameter space is sampled and an optimisation problem is solved for every sampled point for the given design. The decision variables in the optimisation are the control variables and this approach therefore allows the use of the process flexibility in the analysis. Sobol' sensitivity indices are approximated in the course of the GSFA via function evaluations at the sampled points. This step is implemented as a C++ application making use of gPROMS modelling and computational engine. The code is parallelised to be used in a Beowulf cluster under Linux. The solution of several optimisation problems also allows the construction of KPI histograms which are used to quantify the risk and facilitate the decision-making process, and the derivation of an infeasibility probability. Different strategies have been proposed to take into account non-uniform distributions of the uncertain parameters. They include tailored sampling (*e.g.* Sobol'-normal) and re-weighting of a standard Sobol' sample.

The approach to scenario-based optimisation is described in Chapter 5. The solution of this problem provides a new feasible or robust design when the results of the global sensitivity/feasibility analysis and risk quantification are deemed as unacceptable. It should be noted that this approach does not guarantee an improved risk profile (for instance, the deviation of the KPIs in the new design may be worse). Other heuristic approaches could be used to obtain a suitable new design. A reduced set of scenarios is first generated by sampling the space formed by the critical uncertain parameters identified in the global sensitivity/feasibility analysis. The scenario-based optimisation problem is solved using a pseudo-dynamic approach which facilitates the initialisation of complex models. The major focus of the proposed approach is thus how to solve problems which have a relatively large number of scenarios (say, 30-40) and use complex models.

The stochastic design step consists in iterating between the global sensitivity/feasibility analysis and the scenario-based optimisation until the results of the GSFA show that an acceptable design has been found.

This methodology has been tested on the design of a phosgene reactor for which a two-dimensional distributed model was developed. Two uncertain parameter distributions were considered in this eight parameter system: uniform and normal. This allowed the testing of different sampling strategies. The Sobol' approach was found to provide a better coverage of the space and therefore a more realistic assessment of the infeasibility probability. The methodology was carried through two iterations. In the first iteration, three stochastic design steps were undertaken. Following each scenario-based optimisation, an improved

design was found in terms of variability and infeasibility. Although variability is not taken into account explicitly in the problem formulation, the use of the expected performance as an objective does result in an improved risk profile. The GSFA provides a wealth of information. In particular, detailed histograms of the profit reveal a long tail of poor performance for the nominal design: this information is not readily available from simple figures such as means and standard deviation. The case study also allowed the calculation of the cost of uncertainty. In a second iteration of the approach, reduced uncertainty was considered. This radically changed the risk profile of the nominal design and made it much more acceptable.

The main contributions of this work are as follows:

1. an overall iterative approach to tackle process design under technological uncertainty and to support decision-making under uncertainty;

2. an analysis tool, the global sensitivity/feasibility analysis, to evaluate the quantitative risk profile of a given process for a given type of uncertainty. This approach can be applied to large models. It exploits optimally the control structure of the process;

3. a reformulation of the scenario-based optimisation problem so that initialisation difficulties can be avoided;

4. a parallel implementation of the GSFA;

5. the demonstration of the approach on a distributed model of a phosgene reactor with a large uncertainty range.

7.2 Future Work

Three suggestions are made for future work in the context of the proposed methodology: extension to dynamic systems; improvements to sensitivity index calculations; model reduction.

7.2.1 Extension to dynamic systems

So far, the methodology has been developed and tested with steady-state models. The application of the proposed methodology to dynamic systems would extend its benefits to the

analysis of transient conditions. The effects of uncertainty on conditions such as start ups, shutdowns and disturbances during operation could be analysed. The analysis of the process dynamic behaviour requires modifications to the proposed methodology. The global sensitivity/feasibility analysis has to account for additional aspects, such as initial conditions, which may affect the trajectory of the measured variables and the results obtained. Therefore, the definition of the optimisation problem solved for every sampled point will change from a steady state to a dynamic optimisation. For instance, the sensitivity indices can become a function of additional parameters such as initial conditions, interior-point and end-point constraints. This will likely increase the computational complexity of the problem, which may be overcome by the parallel approach.

The pseudo-dynamic optimisation step would also need to be changed to deal with the dynamic behaviour. The objective of this step is to find a new optimal and feasible design for the given dynamic problem. The modifications should allow to define a dynamic problem as one scenario within the overall pseudo-dynamic representation of the scenario-based problem. The overall problem needs to take into account considerations such as those presented for the global sensitivity/feasibility analysis. Time will be a new optimisation variable. The computational requirements for this step are likely to increase and therefore it would be advantageous to parallelise this step.

7.2.2 Improvements to sensitivity index calculations

The sensitivity index calculations can be improved for low-value indices which need a very large number of evaluations to be estimated accurately with the proposed approach. A paper by Saltelli (2002) shows a method to make a better use of the evaluations when calculating sensitivity indices. Further work can be done to obtain good estimates for the sensitivity indices with less samples by using different sampling techniques such as the Scrambled Sobol' sequence (Owen, 1998; Hong and Hickernell, 2003).

7.2.3 Model reduction

Another area which could be explored as future work is model reduction using the results of the global sensitivity analysis. The problem complexity may be decreased by generating a reduced model based on the global sensitivity analysis results. This model reduction may lead to reduced computational time. However, special care must be taken to avoid

reducing the model to a level where the technological risk is not taken into account.

Bibliography

Ahmed, S., and N. V. Sahinidis, "Robust process planning under uncertainty," *Industrial and Engineering Chemistry Research*, **37**, 1883 (1998).

Ahmed, S., N. V. Sahinidis, and E. N. Pistikopoulos, "An improved decomposition algorithm for optimization under uncertainty," *Computers and Chemical Engineering*, **23**, 1589 (2000).

Antonov, I. A., and V. M. Saleev, "An economic method of computing lp_τ-sequences," *USSR Computational Mathematics and Mathematical Physics*, **19**, 252 (1979).

Bellman, R. E., *Dynamic Programming*, Princeton University Press, Princeton, N.J. (1957).

Bellman, R. E., and L. A. Zadeh, "Decision-making in a fuzzy environment," *Management Science*, **17**, B141 (1970).

Benabbas, L., S. P. Asprey, and S. Macchietto, "Curvature-based methods for designing optimally informative experiments in multiresponse nonlinear dynamic situations," *Industrial and Engineering Chemistry Research*, **44**, 7120 (2005).

Bernardo, F. P., E. N. Pistikopoulos, and P. M. Saraiva, "Integration of computational issues in stochastic design and planning optimization problems," *Industrial and Engineering Chemistry Research*, **38**, 3056 (1999).

Bernardo, F. P., E. N. Pistikopoulos, and P. M. Saraiva, "Quality costs and robustness criteria in chemical process design optimization," *Computers and Chemical Engineering*, **25**, 27 (2001).

Bernardo, F. P., P. Saraiva, and E. N. Pistikopoulos, "Inclusion of information costs in process design optimization under uncertainty," *Computers and Chemical*

Engineering, **24**, 1695 (2000).

Bhatia, T. K., and L. T. Biegler, "Multiperiod design and planning with interior point methods," *Computers and Chemical Engineering*, **23**, 919 (1999).

Bhattacharya, S., V. Krishnan, and V. Mahajan, "Managing new product definition in highly dynamic environments," *Management Science*, **44**, S50 (1998).

Biegler, L. T., and I. E. Grossmann, "Retrospective on optimization," *Computers and Chemical Engineering*, **28**, 1169 (2004).

Biegler, L. T., I. E. Grossmann, and A. W. Westerberg, *Systematic Methods of Chemical Process Design*, Prentice Hall PTR, New Jersey, USA (1997).

Book, S., and M. Chernik, "System error analysis based on one-at-a-time perturbations," *Mathematical and Computer Modelling*, **15**, 77 (1991).

Cacuci, D. G., *Sensitivity and Uncertainty Analysis*, Chapman & Hall/CRC, United States of America (2003).

Campolongo, F., and R. Braddock, "The use of graph theory in the sensitivity analysis of the model ouput: A second order screening method," *Reliability Engineering and System Safety*, **64**, 1 (1999).

Caracotsios, M., and W. E. Stewart, "Sensitivity analysis of initial value problems with mixed odes and algebraic equations," *Computers and Chemical Engineering*, **9**, 359 (1985).

Chen, B. H., and S. P. Asprey, "On the design of optimally informative dynamic experiments for model discrimination in multiresponse nonlinear situations," *Industrial and Engineering Chemistry Research*, **42**, 1379 (2003).

Cheng, L., E. Subrahmanian, and A. W. Westerberg, "Design and planning under uncertainty: Issues on problem formulation and solution," *Computers and Chemical Engineering*, **27**, 781 (2003).

Cotter, S., "A screening design for factorial experiments with interactions," *Biometrika*, **66**, 317 (1979).

Cropp, R., and R. Braddock, "The new Morris method: An efficient second-order screening method," *Reliability Engineering and System Safety*, **78**, 77 (2002).

Cukier, R., C. Fortuin, and K. Shuler, "Study of the sensitivity of coupled reaction systems to uncertainties in the rate coefficients. I Theory," *Journal of Chemical Physics*, **59**, 3873 (1973).

Daniel, C., "One-at-a-time plans," *Journal of the American Statistical Association*, **68**, 353 (1973).

Dhole, V. R., and B. Linnhoff, "Total site targets for fuel, co-generation, emissions, and cooling," *Computers and Chemical Engineering*, **17**, S101 (1992).

Diwekar, U. M., "A novel sampling approach to combinatorial optimization under uncertainty," *Computational Optimization and Applications*, **24**, 335 (2003).

Dixit, A. K., and R. S. Pindyck, *Investment under Uncertainty*, Princeton University Press, Princeton, New Jersey (1994).

Douglas, J. M., *Conceptual Design of Chemical Processes*, McGraw-Hill Chemical Engineering Series, McGraw-Hill, New York (1988).

Douglas, J. N., and G. Stephanopoulos, "Hierarchical approaches in conceptual process design: Framework and computer-aided implementation," *Foundations of Computer-Aided Process Design, AIChE Symp. Series*, **91**, 183 (1995).

El-Halwagi, M. M., and V. Manousiouthakis, "Automatic synthesis of mass-exchange networks with single-component targets," *Chemical Engineering Science*, **45**, 2813 (1990).

Floudas, C. A., and G. E. Paules-IV, "A mixed-integer nonlinear programming formulation for the synthesis of heat-integrated distillation sequences," *Computers anc Chemical Engineering*, **12**, 531 (1988).

Georgiadis, M. C., and E. N. Pistikopoulos, "An integrated framework for robust and flexible process systems," *Industrial and Engineering Chemistry Research*, **38**, 133 (1999).

Glavič, P., Z. Kravanja, and M. Homšak, "Heat integration of reactors - I. Criteria for the placement of reactors into process flowsheet," *Chemical Engineering Science*. **43**, 593 (1988).

Gordon, J. S., and D. Goland, "Thermodynamic function of carbonyl chloride." *Journal of Chemical Physics*, **27**, 1223 (1957).

Grossmann, I. E., and D. A. Straub, *Recent Developments in the Evaluation and Optimization of Flexible Chemical Processes*, Computer-Oriented Process Engineering, Amsterdam (1991).

Gustafson, S. A., *Semi-Infinite Programming and Applications, Lecture Notes in Economics and Mathematical Systems*, volume 215, chapter A Three-Phase Algorithm for Semi-Infinte Programming, 138–157, Springer (1981).

Hallale, N., and D. M. Fraser, "Capital cost targets for mass exchange networks. a special case: Water minimisation," *Chemical Engineering Science*, **53**, 293 (1998).

Harmsen, G. J., "Industrial best practices of conceptual process design," *Chemical Engineering and Processing*, **43**, 677 (2004).

Helton, J., "Uncertainty and sensitivity analysis techniques for use in performance assessment for radioactive waste disposal," *Reliability Engineering and System Safety*, **42**, 327 (1993).

Hildebrandt, D., and D. Glasser, "The attainable region and optimal reactor structures," *Chemical Engineering Science*, **45**, 2161 (1990).

Hohman, E. C., *Optimum Networks of Heat Exchange*, Ph.D. thesis, University of Southern California, Los Angeles (1971).

Hong, H. S., and F. J. Hickernell, "Algorithm 823: Implementing scrambled digital sequences," *ACM Transactions on Mathematical Software*, **29**, 95 (2003).

Ierapetritou, M. G., J. Acevedo, and E. N. Pistikopoulos, "An optimization approach for process engineering problems under uncertainty," *Computers and Chemical Engineering*, **20**, 703 (1996a).

Ierapetritou, M. G., and E. N. Pistikopoulos, "Simultaneous incorporation of flexibility and economic risk in operational planning under uncertainty," *Computers and Chemical Engineering*, **18**, 163 (1994).

Ierapetritou, M. G., and E. N. Pistikopoulos, "Design of multiproduct batch plants with uncertain demands," *Computers and Chemical Engineering*, **19**, S627 (1995).

Ierapetritou, M. G., E. N. Pistikopoulos, and C. A. Floudas, "Operational planning under uncertainty," *Computers and Chemical Engineering*, **20**, 1499 (1996b).

Ishii, N., "Life cycle oriented process synthesis at conceptual planning phase," *Computers and Chemical Engineering*, **21**, S953 (1997).

Jacqué, M. L., "Le phosgène," *Chimie et Industrie*, **19**, 24 (1928).

King, C. J., D. W. Gantz, and F. J. Barnés, "Systematic evolutionary process synthesis," *Industrial and Engineering Chemistry: Process Design and Development*, **11**, 271 (1972).

Knuth, D. E., *The Art of Computer Programming*, volume II: Seminumerical Algorithms, Addison-Wesley, MA, USA, second edition (1981).

Kokossis, A. C., and C. A. Floudas, "Optimization of complex reactor networks–I. Isothermal operation," *Chemical Engineering Science*, **45**, 595 (1990).

Kraslawski, A., and L. Nyström, "Fuzzy flexibility indices in process design," *Computers and Chemical Engineering*, **18**, S137 (1994).

Kreisselmeier, G., and R. Steinhauser, "Application of vector performance optimization to a robust-control loop design for a fighter aircraft," *International Journal of Control*, **37**, 251 (1983).

Kucherenko, S., W. Y. Hung, and N. Shah, "High-dimensional Sobol' sequence generator and its applications," Technical report, Imperial College London (2006).

Li, X., and A. Kraslawski, "Conceptual process synthesis: Past and current trends," *Chemical and Engineering Processing*, **43**, 589 (2004).

Linnhoff, B., H. Dunford, and R. Smith, "Heat integration of distillation columns into overall processes," *Chemical Engineering Science*, **38**, 1175 (1983).

Linnhoff, B., and J. R. Flower, "Synthesis of heat exchanger networks. I. Systematic generation of energy optimal networks," *AIChE Journal*, **24**, 633 (1978a).

Linnhoff, B., and J. R. Flower, "Synthesis of heat exchanger networks. ii. evolutionary generation of networks with various criteria of optimality," *AIChE Journal*, **24**, 642 (1978b).

Liu, M. L., and N. V. Sahinidis, "Process planning in a fuzzy environment," *European Journal of Operational Research*, **100**, 142 (1997).

Mauntz, W., "Global sensitivity analysis of general nonlinear systems." Technical report, Centre of Process Systems Engineering, Dept of Chemical Engineering, Imperial College London (2002).

Mehta, V. L., and A. Kokossis, "New generation tools for multiphase reaction systems: A validated systematic methodology for novelty and design automation." *Computers and Chemical Engineering*, **22**, S119 (1998).

Ministry of Munitions, D. o. E. S., *Preliminary Studies for H.M. Factory, Gretna, and Study for an Installation of Phosgene Manufacture*, His Majesty's Stationery Office, London, Great Britain (1920).

Morris, M., "Factorial sampling plans for preliminary computational experiments," *Technometrics*, **33**, 161 (1991).

Nair, S. K., "Modeling strategic investment decisions under sequential technological change," *Management Science*, **41**, 282 (1995).

Ostrovsky, G. M., L. E. K. Achenie, I. V. Datskov, and Y. M. Volin, "Flexibility analysis in the case of incomplete information about uncertain parameters," *Annals of Operations Research*, **132**, 257 (2004).

Ostrovsky, G. M., Y. M. Volin, and D. V. Golovashkin, "Optimization problem of complex systems under uncertainty," *Computers and Chemical Engineering*, **22**, 1007 (1998).

Owen, A. B., "Scarmbling Sobol' and Niederreiter-Xing points," *Journal of Complexity*, **14**, 466 (1998).

Pantelides, C. C., *The Mathematical Modelling of the Dynamic Behaviour of Process Systems*, Centre for Process Systems Engineering, Imperial College London, London SW7 2BY (2003).

Papalexandri, K. P., and E. N. Pistikopoulos, "A multiperiod MINLP model for the synthesis of flexible heat and mass exchange networks," *Computers and Chemical Engineering*, **18**, 1125 (1994).

Paules, G. E. I., and C. A. Floudas, "Stochastic programming in process synthesis: A two stage model with MINLP recourse for multiperiod heat-integrated distillation sequences," *Computers and Chemical Engineering*, **16**, 189 (1992).

Perry, R. H., and D. W. Green, eds., *Perry's Chemical Engineers' Handbook*, McGraw Hill (1997).

Pistikopoulos, E. N., "Uncertainty in process design and operations," *Computers and Chemical Engineering*, **19**, S553 (1995).

Pistikopoulos, E. N., and M. G. Ierapetritou, "Novel approach for optimal process design under uncertainty," *Computers and Chemical Engineering*, **19**, 1089 (1995).

Process Systems Enterprise, Ltd., general PROcess Modelling System, v 2.3 (2006).

PSE Ltd., *gPROMS Advanced User Guide v2.3*, Process Systems Enterprise Ltd., London W6 9DA, United Kingdom (2004a).

PSE Ltd., *gPROMS Introductory User Guide v2.3*, Process Systems Enterprise Ltd., London W6 9DA, United Kingdom (2004b).

Rabitz, H., M. Kramer, and D. Dacol, "Sensitivity analysis in chemical kinetics," *Annual Review of Physical Chemistry*, **34**, 419 (1983).

Rajagopalan, S., M. R. Singh, and T. E. Morton, "Capacity expansion and replacement in growing markets with uncertain technological breakthroughs," *Management Science*, **44**, 12 (1998).

Rooney, W. C., and L. T. Biegler, "Incorporating joint confidence regions into design under uncertainty," *Computers and Chemical Engineering*, **23**, 1563 (1999).

Rooney, W. C., and L. T. Biegler, "Design for model parameter uncertainty using nonlinear confidence regions," *AIChEJ*, **47**, 1794 (2001).

Rooney, W. C., and L. T. Biegler, "Optimal process design with model parameter uncertainty and process variability," *AIChEJ*, **49**, 438 (2003).

Sahinidis, N. V., "Optimization under uncertainty: State-of-the-art and opportunities," *Computers and Chemical Engineering*, **28**, 971 (2004).

Saltelli, A., "Making best use of model evaluations to compute sensitivity indices," *Computer Physics Communications*, **145**, 280 (2002).

Saltelli, A., K. Chan, and E. M. Scott, eds., *Sensitivity Analysis*, Probability and Statistics, John Wiley & Sons LTD, Chichester, England (2000).

Saltelli, A., and I. Sobol', "About the use of rank transformation in sensitivity analysis of model output," *Reliability Engineering and System Safety*, **50**, 225 (1995).

Saltelli, A., S. Tarantola, and K. Chan, "A quantitative model-independent method for global sensitivity analysis of model output," *Technometrics*, **41**, 39 (1999).

Schiesser, W. E., *The Numerical Method of Lines: Integration of Partial Differential Equations*, Academic Press, London (1991).

Schneider, W., and W. Diller, "Phosgene," in *Ullmann's Encyclopedia of Industrial Chemistry*, Wiley-VCH Verlag GmbH & Co. KGaA (2002).

Siirola, J. J., "An industrial perspective on process synthesis," *4th Int. conf. Foundations CAPE, AIChE Symp. Series*, **91**, 222 (1995).

Siirola, J. J., "Strategic process synthesis: Advances in the hierarchical approach," *Computers and Chemical Engineering*, **20**, S1637 (1996).

Smith, E. M. B., *On the Optimal Design of Continuous Processes*, Ph.D. thesis, Imperial College of Science, Technology and Medicine, London SW7 2BY, United Kingdom (1996).

Sobol', I., "Uniformly distributed sequences with an additional uniform property," *USSR Computational Mathematics and Mathematical Physics*, **16**, 236 (1976).

Sobol', I., "On quasi-monte carlo integrations," *Mathematics and Computers in Simulation*, **47**, 103 (1998).

Sobol', I., "Global sensitivity indices for nonlinear mathematical models and their monte carlo estimates." *Mathematics and Computers in Simulation*, **55**, 271 (2001a).

Sobol', I. M., Institute of Applied Mathematics, Moscow, Russia (2001b).

Stephanopoulos, G., and A. W. Westerberg, "Studies in process synthesis – II: Evolutionary synthesis of optimal process flowsheets," *Chemical Engineering Science*, **31**, 195 (1976).

Team, T. L., *LAM/MPI User's Guide*, Indiana University, http://www.lam-mpi.org/, 7th edition (2004).

Umeda, T., T. Harada, and K. Shiroko, "A thermodynamic approach to the synthesis of heat integration systems in chemical processes," *Computers and Chemical Engineering*, **3**, 273 (1979).

Varvarezos, D. K., L. T. Biegler, and I. Grossmann, "Multiperiod design optimization with sqp decomposition," *Computers and Chemical Engineering*, **18**, 579 (1994).

Vassiliadis, V. S., *Computational Solution of Dynamic Optimization Problems with General Differential-Algebraic Constraints*, Ph.D. thesis, Imperial College London, London, United Kingdom (1993).

Wei, J., and M. J. Realff, "Sample average appproximation methods for stochastic minlps," *Computers and Chemical Engineering*, **28**, 333 (2004).

Westerberg, A. W., "A retrospective on design and process synthesis," *Computers and Chemical Engineering*, **28**, 447 (2004).

Yeomans, H., and I. E. Grossmann, "Nonlinear disjunctive programming models for the synthesis of heat integrated distillation sequences," *Computers and Chemical Engineering*, **23**, 1135 (1999).

Yin, K. K., H. Liu, and G. G. Lin, "Stochastic models and numerical solutions for production planning with applications to the paper industry," *Computers and Chemical Engineering*, **27**, 1693 (2003).

Appendix A

Dynamic Optimisation

The algorithm to solve the dynamic optimisation problem formulated with PDAEs involves two different activities: solution of PDAE systems and the optimisation of the dynamic problem. These methods will be briefly reviewed.

A.1 PDAE Solution

The general form of a PDAE system is shown in A.1:

$$\begin{aligned} f(x, x_z, x_{zz}, x_t, y, y_z, y_{zz}) &= 0 \quad \forall z \in (0, L) \\ g(x, y) &= 0 \quad \forall z \in (0, L) \\ C(x(z,0), x_z(z,0), x_t(z,0), y(z,0), y_z(z,0), z) &= 0 \quad \forall z \in (0, L) \\ B^L(x, x_z, y, y_z) &= 0 \quad at \;\; z = 0 \\ B^R(x, x_z, y, y_z) &= 0 \quad at \;\; z = L \end{aligned} \tag{A.1}$$

where the space domain vector is represented by z, $x_t \equiv \partial x/\partial t$, $x_z \equiv \partial x/\partial z$, $x_{zz} \equiv \partial^2 x/\partial z^2$, and so on. f represents the partial differential equations, g the algebraic equations and B^L and B^R the boundary conditions.

The PDAE systems can be solved using the method of lines (Schiesser, 1991) which is schematically shown in figure A.1. The general idea is to convert the system of PDAE to a differential algebraic equation (DAE) system which can be solved by conventional methods.

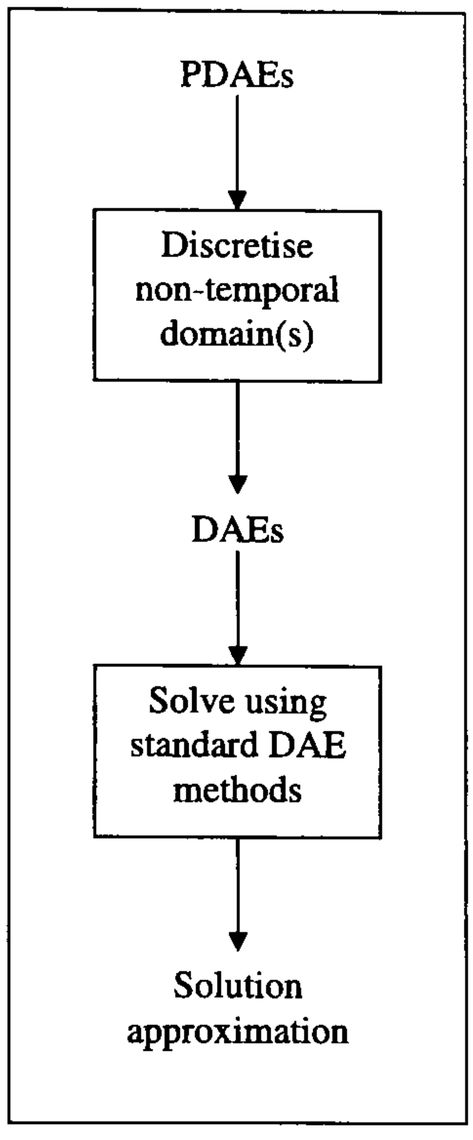


Figure A.1: Schematic representation of Method of Lines

The first step discretises the spatial domain generating a grid. A set of ordinary differential and algebraic equations is then used to approximate problem A.1 to a set of DAEs. Two general methods can be used for the approximation: Finite Difference Discretisation or Polynomial Approximations. The first method approximates the spatial partial derivatives with difference formulae. Taylor expansions are generated around each point in the grid. Three approximations are generated depending on how the Taylor expansions are derived around every point in the grid: backward, forward or centred finite difference. While these three approximations can be used to convert the differential and algebraic equations, f and g, only the backward or forward finite difference can be employed for the boundary conditions. This new set of equations, together with the initial conditions, is used to solve the DAE system by conventional methods.

The polynomial methods try to approximate the spatial variation of the variables with the use of polynomials in z. Since this method enforces the equations at a finite set of points along z, this type of method is called collocation.

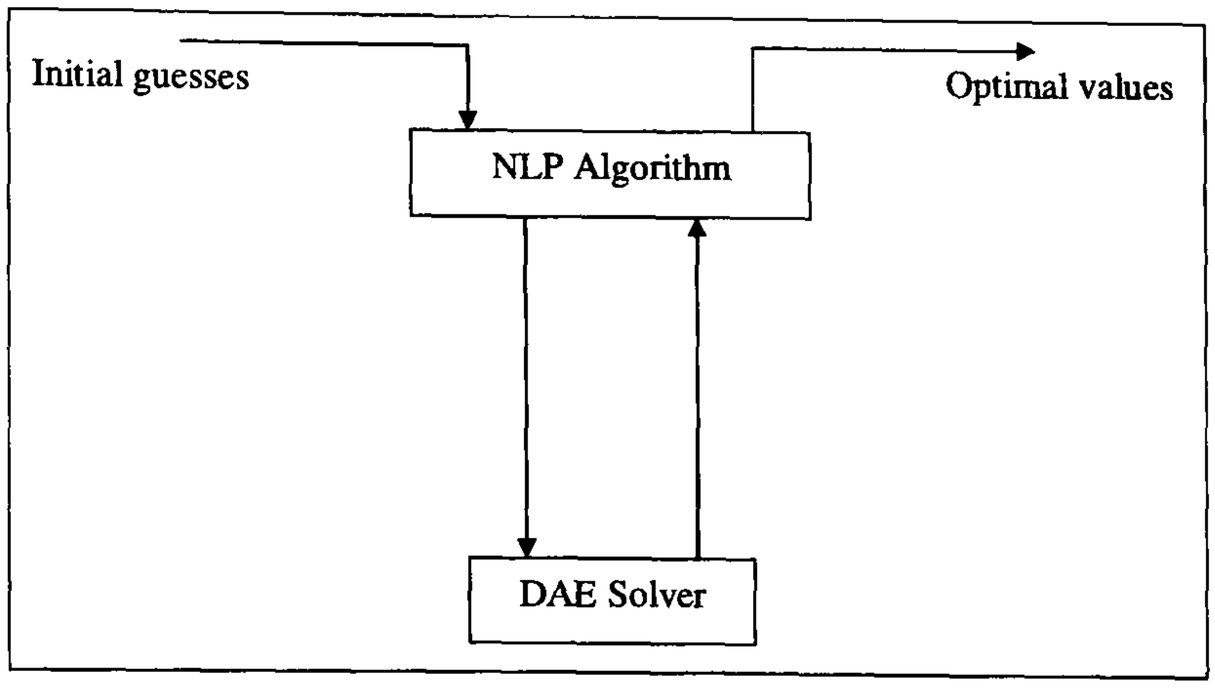


Figure A.2: Schematic representation for solution of dynamic optimisation problem

A.2 Optimisation of Dynamic Problem

The main difficulty with the optimisation of the dynamic problem is its infinite dimensional nature. There are several methods to solve this type of problem. Some of them approximate the infinite dimensional problem by a finite dimensional problem. One such approach is control vector parameterisation (Vassiliadis, 1993).

The control vector parameterisation (CVP) approach is used to divide the time horizon, τ, into a number of elements. The control variables, *u(t)*, are parameterised within each element which helps to convert the equations in the problem to a finite dimensional problem. The parameterisation in each period can take several forms, such as constant, linear or quadratic) and some continuity may be required at the boundaries between intervals.

The resulting optimisation formulation is a nonlinear programming (NLP) problem, which can then be solved by conventional procedures. The overall procedure is summarised in figure A.2.

Appendix B

GSA Files

B.1 Input file for GSA implementation (input.txt)

****

Input file for Parameter Optimisation of Sensitivity Analysis

****

* File Information:

****

gPROMS input file name: E_SENSITIVITY

Output file name: SENSITIVITY

Number of control variables: 4

Number of parameters: 8

Restart previous evaluation: N

Restart increments: 31

* Data on Sensitivity Analysis (Variable Information)

****

Sensitivity coefficient of interest = 1;2;3;4;5;6;7;8

Accuracy = 1e-2

Maximal Nr of samples = 4096

ZeroDefinition =1e-2

RandomOrSobol(Variables) = S

Variable Range:
1:0.04750:0.05250
2:0.04750:0.05250
3:0.0912:0.1008
4:-109336:-111544
5:-220621.5:-225078.5
6:51917.67:63454.93
7:290:296
8:290:296

********** End of Input File **********

B.2 gPROMS file example to call the simpleEvent-FOI foreign object

```
PARAMETER
    theFO        AS  FOREIGN_OBJECT "simpleEventFOI"

UNIT
    OptC AS Dynamic

SET
    theFO        := "DummyFO" ;
    WITHIN OptC DO
        tao      := 0.01/100 ;
        CpCW     := 4.2 ;
        CpCWm    := 4.2*18.015 ;
        DenCW    := 1000 ;
        DenCWm   := 1000/18.015 ;
        Pcw      := 101.324 ;
```

```
U          := theFO.X3 ;
Pi         := 3.1416 ;
RG         := 8.31451 ;
Kinetic    := 4 ;
TO         := 298 ;
beta       := [-1.285E-2, 3.883E-2, 2.463E-2] ;
alpha      := [30.869, 26.929, 60.66] ;
kr         := theFO.X1 ;
kz         := theFO.X2 ;
kzcw       := 0.0006 ;
Nu         := [-1, -1, +1] ;
DenBed     := 800 ;
CpBed      := 0.85 ;
Dr         := 1.0E-3 ;
Dz         := 1.0E-2 ;
NoComp     := 3 ;
Void       := 0.35 ;
    Axial    := [CFDM, 2, 50] ;
    Radial   := [CFDM, 2, 5] ;
END # Within OptC

ASSIGN
    WITHIN OptC DO
        A          := [100, 100, 141.819, 0.127521] ;
        Dhf        := [theFO.X4, 0.0, theFO.X5] ;
        Ek         := [20000, -26233.3, 6000, theFO.X6] ;
        Tcwin      := theFO.X7 ;
        Tin        := theFO.X8 ;

        PPin       := [53.1594, 53.1014, 0] ;
        Vel        := 0.0262759 ;
        Fcw        := 0.312442 ;
        RCW        := 0.375075 ;
```

```
        RZ          := 1.40323 ;
        RR          := 0.357214 ;
    END # Within OptC

PRESET
    RESTORE "OptimisedSim"

INITIAL
    STEADY_STATE

SOLUTIONPARAMETERS
    ReportingInterval := 100 ;
    FPI := "eventFPI" ;
    gRMS := OFF ;

SCHEDULE
    SEQUENCE

        CONTINUE FOR 1
        SAVE "E_Optimised"

        # Now transmit model outputs
        SEND
            SIGNALID "SendOF+ConstraintValues"
            # Output(s)
            OptC.Profit;
        END # Send

    END # Sequence
```

Appendix C

Phosgene Reactor Model

C.1 Nomenclature

Symbols

A	Area
C	Component concentration
Cost	Annualised cost
Cp	Specific heat capacity
D	Dispersion coefficient
E	Internal energy
F	Mass flow
FlowH	Enthalpy flux
h	Specific enthalpy
k	Thermal dispersion coefficient
P	Pressure
pp	Partial pressure
Q	Heat load
r	Reactor's radial domain, [0,RR]
Rate	Reaction rate
Revenues	Product sales revenues
RCW	Cooling jacket radius

RG Universal gas constant

RR Reactor radius

RZ Reactor length

T Temperature

U Overall heat transfer coefficient

V Volume

Vel Feed stream velocity

z Reactor's axial domain, [0,RZ]

Greek symbols

α Specific heat capacity constant term

β Specific heat capacity temperature dependent term

Δ Property difference

ϵ Bed void fraction

π Pi constant

ρ Density

ν Stoichiometric coefficient

Subindexes

0 Reference state

Bed Catalyst bed

cw Cooling water property

f Formation

i No. of component (1-Carbon Monoxide, 2-Chlorine, 3-Phosgene)

in Property at reactor's inlet

out Property at reactor's outlet

r Reactor's radial domain, [0,RR]

reac Reactor measurement

t Transversal measurement

z Reactor's axial domain, [0,RZ]

C.2 Model equations

Material balance

$$0 = -Vel\frac{\partial C_i(z,r)}{\partial z} + D_z\frac{\partial^2 C_i(z,r)}{\partial z^2} + D_r\frac{\partial^2 C_i(z,r)}{\partial r^2} + \frac{D_r}{r}\frac{\partial C_i(z,r)}{\partial r} + \rho_{Bed}\nu_i Rate(z,r)$$

$$\forall z \in (0, RZ),\ \forall r \in (0, RR), i = \{1,2,3\} \qquad \text{(C.1)}$$

Energy balance on reactor side

$$0 = -\frac{\partial FlowH(z,r)}{\partial z} + k_z\frac{\partial^2 T(z,r)}{\partial z^2} + k_r\frac{\partial^2 T(z,r)}{\partial r^2} + \frac{k_r}{r}\frac{\partial T(z,r)}{\partial r}$$

$$\forall z \in (0, RZ),\ \forall r \in (0, RR) \qquad \text{(C.2)}$$

Internal energy

$$E(z,r) = \epsilon\sum_{i=1}^{3}(C_i(z,r)h_i(z,r)) + (1-\epsilon)C_{pBed}\rho_{Bed}(T(z,r)-T_0) - P(z,r)$$

$$\forall z \in [0, RZ],\ \forall r \in [0, RR] \qquad \text{(C.3)}$$

Enthalpy flux

$$FlowH(z,r) = Vel\sum_{i=1}(C_i(z,r)h_i(z,r)) \quad \forall z \in [0, RZ],\ \forall r \in [0, RR] \qquad \text{(C.4)}$$

Specific enthalpy

$$h_i(z,r) = \alpha_i(T(z,r) - T_0) + 0.5\beta_i(T(z,r)^2 - T_0^2) + \Delta H_{fi}$$

$$\forall z \in [0, RZ],\ \forall r \in [0, RR],\ i = \{3\} \qquad \text{(C.5)}$$

Energy balance on cooling jacket

$$0 = -\frac{F_{cw}}{A_{cwt}}\frac{\partial h_{cw}(z)}{\partial z} + kz_{cw}\frac{\partial^2 T_{cw}(z)}{\partial z^2} + \frac{Q(z)}{A_{cwt}}$$

$$\forall z \in (0, RZ) \qquad \text{(C.6)}$$

Specific enthalpy for cooling jacket

$$h_{cw}(z) = C_{p_{cw}}(T_{cw} - 273) \qquad \forall z \in [0, RZ] \qquad \text{(C.7)}$$

Heat load to cooling jacket

$$Q(z) = 2 \cdot \pi \cdot RR \cdot U(T(z, RR) - T_{cw}(z)) \qquad \forall z \in [0, RZ] \qquad \text{(C.8)}$$

Inlet enthalpy flux

$$FlowHin = \frac{Vel\sum_{i=1}^{3}(pp_{i_{in}}(\alpha_i(T_{in} - T_0) + 0.5\beta_i(T_{in}^2 - T_0^2) + \Delta H_{fi}))}{RG \cdot T_{in}} \qquad \text{(C.9)}$$

Total pressure

$$P(z,r) = \sum_{i=1}^{3} C_i(z,r)RG \cdot T(z,r) \qquad \forall z \in [0, RZ],\ \forall r \in [0, RR] \qquad \text{(C.10)}$$

Partial pressure

$$pp_i(z,r) = C_i(z,r)RG \cdot T(z,r) \qquad \forall z \in [0, RZ],\ \forall r \in [0, RR],\ i = \{1,2,3\} \tag{C.11}$$

Initial component concentration

$$C_{i_{in}} = \frac{pp_{i_{in}}}{RG \cdot T_{in}} \qquad i = \{1,2,3\} \tag{C.12}$$

Reactor volume

$$V_{reac} = \pi RR^2 RZ \tag{C.13}$$

Cooling jacket dimensions

$$V_{cw} = \pi(RCW^2 - RR^2)RZ \tag{C.14}$$

$$A_{cw} = 2 \cdot \pi \cdot RR \cdot RZ \tag{C.15}$$

$$A_{cwt} = \pi(RCW^2 - RR^2) \tag{C.16}$$

Cooling jacket flowrate

$$F_{cw} = Vel_{cw}\rho_{cw}A_{cw} \tag{C.17}$$

Reactor inlet flow

$$Fin_i = Vel\pi RR^2 Cin_i \qquad i = \{1,2,3\} \tag{C.18}$$

Reactor outlet flow

$$Fout_i = 2Vel\pi \int_0^{RR} r\ C_i(RZ, r)\ dr \qquad i = \{1,2,3\} \tag{C.19}$$

Product sales revenues

$$Revenues = Fout_{COCl_2} Cost_{COCl_2} \tag{C.20}$$

Annualised reactor cost

$$Cost_{reactor} = 100(V_{reac} + V_{cw})^{0.6} \tag{C.21}$$

Raw material cost

$$Cost_{raw\ material} = Cost_{CO}(Fin_{CO} - 0.5Fout_{CO}) + Cost_{Cl_2}(Fin_{Cl_2} - 0.5Fout_{Cl_2}) \tag{C.22}$$

Cooling water cost

$$Cost_{cw} = Unit\ cost_{cw} F_{cw} \tag{C.23}$$

Boundary equations

Mass balance

$$Inlet : VelC_{i_{in}} = Vel\ C_i(0,r) - D_z \frac{\partial C_i(0,r)}{\partial z} \quad \forall r \in [0, RR],\ i = \{1,2,3\} \tag{C.24}$$

$$Outlet : \frac{\partial C_i(RZ,r)}{\partial z} = 0 \qquad \forall r \in [0, RR],\ i = \{1,2,3\} \tag{C.25}$$

Energy balance

$$Reactor\ centre\ line : \quad FlowHin = FlowH(0,r) - k_z \frac{\partial T(0,r)}{\partial z} \qquad \forall r \in [0, RR] \tag{C.26}$$

$$Reactor\ wall : \quad \frac{\partial T(RZ,r)}{\partial z} = 0 \qquad \forall r \in [0, RR] \tag{C.27}$$

Energy Balance on Cooling System

$$\rho_{cw} Vel_{cw} C_{p_{cw}} (T_{cwin} - 273) = \rho_{cw} Vel_{cw} h_{cw}(0) - kz_{cw} \frac{\partial T_{cw}(0)}{\partial z} \tag{C.28}$$

(C.29)

$$\frac{\partial T_{cw}(RZ)}{\partial z} = 0 \tag{C.30}$$

Reactor centre line

$$\frac{\partial C_i(z,0)}{\partial r} = 0 \qquad \forall z \in (0, RZ),\ i = \{1, 2.\,3\} \tag{C.31}$$

$$\frac{\partial T(z,0)}{\partial r} = 0 \qquad \forall z \in (0, RZ) \tag{C.32}$$

Reactor wall

$$\frac{\partial C_i(z,RR)}{\partial r} = 0 \qquad \forall z \in (0, RZ),\ i = \{1, 2, 3\} \tag{C.33}$$

$$-k_r \frac{\partial T(z,RR)}{\partial r} = U(T(z,RR) - T_{cw}(z)) \qquad \forall z \in (0, RZ) \tag{C.34}$$

BIBL
NDON